Towards Forecast-Informed Sustainable Hydropower Operations

Shahryar Khalique Ahmad

A dissertation

submitted in partial fulfillment of the

requirements for the degree of

Doctor of Philosophy

University of Washington

2021

Reading Committee:

Faisal Hossain, Chair

Bart Nijssen

Erkan Istanbulluoglu

Program Authorized to Offer Degree:

Civil and Environmental Engineering

University of Washington

Abstract

Towards Forecast-Informed Sustainable Hydropower Operations

Shahryar Khalique Ahmad

Chair of the Supervisory Committee:
Professor Faisal Hossain
Civil and Environmental Engineering

To reduce the dependence on fossil fuels, the world needs to mainstream the use of clean and renewable energy sources. Hydropower remains the key renewable source to provide baseload power due to its relatively stable generation and high capacity-factor. However, hydropower operations have historically proven unsustainable due to the impact of dams on the nature and ecosystem. We address the issue of sustainability by proposing a dam operation strategy that is efficient on three fronts: (i) maximizing energy generation while satisfying competing objectives, (ii) feasibility and transferability of dam operation framework, and (iii) environmental and eco-system sustainability.

First, we demonstrate the value of short-term weather forecasts to maximize hydropower benefits by optimizing dam release decisions. By coupling the forecast information with a multi-

objective optimization framework, optimal release decisions were derived that raised total energy generation by 5.6% year-round for Detroit dam in Oregon. Next, to ensure the concept is feasible for application in resource-constrained settings, we developed a fast, skillful, and transferable approach to forecast reservoir inflow. To consider the long-term benefits of dam operations in addition to hydropower generation, we developed a nested optimization technique leveraging both short- and long-term forecasts (termed as co-optimization). The co-optimization, when implemented over a network of dams operated in Upper Colorado Basin, generated 28% higher hydropower annually while satisfying other constraints and competing objectives.

The third aspect to safeguard environmental and ecosystem sustainability was addressed by modeling thermal change in downstream rivers as a function of dam operations. Multi-objective optimization with ecosystem-driven constraints helped realize ecosystem-safe hydropower operations by limiting river temperature alteration within safe bounds. Benefits to hydropower faced tradeoffs under more stringent temperature constraints. To extend our concept over future hydropower dams, we proposed a framework to predict thermal impact of 216 planned dams worldwide. A general homogenized trend of lower highs (reduced river temperatures during summers) and higher lows (warmer temperatures during winters), potentially harmful to native fish species, was predicted across the planned sites. This elucidates the need to incorporate thermal pollution within the dam planning to ensure sustainable hydropower expansion. A decision support system was also developed to facilitate real-world engagement with dam-operating agencies and bridge the gap between research and application domains. It is imperative to mainstream sustainable hydropower operations as an operating standard for existing and future dams and foster the goal of clean energy without sacrificing the societal and ecosystem benefits.

TABLE OF CONTENTS

LIST OF FIGURES

LIST OF TABLES

ACKNOWLEDGEMENTS

First and foremost, all praise and thanks is due to the almighty God for enveloping me with His endless compassion, love, and care at every moment of my life.

I take this opportunity to express the sincerest gratitude to my advisor Professor Faisal Hossain for his supervision, mentorship, encouragement and guidance throughout the research work. He showed a perfect example of both a researcher and an adviser and it has been my fortune and pleasure to work with him. He provided me the freedom to pursue the research that I enjoyed and brought a contagious passion to everything we worked on together. His invaluable guidance during the course of my journey as a graduate student instilled in me the skills necessary for my long-term career goals. I am also grateful to my reading committee members Bart Nijssen and Erkan Istanbulluoglu for their thoughtful insight and suggestions on shaping this dissertation.

I want to express deep gratitude to the current and past members of the SASWE Research Group, in particular, Hisham Eldardiry, Nishan Biswas, Safat Sikder, Indira Bose, Claire Beveridge, Matthew Bonnema, Xiaodong Chen, and Asif Mahmood. Their camaraderie, support, mentorship, encouragement, and friendship made my graduate experience a joy and their suggestions on my research were invaluable.

This acknowledgement is incomplete without the mention of my family members. I want to extend the greatest and deepest appreciations to my parents, Dr. Shakeel Ahmad and Mrs. Shameema Khatoon, and wonderful sister Dr. Shazia Durdana for their endless love, support and encouragement throughout my life.

At the time of writing, Chapter 2 has been published as Ahmad and Hossain (2020a) in *Renewable Energy*, Chapter 3 as Ahmad and Hossain (2019a) in *Environmental Modeling and Software*, Chapter 4 as Ahmad and Hossain (2020b) in *Journal of Renewable and Sustainable Energy*, and Chapter 5 as Ahmad and Hossain (2020c) in *Renewables: Wind, Water, and Solar*. Chapter 6 is under review in *Earth's Future*. These are:

Chapter 2:

Ahmad, S.K., Hossain, F., 2020a. Maximizing Energy Production from Hydropower Dams using Short-Term Weather Forecasts. Renewable Energy, 146, pp.1560-1577. doi:10.1016/j.renene.2019.07.126

Chapter 3:

Ahmad S.K., Hossain, F., 2019a. A Globally Scalable Data-driven Technique for Forecasting of Reservoir Inflow for Hydropower Maximization. Environ. Model. Softw., 119, pp.147-165. doi:10.1016/j.envsoft.2019.06.008.

Chapter 4:

Ahmad, S.K., Hossain, F. 2020b. Forecast-Informed Hydropower Optimization at Long and Short-time scales for a Multiple Dam Network. Journal of Renewable and Sustainable Energy 12. doi:10.1063/1.5124097

Chapter 5:

Ahmad, S.K., Hossain, F., 2020c. Realizing ecosystem-safe hydropower from dams. Renewables: Wind, Water, and Solar, 7(1), pp.1-23. doi:10.1186/ s40807-020-00060-9

Chapter 6:

Ahmad, S.K., Hossain, F., Holt, G., Galleli, S., Pavelsky, T. 2020d. How will Future Dams Modify Temperature of Rivers around the World? Earth's Future (*under review*)

DEDICATION

To my beloved parents, Dr. Shakeel Ahmad and Mrs. Shameema Khatoon, and sister, Dr. Shazia Durdana

Chapter 1. INTRODUCTION

1.1 BACKGROUND INFORMATION

1.1.1 *Significance of Hydropower*

The goal of energy security has been a vital core element for providing sustainable livelihoods across the globe (Romero-Lankao et al., 2017). This goal, however, has been compounded by the complex intertwining of two formidable yet necessary challenges of attaining environmental sustainability and water security. Our environment is already under constantly increasing stress from various human-induced changes and developments and is further worsened by rapidly growing energy demands (Armaroli and Balzani, 2011). The other aspect of water security also demands a similar attention owing to the strong interdependence of energy and water sectors, referred to as the energy-water nexus (Hussey and Pittock, 2012). Water is used in all phases of energy production, and energy is required to extract, pump, and move water for consumption and other uses by humans.

To reduce the dependence on fossil fuels, mainstreaming of clean and renewable energy sources is necessary. The use of wind, water and sunlight to meet electricity demands across the world has been comprehensively explored by Jacobson et al. (2018, 2017, 2014). The future of renewable energy potential has also been projected to lie exclusively in the variable sources of wind and solar power which are claimed to be sufficient to meet the energy demand (Becker et al., 2014; Delucchi and Jacobson, 2011). However, hydropower remains the only dependable source for supplying baseload power (minimum power needed at a steady rate) due to its relatively high capacity factor (Ahmad and Hossain, 2020a; U.S. EIA, 2018; Liu et al., 2019), minimal potential interruptions to the system (Hamlet et al., 2002) and ease of ramping up or down operations. Other advantages that make hydropower a robust and clean energy source that demands due consideration, include its significant operational flexibility with the ability

to store energy (Sørensen, 1981), low operating and maintenance costs (Hamlet et al., 2002), instant power generation (Egre and Milewski, 2002), and its capability to complement intermittent renewables of wind and solar powered energy.

The Sustainable Development Goals (SDGs) agreed by the United Nations in 2015 have led many countries around the world to recognize hydropower as playing a vital role for delivering affordable and clean electricity (Zarfl et al., 2019). The more developed economies of the U.S. and Western Europe are already at an advantage with abundance of hydropower dams built over the past century. In contrast, many countries of Asia, Sub-saharan Africa and South America have planned for expansion of hydropower installation to achieve clean and affordable energy (SDG #7). Despite these differences across countries, the common denominator is the efficiency of hydropower generation which is a unique attribute of dam (used here interchangeably with 'reservoir') operations.

1.1.2 *Current State of Dam Operations*

Management of most reservoirs is currently based on rule curves that outline reservoir storage targets to be met at specific time intervals of the year. The rule curves are historically developed by operating agencies using historical reservoir inflows, physical constraints (e.g., downstream channel capacity), and historical operating objectives (Anghileri et al., 2016). A number of reservoir planning and operation studies have optimized the rules based on the operating purpose and type of reservoir network., subject to different constraints. Lund and Guzman (1999) reviewed a variety of proposed real-time operating policies for multiple reservoir networks operated for water supply, flood control, hydropower, water quality and recreation, and presented conceptual optimal rules for series and parallel reservoir networks. Marques and Tilmant (2013) underscored the economic value of coordination in a large-scale multi-reservoir system in Brazil. Zhou et al. (2016) derived optimal operating rules for multi-reservoir system in China by combining water and power operating rules to coordinate

operations. However, most of these published rules are static ‘rules of thumb’ that need to be ‘nudged’ when circumstances change. This has led to several instances of suboptimal operations that caused heavy damages, especially during highly uncertain flood events. Examples include the 1996 Willamette Valley flood in Oregon (Rose 2016), the 2008 flood in Bihar, India (Meht, 2008), and the recent 2018 flood in Kerala, India (Padmanabhan, 2018). The operations based on static rule curves can also lead to missed hydroelectric energy (Miao et al, 2016). As energy demands are growing rapidly with the increasing population and urbanization, there is a need to meet those using clean sources of generation (Ellabban et al., 2014). However, the current state of hydropower production will soon be incapable to suffice the rising trend of energy demands. The developed world (such as North America or Western Europe) cannot permit new dam constructions because of environmental constraints and regulations and thus cannot expect any significant rise in hydropower capacity installation (Labadie, 2004). The developing nations on the other hand, are faced with increasing environmental and social costs from the numerous small- and large- scale hydropower dams that have been built recently or are planned for in the near future (Collier, 2014; Yüksel, 2019).

This necessitates improving the operational effectiveness of operations for the existing and even planned dams. One such way is to use a scheme of operations that is dynamically updated at shorter timescales and adjusts itself accordingly without the need to refer to static rules. Short-term daily to weekly scale forecasts are indispensable in maximizing societally important benefits of flood control and hydropower generation (Yazicigil et al., 1983; Anghileri et al., 2016). Flood mitigation requires sufficient flood storage before an impending flood, while hydropower generation requires maximizing the economic value of water by releasing most of it through turbines and keeping reservoir at maximum pool to maximize the hydraulic head. Reservoir inflow forecasts, if reasonably

skillful, can help achieve a balance where hydropower can be maximized without compromising flood risk downstream (Jordan et al., 2012; Madsen et al., 2009; Qi et al., 2017).

Further, existing efforts to inform dam operations with forecasts have generally made a distinction concerning the temporal scale of forecast. Short-term forecasts (daily to weekly scale) are incorporated to optimize for short-term (tactical) operational purposes while medium to long-term forecasts (monthly or seasonal scale) are used for long-term (strategic) objectives (Anghileri et al. 2016). Although this is a common notion of using forecast information to optimize reservoir operations, it suffers from drawbacks. Losses can occur to the specified operating purpose due to optimization addressing only the short or long-term objectives but not both (Sreekanth et al., 2012). Therefore, it is imperative to achieve a balance between the immediate and potential future benefits, satisfying both the short and long-term optimality in operations.

1.1.3 *Transitioning Towards Efficient Dam Operations*

Given the limitations in the current state of dam operations and the urgent need to increase the share of renewable energy in the global energy mix, improving hydropower efficiency forms the core objective of this dissertation as illustrated in Figure 1.1. Efficiency of hydropower dam operations entails three key components – (i) maximizing energy generation while satisfying competing objectives, (ii) feasibility and transferability of dam operation framework, and (iii) environmental and ecosystem sustainability. Any water management strategy that lacks on any of these three fronts will result in inefficient energy generation.

First and foremost, because the majority of dams are operated for more than one purpose, it is imperative to design the hydropower operation strategy in a way that is adaptive to the inflow conditions. The dam release decisions should not only maximize energy

generation but also uphold other stakeholder benefits without compromising other purposes. The second and equally significant aspect of energy efficiency is the feasibility of implementing the proposed solution in terms of data requirements and computational resources. This is one of the key mandates as the majority of proposed installed hydropower capacity is planned in developing economies where in-situ data availability and computational resources for complex model simulations is particularly limited. Thirdly, based on the well-known costs to the environment and ecosystem from the existing hydropower operations (Ligon et al., 1995; Tilt et al., 2009), existing efforts to improve dam operations lack on the sustainability front which needs immediate attention.

Figure 1.1 summarizes these three aspects of improving hydropower efficiency (the core objective) and the respective research components. The outer circle denotes tools and techniques used to mainstream the research components in the application domain.

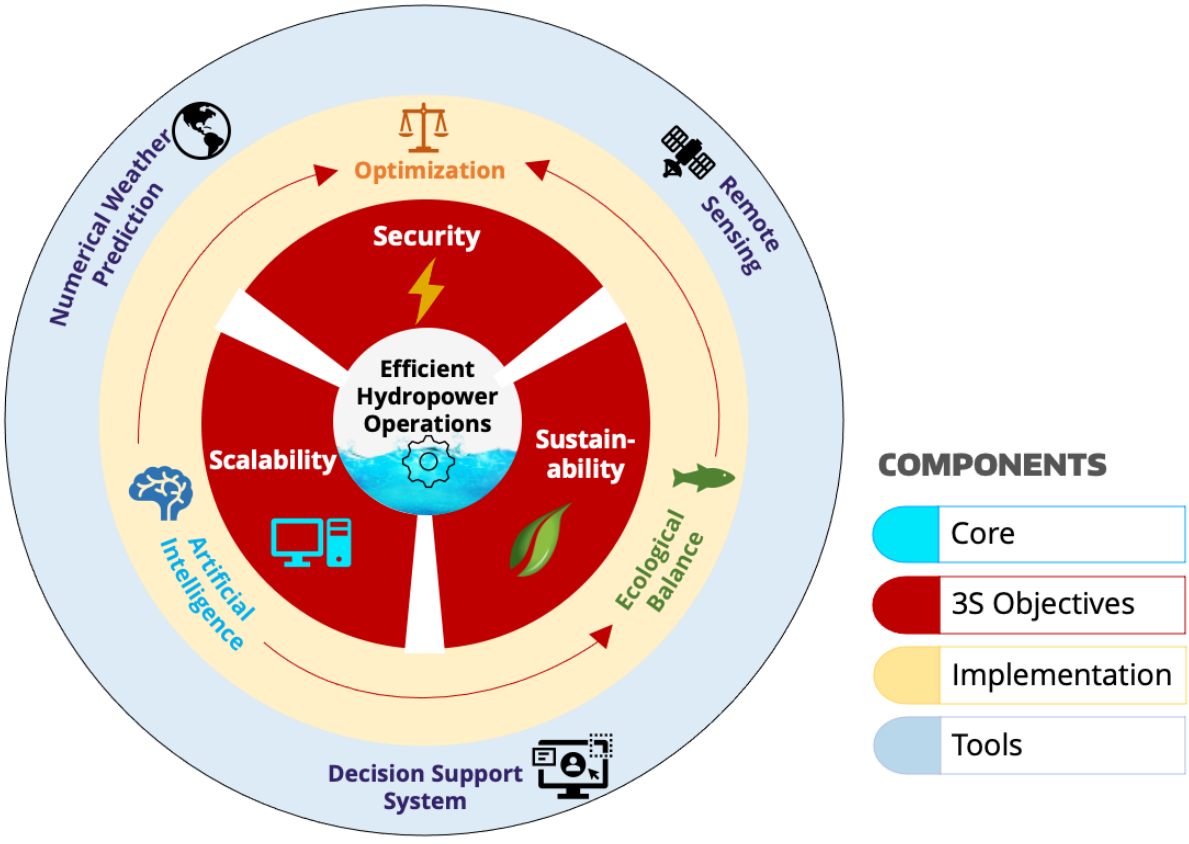

Figure 1.1. Integration of various research components used in this dissertation to address the core objective of achieving an efficient and resilient hydropower generation system.

1.2 RESEARCH OBJECTIVES

The motivation behind this dissertation is to transform the current state of dam operations and realize an operational framework that leads to efficient energy generation on all three fronts. The specific objectives of this dissertation can be summarized as:

(i) To determine the value in informing single and multi-dam operations with forecasts at weather/climate scale toward improving energy generation without compromising other competing objectives.

(ii) To establish a computationally efficient, skillful and globally scalable approach of using forecast information toward optimizing dam operations that is feasible for data/resource-constrained regions.

(iii) To incorporate standards of ecological sustainability within the hydropower operation framework to achieve ecosystem-safe energy generation from existing and planned dams.

The long-term goal of this effort is to result in generation of more energy from fewer dams while adhering to the standards of ecological safety. At the same time, this will provide the dam operating agencies and stakeholders with smarter expansion plans for installing new hydropower capacity.

1.3 APPROACH

The core of this dissertation is organized as follows.

Chapter 2 demonstrates the value of short-term weather forecasts from NWP models in a reservoir optimization framework for maximizing hydropower benefits. Chapter 3 develops a fast, skillful, and transferable approach to forecast reservoir inflow to address resource feasibility of the framework. A decision support system is also presented leveraging the research concepts of the previous two chapters to improve operational decision making.

These two chapters set the foundation of forecast-informed hydropower operations for single dams. Chapter 4 extends this framework to more common real-life networks of multiple dams using both long-term (seasonal) and short-term (daily) forecasts to maximize hydropower generation. Chapter 5 focuses on the ecological sustainability aspect of hydropower operations. By modeling thermal change in downstream rivers as a function of dam operations, additional constraints are imposed on the optimization framework to realize ecosystem-safe hydropower operations. Finally, chapter 6 proposes a solution to predict thermal impact of planned hydropower dams worldwide and facilitate expansion of hydropower infrastructure in an environmentally sustainable way.

Chapter 2. VALUE OF SHORT-TERM WEATHER FORECASTS IN MAXIMIZING HYDROPOWER PRODUCTION

Note: This chapter has been published mostly in its current form in the journal Renewable Energy (Ahmad and Hossain, 2020a). Used with permission from Elsevier.

Ahmad, S.K., Hossain, F., 2020a. Maximizing Energy Production from Hydropower Dams using Short-Term Weather Forecasts. Renewable Energy, 146, pp.1560-1577. doi:10.1016/j.renene.2019.07.126

ABSTRACT

This study explores the maximization of hydropower generation by optimizing reservoir operations based on short-term inflow forecasts derived from publicly available numerical weather prediction (NWP) models. Forecast fields from the NWP model of Global Forecast System (GFS) were used to force Variable Infiltration Capacity (VIC) hydrologic model to forecast reservoir inflow for 1-16 days lead time. The optimization of reservoir operations was performed based on the forecast of inflow. The concept was demonstrated for two dams in the United States. Optimal operations over two-year return period storm events produced additional benefits of 68.1% and 80.9% for Pensacola and Detroit dams, respectively, while optimization over a longer ten-month period for Detroit dam raised the total energy by 5.6% over the observed generation. The optimization not only improved hydropower generation, but also helped satisfy the goals of flood control and dam safety. The study clearly underscores the additional value of weather forecasts that are available publicly and globally from NWP models for any dam location for hydropower maximization. Given the on-going effort to coordinate strategies for sustainable energy production from renewable energy sources, it is timely that this concept be expanded further to current hydropower dam sites around the world. This can

help reduce dependence on fossil-fuel based energy production and shift towards greener sources using existing hydropower infrastructure.

2.1 INTRODUCTION

Improving production from renewable energy sources is required in reducing the dependence on fossil fuels and addressing the global energy security in a sustainable way. As envisioned by (Jacobson et al., 2017), unless a replacement energy infrastructure is developed well ahead of time, economic, social and political instability may ensue due to heavy fluctuation in the supplies and price of fossil fuel (Department of Energy, 2016). The renewable sources of energy are not subject to such price fluctuations as they come from the available natural sources of water, sunlight, wind, tides etc. (Vieira et al., 2009). A recent study concluded that the use of wind, solar, hydroelectric, tidal and geothermal energy is the most beneficial, among several other alternatives, for addressing pollution, public health, global warming, and energy security (Jacobson, 2009).

The use of wind, water and sunlight to suffice for the electricity demands within U.S. as well as worldwide has been explored by Jacobson et al. (2014; 2018; 2017; 2011). Some of these studies have projected the future renewable energy potential to lie exclusively in the variable sources of wind and solar power and claimed them to be sufficient to meet the energy demand (Heide et al., 2010; Delucchi et al., 2011; Becker et al., 2014; Jacobson and Delucchi, 2011). However, hydropower remains a stable renewable source to generate the baseload power (minimum power needed at a steady rate) due to its relatively high capacity factor (Energy Information Administration, 2018; Tiu et al., 2019) and minimal potential interruptions to the system (Hamlet et al., 2002; Spector, 2015). Factors that further necessitate studying hydropower systems include its significant operational flexibility with ability to store energy (Sørensen, 2002), instant power generation (Egre and Milewski, 2002), low operating

and maintenance costs (Hamlet et al., 2002), and capability of integration with intermittent renewables (Kougias et al., 2016). This is manifested in recent effort of wind-hydro combination projects by the German firm *Max Bögl* (Grumet, 2016).

Within the U.S., over the past 65 years (1950-2015), hydropower has contributed 10% to the total and 85% to the renewable power generation (Department of Energy, 2016). However, the installation of newer hydropower capacity has declined in the past couple of decades. According to the U.S. Department of Energy, the amount of nation's net electricity generation contributed by hydropower has decreased, from 30% in 1950 to 7% in 2013, as nuclear power, coal, natural gas, and other sources were added to the nation's energy portfolio to meet rising demands. In the last decade, no large-scale hydropower dam project, exceeding 500 megawatts (MW), has been constructed in the U.S. due to factors such as lower economic growth, concerns related to environmental impacts, stagnant energy market, and uncertainties owing to the recent breakthroughs in the shale gas and oil industries (Miao et al., 2016). Figure 2.1 illustrates this stagnation observed in the growth of hydropower capacity after 1990. Further, as most economical hydropower sites in U.S. have already been explored over the previous century, any rise in the hydropower infrastructure is hardly expected (Labadie, 2004). However, given that large-scale development of new hydropower dams has stagnated in the developed world such as the U.S., it is worthwhile to explore how existing infrastructure can be maximized of its operational effectiveness to provide more power to the energy grid by optimizing the operations (Block, 2011).

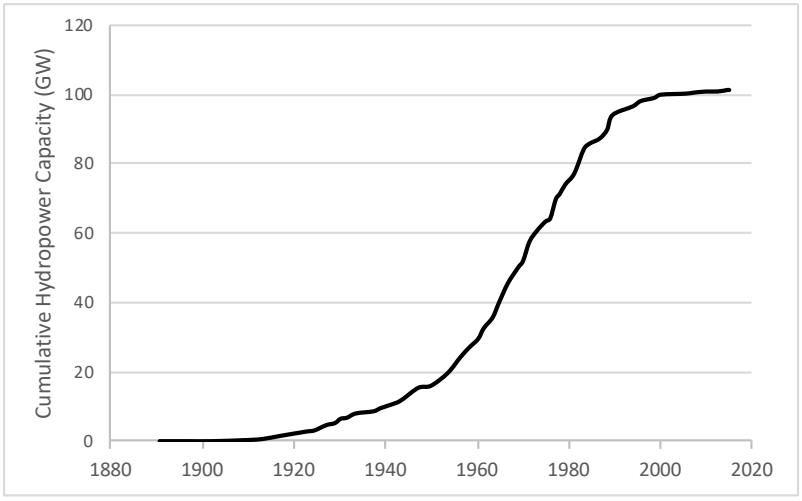

Figure 2.1 Cumulative installed hydropower capacity from 1890-2015 over the United States (Data from Department of Energy, 2016)

The current management of most federal reservoirs at daily time scale is based on rule curves that outline the reservoir storage targets to be met at specific time intervals of the year. The rule curves were designed based on existing storage volumes using a climatology of historical flow observations (Lee et al., 2009; Ficchi et al., 2016). Operating strictly based on these rules, without considering the altered demands or changes in inflow patterns (Farmer et al., 2016; Hossain et al., 2012) can cause mishandling of an impending and unexpected reservoir inflow situation at the weather scale. Such a situation can lead to missed hydroelectric energy (Miao et al., 2016). For example, in a weaker-than-average month of the flood season, lowering the pool to rule curve level too early can result in significant loss in power generation, which could be avoided if the inflow forecasts are made ahead of time. Thus, it is timely to leverage the advancements in atmospheric modeling for forecasting the weather (Bauer et al., 2015) and optimization techniques to achieve the goal of maximizing hydropower energy and realize more efficient and 'smart' reservoir operations management.

The numerical weather prediction (NWP) weather models from various meteorological agencies produce weather scale forecasts fields of precipitation, temperatures, wind speed, soil moisture etc. in three dimensions over the entire globe. These publicly available forecasts represent an underutilized low-hanging fruit for the hydropower community. Currently, the

integration of such forecasts into existing water management decision processes at weather scale is not yet popular or mainstream due to the traditional risk averse nature of water managers. The major concerns include low forecast skill and mismatch in the scales of forecasts from those required by the stakeholders (Lee et al., 2009; Goddard et al., 2010; Anghileri et al., 2016). However, a recent study concluded that the forecast skill of NWP models at a lead time of 7 days has improved from 50% in 1995 to more than 70% in 2015 (Sørensen. 1981). Such an improvement can capture the peaks of a flood event and can be utilized to adjust the dam operations accordingly. Reservoirs in the snow-dominated regions like the west coast (e.g. Columbia River basin) frequently use seasonal projections of climate, snowpack forecast etc. to optimize their operations (Anghileri et al., 2016). Ongoing projects such as Integrated Forecast and Reservoir Management (INFORM) (Georgakakos et al., 2007) and Forecast Informed Reservoir Operations (Center for Western Weather and Water Extremes, 2016), that have focused over specific watersheds, are also utilizing short-term weather forecasts for operating the reservoirs. Another issue is the coarse resolution of the NWP forecast fields that are often not detailed enough to be applied over the relatively small reservoir catchments. To address this scale limitation, dynamic downscaling technique can be used to resolve the atmospheric processes at finer spatial scales (Murphy, 2000; Sikder, 2016; Teutschbein, 2011). To the best of our knowledge, there has not been any study to explore the value of dynamically downscaled NWP based forecasts specifically for hydropower maximization.

To utilize the forecast inflow information for generating more energy, the reservoir system needs an optimal and more informed set of release decisions updated dynamically based on the current reservoir state and future inflow. Various optimization techniques have been proposed in the past, and an extensive literature review and evaluation of different state-of-the-art approaches can be found in (Yeh, 1985; Rani and Moreira, 2010; Ahmad et al., 2014). The optimization objective is the key towards optimizing operations as there are a plenty of studies

focusing on single user benefits. These include optimizations for hydropower production (Yasar, 2016; Barros et al., 2003; Jothiprakash and Arunkumar, 2014), flood control and security (Hsu and Wei, 2007; Windsor, 1973), water supply (Ji et al., 2016; Neelakantan et al., 1999), irrigation and crop planning (Georgiou and Papamichail, 2008; Sadati et al., 2014) and environmental concerns (Miao et al., 2016). However, due to the wide-ranging diversity of property rights and stakeholders, optimizing for a single stakeholder is ill-advised, rather the competing purposes (such as flood control and irrigation) needs to be balanced for extracting equitable benefits out of the existing infrastructure. In several multi-objective optimization studies (Yeh and Becker, 1982; Ding et al., 2015; Reddy and Kumar, 2006; 2007; Khu and Madsen, 2005; Ngo et al., 2007; Ahmadi et al., 2014; Croley et al., 1979), the focus has been on the dams with significantly large reservoir storage capacity. The value of weekly streamflow forecasts was evaluated by (Georgakakos, 1989) over three different reservoir systems. Wasimi and Kitanidis (1983) analyzed the daily forecasts specifically to minimize flood damage from multi-reservoir system operations during floods. Short-term forecasts, as used here, are likely more valuable for the dams with reservoir capacity smaller than the annual inflow volume (Anghileri et al., 2016). This study specifically explores such dams, usually unaddressed in the existing literature, for hydropower operations incorporating the weather-scale forecasts maintaining flood and dam safety. Further, as underscored by (Krzysztofowicz, 2001), the uncertainty of hydrologic forecasts must be considered to avoid fatal decisions. A scheme for obtaining probabilistic inflow forecasts based on ensemble NWP fields is also described.

Thus, the key novel elements that distinguish this study from the existing literature include: (a) demonstration of the value of publicly available, dynamically downscaled NWP-based forecasts, to obtain reservoir inflow forecasts; (b) derivation of probabilistic forecasts using NWP forecast fields; (c) focusing on small-medium storage dams that receive

unregulated inflow; (d) coupling of the forecasts with reservoir optimization for hydropower maximization without compromising downstream flood safety (Ahmad and Hossain, 2020a). Most of the published literature, to the best of our knowledge, focus on flood control or hydropower but never together despite the obvious and competing constraints each pose on reservoir operations.

The overarching research question addressed is – *can short-term weather forecasts from numerical weather prediction improve the hydroelectric energy production for small and medium storage dams without compromising flood security, dam safety and environmental flow constraints?* Hereafter 'short-term' will be used to refer to a period of up to 16 days (forecast horizon of the NWP model considered here). A schematic of the approach highlighting the major components of the study is shown in Figure 2.2 and is explained in the following sections.

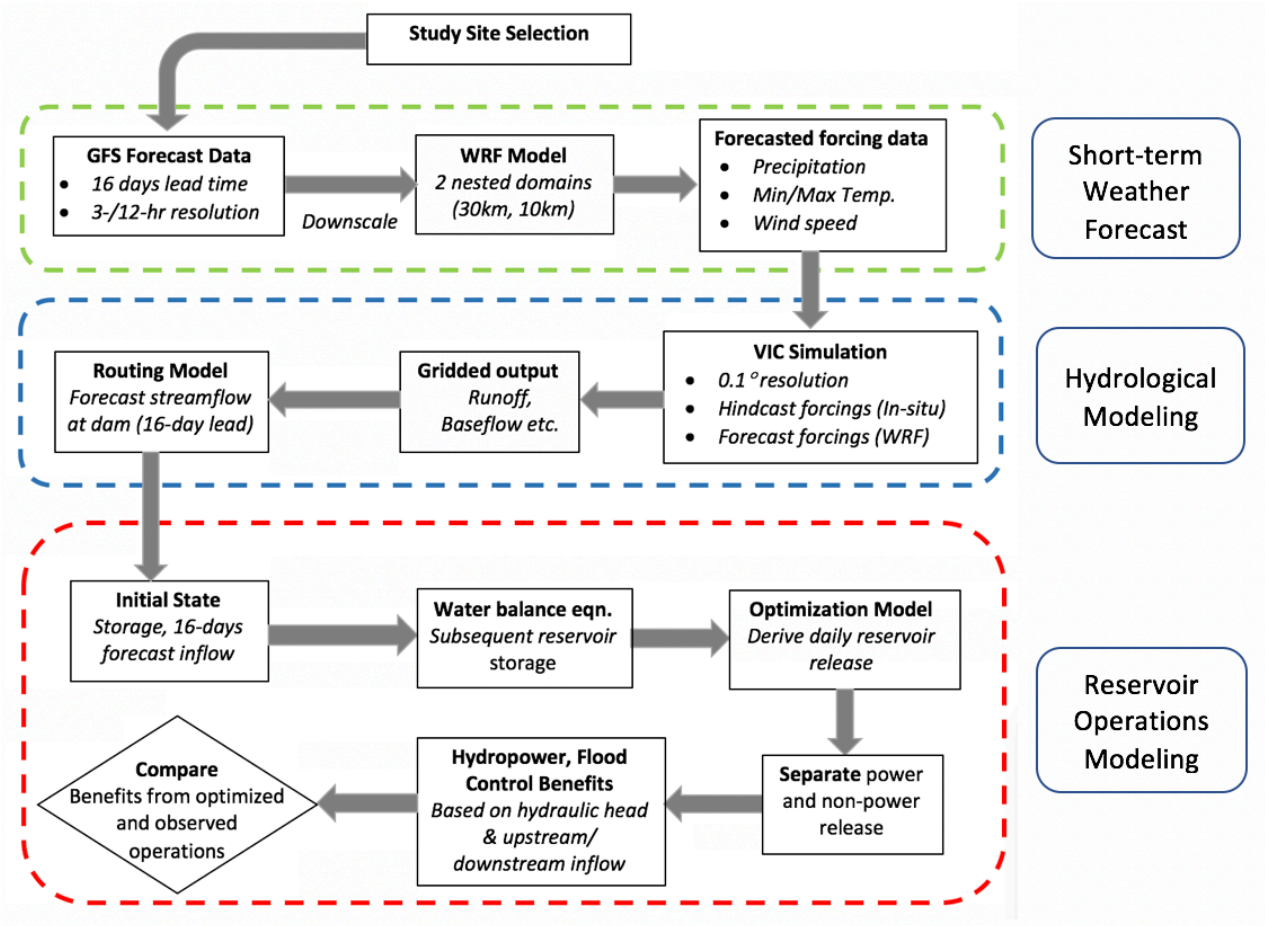

Figure 2.2 Illustration of the approach used in this study. Green box – forecasting; Blue box – hydrologic modeling; Red box – optimization component. VIC is the hydrologic model for predicting inflows. GFS is NOAA's Global Forecasting System for weather forecasts.

2.2 Material and Methods

2.2.1 *Study Region and Data*

An exploration was made for dams satisfying the following criteria: (i) operated for hydropower generation or flood control as their primary or secondary purpose, (ii) have reservoir storage capacity less than a threshold of 1,700 kaf (2.1 km^3) (98^{th} percentile value for reservoir storage within U.S., see Figure 2.3), (iii) located upstream in the dam network (in case of a multi-reservoir system) to receive unregulated inflow, to facilitate hydrological modeling, and (iv) reservoir storage capacity smaller than annual inflow volume for the short-term forecasts to be valuable. Out of the several potential locations, Detroit dam in Oregon and Pensacola dam in Oklahoma, were selected based on the data availability and processing time constraints. Both the Detroit dam, located at the North Santiam River forming Detroit Lake, and Pensacola dam on the Neosho River forming Grand Lake are primarily used for hydropower and flood control. The powerhouse at Detroit dam contains two Francis turbine units with a combined nameplate capacity of 100MW, while Pensacola dam, Oklahoma's first hydroelectric power plant, consists of six turbine generator units with the nameplate capacity of 120MW. The observed streamflow data was obtained from the U.S. Army Corps of Engineers (USACE) (USACE Northwestern Division, 2017; Monthly Charts for Grand Lake, 2018). The reservoir storage capacity and ratio with annual inflows are shown in Table 2.1. Comparison of Storage Capacity and Annual Inflow for the two dams and locations of the selected dams in Figure 2.4.

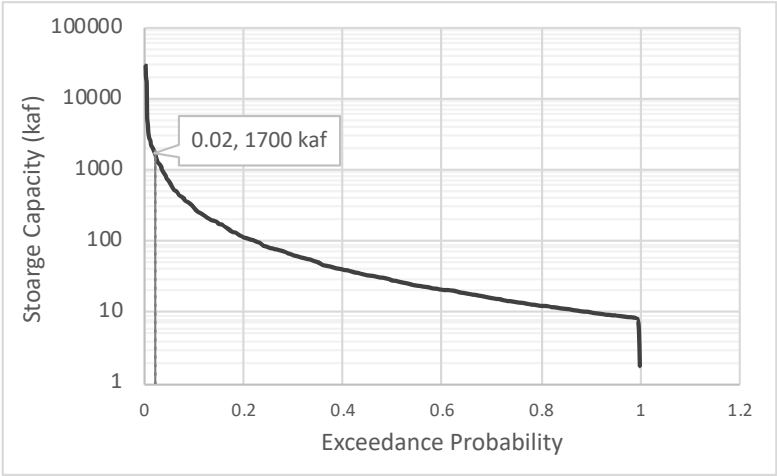

Figure 2.3 Distribution of the storage capacity of dams in U.S. Data obtained from Global Reservoir and Dam (GRanD) database (Lehner et al., 2011).

Table 2.1. Comparison of Storage Capacity and Annual Inflow for the two dams

Dam	**Drainage Basin Area (km^2)**	**Storage Capacity (km^3)**	**Annual Inflow (km^3)**	**Capacity-Annual Inflow Ratio**
Detroit	1435.4	0.56	1.75	0.32
Pensacola	26847.9	2.06	7.40	0.28

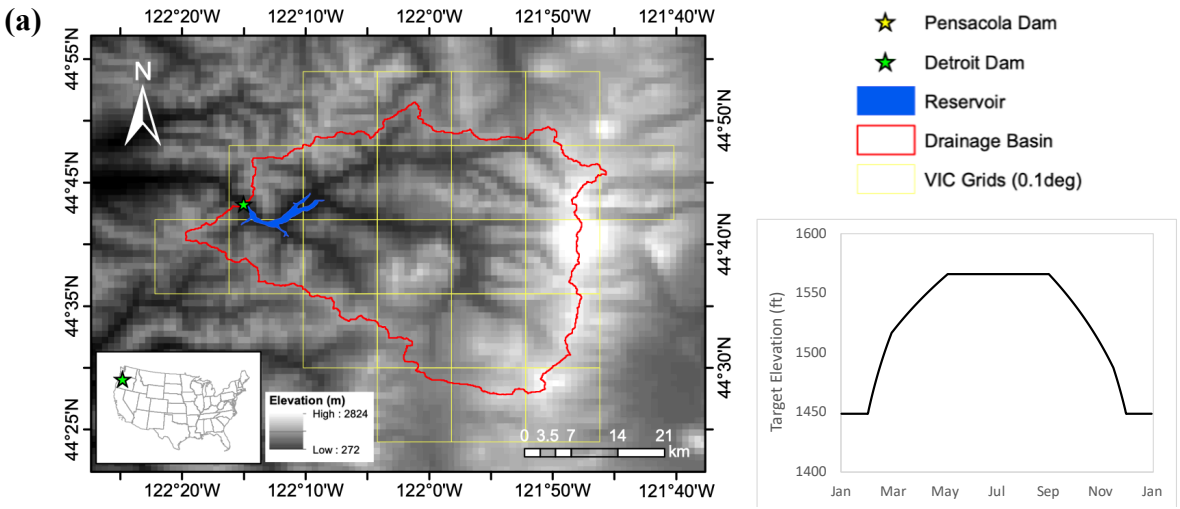

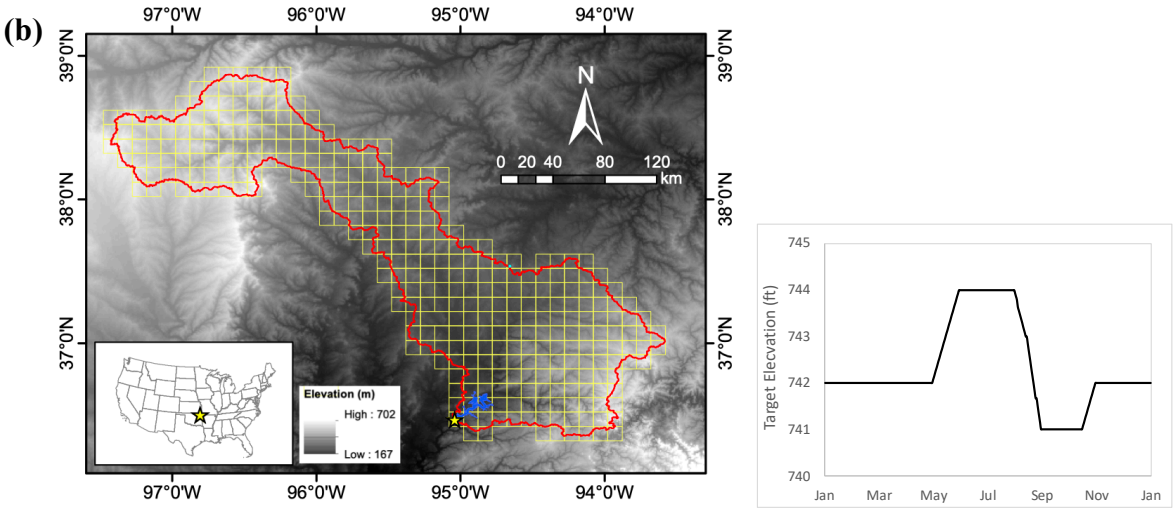

Figure 2.4 Location, drainage boundaries, VIC model grids (0.1˚) on the left panel and rule curves for (a) Detroit Dam, OR; (b) Pensacola Dam, OK, on the right panel (1ft = 0.305m)

2.2.2 *Short-term NWP based forecasts*

Real-time short-term (1-16 days) forecast data from the Global Forecast System (GFS) global-scale NWP model was acquired at 0.5˚ resolution. The global forecasts are produced four times a day for 1-16 days lead time in almost real-time by National Centers for Environmental Prediction (NCEP) (National Centers for Environmental Information, 2018). Dynamic downscaling was performed using the numerical Weather Research Forecasting (WRF) model to output forecasts at 0.1˚ resolution. WRF, a mesoscale atmospheric numerical modeling system, has demonstrated its capability for constructing the atmospheric conditions, at both local and regional scales (Chen et al., 2017; Skamarock et al., 2008). Two nested domains of 10 km and 30 km were used for both the dams as shown in Figure 2.5**Error! Reference source not found.**.

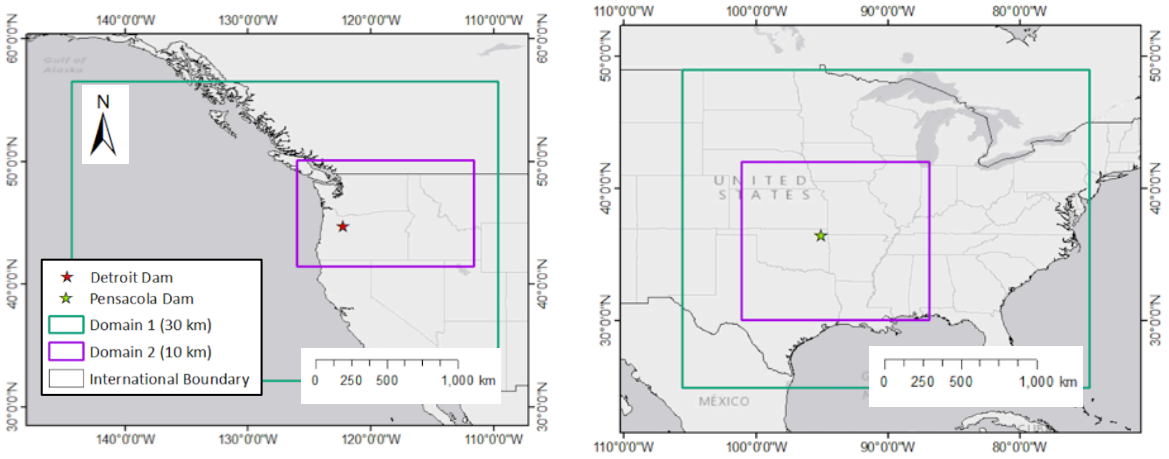

(a) (b)

Figure 2.5 The nested domains for WRF simulation at 30km and 10km, for (a) Detroit Dam, OR and (b) Pensacola Dam, OK.

In a numerical model like WRF, the Microphysics (MP) and Cumulus Parameterization (CP) schemes are the controlling factors for precipitation as reported in existing literature (Stensrud, 2007). As the Detroit dam lies in the Pacific Northwest region, the model configurations were inherited from the forecast model runs of Department of Atmospheric Sciences at the University of Washington (Pacific Northwest Mesoscale Model Numerical Forecast Information, 2017). The Thompson graupel scheme was considered for MP and Grell-Devenyi ensemble scheme for CP. For Pensacola dam, the Morrison microphysics scheme was used as recommended by Chen et al. (2016) for extreme storm simulations. Appendix A evaluates the performance of WRF setup for both the dams.

2.2.3 *Hydrological Model*

The macroscale semi-distributed Variable Infiltration Capacity (VIC) hydrologic model (Liang et al., 1994; 1996) was chosen to model the reservoir inflow. The VIC model is forced with the time series of gridded precipitation, minimum and maximum temperature, and wind speed. The macroscale model was run at a daily time scale at 0.1˚ spatial resolution to ensure that the basin contains enough grid cells for simulation. The hindcast forcings were obtained

from NCDC Global Surface Summary of the Day data (NOAA Data Catalog, 2017) while the WRF-downscaled GFS fields provided the forecast forcings for the VIC model. To obtain the inflow at the downstream station of basin, routing of streamflow was performed separately using the routing model of Lohmann et al. (1996; 1998). Model calibration was performed by adjusting the parameters of VIC model that govern baseflow recession, infiltration, and soil layer depths to match the simulated streamflow with reference data, minimizing the root mean squared error (RMSE). The calibration and validation details of VIC model are provided in Appendix A.

2.2.4 *Reservoir Operations Model*

The next step (Figure 2.2, red box) is to model the reservoir operations using the forecast inflow information by optimizing the releases from the reservoir to maximize hydropower generation without compromising the dam's flood control strategy. Optimizing at the daily time step is most suitable when it comes to real-time operations of small and medium-storage dams. A small dam operator is very unlikely to be making decisions on reservoir releases for such dams at frequencies higher than a day.

2.2.4.1 Optimization Strategy

In general, setting up the reservoir's optimization framework involves three components – 1) advanced scheduling of water releases, 2) useful inflow forecasts that serve as input data, and 3) and optimization model that utilizes forecast information to the best advantage (Yeh, 1985). A major limitation in operating the reservoirs occurs during the flood/peak flow seasons when the high uncertainty in predicting a flood peak leaves the dam operator uncertain on much water to release to balance the various stakeholder benefits. The short-term forecast information was utilized here to provide the operator with a release policy optimized to simultaneously maximize benefits from the conflicting objectives.

To minimize the effect of reduced forecast skill with increasing lead times (see Appendix A), the optimization strategy sequentially updates NWP-based (downscaled by WRF) flow forecasts every other day. Evaluation is performed by calculating optimized hydropower benefits (*optimized* HP) using the optimized releases while passing the observed inflow into the system. The *optimized HP* benefits were compared against the observed benefits (*observed HP*) using observed operations without any optimization/forecasts. The observed benefits correspond to the real-world power generation data obtained from USACE that operates the two dams. The optimized hydropower benefits (megawatt-hours, MWh) were calculated as a product of hydraulic head and power release (via penstocks), considering the turbine efficiency, operating hours and the capacity factor (ratio of actual hydropower produced to the maximum possible over a period).

2.2.4.2 Optimization Objectives and Constraints

Reservoir operations were formulated as a Multi-objective Optimization Problem (MOP) based on a Pareto optimal set of solutions with the objective functions of hydropower maximization and flood control (Madsen et al., 2009). The two objectives are mutually conflicting, since maximizing hydropower production requires higher reservoir storage to produce more power, while for minimization of the flood risk, more water needs to be released to ensure enough storage when the peak inflow hits the reservoir. The Non-dominated Sorting Genetic Algorithm (NSGA-II) (Deb et al., 2000) was used to yield the Pareto front of the optimal solutions from which an appropriate alternative can be chosen at various satisfaction levels of both the objectives [66]. The two conflicting objectives are formulated below.

1. Minimize the deficit in hydroelectric power production (MW) from the maximum generation capacity of the powerplant (HP_{max}),

$$\min f_1(MW) = HP_{max} - \sum_t \epsilon \cdot \Delta t_{turb} \cdot (HF_t - HT_t) \cdot R_{p,t} \qquad (2.1)$$

2. Minimize the absolute value of deviations of reservoir elevation (H) from the target rule curve level (T) over the optimization horizon. It is represented as,

$$\min f_2(ft) = \sum_t |H_t - T_t| \quad (2.2)$$

$t -$ 1-16 days (optimization horizon)

HF – Reservoir forebay water level (ft)

HT – Reservoir tailrace water level (ft)

ϵ – Turbine efficiency

Δt_{turb} – Turbine operating hours

$R_p -$ Power release from turbines (cfs)

Several constraints were imposed on the optimization problem in the interest of downstream stakeholders, dam safety and environmental concerns. The power and spillway release from the reservoir were limited by the turbine and spillway capacity. The minimum for reservoir storage was set to 95% of the historical minimum and the maximum to the flood control pool while following the storage-volume continuity. The total release was bounded between the environmental flow limit and a safe threshold to prevent flooding at a downstream control station. The mathematical formulation of the constraints is given in Appendix A.

2.3 RESULTS

Three case studies are presented for forecast-based hydropower maximization using optimized reservoir operations. Two of them were performed over a single storm flow event each for Detroit and Pensacola dams, while a third long-term assessment was performed over a continuous period of ten months for Detroit dam with a long dry spell.

2.3.1 *Detroit Dam – Single Event Assessment*

The various pools of the reservoir along with the constraints used in setting up the optimization model are shown schematically in Figure 2.6. The maximum total release was set to control

the downstream point of Mehama to a threshold of 9000 cfs (255 m^3/s) to prevent downstream flooding.

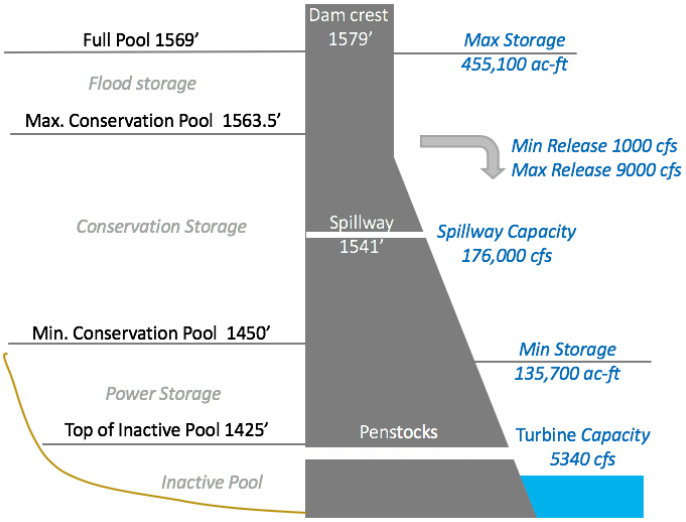

Figure 2.6. Cross-section of Detroit dam (not to scale) showing relevant pool elevations (from mean sea level, MSL) along with the optimization constraints obtained from USACE. (1 ft = 0.305 m, 1 cfs = 0.028 m^3/s, 1 ac-ft = 1233.48 m^3)

The flow event of 21 Dec 2014 with peak inflow of 24,170 cfs (684 m^3/s) (yearly-scale magnitude) was selected. As the turbine operating characteristics vary over an event or a season, model for hydropower estimation (MWh) based on available daily energy generation data (MW) was developed. Linear regression was performed between the energy generation (in MWh) and the product of hydraulic head ΔH and power release R_p (correlation coefficient, $R^2 = 0.93$) to obtain an average estimate of 19.72 hours for turbine's operating hours coupled with its efficiency (the constant $\epsilon \cdot \Delta t_{turb}$ in equation 2.1). Although the linear model gives a reasonable approximation for hydropower production function, detailed data on the turbines' characteristic curves and their operating schedules will be sought from dam operating agencies in a future work.

The 16-day forecast inflow obtained using the VIC model forced with WRF-downscaled forecasts for lead times of 3, 5 and 9-days over the selected event are shown in Figure 2.7(a).

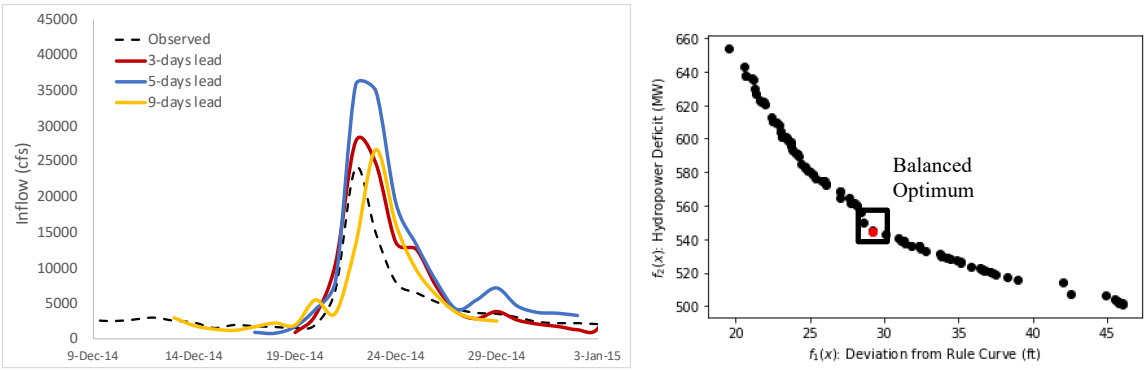

(a) (b)

Figure 2.7. (a) VIC-modeled 16-day forecast flow forced with WRF-downscaled forecast fields, for lead times of 3, 5 and 9 days for Detroit dam, OR; (b) Non-dominated solutions on the Pareto front and the selected balanced optimum obtained between the objectives of hydropower deficit and deviation from rule curve (to be minimized). (1 cfs = 0.028 m^3/s)

The optimized release policy was obtained with the optimization starting on Dec 11. A set of 100 non-dominated points on the tradeoff curve (Pareto front) obtained between the two competing objectives are shown in Figure 2.7(b) for the first day of optimization. A balanced optimum solution was chosen on the Pareto front giving equal priority for hydropower deficit and flood risk (in terms of deviation from rule curve) and aiming at concurrently minimizing both the objectives. The conflicting nature of the two objectives can be clearly observed from the shape of the Pareto curve.

The optimal release of the first two days were implemented while the later ones were revised in the next model run on Dec 13 using updated forecasts. The sequential updating of forecasts was continued every alternate day until Dec 19. This resulted in the optimized release as shown in Figure 2.8(a). While the releases and elevations from Dec 11-19 are obtained by

sequentially updating the forecasts, the values afterwards are obtained from the last optimization run of Dec 19.

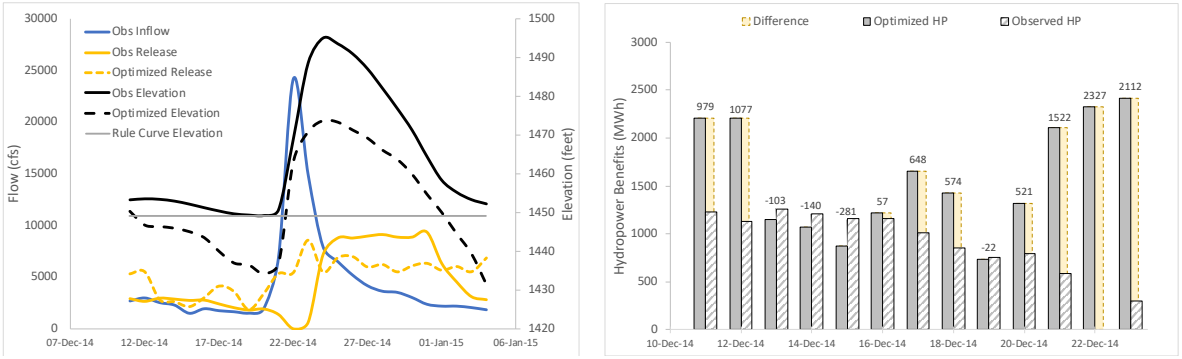

(a) (b)

Figure 2.8. (a) Optimized releases and elevations from the sequentially updated forecasts from Dec 11-19, along with the respective observed values, (b) Daily comparison of hydropower benefits (MWh) from optimized and observed operations (Detroit dam, OR). 'HP' stands for Hydropower; yellow bars and labels show the difference in benefits from the two set of operations.

As can be seen from Figure 2.8(a), the optimized operations result in a higher release as soon as the peak inflow is forecasted due to which the reservoir levels (black dashed curve) drop down within dam's safety limits, and then surges as the peak hits the reservoir. The elevation at the end of the optimization period, however, has a slightly higher deviation from the rule curve (compared to the observed value) as the sequential updates to forecasts have only been made till Dec 19. An o*ptimized hydropower benefit* of 20,720 MWh was obtained in comparison to the observed production of 11,450 MWh over Dec 11-23. Thus, an additional benefit of 9,270 MWh of hydropower could have been generated before and during the peak inflow event based on weather forecasts and optimization. The daily comparison of hydropower benefits from the optimized and observed operations is shown in Figure 2.8(b).

2.3.2 *Pensacola Dam – Single Event Assessment*

Similar to Detroit dam, we identified the dam's relevant pools, the operating constraints and turbine features, as depicted in Figure 2.9. The optimization constraints for Pensacola dam were obtained from USACE. For the maximum total release, the threshold of 30,000 cfs (849 m^3/s) was selected as a flood-safe value of streamflow at the downstream USGS gage of Neosho River (site ID - 07190500). Other constraints are summarized in Appendix A.

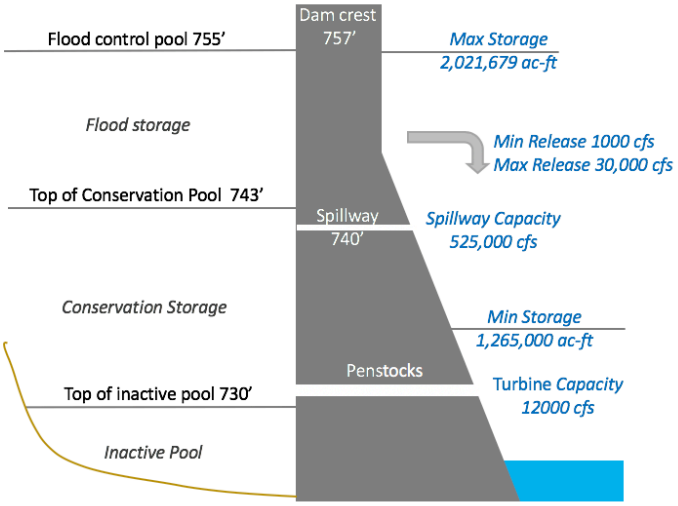

Figure 2.9. Cross-section of Pensacola dam (not to scale) showing relevant elevations (from mean sea level, MSL) and the selected constraint values obtained from USACE. (1 ft = 0.305 m, 1 cfs = 0.028 m^3/s, 1 ac-ft = 1233.48 m^3)

The inflow event of 22 Mar 2012 with a peak flow of 82,350 cfs (2332 m^3/s) was chosen for Pensacola dam. As the actual hydropower data (MWh) is not provided on USACE data portal, an estimate of turbine's operating hours and efficiency could not be obtained. Hence, a value, close to that for Detroit, of 20 hours was chosen for the constant in hydropower equation ($\epsilon \cdot \Delta t_{turb}$) (equation 2.1), as both the dams have similar installed hydropower capacities. The 16-day forecast inflow modeled for lead times of 3, 5 and 9-days is shown in Figure 2.10(a).

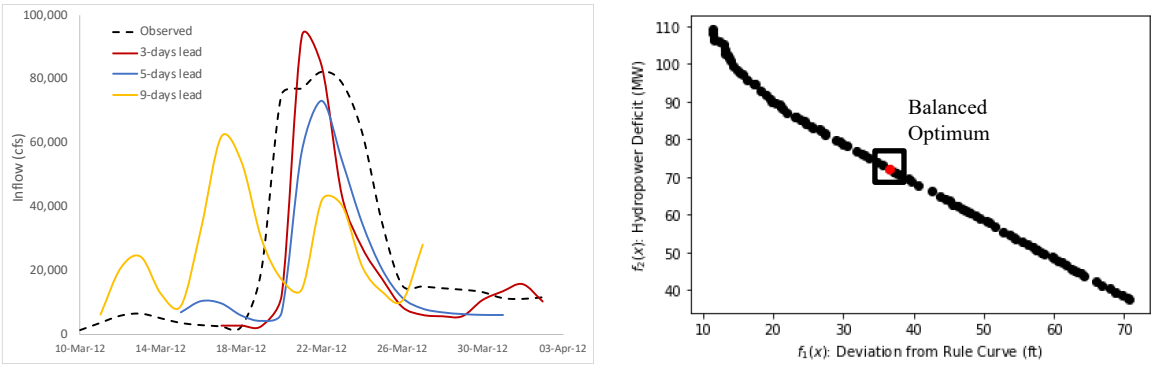

(a) (b)

Figure 2.10. (a) VIC-modeled 16-day forecast flow, forced with WRF-downscaled forecast fields, for lead times of 3, 5 and 9 days; (b) Pareto front and the selected balanced optimum obtained between the two objectives, Pensacola dam, OK.

The Pareto front with the non-dominated solutions and the chosen balanced optimum is shown in Figure 2.10(b). The optimization based on sequential updates to WRF forecasts for this dam revealed *optimized hydropower benefit* of 31,650 MWh from Mar 11-24, as compared to the *observed benefit* of 18,825 MWh. Again, an additional production of 12,825 MWh pre- and over the peak flow event was realized. The optimized releases and reservoir elevations are compared with the respective observed values in Figure 2.11(a) and the daily hydropower benefits plotted in Figure 2.11(b).

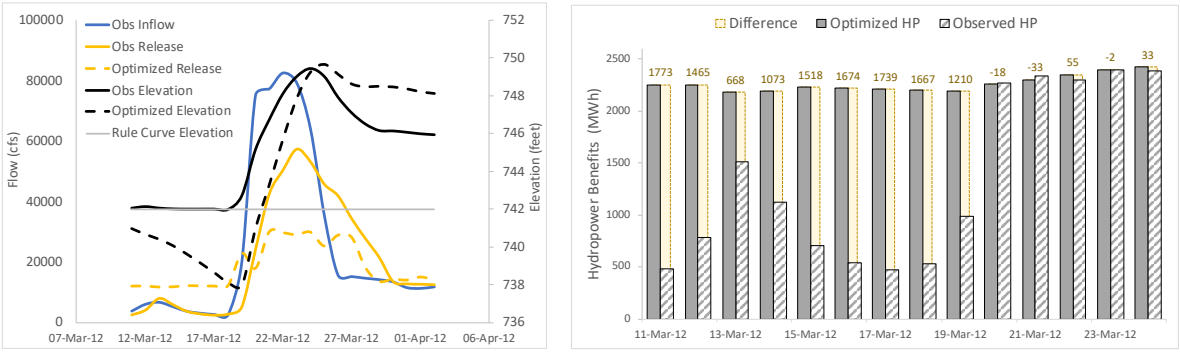

(a) (b)

Figure 2.11. (a) Optimized releases and elevations updating forecasts every alternate day from March 11-17, with the respective observed values; (b) Daily comparison of hydropower benefits (MWh) obtained using observed and optimized operations (Pensacola dam, OK).

'HP' stands for Hydropower; yellow bars and labels show the difference in benefits from the two set of operations.

2.3.3 *Long-term Assessment of Hydropower Benefits*

To put our concept to test in the practical world, the reservoir operations model for hydropower maximization using WRF-downscaled forecasts were automated through an online decision support system (see http://depts.washington.edu/saswe/damdss) for Detroit dam. The long-term results obtained from Dec 2017 to Sep 2018 (10 months), consist of both wet and dry seasons. A 16-day optimized operation schedule was derived using the WRF model's downscaled GFS forecasts. Using the actual inflow that occurred during the day and the respective optimized releases, final reservoir storage was computed by satisfying the storage-volume continuity (see Appendix A.3). The final storage of the first day served as the next day's beginning storage to obtain the next set of optimized releases using the updated forecasts. The model was run for all the ten months using such daily sequential updates. A similar update process was followed by (Alemu et al., 2011) at a weekly scale. The inflow forecasts generated over the selected 10-month period are compared with the observed values in Appendix A.2.

The hydropower benefits from the optimized operations are compared with the observed power generation data from USACE in Figure 2.12, plotted together with the respective inflow and release. The plots suggest that during the peak flow seasons, optimized policy results in higher release ahead of the event leading to higher energy generation. For low flows, the optimized release is constrained by the environmental flow limit of 1000 cfs, although the actual operations go below this limit on a few days. The total optimized hydroelectric energy (*optimized HP*) of 258,120 MWh was obtained over the 10-month period in comparison to the observed benefit (*observed HP*) of 244,490 MWh. Thus, an additional hydropower benefit of 13,630 MWh (optimized minus observed hydropower) was obtained

over the longer term that included both wet and dry seasons. The highest benefits in energy were obtained when a peak inflow occurs, as that is when the dam operator is most uncertain on the release to be made often leading to 'missed hydropower.' There are also episodes when the energy generation from observed operations exceeded the optimized ones (red bands in Figure 2.12) that occur during the low flow periods, generally after a peak inflow event. This is because, during peak inflow, dam operations hold the water back for preventing the flood downstream due to high uncertainty in future flows. Once the peak flow recedes, the dam operator is bound to release more water brought in by the peak flow event, which increases hydropower production, but also causes high spillway releases increasing downstream risk of flooding. The optimized operations, on the other hand, use the forecasts to release early the water already stored before peak arrives at the reservoir in a controlled manner without causing spillway. This generates a consistent amount of energy before and after the peak flood event. The other objectives (of flood control and dam safety) were also not compromised by keeping the reservoir below the safe release threshold of downstream flooding and satisfying the environmental flow constraints. Thus, in a longer period, the concept has potential in producing more energy benefits with reduced flood risk, overcoming the concerns of false alarms and false low flows, when operationalized in real-time operations over the existing infrastructure.

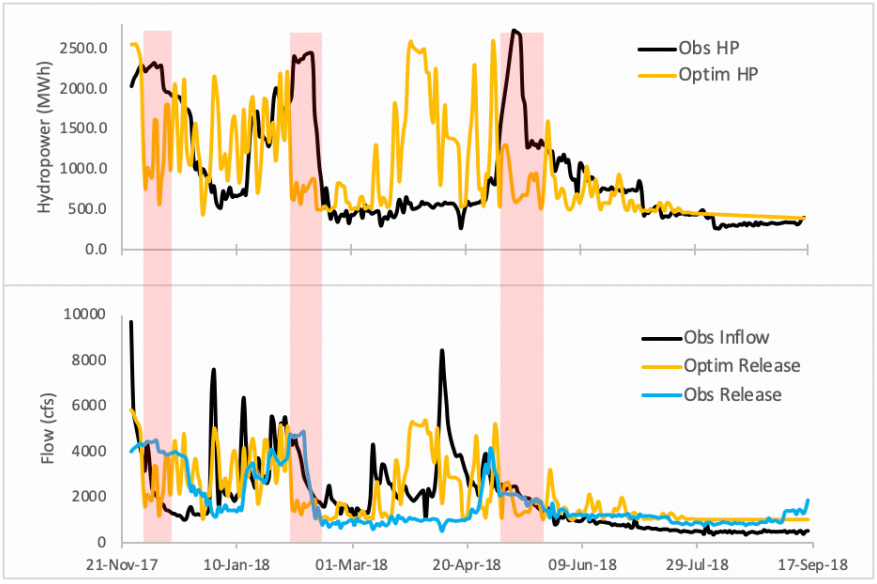

Figure 2.12. Optimized hydropower benefits obtained by sequentially updating forecasts every day for Detroit dam, compared with the observed benefits (top); optimized and observed release policy compared along with the observed inflow (bottom). Red bands highlight the days when optimized power was exceeded by the observed power generation.

2.4 Improvements in NWP-based Reservoir Inflow Forecasting

2.4.1 *NWP-based Probabilistic Inflow Forecasts*

To incorporate the uncertainty in forecasts, an ensemble of streamflow forecasts was obtained based on Global Ensemble Forecast System (GEFS) forcings. The 21-member ensemble forecast fields from GEFS were used to force the VIC hydrological model and obtain ensemble of inflow forecasts for 1-16 days. The peak flood event of Mar 2012 over Pensacola dam was chosen for demonstrating the value of available NWP ensemble fields in capturing the uncertainty in flow forecasts. The mean, minimum and maximum forecast flow from the 21-member GEFS ensembles for lead times of 3, 5, 7 and 9 days is shown in the Figure 2.13 for the peak flow event. A comparison of forecasting accuracy based on the average GEFS scenario against WRF-downscaled GFS is shown in Table 2.2, which suggests clear benefits of using probabilistic forecasts likes GEFS over the WRF simulation.

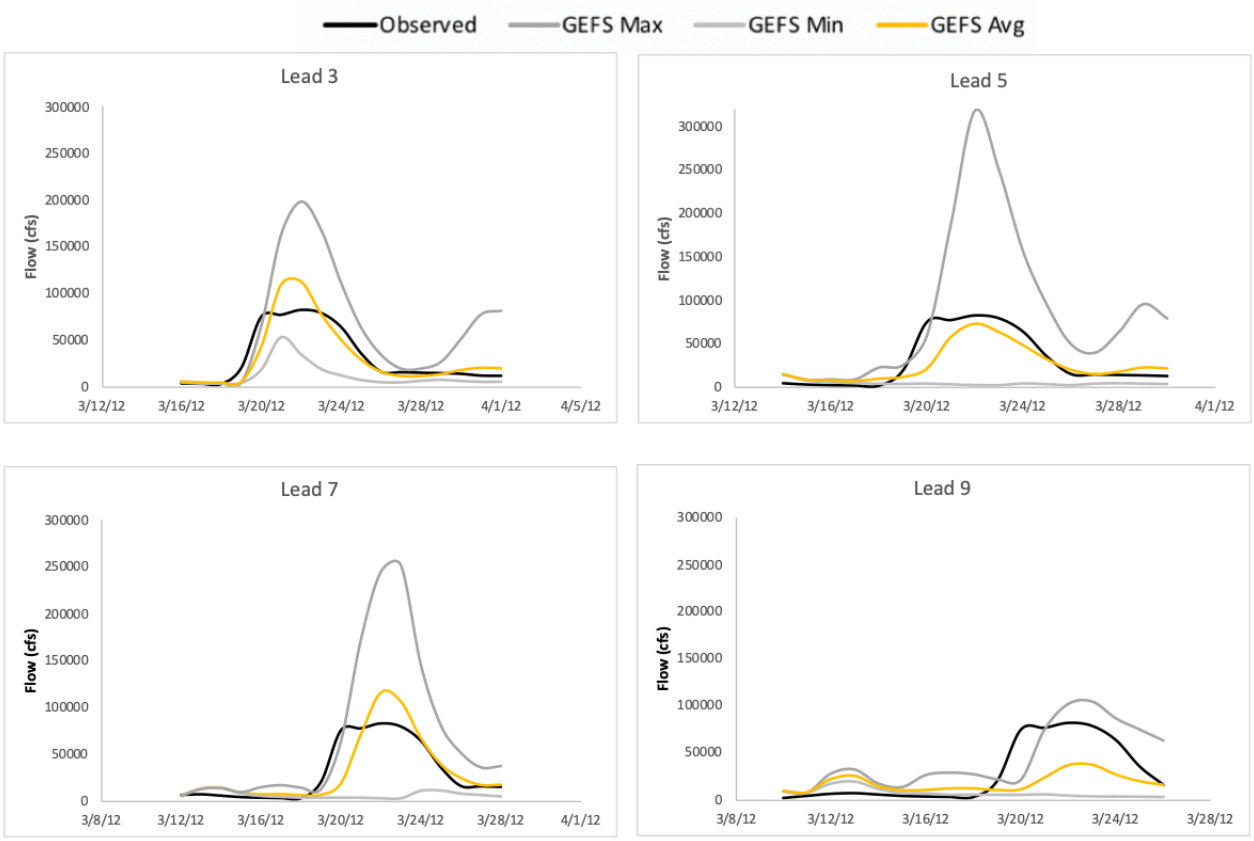

Figure 2.13. Ensemble forecast inflow corresponding to mean, minimum and maximum of the 21 ensemble members of GEFS forecast fields over Mar 2012 event for Pensacola dam.

Table 2.2. Comparison of the forecast flow performance from average GEFS scenario and WRF-downscaled GFS fields over Mar 2012 event for Pensacola dam.

	L3		L5		L9	
Metric	**WRF**	**GEFS**	**WRF**	**GEFS**	**WRF**	**GEFS**
Correlation	0.817	0.905	0.556	0.887	0.002	0.691
RMSE (cfs)	20827.0	14977.1	28407.2	15964.9	34934.1	28298.5
NRMSE	0.678	0.501	0.908	0.515	1.090	0.868

2.5 DISCUSSIONS

2.5.1 *Performance Assessment - Hydropower versus Flood Control Benefits*

In order for the proposed optimization strategy to be effective, the two competing objectives of hydropower and flood control need to be satisfied simultaneously. For the Pensacola dam, during the Mar 2012 peak event, the proposed optimization strategy was able to generate an additional 12,825 MWh of energy on top of the production from observed

operations. This amounts to a revenue of $1,251,720 using the average residential electricity rate of 9.76¢/kWh in Oklahoma City (Oklahoma City Electricity Rates, 2018). At an average electricity consumption of 900 kWh per month per US household, this additional energy can fulfill the demands of around 11,545 more households for one month. For the competing flood control objective, the performance was assessed from the reduction in the outflow peak over the event. For the selected event, a maximum observed release of 57,211 cfs (1620 m^3/s) was limited to just 30,000 cfs (849 m^3/s) (~47.5% reduction) as a safe threshold to prevent flooding downstream.

For Detroit dam's single event assessment, the proposed optimized operations were able to generate an additional 9,270 MWh of hydropower (on top of the observed value). Again, this energy equivalent to revenue of $908,460 at a rate of 9.8¢/kWh in Oregon (Oregon Electricity Rates, 2018) that can power up to 8,345 US households for a month. For the long-term assessment over ten months (with inflows lower than the considered individual peak events), the additional energy amounted to 13,630 MWh (5.6% increase over the observed energy) and the optimization strategy was most effective during the high inflow periods. The reservoir release was kept under the flood-safe limit of 9000 cfs (255 m^3/s) for the downstream control station. Thus, the proposed optimization strategy not only generates more hydroelectric power but also addresses the other key objective of reducing the flood risk.

The two dams for the case study assessments were chosen in different hydrological regimes with varying characteristics. As the Detroit dam lies in with steep terrain with small sized basin and fast hydrological response, the rainfall quickly gets converted into runoff with a lesser time of concentration. However, Pensacola dam possesses a flatter terrain with longer rivers resulting in higher time of concentration. Thus, the successful assessment over both the dams, over individual high inflow events as well as operationally over longer term, illustrates the robustness of the concept.

2.5.2 *Scalability of Hydropower Maximization*

While the dams selected for study have different hydrologic regimes, catchment characteristics and reservoir inflows, the variation is certainly much higher across the dams over U.S. and the globe. This variation cannot be captured by the analysis presented in this study. Also, this study was limited in terms of the computational resources to simulate WRF model (for downscaling GFS forcings and generating inflow forecasts) for a year-long period over the Pensacola Dam. This will be considered in the next chapter by using computationally efficient ANN to forecast inflows and optimize reservoir operations. The practitioners are encouraged to study and extend the framework of optimization to improve the hydropower generation scenario using weather forecast information over other dams suitable for such kind of exploration. These include the dams that are (a) powered, (b) have small to medium reservoir storage capacity, and (c) upstream in the dam network receiving unregulated flow. An analysis over the U.S. dams revealed 525 dams satisfying these criteria, amounting to 23% of the 2248 powered dams (NHAAP Existing Hydropower Assets, 2017). These dams are shown in Figure 2.14 and are the sites for further exploration of their suitability for the concept. We believe that the concept, if extended to a good fraction of such dams, has the potential to bring the nation closer to an energy infrastructure independent of the fossil fuels and other non-renewable sources.

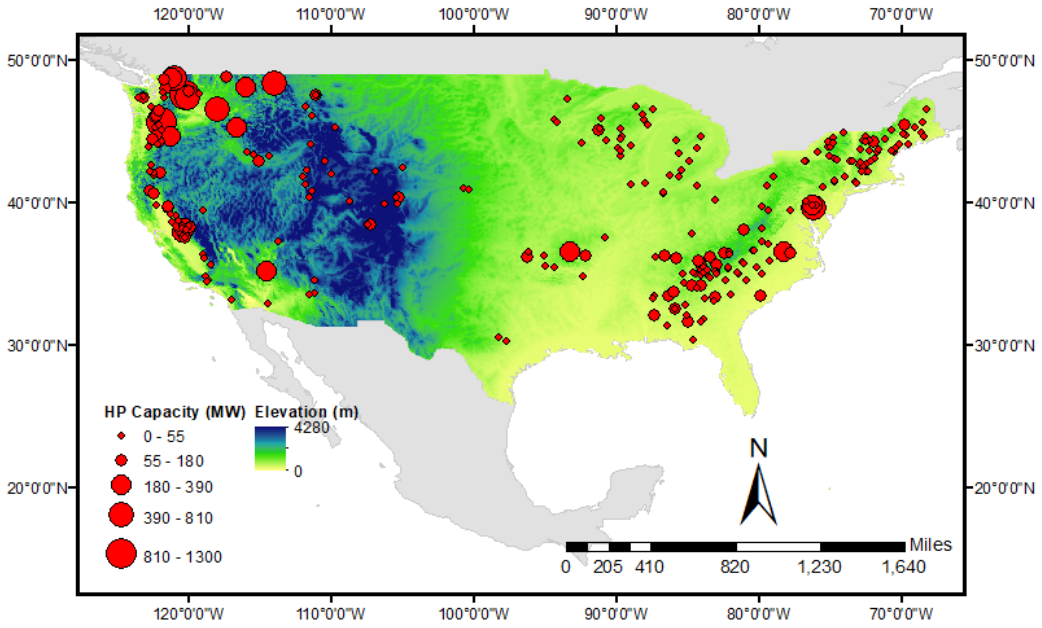

Figure 2.14. Locations of upstream dams receiving unregulated inflow to be explored of their suitability for weather forecast use in optimizing reservoir operations.

2.6 CONCLUSIONS

The purpose of this study was to evaluate the potential of short-term weather forecasts to extract more hydroelectric energy, without compromising other competing objectives. The NWP model-based weather forecasts, their dynamic downscaling, hydrologic modeling, and the optimization algorithm were coupled with reservoir operations model to obtain the optimized release policy for maximizing energy production. The concept was demonstrated over Detroit and Pensacola dams with varying hydrological characteristics receiving unregulated inflow. Performance assessment over two-year return period storm events produced benefits of 12,825 and 9,270 MWh for Pensacola and Detroit dams, respectively, while optimization over a longer ten-month period (of wet and dry seasons) for Detroit dam raised the total energy production by 5.6% over the observed scenario. The optimization not only benefitted the hydropower, but also helped satisfy the goals of flood control and dam safety. The Pareto optimality allows the operator to choose an appropriate optimal solution

depending on the prevailing circumstances in operating the reservoir. It should be noted that, at least for the type of dams demonstrated here, the forecasts help the most during the peak flow (wet) period when uncertainty in the reservoir inflow is high causing over-conservative operations. Nevertheless, the long-term benefits of maximizing the hydropower every day, even in small amounts, is a low-hanging fruit that should not be overlooked, rather be explored to its depth to realize a more sustainable framework for reducing the dependence on fossil-fuel based energy generation.

The 21-member ensemble GEFS forecast fields forced VIC model to generate probabilistic reservoir inflow forecasts over a peak inflow event for Pensacola dam. The average GEFS scenario performed better than the WRF downscaled forecasts. The improved inflow forecasts with the uncertainty estimates (from probabilistic forecasts) can benefit the optimization model and arrive at optimal decisions different confidence levels.

Combining optimization and simulation models for managing water resources in a real-world setting has not been fully realized yet (Sechi and Sulis, 2009). By using real data on real dams with real-world constraints, we have demonstrated very clearly that the currently available weather forecasts from NWP models have a lot to offer to address energy security. This will allow the dam operators to make decisions based on an improved advisory in real-time to achieve more efficient hydropower generation (more power with same or less impounded water) and reduce our impact on the natural world.

The next challenge is to make the publicly available NWP forecasts more accessible to dam operators and decision makers in nations with limited in-situ data and computational resources. This is addressed in the next chapter (Chapter 3) using a data-driven technique that is computationally efficient, transferrable, and skillful in forecasting reservoir inflow.

Chapter 3. DATA-DRIVEN TECHNIQUE FOR FORECASTING RESERVOIR INFLOW: APPLICATION FOR HYDROPOWER MAXIMIZATION

Note: This chapter has been published mostly in its current form in the journal, Environmental Modelling & Software (Ahmad and Hossain, 2019a). Used with permission from Elsevier.

Ahmad S.K., Hossain, F., 2019a. A Globally Scalable Data-driven Technique for Forecasting of Reservoir Inflow for Hydropower Maximization. Environ. Model. Softw., 119, pp.147-165. doi:10.1016/j.envsoft.2019.06.008.

ABSTRACT

A generic and scalable scheme is proposed for forecasting reservoir inflow to optimize reservoir operations for hydropower maximization. Short-term weather forecasts and antecedent hydrological variables were inputs to a three-layered hydrologically relevant Artificial Neural Network (ANN) to forecast inflow for 7-days of lead time. Application of the scheme was demonstrated over 23 dams in U.S. with varying hydrological characteristics and climate regimes. Probabilistic forecast was also explored by feeding ANN with ensembles of weather forecast fields. Results suggest forecasting skill improves with decreasing coefficient of variation in inflow and increasing drainage area. For forecasts at 7-day lead time, Nash-Sutcliffe Efficiency was higher than 0.5 for 48% of the sites. Forecast-informed operations were simulated using a rolling horizon scheme and assessed against benchmark control rules that ignore forecasts. Over two years of assessment for Pensacola dam (Oklahoma), additional 5.2% of energy could have been harvested without compromising flood risk relative to the benchmark. A web-based decision support system, operational over Detroit dam (Oregon), was presented to promote engagement of dam operators and leverage the advances in weather

forecasting and hydrological modeling toward operational decision-making. This study reinforces the potential of a numerically efficient and skillful reservoir inflow forecasting scheme to address water-energy security challenges and bridge the gap between research and application domains.

3.1 INTRODUCTION

In the previous chapter, a proof-of-concept was presented to demonstrate the value in weather-scale forecasts from NWP models in improving hydropower generation. This chapter will address the resource feasibility aspect of this concept. By proposing a novel data-driven technique of forecasting reservoir inflow, the chapter aims at improving the accessibility of these NWP forecasts to dam operators and decision makers.

Most of the world's artificial reservoirs are operated at daily or longer time scales based on rule curves that were designed using a climatology of historical flow observations and pre-dam storage volumes (Lee at al., 2009; Ficchi et al., 2015; Yazicigil et al., 1983). Rule curves outline the reservoir storage targets that need to be met at specific times of the year. Operating strictly based on these climatology-based rules can lead to mishandling of an unexpected peak reservoir inflow event (Miao et al. 2016). For instance, in a relatively dry flood season, lowering the pool to rule curve level can result in significant loss in hydropower generation, which could be avoided if weather forecasts were made ahead of time.

For efficient operations of a single/multipurpose reservoir system, the information about forecast inflow into the system is an important part of the real-time decision-making process. Short-term daily to weekly scale forecasts are indispensable in maximizing societally important benefits of flood control and hydropower generation (Yazicigil et al., 1983; Anghileri et al., 2016). Flood mitigation requires sufficient flood storage before an impending flood, while hydropower generation requires maximizing the economic value of water by

releasing most of it through turbines and keeping reservoir at maximum pool. Reservoir inflow forecasts, if reasonably skillful, can help achieve a balance where hydropower can be maximized without compromising flood risk downstream (Jordan et al., 2012; Madsen et al., 2009; Qi et al., 2017). Often, this is achieved by proactive storage or release from reservoir in anticipation of reservoir inflow. Recently, a study on two dams in US showed application of Numerical Weather Prediction model (NWP)-based reservoir inflow forecasts for optimizing the reservoir operations (Ahmad et al., 2018). Significant hydropower benefits were demonstrated without compromising the flood control objective. Ongoing projects such as Integrated Forecast and Reservoir Management (INFORM) (Georgakakos et al., 2007) and Forecast Informed Reservoir Operations (FIRO Overview, 2017), focused over specific watersheds, are also utilizing short-term weather forecasts for operating the reservoirs.

The NWP models from various meteorological agencies produce weather-scale forecast fields of temperatures, wind, precipitation, soil moisture in three dimensions over the entire globe. These publicly available forecasts represent an underutilized resource for the hydropower community, due to concern over fossil-fuel based environmental degradation (Dudhani et al., 2006; Li, 2005). Moreover, efficient management of hydropower facilities is essential for emerging economies where demand for energy often exceeds supply or generation capacity (Asif and Muneer, 2007). As more hydropower dams are constructed, especially in developing nations, achieving the highest possible operational efficiency using available weather forecasts can address the growing resource needs of today. The challenge today is to convert the global and public availability of weather forecasts to locally actionable data as reservoir inflow forecast, and thus mainstream their use in the operational world.

However, there are logistic hurdles to globalizing hydropower maximization techniques based on NWP-based reservoir inflow forecasts. Even if the forecasts achieve certain level of accuracy, adequate computational resources are required to capture sudden peak flow events

considerably faster than real-time. This is because at a global scale, the NWP models lack sufficient detail to force hydrological models over the reservoir catchments where precipitation can often exhibit higher spatial variability (Flint and Flint, 2012; Do Hoai et al., 2011). Dynamic downscaling techniques have subsequently emerged in recent past that are known to be locally constrained rendition of weather forecasts at hydrologically relevant scale (Wilby and Wigley, 1997). However, dynamic downscaling is computationally intensive and not feasible for computationally constrained settings of most operational reservoir management agencies around the world. For example, a study on flood forecasting in Houston, TX found that it takes nearly 7 to 20 hours for dynamically downscaling of NWP forecasts for 24-hr lead-time depending on the configuration of CPU available in the current market (Sikder et al., 2019).

In summary, there are two important hurdles for operationalization of reservoir inflow forecasts in real-time reservoir optimization models around the world. These are: 1) uncertainty in inflow forecast (Zhao et al., 2011; Georgakakos et al., 2008; Faber and Stedinger, 2001), and 2) computational burden of deriving these reservoir inflow forecasts (Cheng et al., 2014).

For large-scale applications of NWP forecast fields in optimizing reservoir operations for hydropower maximization, an alternate and scalable numerical scheme is required. Such a scheme should have the following desired properties: 1) it has to be numerically efficient and considerably faster than real-time for practical operations; 2) it has to allow rapid multi-year historical assessment to understand risks of false positives and negatives in operations; 3) it has to be effective in limited in-situ hydrologic data settings for application in developing countries; and 4) it has to be skillful and yield physically realistic forecasts for streamflow over the forecast horizon.

Our selected scheme that we present here with such desired features is the data-based technique of Artificial Neural Networks (ANN) tailored for reservoir inflow forecasting. The

ANN technique, over the last two decades, has proven to be an efficient supplement to modeling qualitative and quantitative water resource variables and capturing the nonlinearity in flow (Maier et al., 2010; Jain et al., 2009; Maier and Dandy, 1996; Hutton and Kapelan, 2015; Wei, 2016; Govindaraju and Rao, 2000; Wu et al. 2014). As noted by ASCE Task Committee on Application of ANNs in Hydrology (2000), ANNs are robust tools for many of the complex hydrological modeling problems. The review of relevant research on ANNs by Maier et al. (2010) suggest that a vast majority of studies have focused on flow prediction. Daily short-term flow forecasting using ANN has been explored, amongst others, by Birikundavyi et al. (2002), Kişi (2005), Wu et al. (2009), Coulibaly et al. (2000) and Zemzami et al. (2016). As required in all modelling efforts, following good practice that increases the credibility and impact of modelling results (Jakeman et al., 2006; Welsh, 2008), is particularly important for ANN models that are developed using available data and not explicitly based on underlying physical processes. For the input nodes, past conditions of streamflow and hydro-meteorological variables are commonly used in predicting future flow. Studies also used other predictor combinations such as flow length and travel time (Akhtar et al., 2009), previous day's rainfall and temperature (Lorrai and Sechi, 1995), flow, rainfall and evapotranspiration (Anctil et al., 2004), soil moisture deficits and runoff (Cheng and Noguchi, 1996). Bartoletti et al. (2018) eliminated the redundancy in antecedent rainfall using the data-driven Principal Component Analysis technique. However, to the best of our knowledge, there is no work on the use of freely available global NWP weather forecasts as ANN inputs.

Several studies using only the antecedent conditions have indicated the inability of ANN to capture the flow peaks (e.g., Campolo et al., 1999; Sudheer et al., 2003; Wu et al., 2009; De Vos and Reintjes, 2005). To provide an accurate estimate of peaks, it is necessary to remove the local variations caused by extreme flows from the time series function being mapped. Streamflow transformation is used to simplify the data structure following a

convenient statistical model (Sudheer et al., 2003). As found by Zemzami et al. (2016), separation of streamflow into baseflow and runoff components improved the peak flow estimation and hence, it was incorporated in the present research. The runoff component was transformed by a moving average procedure to improve the peak flow prediction. Further, studies on ANN-based reservoir inflow prediction have primarily focused over only a specific reservoir system. In an effort to demonstrate global scalability, application of any proposed inflow forecasting scheme extending over multiple dams with varying hydro-climatic and geographic characteristics is necessary.

Further, the awareness and expertise required to set up the framework for forecast-informed dam operations is mostly limited to scientific community and does not extend to the application world and real-life decision-making. Also, multiple uncertainties exist in the optimal decision-making process presenting risks to the end-user decisions (Zhu et al., 2017). This limits the advancements in atmospheric modeling to benefit the water managers until creative and user-friendly solutions are devised to improve engagement and help managers understand the practical value of advancements. To empower and actively engage the dam operators, a dam user-driven decision support system (DSS) is needed that not only visualizes the weather forecast data, but one that forecasts the reservoir inflow, optimizes the release decisions and allows enough operator-driven flexibility to tweak constraints, and then predicts the optimized release and storage decisions.

The innovative aspects of this study include development of ANN model based on the coarser scale forecast fields of 1-7 days lead from NWP weather models to predict basin-scale hydrology (Ahmad and Hossain, 2019a). The technique was tested over an inventory of 23 dams with widely varying hydrological characteristics and local climate regimes. A comprehensive validation framework was employed to assess the skillful and physical realism of the modeled forecasts. The probabilistic nature of inflow forecasts was addressed by

obtaining an ensemble of forecast flow derived from ensemble of weather forecast. The forecasts were further incorporated in a reservoir optimization model for maximizing the daily hydropower generation while meeting other dam management constraints and regulations. The specific research questions of this study are: (1) *Can the use of ANN with pertinent hydrologic knowledge be computationally efficient, skillful and globally scalable in forecasting the reservoir inflow over short term forecast horizon (1-7 days)?* (2) *What role does the hydrological characteristics of the upstream basin and local climate zone play in driving the forecast skill of the designed ANN model?* (3) *Can such fast inflow forecasts be used to optimize the reservoir operations to improve energy generation without compromising flood or dam safety?*

In order to empower the stakeholder agencies with advancements in atmospheric science, modeling, and optimization techniques, we also developed an open-source DSS that knits together the complex models and simulations running in the backend, with a frontend visualizer that is user-friendly and easy to follow (Ahmad and Hossain, 2019b). This DSS is also designed to provide a continuous assessment of the modeled results that helps the decision-maker gauge the performance against the reference (observed) variables in the retrospective mode. The end goal was to help the dam operator realize 'smarter' dam operations by the forecast-informed advisory, so that the release decisions are optimal in satisfying different downstream stakeholder needs.

The rest of this study is organized as follows. In the next section we discuss the selection of dam sites for application of the proposed technique, followed by a description of datasets used. This is then followed by a detailed methodology and different components involved in Section 3.3. The case study results of ANN-based forecasts over the database of dams and its application for optimization of reservoir operations are presented in Section 3.4, followed by a description of DSS in Section 3.5 and discussion and concluding remarks in Section 3.6.

3.2 Study Sites and Hydrometeorological Data

In order to address the first two research questions, 23 dams located in various climate zones of the contiguous U.S. (CONUS) were selected. All selected dams receive unregulated flow and are operated for a variety of purposes such as flood control, hydropower generation, water supply, irrigation and recreation. Fifteen of these dams are powered. The dam inventory also represents a wide range of upstream catchment area, topography, hydrological characteristics, flow patterns, reservoir storage and installed hydropower capacity. The dams are shown in Figure 3.1 by location and size of upstream drainage area. Apart from the study sites within US, six dam sites in large river basins of Ganges, Brahmaputra and Mekong were identified. Table 3.1 presents the information about the selected study sites with descriptive statistics of the original flow data over 2007-2014.

Data for this study over the CONUS are as follows: (a) deterministic and ensemble forecast hydro-meteorological forcing fields, (b) basin's antecedent conditions, and (c) current reservoir state. The deterministic forecast fields of precipitation, temperature and windspeed were acquired from the Global Forecast System (GFS) global-scale Numerical Weather Prediction model at 0.5˚ resolution for 1-7 days lead-time with a 3-hourly temporal resolution. The archived data is available from Oct 2006, due to which the period of analysis in this study was set to 2007-2017 and all the other datasets were gathered over this period. For the ensemble forecast fields, NOAA's Global Ensemble Forecasting System Reforecast (version 2) dataset (GEFS/R) (Hamill et al., 2013) with 11-member ensemble of forecasts at 1˚ resolution was used. The antecedent precipitation over the basin was obtained from the Climate Hazards Group InfraRed Precipitation with Station data (CHIRPS) gridded rainfall time series at 0.05˚ resolution (Funk et al., 2015), antecedent temperature and windspeed from in-situ Global Surface Summary of the Day (GSOD) data (Global Surface Summary of the Day, 2018) and antecedent soil moisture from Global Land Data Assimilation Systems (GLDAS). All the

gridded datasets were processed to calculate the basin-averaged values to be used as inputs to ANN. The antecedent observed reservoir inflow for US dams was obtained from the dam operating agencies of US Army Corps of Engineers (USACE) and US Bureau of Reclamation (USBR). State of current reservoir storage and headwater level was acquired from the respective agencies' data portals. The climate zones for each dam were extracted from Köppen-Geiger climate classification (Peel at al., 2007). For the real-time forecasting and reservoir operation purpose, a forecast horizon of 1–7 days ahead was chosen.

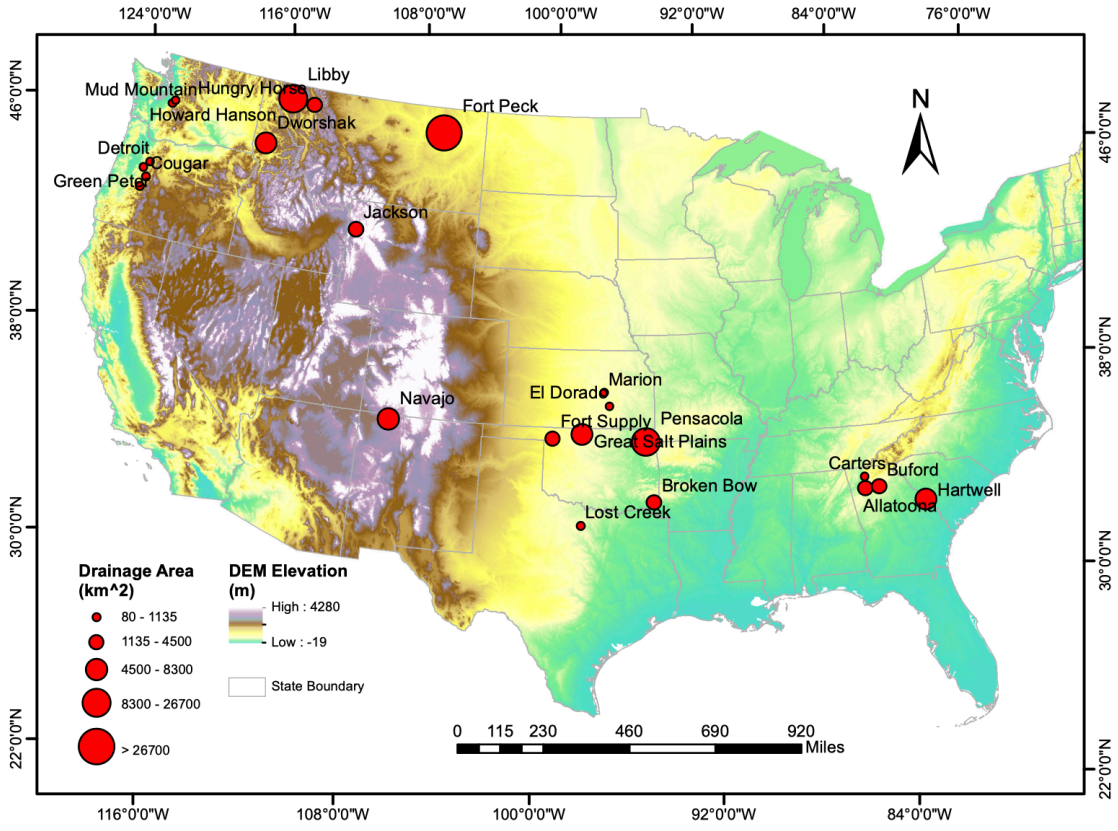

Figure 3.1 Selected inventory of 23 dams, receiving mostly unregulated flow, for application of ANN-based inflow forecasting. The markers are sized by the area of upstream drainage basin.

Table 3.1 Selected study dams (in CONUS) and stations (on river basins in Asia) for application of ANN based flow forecasting technique with descriptive statistics of the basin/flow. 'MRB' refers to Mekong River Basin.

#	Dam/Station Name	Mean Flow (cfs)	Std. Dev of Flow (cfs)	COV	Drainage Area (km^2)	Reservoir Storage (km^3)	Koppen Climate Class	State/ Basin
1	*Allatoona*	1447.33	2214.58	1.53	2893	0.83	humid subtrp	GA
2	*Broken Bow*	1375.51	3597.79	2.62	1995	1.98	humid subtrp	OK
3	*Buford*	1714.45	2238.86	1.31	2694	3.15	humid subtrp.	GA
4	*Carters*	562.86	649.33	1.15	966	0.58	humid subtrp	GA
5	*Cougar*	933.91	850.65	0.91	544	0.27	mediterranean	OR
6	*Detroit*	2207.62	2052.71	0.93	1134	0.56	mediterranean	OR
7	*Dworshak*	5731.71	6543.91	1.14	6320	4.39	cold dry	ID
8	*Eldorado*	191.45	757.38	3.96	606	0.30	cold humid	KS
9	*Fort Peck*	10282.50	9562.12	0.93	149508	23.56	semi-arid	MT
10	*Fort Supply*	43.11	103.68	2.41	4978	0.12	humid subtrp.	OK
11	*Great Salt*	413.68	1142.63	2.76	717	1.22	humid subtrp.	OK
12	*Green Peter*	1572.91	2122.20	1.35	8288	0.53	mediterranean	OR
13	*Hartwell*	3150.38	3601.98	1.14	5408	4.24	humid subtrp.	GA
14	*Hills Creek*	1198.80	1134.96	0.95	1008	0.44	mediterranean	OR
15	*Howard*	1070.65	1297.74	1.21	572	0.17	cold humid	WA
16	*Hungry Horse*	3949.58	5624.46	1.42	4248	3.68	cold humid	MT
17	*Jackson*	1478.85	2072.66	1.40	2134	1.08	cold humid	WY
18	*Libby*	12252.60	15028.93	1.23	23403	7.43	cold humid	MT
19	*Lost Creek*	1861.67	1034.76	0.56	88	0.03	humid subtrp.	TX
20	*Marion*	93.28	389.11	4.17	518	0.23	cold humid	KS
21	*Mud Mountain*	1653.07	1289.34	0.78	1036	0.13	temperate	WA
22	*Navajo*	1017.90	1112.65	1.09	8262	1.28	cold humid	NM
23	*Pensacola*	8669.14	15613.03	1.80	26672	2.71	humid subtrp.	OK
Large Basin Stations:								
1	*Hardinge Bridge*	9739.14	12406.50	1.27	985259	-	humid subtrp.	Ganges
2	*Bahadurabad*	17787.32	16055.54	0.90	525349	-	tropical/ humid subtrp.	Brahm-aputra
3	*Vientiane*	3951.18	3350.90	0.85	90469	-	tropical	MRB
4	*Pakse*	9670.50	9399.63	0.97	349928	-	tropical	MRB
5	*Stung Treng*	13663.62	13061.23	0.96	445074	-	tropical	MRB
6	*Kampong. Cham*	14882.85	15374.09	1.03	470737	-	tropical	MRB

3.3 METHODOLOGY

The experimental approach followed in the study is shown in Figure 3.2 and described in the following sections.

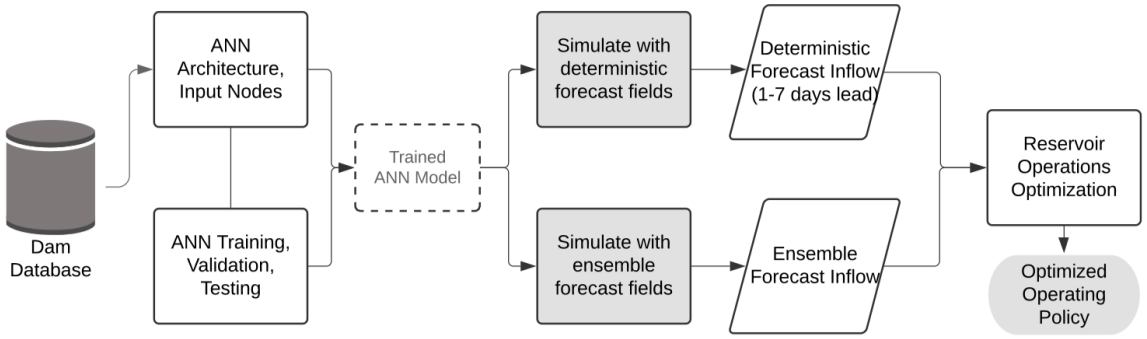

Figure 3.2 Experimental approach showing development and testing of ANN architecture, and its integration with the reservoir operations optimization to achieve hydropower maximization.

3.3.1 *Proposed ANN Architecture*

The ANN architecture used here is the multilayer feedforward neural network. This is one of the most popular architecture used for streamflow forecasting (Wu et al., 2009). It involves input, hidden and output layers where the hidden layer allows the network to perform complex nonlinear mapping between the input and output variables (Coulibaly et al., 2000; Funuhashi et al., 1989). A three-layered ANN with one hidden layer was implemented. Many experiments in the past have confirmed this to be adequate for most forecasting problems (Lippmann, 1987; Zhang et al., 1998; Coulibaly et al., 2000). The network's ability to learn from training data and generalize depends on the number of nodes in input and hidden layers.

The sum of the weighted nodes of a layer form input to a transfer function that determines the output of that node. Nonlinear functions allow the network to learn nonlinear relationships between input and output vectors. The S-shaped log sigmoidal function was employed that acts as a squashing function bounding the output between zero and one and is the most commonly used for hidden layer nodes (Zealand et al., 1999). The output y_j from the j^{th} neuron of the layer is:

$$y_j = \frac{1}{1+e^{-\left(\Sigma w_{ji} x_i\right)}} \quad (3.1)$$

where, w_{ji} = weight of the connection joining the j^{th} neuron in a layer with i^{th}neuron in the previous layer, and x_i= value of the i^{th}neuron in the previous layer. The linear function, as recommended for the nonlinear regression problems, was used for the output node activation.

3.3.2 *ANN input predictors*

Selection of input nodes for developing an ANN model is a difficult task that needs attention and a good understanding of the underlying physical processes. Relying solely on the model to identify critical inputs from a large subset can lead to misconvergence, poor accuracy and curse of dimensionality (Bowden et al., 2005). Sudheer et al. (2002) proposed a better alternative to the popular trial-and-error approach, utilizing the statistical properties (cross-, auto- and partial autocorrelation) of the observed data series for identifying appropriate input vector to the network.

The candidates for the input layer nodes for the proposed ANN scheme were: (1) NWP forecasts of precipitation, temperature and windspeed, obtained from the GFS model, produced at 0.5˚ resolution; (2) antecedent precipitation over the basin, (3) antecedent streamflow into the reservoir; and (4) antecedent baseflow. The gridded hydrometeorological inputs were obtained as daily basin-averaged values over the dam's upstream catchment area. The flow series can be viewed as the sum of baseflow and runoff signals, which when selected adequately as ANN inputs can improve model performance (Zemzami et al., 2016). The baseflow was separated from the daily observed reservoir inflow using the Recursive Digital Filter (RDF). RDF has been shown to perform better than other filtering techniques (Corzo et al., 2007; Zemzami et al., 2016). The general form of the filter is:

$$b_k = \frac{[(1-BFI_{max})\cdot a\cdot b_{k-1}+(1-a)\cdot BFI_{max}\cdot y_k]}{1-a\cdot BFI_{max}} \quad (3.2)$$

$$r_k = y_k - b_k \quad (3.3)$$

where, y_k is the total streamflow, b_k is the separated baseflow and r_k is runoff component at time k. It involves two filter parameters that need prior calibration: a, the recession constant and BFI_{max}, the maximum value of the baseflow index that can be modelled by the algorithm (Eckhardt et al., 2004). The initial baseflow, b_0 is also an unknown (assumed zero in this study for simplicity).

The runoff signal exhibits high local variations due to varying skewness in the data series especially for the smaller drainage areas. This can lead to underestimation of peak flow. An appropriate data transformation is needed to reduce these variations and improve the performance (Sudheer et al., 2003). The moving average method was used here that is also found to improve the time lag in modeled peaks flows (De Vos and Reintjes, 2005). The moving average smoothens flow time series by replacing each data point with the average of previous K data points, K being the length of the memory window, with same weight applied to each data point. Instead of the antecedent runoff time series, the moving average over total streamflow was applied to obtain the input node. Once the candidate predictors were identified, the statistical properties of cross- and partial autocorrelation between the predictors and the streamflow were used for finding the optimal number of antecedent days for each variable. The number of hidden layers in the architecture and the baseflow parameters were selected using a trial-and-error procedure. With this configuration, a sensitivity analysis was performed where ANN was trained with different combinations of antecedent/forecast predictors to select the best combination of input predictors for the study sites. This procedure for input predictor selection is schematically shown in Figure 3.3.

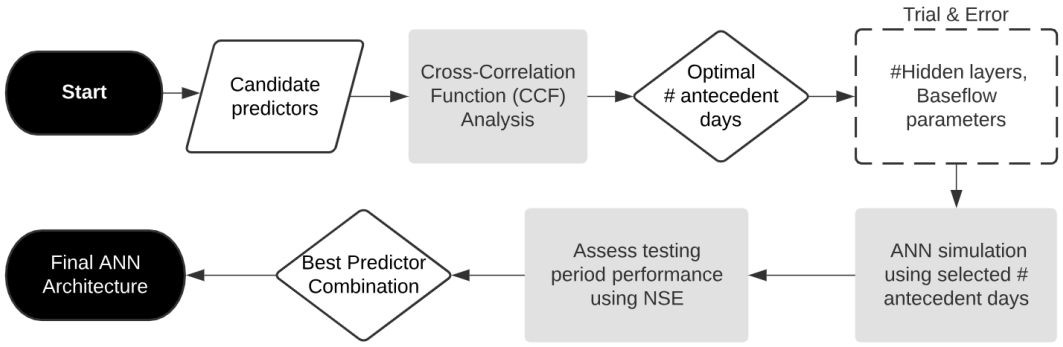

Figure 3.3 A schematic of different steps involved in building the ANN architecture and input predictor combination.

3.3.3 *ANN training algorithm*

The training of an ANN, or determining the weights of the ANN nodes, was performed using a learning algorithm to minimize an error function by providing input-output examples (training data). As found by several studies, the Levenberg-Marquardt (LM) training method is the most effective method for feed-forward neural networks with respect to the training precision (Liu, 2010; Kişi, 2007; Sun et al., 2016; Anctil et al., 2004). The algorithm blends the stability of steepest descent method and the speed advantage of Gauss–Newton algorithm providing a robust way to find the optimal weights, without having to compute the Hessian matrix (More 1978). The MATLAB implementation of LM training in the Neural Network Toolbox was used here (The Mathworks Inc., Natick, Massachusetts).

The most critical issue in training a multi-layer ANN is its ability to generalize the modeled outputs. While an overly complex ANN structure can potentially fit the noise in the training data leading to the overfitting, an insufficient level of complexity can result in lack of generalization ability that fails to detect regularities in the data set, which is also known as underfitting (Coulibaly et al., 2000). To avoid these issues, the early stopped training approach (STA) is incorporated within the LM training. The STA involves dividing the entire data into

three subsets – (i) a *training set,* which is used to compute the gradient and update the weights and biases of the network, (ii) *validation set* over which the errors are monitored during the training process and is used to decided when to stop training, (iii) *test set,* which is not used in the training process but is used to assess the expected performance in the future. During the initial phase of training, the training and validation set errors decrease. However, when the network begins to overfit the data, the error on the validation set typically begins to rise. When the validation error increases for a specified number of iterations, the training is stopped, and the weights and biases at the minimum of the validation error are returned. This threshold number of iterations is chosen to be six in this study. As recommended by Maier and Dandy (2000), this threshold avoids any utilization of validation/test set data during the training process, either to optimize the network inputs and parameters or to decide when to stop training.

Another method to improve the generalization, called regularization was used that modifies the performance function for training. The procedure adds a term to the performance function consisting of the mean of the sum of squares of the network weights and biases. This causes the network to have smaller weights and biases and forces the network response to be smoother and less likely to overfit. The performance ratio of 0.5, which gives equal weight to the mean square errors and the mean square weights was chosen.

The daily inflow forecast over 7-day horizon was obtained using an iterative multi-step forecasting method. The ANN modeled flows at the first lead-time are used as the antecedent flow conditions for the next step's model input, including all other past information. With each subsequent lead-time, ANN's own outputs are used iteratively to model the 7-day ahead forecasts. The metrics used for assessing the ANN performance include Nash Sutcliffe Efficiency (NSE), Root Mean Square Error (RMSE), Correlation (R^2) and Mean Absolute Error (MAE).

3.3.4 *Forecast performance assessment*

To ensure that the trained ANN model does not contain known or detectable flaws and can be used with confidence over any unseen data, a comprehensive assessment was performed using different facets of the modeled ANN flow. Specifically, three aspects of the model validity are considered here, namely (a) *replicative validity*: how well the ANN model can capture the general underlying relationship in the calibration data (b) *predictive validity*: the ability of the model to generalize or learn the specific patterns in the calibration data, (c) *structural validity*: plausibility of the model when compared with a priori knowledge (Humphrey et al., 2017). For, the replicative validity, the model fit is evaluated, and residuals are analyzed for violation of error model assumptions using graphical plots of predictions and residuals. The predictive validity is ensured by demonstrating the model's performance on an independent test set in addition to the training and cross-validation sets such that there is no overfitting and underfitting. Lastly, for structural validity, the relative contribution of each input predictor to the model output is assessed using a sensitivity analysis (described in section 4.1). The more complex methods to quantify relative importance of inputs found in literature are skipped here as replicative and predictive validity are most important for forecasting problems. For further details, the reader is referred to Humphrey et al. (2017) who proposed such a validation framework for multilayer ANNs.

3.3.5 *ANN-based forecasts for reservoir operations optimization*

The inclusion of forecast variables as a part of ANN input predictor set allows for using different forecast products to model the forecast flow. The trained ANN model when fed with the GFS and GEFS-based deterministic and ensemble forecast fields, respectively, over the test period results in deterministic and ensemble members of forecast for 1-7 days lead time. The forecast flow was used to optimize the release decisions to maximize the hydropower

generation, without compromising the flood control and dam safety. The focus in this study is on dams that overwhelmingly require daily or longer time horizon for decision-making. Hence, the optimization was set up with daily temporal scale over a horizon of 1-7 days. The study formulates the following two operating schemes to demonstrate the application and value of forecast flows in reservoir operations.

3.3.5.1 Forecast-guided operations using model predictive control scheme

This scheme is devised to simulate the reservoir operations using short-term deterministic forecasts over 1-7 days lead-times to generate daily release decisions that are optimal according to a constrained objective function. The release at first time step was implemented while the later ones were revised at the next step's model run using updated forecasts. Such a strategy termed as Model Predictive Control (MPC) (or 'rolling horizon'), was proposed by Mayne et al. (2000) and implemented by Turner et al. (2017). The objective in this study was set to minimize the hydropower deficit from maximum installed capacity (or, to maximize energy generated) over the forecast horizon based on the optimized releases. The end-state of reservoir at the end of 7^{th} day is controlled using a penalty function that considers the reservoir state beyond the forecast horizon. This penalty function was proportional to the amount of deviation of the terminal reservoir level from the rule curve specified level. During the flood seasons, excessive spillway release was kept in check to minimize potential downstream damage. If a flood event is forecasted causing the reservoir level to reach the flood storage pool, the penalty function was modified to the sum of spillway release from the reservoir over the 7-day period. Thus, the selected penalty function grants preference to those release decisions that either minimize large deviations from rule curve specified levels or minimize the downstream flood risk, based on the season of reservoir operation.

The major objective of energy maximization and the penalty function were implemented in the form of a Multi-objective Optimization Problem (MOP) seeking Pareto

optimal set of solutions (Madsen et al., 2009). The suitability of Pareto optimal solutions for MOPs in reservoir operations has been demonstrated, amongst others, by Chen et al. (2017), Yang et al. (2015) and Giuliani et al. (2016). The Non-dominated Sorting Genetic Algorithm (NSGA-II; Deb et al., 2000) was used to yield the Pareto front of the optimal solutions, where none of the objective functions can be improved further without violating the other.

Several constraints were imposed for optimizing the reservoir releases in the interest of downstream stakeholders, dam safety and environmental concerts. Logistical constraints included turbine and spillway capacity limiting the power and spillway release and storage-volume continuity. The minimum reservoir storage was set to 95% of the historical minimum while limited by the flood control pool. The flood control constraint was implemented by limiting the total release to a safe threshold considering downstream flooding. The environmental flow was used to set the minimum release. The mathematical formulation and details of the constraints and objective functions are given in Appendix A.3.

3.3.5.2 Benchmark scheme

To assess the performance and value of optimizing the reservoir operations using the flow forecasts, a benchmark operating scheme is needed. In reality, dam operations would take into account many other factors that cannot be easily accommodated in a scientific analysis including regulatory requirements, power grid requests for hydropower dispatch, and recreation demands from local agencies. Thus, the hydropower benefits cannot be directly compared against the respective benefits from actually observed operations. Hence, a customized operation scheme was designed targeted specifically at maximizing the hydropower objective function (Turner et al. 2017). As proposed by Turner et al. (2017), the control rules were designed in the form of look-up table where the optimal release is specified as a function of two state variables – the reservoir storage level and season of year. We followed here the most rigorous way of designing such rules by optimizing the operations using the

observed time series data over 24 years from 1995-2018. The objective function was to maximize the total energy generated by the reservoir (which is the same objective as used for the optimization based on the forecasts). Although, the forecast-guided operations were obtained using daily optimization, a monthly time step was chosen to obtain the control release policy for benchmarking considering the huge number of data points to optimize over at daily scale.

3.3.6 *ANN-based ensemble forecasting*

The inherent uncertainty in the forecast variables of precipitation and temperature from the NWP models propagate in the modeled flow forecasts. To account for this uncertainty in modeled flow, the input predictors of forecast precipitation and minimum and maximum temperature from the ensemble forecast product of GEFS were inputs to the selected ANN configuration. Corresponding to each of the 11 GEFS ensemble members, 11 different realizations of the 1-7 days lead time forecast flow were obtained from the ANN model. The numerically fast ANN technique allowed the simulation of all the ensemble members in minimal processing time.

Next, the optimization model, set up to use deterministic forecasts, was simulated with three scenarios of GEFS-based forecast flow – the minimum, maximum and average of the ensemble inflow members. Maximizing the objective function value across all ensemble members to optimize decisions will undermine the dam operator's ability to adjust release in response to new information (Turner et al. 2017). The use of multi-stage stochastic optimization for optimization based on ensemble forecasts can also be found in literature (Xu et al. 2015; Fan et al., 2016). However, due to its computationally demanding requirements and complex implementation, we have limited the study here with a deterministic rolling horizon

type optimization for probabilistic forecast using minimum, maximum and average of the ensemble scenarios.

3.4 RESULTS

The ANN based forecasting was tested for each of the 23 selected dam sites and the performance was assessed individually. The ensemble forecasting was applied to 3 dams for demonstrating the concept and performance. Finally, the reservoir operations optimization using the modeled forecasts is shown for a single dam. The detailed results are described in the following sections.

3.4.1 *ANN architecture and input selection*

For arriving at the optimal input combination, first the number of antecedent days for the candidate predictor variables, as identified in section 3.2, was determined using the statistical properties of the respective time series. We chose to perform this analysis first for one of the dams, Pensacola dam (located in Oklahoma, USA), to obtain an estimate of probable predictors and then tested the configuration for other dams.

The cross-correlation function (CCF), measuring the similarity of a time series with the lagged versions of another, was obtained for the antecedent variables of precipitation, baseflow, temperature, windspeed, against the observed streamflow series at various lags. Partial autocorrelation of observed streamflow was plotted to assess the predictability in the antecedent flow. As shown in Figure 3.4(a), the cross-correlations decay with increased lags and are significantly high for precipitation and baseflow for use as predictors for ANN. The streamflow PACF indicates significant correlation up to lag 3 and falls sharply thereafter below the confidence limits. For the moving averaged streamflow as input, the best value of memory window length, K, was determined using the cross-correlation between streamflow and

antecedent moving-averaged flow as plotted in Figure 3.4(b) for K values of 3, 5 and 8 for the Pensacola dam. From the CCF plots, it can be observed that the moving average flow correlates differently at different lags based on the window size. For each lead-time, the window size giving the best cross-correlation was identified to obtain the optimal K value.

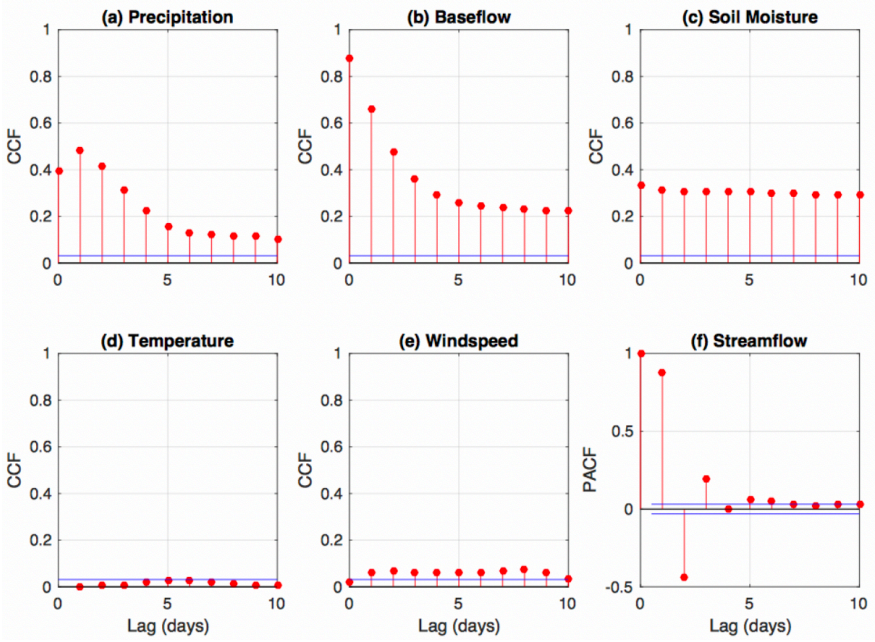

(a)

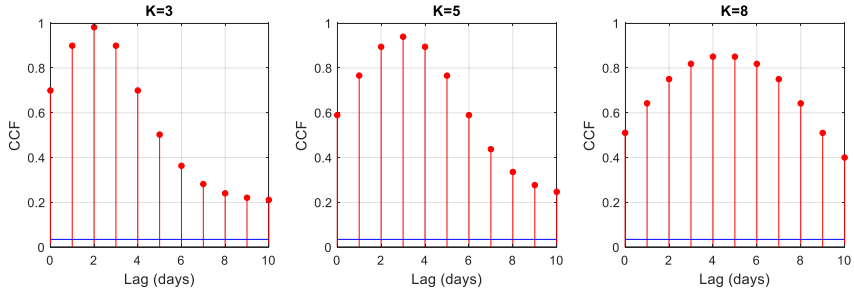

(b)

Figure 3.4 *Upper panel* (a) Cross-correlation functions (CCF) between with observed reservoir streamflow and antecedent (a) precipitation, (b) baseflow, (c) soil moisture, (d) temperature, (e) wind speed, and (f) Partial autocorrelation function for streamflow. *Lower panel* (b) CCF for antecedent moving average inflow over different window lengths against observed flow for Pensacola dam over the training period. The blue lines show 95% confidence bands around zero.

Based on this CCF based analysis, following values were selected for antecedent moving averaged streamflow: $K = 3$ for lead times of 1 and 2 days, $K = 5$ for lead time of 3 days and $K = 8$ for lead times of 4 to 7 days. Three days of antecedent streamflow were also used for forecasting beyond lead-time of 3 days. Two and three days of antecedent precipitation and baseflow were considered, respectively, while the temperature, soil moisture and windspeed were ignored due to lower CCF values. In applying the filter for baseflow separation, the values of 0.05 and 0.73 were found for a and BFI_{max}, respectively using a trial-and-error procedure for Pensacola dam. In addition to these antecedent variables, the forecast forcings of precipitation and temperature (minimum and maximum) were also provided as input nodes to ANN pertaining to the respective lead time of forecasting.

Next, to select the final set of input nodes and to assess the relative contribution of each predictor, the ANN was simulated with different combinations of predictors. This demonstrates the structural validity of the selected model as explained in section 3.4. The configuration was kept same across all the dams to allow fair assessment across all 23 dams and keep the sensitivity analysis simple. The sensitivity analysis is also advantageous as it can inform if the ANN model trained using a particular set of inputs is robust enough to be scalable to locations with varying characteristics.

Table 3.2 NSE (testing period) averaged for all 23 dams and examples for two dams, using different predictor combinations. P_a: antecedent precipitation (2 days), P_f: forecast precipitation (1 day), T_f: forecast min and max temperature (1 day each), B: antecedent baseflow (3 days), Q: antecedent streamflow(observed/moving-averaged). The row in bold is the selected best combination.

Predictor Combination	**Average NSE (all 23 dams)**			**Pensacola Dam**		**Green Peter Dam**	
	L1	**L4**	**L7**	**L1**	**L7**	**L1**	**L7**
P_a, T_f	0.095	-0.030	-0.036	0.269	0.132	0.437	0.173
P_f, P_a, T_f	0.177	0.108	0.063	0.370	0.128	0.529	0.324
B	0.670	0.371	0.286	0.470	0.175	0.751	0.280
Q	0.652	0.347	0.272	0.683	0.183	0.752	0.292

Q, B	0.669	0.366	0.253	0.812	0.151	0.757	0.319
T_f, Q, B	0.551	0.416	0.327	0.598	0.256	0.766	0.411
P_f, P_a, T_f, B	0.730	0.451	0.231	0.815	0.252	0.897	0.482
P_f, P_a, Q, B	0.771	0.396	0.306	0.799	0.164	0.889	0.459
P_a, T_f, Q, B	0.654	0.331	0.327	0.762	0.202	0.746	0.460
$\boldsymbol{P_f, P_a, T_f, Q, B}$	**0.743**	**0.481**	**0.342**	**0.838**	**0.268**	**0.910**	**0.455**

For assessing the performance, the NSE was calculated for each lead-time of the modeled flow. Using the ANN configuration that yielded the highest average NSE across all the dams, the best combination of input nodes was derived. The period of Jan 2007 to Aug 2014 was used as the *training set*, while the *validation* and *testing sets* extended from Sep 2014 – Oct 2015 and Nov 2015 – Dec 2017, respectively. Table 3.2 demonstrates the sensitivity analysis carried out with the different configurations, tabulating the average NSE values for lead times of 1, 4 and 7 days over all the dams during the testing period. The individual dam NSE values are shown only for Pensacola and Green Peter dams for the sake of brevity, for the lead times of 1 and 7 days.

Table 3.2 gives the value that each individual predictor adds to the ANN forecast skill. It can be seen that, although the antecedent and forecast precipitation and temperature have little value by themselves, they generally improve the performance when used in combination with the flow variables. Although exceptions exist to this trend when only NSE is considered as a measure of performance as in Table 3.2, the skill is improved in terms of minimized lag between the peaks in the modeled and observed flow. This is more visible from the lagged correlations between the two streamflow time series plotted in Figure 3.5, where higher correlation value close to lag 0 represents better performance with reduced peak time lagging. Using only the base flow and moving average flow as predictors (Figure 3.5a and Figure 3.5c), the peak correlation occurs at a higher lag due to which the modeled peaks exhibit time lagging. However, as Figure 3.5b and Figure 3.5d show, the lag is reduced significantly when forecast

precipitation and temperature are included. The correlation values at lag zero increase in the latter combination.

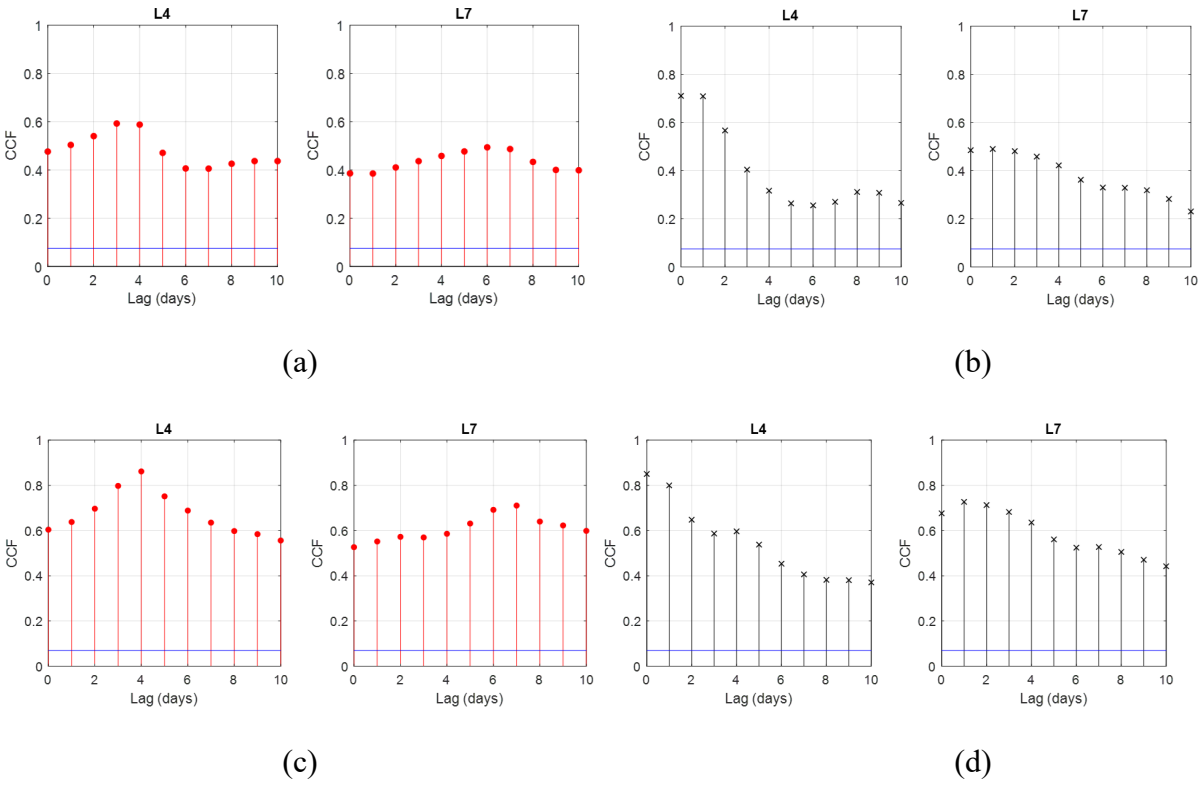

Figure 3.5 Lagged cross-correlations between the modeled and observed streamflow for Pensacola dam using (a) only base flow and moving average flow, (b) using also the antecedent/forecast precipitation and temperature as predictors in addition to antecedent flow. (c) & (d) same evaluation but for Green Peter dam. Higher correlation value close to lag 0 represents better performance with reduced peak time lagging. Blue lines mark 95% confidence bands around zero.

Based on this analysis, the final predictor combination for the ANN is selected as: antecedent precipitation (2 days), antecedent baseflow (3 days), antecedent streamflow (3 days; for lead times of 4-7 days), antecedent moving average flow (3-, 5- and 8-day window based on lead time), forecast precipitation (1 day) and forecast min/max temperature (1 day each). The final ANN architecture selected is shown in Figure 3.6.

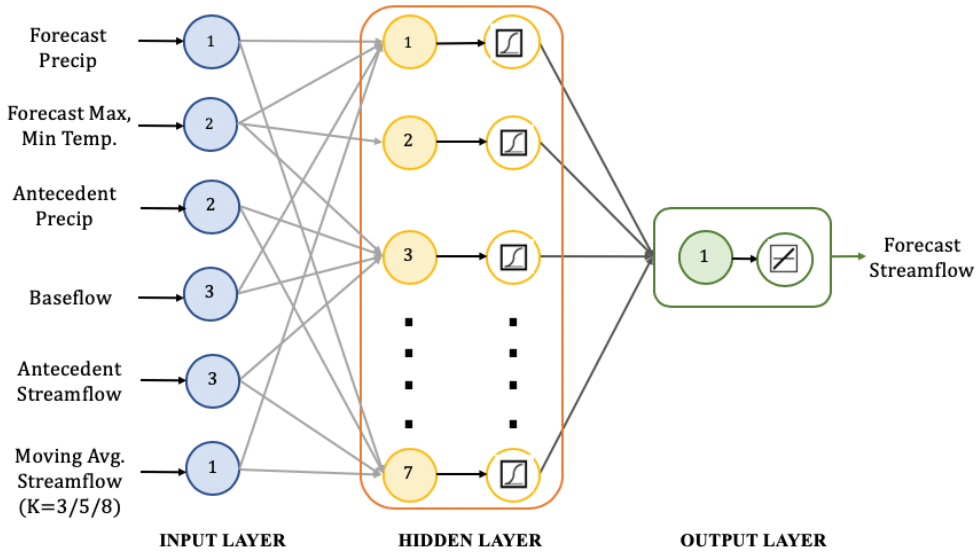

Figure 3.6 Three-layered ANN architecture and the selected input nodes with log sigmoid and linear transfer functions for hidden and output layers, respectively. Numbers on input nodes represent selected number of antecedent/forecast days. *K* is the window length for moving average streamflow that is varied with lead time of forecasting.

3.4.2 *ANN-based forecast assessment*

Using the optimal combination of predictor nodes from section 4.1, the ANN model was simulated for the selected 23 dams and the skill in forecast was assessed using various metrics of evaluation over the testing period.

To assess the predictive validity, the evaluation of the modeled flow was performed over completely independent test set using metrics of NSE, Correlation, and MAE. Table 3(a) summarizes the metrics for each of the 23 dams. The six stations on Ganges, Brahmaputra and Mekong river basins over which the ANN model was setup are also included in the evaluation for the sake of comparison in Table 3.3(b). The plots of the observed and modeled flow time series are shown in Figure 3.7.

The replicative validity is assessed using (i) scatter plot of observed and modeled flow, and (ii) time series of standardized residuals. Scatter plot of the observed and modeled flow data in Figure 3.8(a) shows robust performance, where systematic divergence from the 1:1 line

indicates unmodeled behavior. The time series of the standardized residuals, as plotted in Figure 3.8(b) identifies any serial correlation in the residuals that suggests unmodeled deterministic behavior. The standardized residuals were calculated as raw residuals divided by their estimated standard deviation. An ideal plot of residuals should lie randomly within a horizontal band with no visible patterns.

Table 3.3 (a) Evaluation of ANN flow forecasts for 23 dams stating NSE, Correlation and MAE for lead times of 1, 4 and 7 days.

	Dam Name	NSE			Correlation			MAE (cfs)		
		L1	L4	L7	L1	L4	L7	L1	L4	L7
1	**Libby**	0.974	0.871	0.780	0.987	0.933	0.886	1256.2	2413.7	3325.6
2	**Jackson**	0.958	0.850	0.771	0.979	0.922	0.880	223.2	411.9	519.7
3	**Dworshak**	0.955	0.812	0.681	0.978	0.902	0.828	707.8	1698.2	2370.5
4	**Hungry Horse**	0.920	0.746	0.649	0.960	0.873	0.822	665.1	1199.4	1462.6
5	**Navajo**	0.917	0.819	0.703	0.960	0.905	0.841	221.2	345.7	468.0
6	**Great Salt**	0.910	0.754	0.455	0.956	0.872	0.684	278.9	541.8	821.2
7	**Lost Creek**	0.908	0.711	0.580	0.953	0.852	0.767	179.2	382.8	466.0
8	**Cougar**	0.885	0.496	0.456	0.942	0.735	0.682	129.4	302.0	354.6
9	**Hills Creek**	0.864	0.670	0.502	0.930	0.827	0.714	193.2	376.6	444.3
10	**Detroit**	0.843	0.720	0.606	0.920	0.849	0.780	364.5	553.0	703.0
11	**Pensacola**	0.838	0.517	0.268	0.922	0.724	0.519	3031.8	5545.8	6697.6
12	**Fort Peck**	0.777	0.329	0.240	0.883	0.584	0.539	792.6	1542.3	1955.3
13	**Mud Mountain**	0.746	0.280	0.406	0.868	0.534	0.639	329.3	606.7	501.4
14	**Howard**	0.717	0.457	0.238	0.859	0.819	0.550	318.7	419.8	505.6
15	**Buford**	0.678	0.465	0.326	0.835	0.704	0.578	584.3	863.0	791.2
16	**Hartwell**	0.632	0.433	0.340	0.799	0.693	0.604	1456.6	1951.5	2072.3
17	**Carters**	0.624	0.414	0.242	0.835	0.689	0.521	218.6	277.6	310.8
18	**Allatoona**	0.571	0.524	0.376	0.769	0.726	0.617	705.8	597.1	749.5
19	**Eldorado**	0.566	0.100	0.036	0.769	0.326	0.223	176.2	257.7	287.7
20	**Green Peter**	0.531	0.331	0.133	0.741	0.611	0.427	219.6	295.7	336.4
21	**Broken Bow**	0.517	0.167	0.140	0.731	0.408	0.388	820.9	1355.2	1484.6
22	**Fort Supply**	0.246	-0.33	-0.29	0.68	0.389	0.267	11.8	16.3	15.1
23	**Marion**	0.323	-0.092	0.063	0.630	0.365	0.254	89.0	129.1	115.1

Table 3.3 (b) Evaluation of ANN flow forecasts for six stations of Ganges, Brahmaputra and Mekong river basins, comparing the NSE and Correlation

#	Station Name	NSE			Correlation		
		L1	L4	L7	L1	L4	L7
1	**Hardinge Bridge**	0.945	0.936	0.930	0.973	0.969	0.965
2	**Bahadurabad**	0.892	0.893	0.872	0.945	0.945	0.934
3	**Vientiane**	0.990	0.880	0.810	0.990	0.940	0.910

4	**Pakse**	0.990	0.950	0.890	1.000	0.980	0.950
5	**Stung Treng**	0.990	0.940	0.900	1.000	0.970	0.950
6	**Kampong Cham**	0.990	0.960	0.900	1.000	0.980	0.960

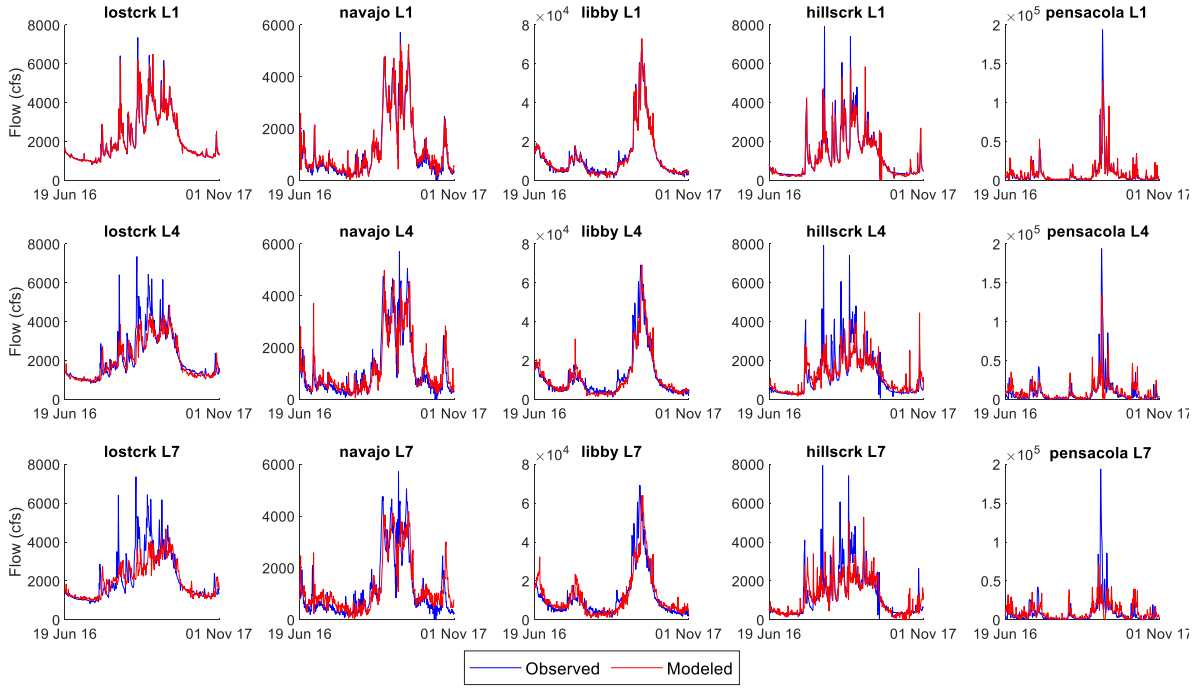

Figure 3.7 ANN modeled flow plotted against observed values over testing period for 1, 4, and 7-days lead time (L1, L4, and L7) for Lost Creek, Navajo, Libby, Hills Creek and Pensacola dams.

Figure 3.7 and Figure 3.8 suggest that the forecast skill decreases with increasing lead-time as expected, however the scatter plot of the observed and modeled flow fits well across the 1:1 line. The standardized residuals are mostly randomly distributed around the zero line, though the peak flow season has a few negative residual points for lead times of 4 and 7 days, corresponding to the underestimations in modeled flow. The performance for Pensacola dam is specifically affected by an unusually extreme peak event that hit the reservoir during the testing period, the likes of which did not occur over the training set of data. This causes heavy underestimations in the flow forecast over the event. A longer training period is required to

improve the performance over such extreme peak flow events. Apart from this exceptional peak event, serial correlation in the residuals is mostly minimal across dams.

After assessing model validity, the next step in the ANN performance assessment is to compare the performance across the 23 dams (and 6 large-scale basin stations) as a function of dam's hydrologic and climate characteristics. Three factors were used to capture the varying characteristics –upstream drainage area of dam, local climate according to Köppen-Geiger climate classes, and coefficient of variation (COV) of observed streamflow, defined as ratio of the standard deviation of the inflow time series (over training period) to its mean value. COV is a measure of variability of the incoming flow into the reservoir. Figure 3.9(a) below plots the distribution of NSE values for lead-time of one and seven days (measure of ANN performance) over the testing period, as a function of the COV for each dam. The respective climate class-based distribution of the NSE values for each dam is shown in Figure 3.9(b). COV is shown on the same plot in the bottom panel.

Figure 3.9(a) reveals strong negative signal between the COV and forecast skill. The six stations in large river basins perform very well (Table 3.3(b)) with much larger catchment areas and smaller variation in flow due to monsoonal hydrology. From Figure 3.9(b), it is evident that the performance improves as the drainage area increases especially for the cold humid and humid subtropical class dams. The Mediterranean class dams perform well even for smaller reservoirs due to the similar flow characteristics in all the four dams (COV ~1 and mean flow ~1500cfs). Appendix B shows the map of climate class with ANN performance for each dam. The two exceptions from the expected trend, encircled in red, are explained below:

1. The Fort Supply dam, in humid subtropical climate, receives very low flows with a mean value of 43 cfs over the training period and 18 cfs over validation/testing, leading to high COV. This results in offsetting the effect of average drainage area and makes it harder for ANN to learn the flow pattern.

2. The Fort Peck with drainage area is 149,508 km^2 (not shown entirely in Figure 3.9(b) due to scaling issues) is the only dam to have a few regulating flow structures upstream. A part of annual inflow is contributed by the releases from other upstream dams in addition to the natural unregulated component, which deteriorates the NSE value at higher lead times and again counterbalances the effect of very high drainage area.

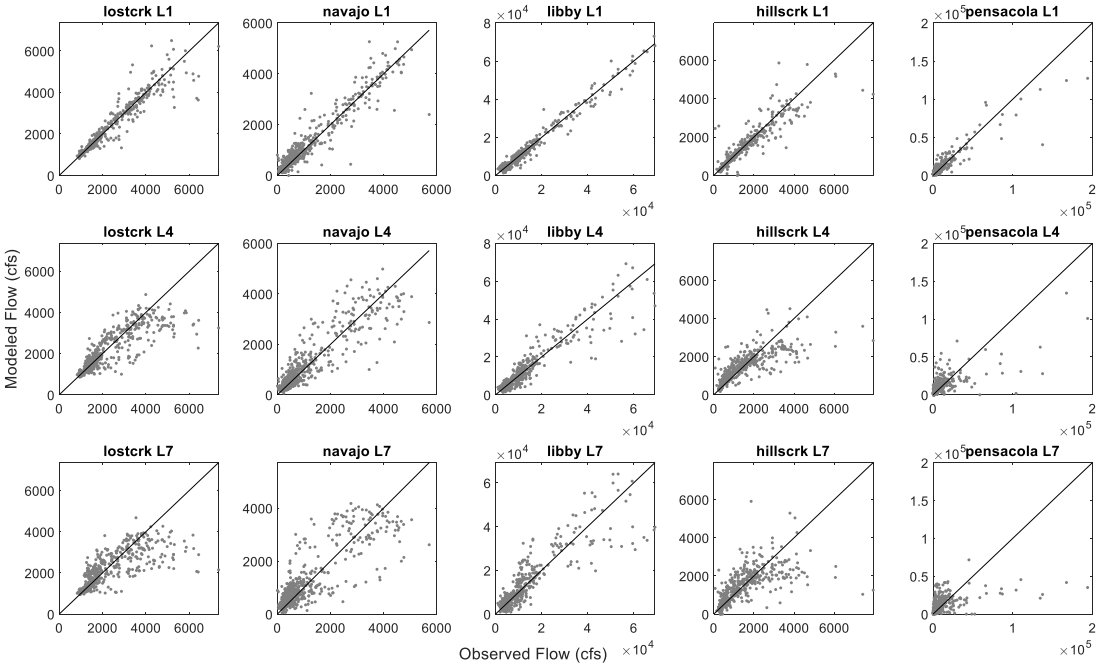

(a)

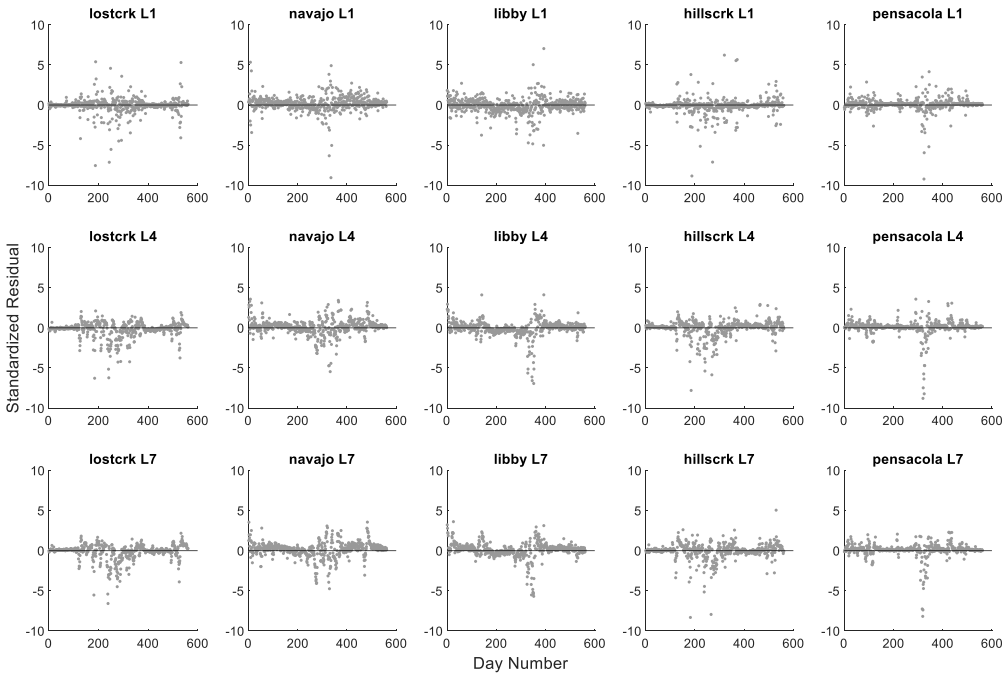

(b)

Figure 3.8 (a) Scatter plot of the forecast and observed flow for 1, 4 and 7-days lead times; (b) Standardized residuals plotted with time over testing period to identify serial residual correlation for Lost Creek, Navajo, Libby, Hills Creek and Pensacola dams.

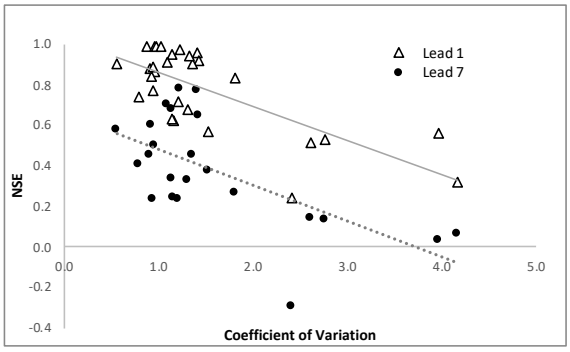

(a)

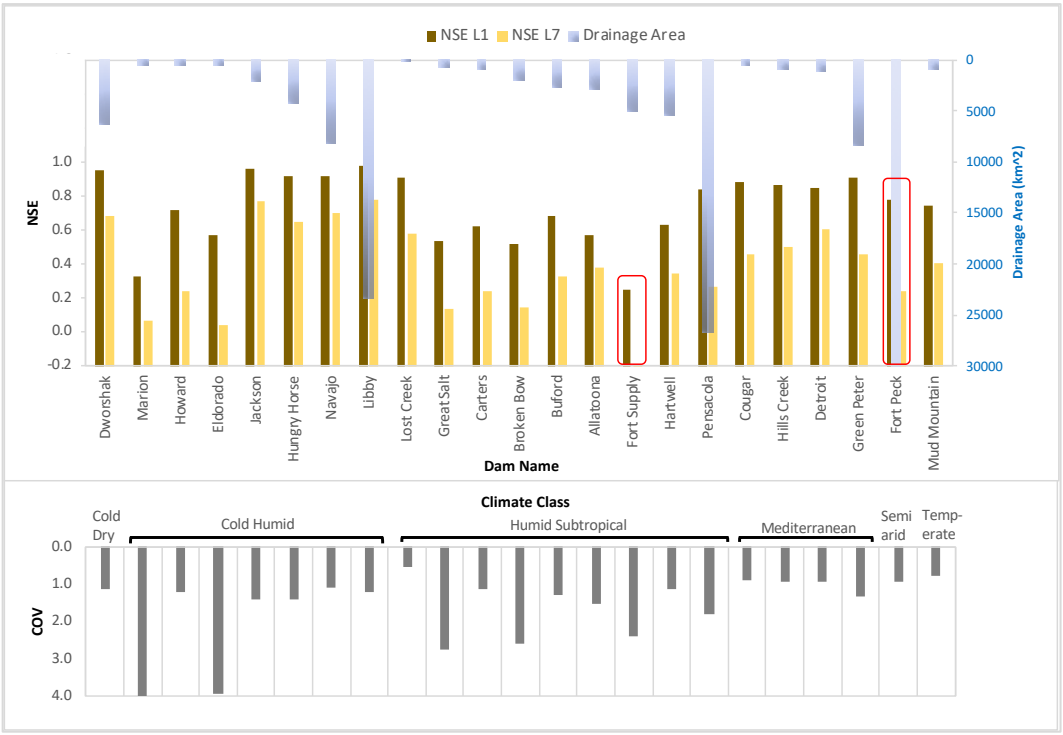

(b)

Figure 3.9 (a) ANN performance in terms of NSE values at lead time of 1 and 7 days (L1 and L7) plotted against the coefficient of variation (COV) for all the 23 dam sites including the additional 6 large-scale basin stations. (b) Distribution of NSE values (left y-axis) for each dam at L1 and L7 with drainage area (right y-axis) in the upper panel. The respective local climate class and COV is plotted in the lower panel. The dams in each climate class are sorted in order of decreasing drainage area. The two exceptions – Fort Supply and Fort Peck not following the expected trend are encircled in red.

3.4.3 *ANN-based ensemble forecasts*

Feeding the ANN with ensemble of forecast predictors from GEFS resulted in ensemble members of the forecast flow and estimates of flow uncertainty. The spread and mean of the forecast flow were calculated. The application is demonstrated over a single peak flow event for three dams. These are: (i) Pensacola dam with peak event of May 2015, (ii) Detroit dam with peak event of Dec 15, (iii) Jackson dam with peak event of May-Jun 2016. The results of ensemble forecasts compared with the deterministic (using GFS forcing fields from section

4.2) and observed flows are shown in Figure 3.10. The mean of the ensemble forecasts usually corresponds well with the deterministic forecasts except during the high flow events when the ensemble spread is higher. The increase in forecast flow uncertainty with lead-time is also visible from the Figure 3.10 for the selected dams.

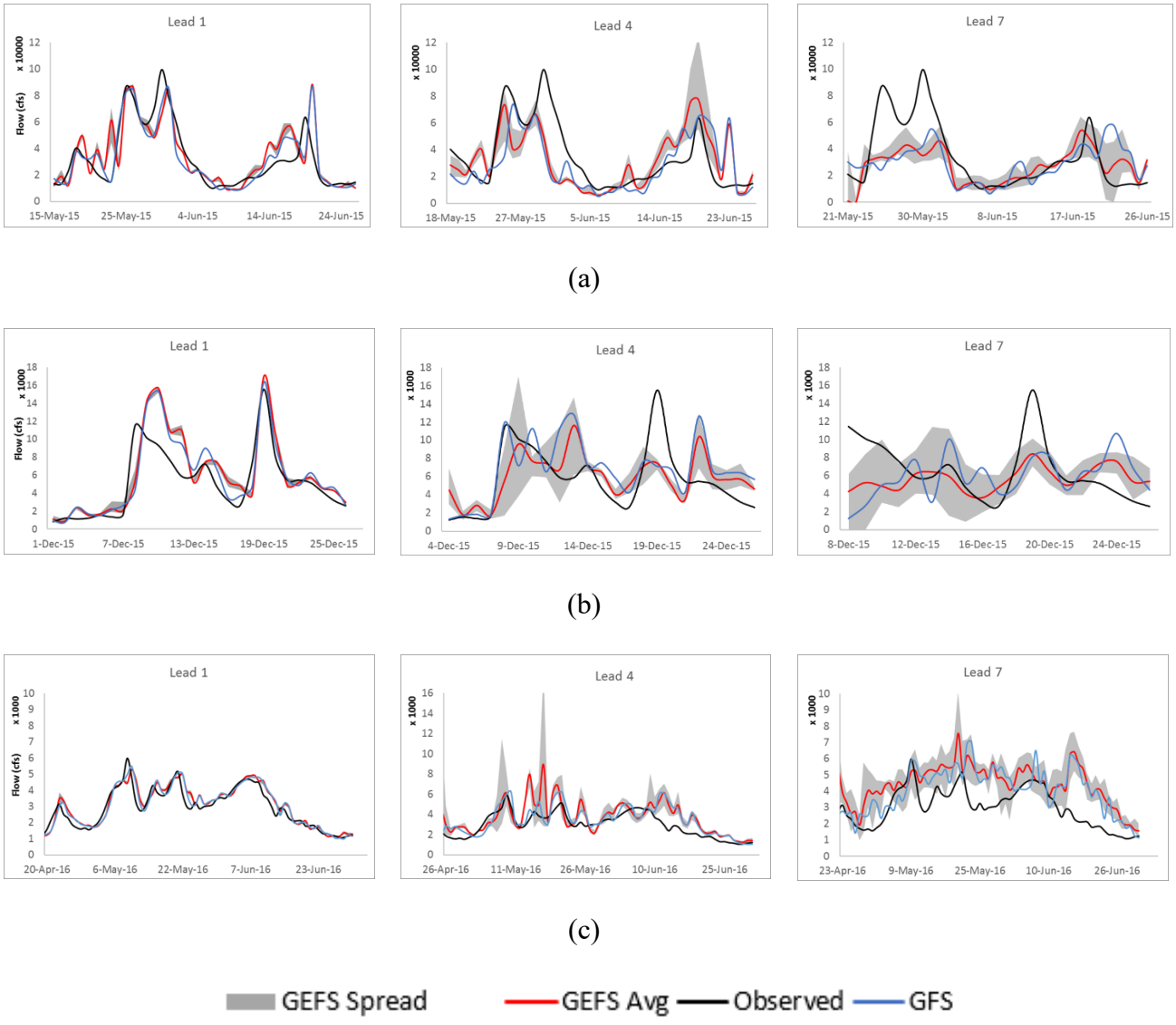

Figure 3.10 Ensemble forecasts (average and spread) obtained by feeding ANN with ensemble forecast fields from GEFS, compared with the observed flow and deterministic forecasts (feeding ANN with GFS forecasts) for: **(a)** Pensacola dam, **(b)** Detroit dam, and **(c)** Jackson dam, at lead times of 1, 4 and 7 days.

3.4.4 *Reservoir operations optimization using deterministic forecasts*

To demonstrate the optimization of reservoir operations based on the ANN-based forecasts, the Pensacola dam was selected. A schematic of dam specifics with key operating constraints is shown in Figure 3.11(a). The observed data of inflow, releases and hydropower generation were obtained from the USACE (Monthly Charts for Grand Lake, 2018).

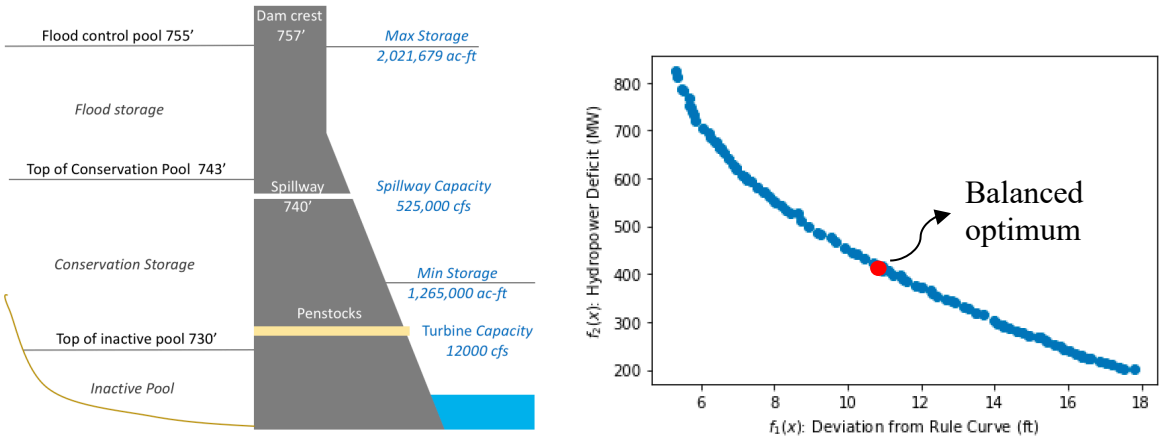

(a) (b)

Figure 3.11 (a) Specific pools and constraints used for optimization with pool levels above mean sea level; (b) Solutions on the Pareto front and a sample balanced optimum between the energy maximization and penalty function for Pensacola Dam in Oklahoma.

3.4.4.1 Forecasts based Model Predictive Control Scheme

The optimization using data-driven inflow forecast was performed over a period of two years (Sept 2014 – Aug 2016) for Pensacola Dam. The period was selected to ensure it does not entail the training set of ANN. The optimization problem is solved at each time step applying NSGA-II technique, yielding the optimal release sequence for the horizon of 1 to 7 days. With the MPC strategy, the first of these is implemented in simulation and the remainder are subsequently updated next day when a new forecast is issued. A balanced optimum solution was chosen on the Pareto front for flood and non-flood seasons to maximize hydropower and minimize the penalty function. An example Pareto-optimal solution front between the

hydropower deficit minimization and penalty function (in terms of deviation from rule curve) and a sample balanced solution over the front is shown in Figure 3.11(b). The optimized release decisions over the 2-year period are compared with the actual observed operations in Figure 3.12(a), while the resulting reservoir headwater levels based on optimized and observed releases are compared in Figure 3.12(b).

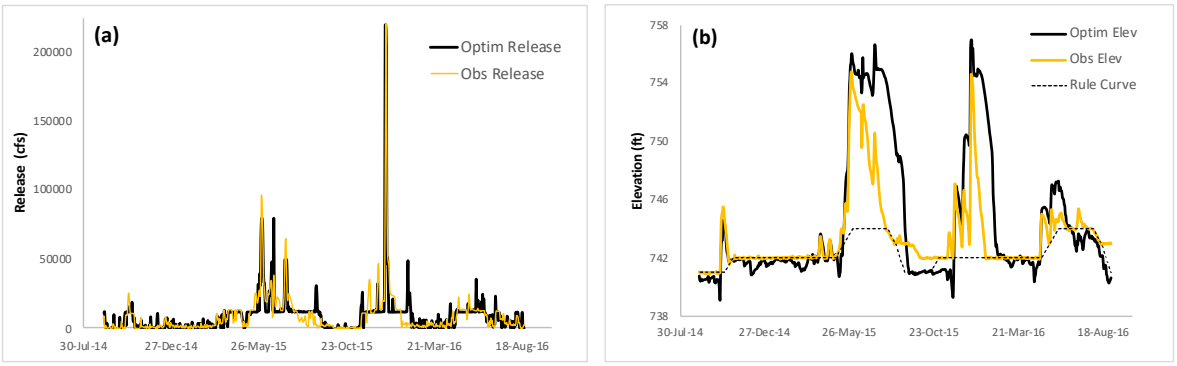

Figure 3.12 (a) Optimized release policy using the ANN forecasted inflow, compared with the observed operations; (b) Resulting reservoir headwater levels using optimized and observed releases, and the rule curve for Pensacola dam from USACE

3.4.4.2 Benchmark Scheme

The benchmark operating scheme, in the form of control rules or look-up table, was designed to assess the performance of optimized operations based on forecasts. The computations over the 24-year period (1995-2018) at monthly time step were performed using the R package '*reservoir'* (Turner and Galelli, 2016) with the '*sdp_hydro'* function that implements Stochastic Dynamic Programing under given constraints and constants. Release was discretized into 50 uniform values up to the maximum release threshold (see Appendix B),

while the storage was discretized into 200 values within the set bounds.

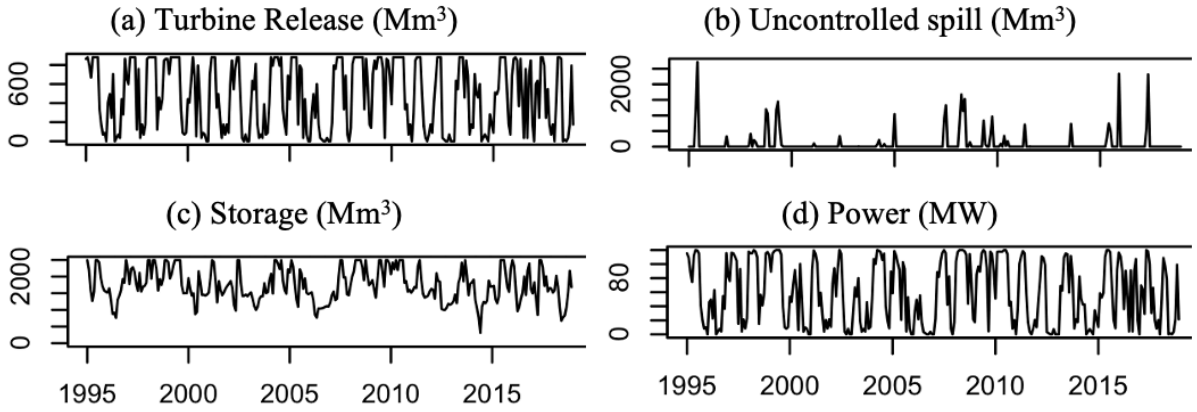

Figure 3.13 shows the optimal release decisions, storage behavior and power generated under control rules.

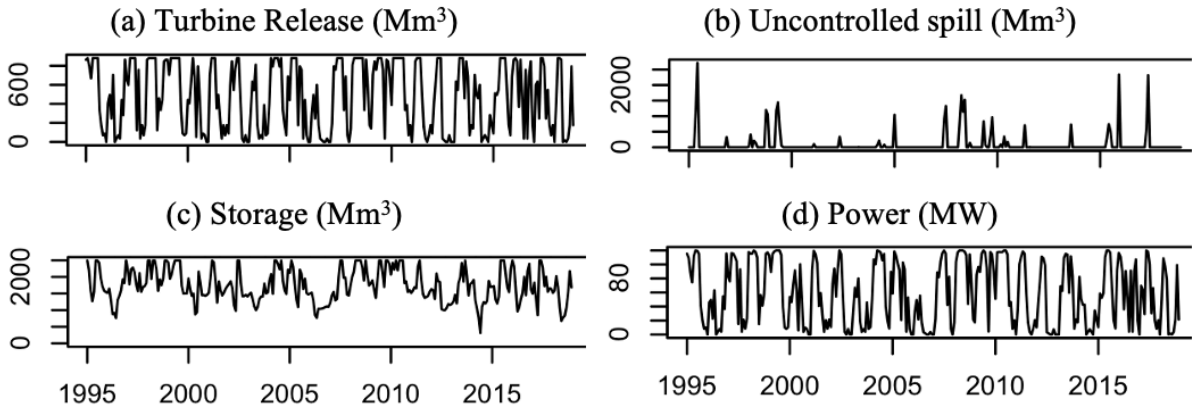

Figure 3.13 Reservoir operating policy and resulting reservoir behavior at monthly scale based on the benchmark control rules designed specifically for hydropower maximization neglecting the forecasts using the R package '*reservoir'* (after Turner and Galelli, 2016).

3.4.4.3 Comparison of forecast-based optimization with the benchmark

To assess the optimization performance, two hydropower benefits were calculated: (i) *optimized HP*: hydropower generation resulting from the optimized releases based on the ANN inflow forecasts while passing the observed inflow into the system; (ii) *benchmark HP*: hydropower generated from benchmark control rules-based operations. Over the two years of assessment (Sep 2014-Aug 2016) that includes flood and non-flood seasons, the *optimized HP*

was 954,061 MWh in comparison to the *benchmark HP* of 906,807 MWh. Thus, the optimized release decisions resulted in an additional and 'flood-safe' hydropower production of 47,253 MWh amounting to $4,611,892 using the average residential electricity rate in Oklahoma City of 9.76¢/kWh (Electricity Rates, 2018). At an average electricity consumption of 900 kWh per month per US household, this much of energy can fulfill the demands of around 45,530 households for one month.

For the penalty function addressing flood control during peak flow seasons, two peak events in the two-year period of assessment were analyzed for the improvement in peak release reduction. The ANN forecast flow over each of these events is shown in Figure 3.14.

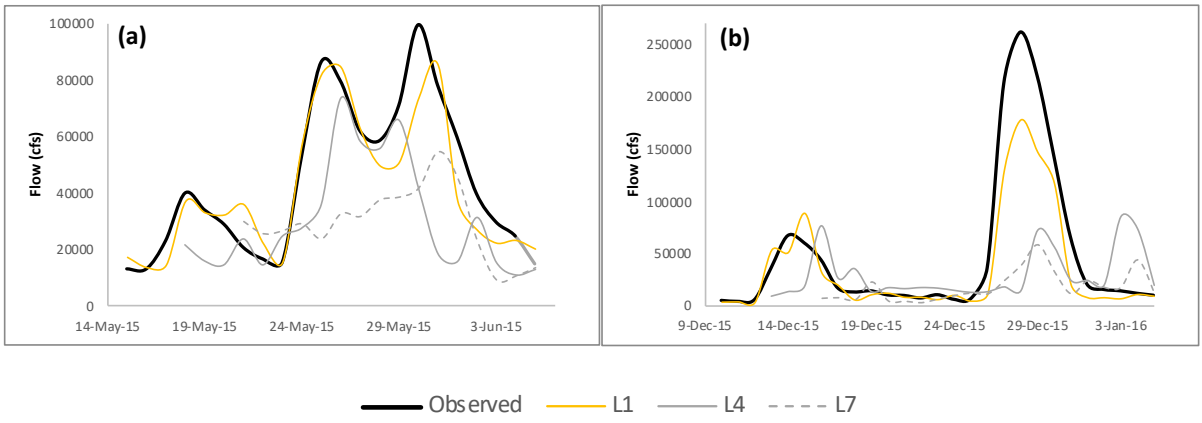

Figure 3.14 ANN forecast flow for lead times of 1, 4 and 7 days over the Pensacola dam's peak inflow events of (a) May 2015 with peak flow of 99,700 cfs and (b) Dec 2015 of 221,360 cfs

The underestimation is much higher in the second peak flow event with increasing lead-time as the event of such a magnitude is quite rare making it difficult for ANN to learn. Due to this underestimation, as the optimization over 7-day horizon proceeds, the pre-event releases are triggered only very close to the event and not much improvement is achieved in downstream flood control. While on the contrary, for the May 2015, with better forecast skill, the optimal releases are bounded within the safe threshold of 30,000 cfs for most days and the peak release reduced by ~18% to 80,000 cfs on May 30 (see Figure 3.12(a)). The operations improved in

terms of the resulting reservoir levels being closer to rule curve as compared to the observed operations during drawdown and dry seasons, as shown in Figure 3.12(b).

3.4.5 *Reservoir operations optimization using ensemble forecasts*

The ensemble of the forecasts was assimilated into the reservoir operations optimization. The optimization model as setup in section 4.2 was simulated with three scenarios of GEFS-based forecast flow – the minimum, maximum and average of the ensemble inflow members. The technique is illustrated using the peak flow event of May 2015 over Pensacola dam. The GEFS ensemble-based inflow forecasts, as shown earlier in Figure 3.10(a), were used to simulate the optimization model. The optimized releases and resulting reservoir elevations from each ensemble scenario and from previously obtained GFS-based forecasts are plotted in Figure 3.15.

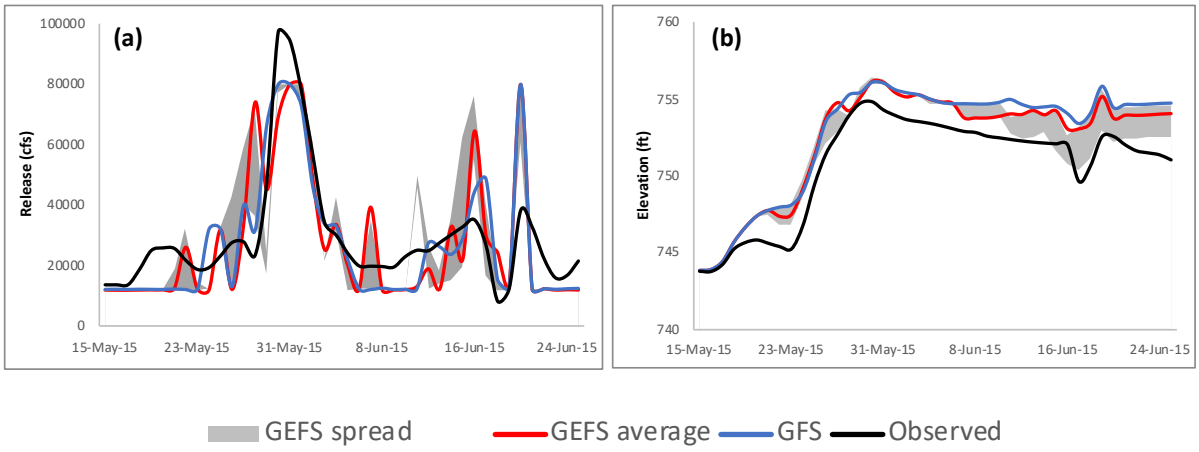

Figure 3.15 Optimized release decisions using rolling horizon optimization and resulting reservoir elevation behavior based on average, min and max of the GEFS ensemble flow forecasts. Spread is obtained based on the minimum and maximum values of the optimized variables. The respective variables from GFS based deterministic forecasts and observations are also shown.

Figure 3.15(a) and Figure 3.10(a) suggest that the uncertainty in inflow forecasts, which is minimal for lead-time of one day and increases afterwards, translates into the corresponding

uncertainty in the release decisions. However, as the optimization proceeds on a rolling horizon basis, the more certain and skillful forecasts are ingested to generate optimal release decisions that minimize the uncertainty in the policy and resulting reservoir storage behavior.

3.5 Decision Support System for Smart Dam Operations

To facilitate real-world engagement with dam-operating agencies in the decision-making process, a web-based open-source decision support system (DSS) was developed. The purpose of DSS is not to replace but rather to improve human decision-making in making informed choices to achieve this objective. We call this DSS 'Intelligent Dam DEcisions and Assessment' (iDDEA) as described in section 3.5.1 (Ahmad and Hossain, 2019b). The iDDEA DSS is currently operational and hosted at http://depts.washington.edu/saswe/damdss/. To ensure reproducibility of the DSS for other regions of interest and to provide a platform for assessing the necessary scripts for customization, a GitHub repository (https://github.com/shahryaramd/iDDEA) has been set up for all the frontend script and libraries, and necessary scripts and model configuration files for the backend architecture, that anyone can download to start customizing the iDDEA DSS.

We incorporate here a bipartite approach as described by Gachet & Haettenschwiler (2003), for developing the DSSs, which decouples the decision support system into the contents, i.e. frontend, and the container i.e. backend. This architecture is shown in Figure 3.16, highlighting the interaction between the two top-level components along with their individual sub-constituents.

For operationalizing the DSS, Detroit dam in Oregon was chosen based on its hydrologic characteristics and long record of the observed data. It has been operational over Detroit dam since December 2017 and is regularly monitored by USACE as well as stakeholders from various other regions.

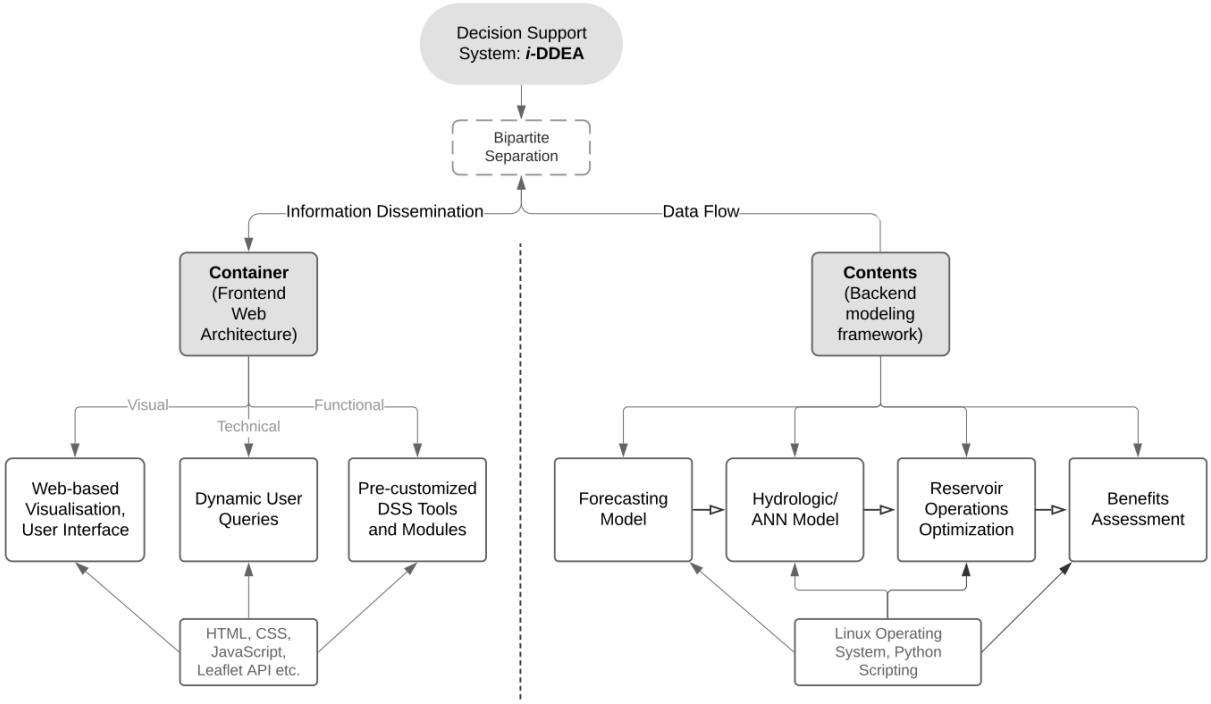

Figure 3.16 The overall architecture for iDDEA, based on a bipartite approach that separates the DSS into two major components – contents (here backend models) and container (the frontend web platform). The approach facilitates the independent reuse of the two components for easy customization. The DSS is hosted at http://depts.washington.edu/saswe/damdss/.

3.5.1 *Backend architecture*

The backend of the DSS comprises of four different modules embedded into a framework, to produce optimized reservoir releases for one week of lead time. The modules are coupled with each other, where one's output becomes the input to the next to generate the different results that serve as the content for the frontend template-based architecture. Because the DSS backend is designed to be model-agnostic, two different models were implemented for generating the reservoir inflow forecasts – one that uses the VIC hydrologic model (described in Chapter 2), while other using the ANN model (described in current chapter). The reservoir inflow forecasts are then passed to reservoir operations model integrated with the backend to generate optimal release decisions to be disseminated via frontend.

In addition to the optimal release advisory generated using the forecasts-informed reservoir optimization, iDDEA also provides a realtime assessment of the disseminated advisory. The optimized release decisions are compared with the observed operations retrospectively over the past week in terms of the respective hydropower benefits.

3.5.2 *Frontend architecture*

The other component that serves as the link between the complex models running in the backend and the user (dam operator) is the frontend or visualization framework of the iDDEA DSS. This framework is organized into several modules to help achieve the desired characteristics of the DSS. The three main aspects of the user experience considered here are – visual, functional and technical elements that are implemented using various open-source tools, libraries and Application Program Interfaces (APIs). The functional elements, as considered here, constitute the overall space, navigation, content and logos, and their respective formatting. The technical and visual aspects include the dynamic querying and visualization of timeseries/raster products on the web map, respectively (Ahmad and Hossain, 2019b).

The first module of the frontend architecture is the advisory on processed forecasts for hydrological variables and inflow into the reservoir for 7 days lead time. The visualization informs the dam operator about the amount of water flowing into the system in the next two weeks and if any precautions are necessary in light of a potential flood event. Two options are available for the source of inflow forecasts – VIC based and data-based (ANN). Based on the forecast inflow, the optimization model running in the backend produces an optimized set of releases to be made from the reservoir based on the current reservoir storage and future inflow. The next module is developed to perform a retrospective assessment of the optimization-based decisions on the basis of additional energy benefits. The ‘Assessment’ tab presents the user with two options – ‘Weekly Hydropower Assessment’ and ‘Weekly Forecast Assessment.’

Finally, the DSS allows the user to visualize the actual operations as streamed from the USACE's data portal.

3.6 DISCUSSION

A data-driven weather forecast-based reservoir inflow forecasting using ANN technique was developed with a comprehensive validation and testing framework. In addition to the antecedent conditions, short-term forecast fields from the GFS model were used as inputs to train a three-layered ANN. By using a transformation of antecedent flow time series along with the forecast fields of precipitation and temperature, time lag in peak flow prediction was significantly improved. Six stations (with no dams) on large river basins of Ganges, Brahmaputra and Mekong were also included in the assessment. Superior performance was observed for these international basins due to their large basin area and strong seasonal hydrology due to the predictable monsoon. The forecast skill assessment suggested that the technique performs reasonably well with NSE value greater than 0.5 for 48% of the sites (including those on larger basins) for forecasts at lead-time of 7 days. This suggests that the same ANN configuration is able to capture the flow variations across a variety of dams.

The performance across the different dams also revealed trends pertaining to flow characteristics and area of the upstream catchment. As reservoir receives inflow that is more variable over the annual scale with less visible seasonal patterns, reflected by a high COV value, the forecast performance decreases. This can be explained as the ability of ANN to learn from the limited training provided in this study is not sufficient when the variability in the flow is too high. An improved performance can be achieved for such basins using a longer training period with varying flow regimes. Apart from COV, another factor controlling the flow characteristics and the forecast skill is the drainage area of the basin. Decreasing drainage area makes the basin hydrologically more responsive with lower times of concentration and the

basin generates flashier peak flows with lesser seasonal patterns. This deteriorates the forecast skill especially with the increasing lead-times. Furthermore, although the performance of dams in Mediterranean climate zone is generally better than dams in other climates, there is no remarkable trend as a function of local climate. This in fact verifies the robustness of the selected ANN architecture's learning ability across diverse hydro-climatologic conditions. The results also prove the global scalability of the proposed technique, as the forecast performance was tested here for a wide range of hydrologically different dam sites (as well as undammed river stations in large river basins of Asia) and in different climates.

As the deterministic flow forecasts from ANN model were not able to capture the inherent uncertainty present in the streamflow estimates, an ensemble of forecast fields was assimilated into the trained ANN to propagate the uncertainty. The results revealed that the highest spread in ensemble flow forecasts occurs during the peak flow seasons when the inflow into reservoir is most uncertain. This is the regime when the dam operators can benefit most from these forecasts. Providing the operating agencies with the ensemble forecasts during flood seasons can help increase the odds of operating for the flows of high probability of occurrence and improve the energy generation without risking the flood control.

The forecasting technique was then coupled with a reservoir optimization model for maximizing the hydropower generation without compromising flood control and dam safety. A rolling horizon scheme was employed to obtain optimal release policy over the horizon of 1-7 days. A benchmark policy, obtained as look-up table by neglecting the forecasts but optimized for energy generation, provided a fair benchmark to compare hydropower benefits from the forecast-based optimal operations. The long-term assessment over two years yielded significant benefit over the benchmark policy with reduced flood risk downstream.

Short-term ensemble forecasts were also explored in this study. The reservoir operations optimization model was also simulated using the different scenarios (min, max and

average) of the flows over the forecast horizon. The uncertainty in the release decisions was propagated by the corresponding spread of the ensemble forecast flows, although the effect was undermined due to the continual updating of forecasts every day during the optimization process. It should be mentioned that uncertainty (spread) in the ensemble flow forecasts, which is highest at times of extreme peak flow, also leads to the uncertain operating policy mostly during the peak flow times. This implies that the use of ensemble forecasts can be most efficient during the seasons of high flow and should be avoided over drier periods.

The proposed ANN scheme that is numerically fast and efficient for forecasting of reservoir inflow allowed an assessment over multiple years and multiple sites using computationally modest resources. The proposed ANN technique is appropriate for global scale operationalization of short-term reservoir inflow forecasts for any dam site provided the training data are selected carefully with acute hydro-climatic understanding of the basin. The inputs used herein are freely and globally available. Such a technique also allows long-term risk assessment of historical operations by directly incorporating the forecast fields from NWP models. The optimization using Pareto optimality concept allows the operator to choose an appropriate optimal solution depending on the prevailing circumstances and analyzing the tradeoff between the conflicting objectives.

Finally, the generic open-source DSS, iDDEA, proposed here promotes engagement of dam operators to leverage the advances in weather forecasting and hydrological modeling in operational decision-making. The development of open-source and nonproprietary tools has now made it possible for the water resources community to benefit from the advancements in the fields of atmospheric modeling, modeling, and optimization techniques. To ensure maximum uptake of science and models, a web based DSS makes a perfect case to inform the dam operator about the most optimal set of decisions meeting the needs of different involved stakeholders of a hydropower infrastructure.

3.7 CONCLUSIONS

In this chapter, a data-driven and weather forecast-based reservoir inflow forecasting scheme is proposed for forecasting reservoir inflow to optimize reservoir operations for hydropower maximization. Short-term weather forecasts and antecedent hydrological variables were inputs to a three-layered feedforward Artificial Neural Network (ANN) to forecast inflow for 7-days of lead time. The scalability of the concept was proven by applying it over an inventory of 23 dams receiving unregulated natural inflow with varying hydrological and climate characteristics. A consistent ANN architecture and input predictor configuration was used to allow a fair comparison across dams. In addition to the antecedent conditions, short-term forecast fields from the GFS model were used as inputs to train a three-layered ANN. The forecast skill assessment suggested reliable performance with NSE value greater than 0.5 for 48% of the sites (including those on larger basins) for 7-day lead forecasts. These ANN-derived forecasts were used to perform multi-objective optimization under a rolling horizon scheme. Over two years of assessment for Pensacola dam (Oklahoma), additional 5.2% of energy could have been harvested without compromising flood risk relative to the benchmark. A web-based decision support system, operational over Detroit dam (Oregon), was presented to promote engagement of dam operators and leverage the advances in weather forecasting and hydrological modeling toward operational decision-making.

At this point, we have demonstrated the potential of a numerically efficient and skillful reservoir inflow forecasting scheme to address water-energy security challenges and bridge the gap between research and application domains. The next task is to implement this concept over complex and more common networks of multiple dams and using forecasts at multi-temporal scales. This challenge is tackled in Chapter 4.

Chapter 4. FORECAST-INFORMED HYDROPOWER OPTIMIZATION AT LONG AND SHORT-TIME SCALES FOR A MULTIPLE DAM NETWORK

Note: This chapter has been reproduced from Ahmad and Hossain (2020b) with the permission of AIP Publishing.

Ahmad, S.K., Hossain, F. 2020b. Forecast-Informed Hydropower Optimization at Long and Short-time scales for a Multiple Dam Network. Journal of Renewable and Sustainable Energy 12. doi:10.1063/1.5124097

ABSTRACT

This study presents a scheme for co-optimizing the long-term (seasonal) reservoir operating objectives with the short-term (daily) objectives for multi-dam networks to maximize hydropower generation. Long-term optimal reservoir storage provides temporal space to optimize operation of the dams at short-term based on forecasted reservoir inflow. The study asks if there is an added benefit of co-optimization of operations at long- and short-term scales for hydropower generation. Multi-objective optimization problem at both the temporal scales was simultaneously solved considering Pareto optimality between conflicting objectives. Constraints pertaining to flood control, dam safety and environmental flow were imposed. The proposed scheme was implemented over a network of Blue Mesa, Morrow Point, and Crystal dams in the Upper Colorado Basin. Ensemble forecast forcings from publicly available numerical weather prediction (NWP) and climate models were used as inputs for the daily- and monthly-scale inflow forecasts. Results show an improvement of 41%, 27% and 15% in hydropower generation using the co-optimization during wet, moderate and dry years, respectively, against a benchmark that neglects inflow forecasts. The study demonstrates added

benefit of co-optimizing the operations for hydropower generation based on short- and long-term forecasted reservoir inflow. Given that most dams today operate as a network in a river basin, we recommend moving away from single dam and single timescale optimization to a multiple-dam with long- and short-term scale co-optimization-based operations to make renewable energy generation more efficient.

4.1 INTRODUCTION

In the preceding chapter, we demonstrated the value in using data-driven approach for computationally efficient and skillful streamflow forecasting. This chapter deals with extending this approach over complex and more commonly occurring networks of multiple dams. The use of forecasts at multi-temporal scales is also explored here.

One of the least expensive and stable sources of energy with significant operational flexibility and instant power generation capability is conventional hydropower (Holmes and Papay, 2011). Hydropower has experienced comparatively much less periods of fluctuations in yield unlike wind or solar that are dependent on geographic location and ambient weather conditions (DOE 2016). To reduce the dependence on fossil fuels and promote the use of clean and renewable energy sources, the operations of hydropower dams (used here interchangeably with 'reservoirs') need to play a critical and central role. Hydropower dams that already exist are not getting phased out globally anytime soon despite the well-known costs to the environment and ecosystem services (Ligon et al., 1995; Tilt et al., 2009). Thus, efficiently managing such a resource has the potential to not only expand clean (i.e., non-fossil fuel) energy generation but also to provide resilience against extreme hydrological events, drought management and flood protection (Yang et al., 2017). As the growing population's demand for water and the resulting water stress continues to increase, building newer dam infrastructure is not a fool-proof solution and is much debated in the literature (Manyari and de Carvalho Jr,

2007; Tilt et al., 2009). Rather, if the existing dams are operated more efficiently, higher energy benefits can be achieved without building new hydropower dams. In other words, improved performance of hydropower operations can generate more energy from less dams, while providing the planned hydropower systems with smarter expansion plans (Marques and Tilmant, 2013).

Researchers and policy makers, over the past century, have been making efforts to improve the reservoir operations to better satisfy the demands of stakeholders. A major challenge towards improving the operational effectiveness of reservoirs is to integrate the forecast of weather and climate information with real-time operating policy (Dong et al., 2006). A distinction is generally made concerning the temporal scale of forecasts where short-term forecasts (daily to weekly scale) are incorporated to optimize for short-term (tactical) operational purposes while medium to long-term forecasts (monthly or seasonal scale) are used for long-term (strategic) objectives (Anghileri et al. 2016). Although this is a common notion of using forecast information to optimize reservoir operations, it suffers from drawbacks. Losses can occur to the specified operating purpose due to optimization addressing only the short or long-term objectives but not both (Sreekanth et al., 2012). Real-time operations typically rely on forecasts with a horizon of only a few days because of degrading skill in forecasts with increasing lead time (Celeste et al., 2008). However, relying only on the short-term forecasts for reservoir operations optimization results in a short-sighted policy that does not dovetail the longer-term goals. Such release decisions optimal only over short-term are prone to sub-optimality when the performance is assessed over the seasonal or annual scale (Xu et al., 2015; Sreekanth et al., 2012). Likewise, when the optimization problem addresses only the long-term planning of the reservoir operations, it uses seasonal hydro-climatic information that can introduce large inflow uncertainty at shorter time scales. Bias in long-term forecasts of inflow and conflicts between long and short-term operation goals can again lead

to a suboptimal policy over the long-term as well as over episodic extreme events (Xu et al., 2015). Therefore, it is imperative now to achieve a balance between the immediate and potential future benefits, satisfying both the short and long-term optimality in operations. Large dams that operate as a network can optimize their monthly storage and release based on seasonal (long-term) forecast of inflow. Such long-term optimization provides temporal solution space to optimize and tailor the operations of the dams at short-term (daily) scale based on reservoir inflow using weather-forecasts. We demonstrate this concept schematically in Figure 4.1.

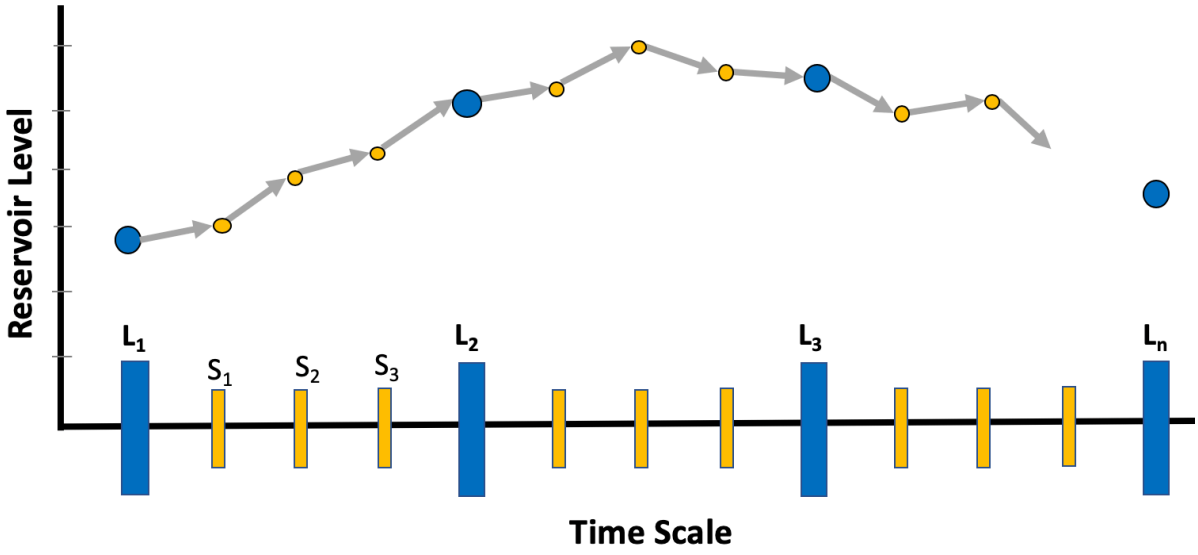

Figure 4.1 Schematic showing the concept of co-optimization where the long-term optimal goals are dovetailed with the short-term optimal reservoir operations. Blue bars (L_1, … L_n) are long-term forecast horizon units (or lead times) for obtaining storages optimized for long-term benefits while yellow bars (S_1, … S_n) denote short-term optimization horizon. The corresponding short-term optimal operations (grey arrows) result in the levels (yellow circles) that are also optimal with the long-term goals (blue circles). The co-optimization uses temporal solution space to tailor the short-term operating policy within the long-term horizon.

Dams are seldom operated individually and are usually connected in a network, often to form a multi-reservoir system with a cascade of reservoirs in series and occasionally in parallel. Operating the entire system in coordination with each dam is essential for improving the

operational efficiency and maximizing the overall benefits to the stakeholder with conflicting interests (Xu et al., 2015). Joint operation considers the storage variation in each linked reservoir and subsequently results into a set of optimal releases with simultaneous evaluation of numerous trade-offs in the best interest of each reservoir. Operating rule curves are often used to guide the operations of system of dams outlining the reservoir storage targets to be met at specific times of the year. The rules are historically developed by respective operating agencies using historical reservoir inflows, physical constraints (e.g., downstream channel capacity), and historical operating objectives (Anghileri et al., 2016). A number of reservoir planning and operation studies have optimized the rules based on the operating purpose and type of reservoir network. Lund and Guzman (1999) reviewed a variety of derived real-time operating policies for multiple reservoir networks operated for water supply, flood control, hydropower, water quality and recreation, and presented conceptual optimal rules for series and parallel reservoir networks. Marques and Tilmant (2013) underscored the economic value of coordination in a large-scale multi-reservoir system in Brazil. Zhou et al. (2016) derived optimal operating rules for multi-reservoir system in China by combining the water and power operating rules to coordinate operations. However, most of these published rules are static 'thumb rules' that cannot be relied upon when the circumstances change. For example, during extreme events of unprecedented magnitude, relying upon such rules does not guarantee the best degree of resilience or downstream safety. This necessitates a scheme of operations that is dynamically updated at shorter timescales and adjusts itself accordingly without the need to refer to static rules.

The dimensionality problem in optimizing larger systems is tackled using the aggregation of multiple reservoirs to convert into an equivalent single-reservoir optimization problem (Liu et al., 2011). This is then followed by a disaggregation scheme to obtain solutions for the single reservoirs (Saad et al., 1994). Fang et al. (2014) proposed hedging rule based on

an aggregated reservoir and storage allocation rule to specify release from each reservoir. Archibald et al. (1997) included a two-dimensional representation of the rest of the system to the equivalent aggregated reservoir. Another commonly applied approach is to optimize the releases and stored energy instead of the objective or cost function. For example, Becker and Yeh (1974) and Li et al. (2012) proposed optimal operations model that minimized the loss of release or stored energy. Furthermore, a general rule for increasing hydropower is to prioritize storage in reservoirs with highest energy production (Marques and Tilmant, 2013). However, such an approach is biased as the most 'efficient' reservoir that needs the least amount of release per unit energy generated always gets more load leading to faster storage depletion, reducing its productivity (Xu et al. 2015).

A vast majority of literature on deriving optimal operation rules has paid attention to either short-term or long-term forecast-based optimization. The value of long-term inflow forecasts (monthly to seasonal scale) has been demonstrated for flood control operations (Anghileri et al., 2016), hydropower operations (Hamlet et al. 2002; Block, 2011; Maurer and Lettenmaier, 2004; Alemu et al., 2010), irrigation and water supply (Sankarasubramanian, 2009; Georgakakos et al., 2005) and drought management (Golembesky et al., 2009). On the other hand, a few of the studies on short-term (daily to weekly) forecasts, specifically for hydropower maximization, include Ahmad et al. (2020), Monteiro et al. (2013), Madsen et al. (2009), and Fan et al. (2016). There are only a handful of studies that have focused on integrating the long-term optimization module with the short-term (daily) operations as a co-optimization strategy.

One of the first efforts to integrate the optimization models at different temporal scales was proposed by Becker et al. (1976) and Yeh (1979) for the operation of California Central Valley Project. The procedure optimizes a monthly model over one year and uses the monthly ending storages into a daily model followed by using the daily releases into an hourly model.

Georgakakos (2006) used a similar concept for developing multilayer operation model for Nile Basin. Dong et al. (2006) assessed the effect of flow forecasting quality on the benefits of single-reservoir operation. The ending monthly storage from a long-term optimization model were input as constraints to the short-term daily model. However, the long-term model uses monthly average of the observed flow series which results in a single static long-term policy and is not updated as the optimization progresses in time. Also, different levels of noise were added synthetically to the observed inflow to obtain the short-term forecasts. Synthetic forecasts render the optimization results sensitive to the added noise which are not representative of the actual value in the concept when it is operationalized. Celeste et al. (2008) integrated daily and monthly optimization models over a single reservoir operated for water supply. A deficit term was obtained from the long-term release policy representing how well the demands are met so as to trigger hedging during the short-term operations. This approach does not guide the short-term policy at each time step of the optimization horizon, rather the operations are only affected when the deficit exceeds a certain threshold. Sreekanth et al. (2012) generated synthetic forecast flows to demonstrate the nesting of long-term optimization with the short-term model at a time step of 5 days over a single reservoir in South India. Simple linear constraints were used for using the information from long-term model into the short-term optimization procedure. Xu et al. (2015) established a short-term operation model first to minimize the operation cost and then the non-dominated set of solutions was used as input to a long-term model to select the best strategy for both the temporal scales. Again, historical inflows were used to represent the possible flow scenarios to occur in the future.

Given the history of multi-reservoir optimization, there still remain a few gaps that necessitate attention from the scientific community:

(a) There are hardly any studies that integrate the short and long-term operating objectives simultaneously as a co-optimization problem while updating the optimal polices at both time scales for a multi-reservoir system, specifically for hydropower operations.

(b) The existing studies on co-optimization at the two timescales have only used synthetically generated forecasts by adding noise to the observed inflow time series which does not represent the true value in such a concept when applied operationally.

(c) Although there have been efforts to study the effect of the quality of flow forecasts on resulting optimal policy, no comprehensive framework has been developed to assess the added value in co-optimization of the operating policy at short and long-term scales against a conventional baseline with no optimization for multiple dam networks.

To address these unresolved issues for hydropower generation in the context of renewable energy sustainability, the present study uses a real-time weather forecasting model at short-term (daily) and seasonal climatic model at long-term (monthly) temporal scales to obtain flow forecasts for the co-optimization model (Ahmad and Hossain, 2020b).

The specific research questions addressed here are: *(1) What is the added value of co-optimization in time and space dimension over a multi-dam network operated for hydropower operations? (2) How sensitive is the optimal reservoir operating policy to the skill in short and long-term flow forecasts?*

The study is organized as follows. In the next section, the selected site and necessary datasets for the application of the proposed technique are described. This is then followed by a detailed description of the forecasting and reservoir operations optimization model as well as the evaluation framework in Section 4.3. The case study results of the application of short- and long-term forecasts for optimization using different strategies for evaluation are presented in Section 4.4. A sensitivity analysis of the skill of long-term forecasts is also included, followed by discussion and concluding remarks in Section 4.5.

4.2 STUDY SITE AND DATASETS

4.2.1 *Multi-Dam Network and its Operations*

The dam network chosen for the demonstration of the proposed technique is one of the four units of Colorado River Storage Project called Wayne N. Aspinall Unit. The unit is comprised of a series of three dams - Blue Mesa Dam, Morrow Point Dam, and Crystal Dam in the Upper Colorado Basin along the Gunnison River which flows further down into the Colorado River. The dams were constructed between 1963 and 1977 and are operated by the U.S. Bureau of Reclamation (USBR). A schematic of the reservoir connections and relevant hydrological stations is shown in Figure 4.2 (USBR, 2004). The drainage basin of Blue Mesa dam used for reservoir inflow modeling is also shown. Table 4.1 summarizes the characteristics of dams and powerplants in the Unit.

Table 4.1 Relevant characteristics of the dams, reservoirs, and powerplants in the Aspinall Unit.

Dam, Reservoir and Powerplant characteristics	**Blue Mesa**	**Morrow Point**	**Crystal**
Dam Type	Earthfill embankment	Double-Curvature Thin-Arch	Double-Curvature Thin-Arch
Dam Height (ft)	502.0	468.0	323.0
Spillway Crest Elevation* (ft)	7487.9	7123.0	6756.0
Crest Elevation* (ft)	7528.0	7165.0	6772.0
Total Storage Capacity (acre-ft)	940,700	117,190	25,240
Total Installed Capacity (MW)	86.4	173.3	32.0
Production Mode	Peaking	Peaking	Base Load
Number of Turbines	2	2	1
Turbine Flow Capacity (cfs)	3400	5400	2150
Bypass Capacity (cfs)	4500	1500	1900
Spillway Capacity (cfs)	34000	41000	41350

* Above mean sea level

The upstream-most and largest reservoir, Blue Mesa, is responsible for the primary water storage in the system. The powerplants at Blue Mesa and Morrow Point are highly

flexible with the release rates and can be operated to provide peaking power. The five turbines at the three dams

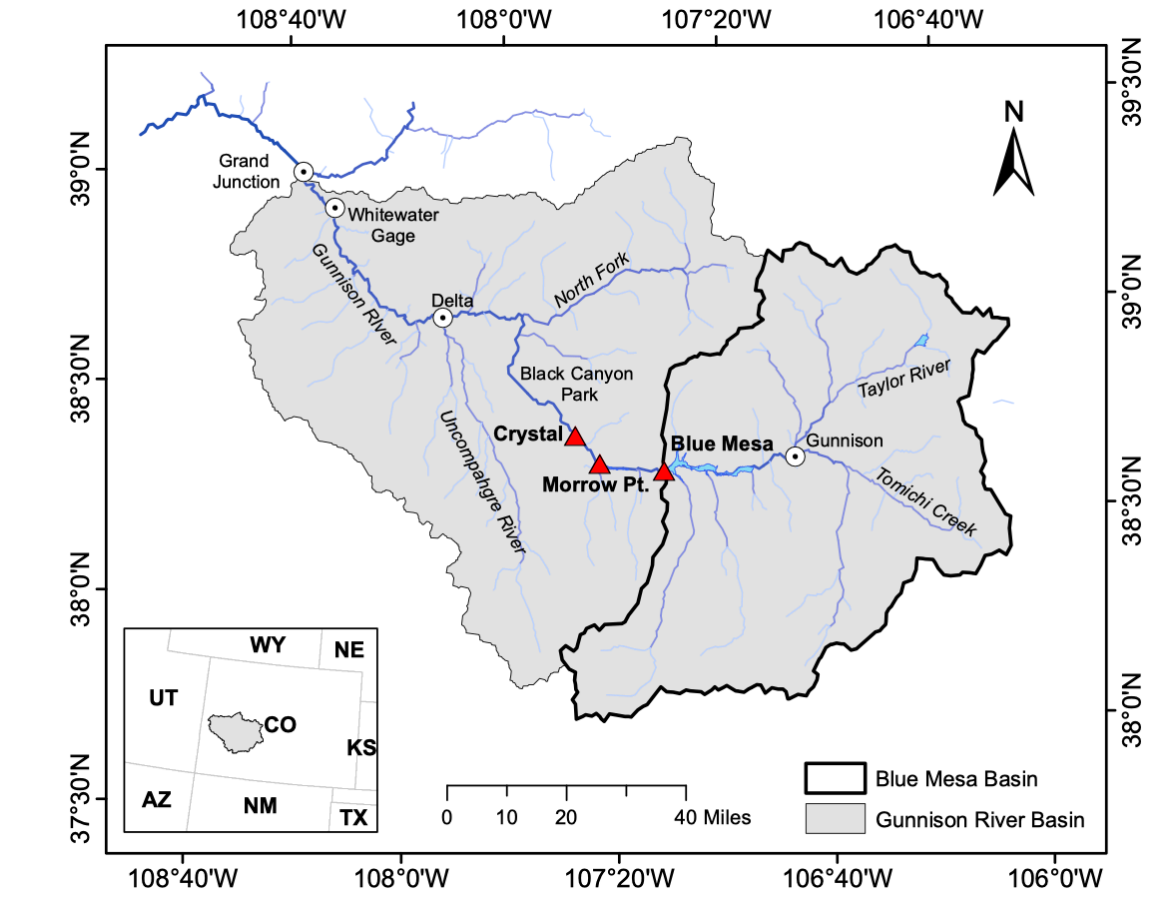

(a)

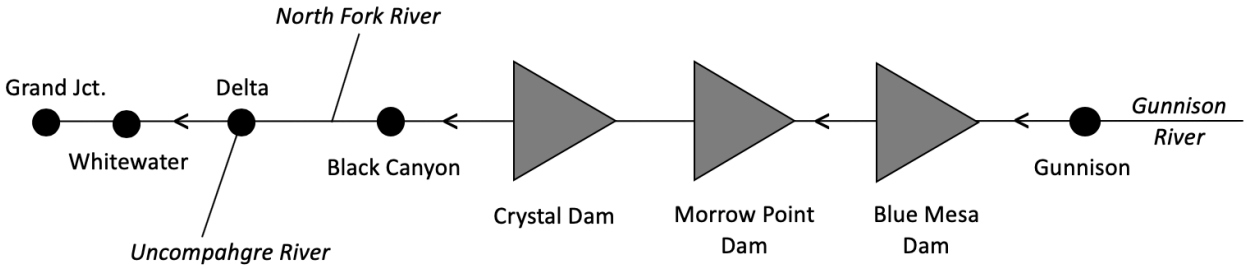

(b)

Figure 4.2 (a) Dams in the Aspinall Unit, pertinent hydrological stations, Gunnison River and Blue Mesa drainage basins; (b) Simplified schematic showing the dam connections and relevant stations (not to scale). Arrows show the flow direction (upstream to downstream).

are capable of generating up to 291 megawatts (MW) of electricity. The powerplant at Morrow Point produces largest amount of energy, around twice as much as Blue Mesa. Crystal Reservoir serves as a regulation reservoir to stabilize flows to the Gunnison River and is usually operated under constraints to regulate downstream flows. The dam releases can be made via powerhouses/penstocks, bypass or spillway routes. The USBR manages the releases within certain sideboards that include annual snowpack conditions, senior water rights, minimum downstream flow requirements, powerplant and outlet capacities, reservoir elevation goals, fishery management recommendations, dam safety and other considerations. Certain operational goals are mandated to honor these sideboards which were used to design constraints for the optimization model. These goals include but are not limited to the following (see Figure 4.2 for hydrological stations):

a) The desired Whitewater gage peak flow (USGS station 09152500) to be obtained every year based on the April-July forecasted inflow into Blue Mesa reservoir.
b) Flow at Gunnison River above the confluence with Uncompahgre River to be kept below 15,000 cfs.
c) Peak releases be typically made between May 10th and June 1st, giving priority to powerplants followed by bypasses and spillways.
d) Blue Mesa Reservoir to be kept at or below 7,490 feet (580,000 acre-feet live storage) by December 31st to provide storage for next spring's runoff and minimize upstream icing.
e) Minimum downstream flow through the Black Canyon of the Gunnison National Park and Gunnison Gorge National Conservation Area is 300 cfs, except in severe drought when flow may be reduced.
f) Maximum releases from Crystal Dam, outside of the peak flow period, be limited to the 2,150 cfs powerplant capacity.

Daily ramping rates at Crystal Dam limited to increases in 500 acre-ft and decreases of 400 acre-ft per day.

4.2.2 *Operational and Hydrometeorological Data*

The observed operational data for the Aspinall Unit was obtained from the USBR's data portal (https://www.usbr.gov/rsvrWater/HistoricalApp.html; Aspinall Unit Water Operations, 2019) that include observed inflows, releases, reservoir elevation, storage and hydropower generated. The operational data was used for setting up the optimization model as well as in calibration and validation of the forecasting models. The hydro-meteorological forecast forcings, basin's antecedent conditions, and current reservoir state (from USBR) were inputs to the inflow forecasting model. The forecast fields of precipitation, temperature and windspeed were acquired from the Global Forecast System (GFS) global-scale NWP model at 0.5˚ for 7 days lead time with a 3-hourly temporal resolution. To include the uncertainty estimates in the forecast flow, NOAA's Global Ensemble Forecasting System Reforecast (version 2) dataset (GEFS/R) (Hamill et al., 2013) with 11-member ensemble of forecasts at 1˚ resolution was used. The average scenario of the ensemble members was used for optimizing the reservoir operations. The antecedent basin precipitation was obtained from the Climate Hazards Group InfraRed Precipitation with Station data (CHIRPS) gridded rainfall time series at 0.05˚ resolution (Funk et al., 2015). The gridded datasets were converted into basin-averaged estimates for inputs to the forecasting model.

For the monthly-scale long-term forecasting model, in addition to the antecedent monthly streamflow, the ensemble seasonal forecast forcings from the climate model suite of North American Multi-Model Ensemble (NMME) were used (Kirtman et al., 2014). The diversity of models in NMME provides a superior representation of multi-model uncertainty in seasonal forecast skill, on average, relative to other seasonal prediction systems. Because it is computationally challenging to use each of the ensemble models present in the NMME suite

for optimization, two models were chosen to obtain enough ensemble members that are representative of the uncertainty in modeled forcings. These were: (i) Climate Forecast System version 2 (CFSv2) for monthly precipitation fields (Saha et al., 2014), and (ii) Geophysical Fluid Dynamics Laboratory (GFDL) CM2.1 model for sea surface temperature fields (Delworth et al., 2006). An additional predictor of the SST anomaly-based index of Niño 3.4 was also used for the monthly forecast model, retrieved from the National Oceanic and Atmospheric Administration Earth System Research Laboratory (NOAA-ESRL) (http://www.esrl.noaa.gov/psd/data/climateindices/list/). The period of analysis used to setup the long-term forecasting model extended from 1980-2018, while that for short-term weather forecasting ranged from 2007-2018.

4.3 METHODS

The general approach followed in this study and the experimental components are schematically shown in Figure 4.3. The following sections describe the methodological components in detail.

4.3.1 *Short-term ensemble flow forecasting*

To obtain the short-term forecasts for 7 days lead time for inflow into each of the three reservoirs in the dam network, two kinds of models were incorporated: (i) Data-based artificial neural networks (ANN) model for Blue Mesa dam which is the most upstream in the multi-dam network, (ii) Linear regression model for the Morrow Point and Crystal dams which lie downstream. The ANN model was specifically chosen for Blue Mesa dam because it receives most of the unregulated flow and the nonlinearities in the hydrological response are most suited for a complex model like ANN. However, for the next two downstream dams, the inflows are highly dependent on the release from the upstream dam and hence do not require complex

modeling exercise. As the skill in modeling the system inflow is mostly driven by the most upstream Blue Mesa dam, the focus was to improve the quality of Blue Mesa's forecast inflow using ANN. The specifics of the ANN model are described next followed by the linear regression model and ensemble forecast processing.

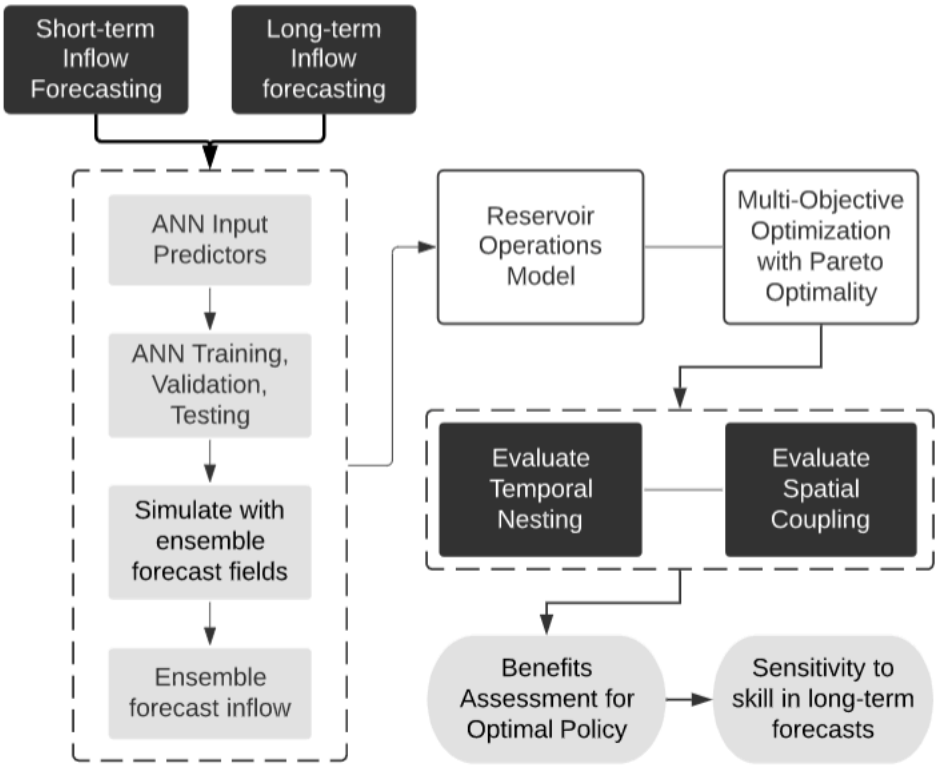

Figure 4.3 Schematic of the approach showing key experimental components of the study. See Table 4.4 for explanation of the evaluation framework strategies.

4.3.1.1 ANN model for daily flow forecasting

The daily forecasting model is based on a feedforward neural network involving input, hidden and output layers. Considering the reservoir and basin characteristics, the candidate input layer nodes were identified as: (i) forecast fields of precipitation and temperature, obtained from the GFS model at 0.5˚ resolution; (ii) antecedent precipitation over the basin, (iii) antecedent streamflow into the reservoir; and (iv) antecedent baseflow. A procedure was followed similar to that used by Ahmad et al. (2019) for selecting the optimal set of input predictors to this ANN model. The final predictor set included antecedent precipitation (2 days), antecedent baseflow

(3 days), antecedent inflow (1/2/3 days based on lead time), antecedent moving average inflow (3/5/8-day window based on lead time), forecast precipitation (1 day) and forecast min/max temperature (1 day each). The configuration of the short-term ANN model is shown in Figure 4.4. The ANN was trained using Levenberg-Marquardt (LM) method and measures of early stopped training (STA) and regularization were taken to avoid overfitting and lack of generalization (underfitting). The period of Jan 2007 to Aug 2014 was used as the *training set*, while the *validation* and *testing sets* were selected as Sep 2014 – Oct 2015 and Nov 2015 – Dec 2017, respectively.

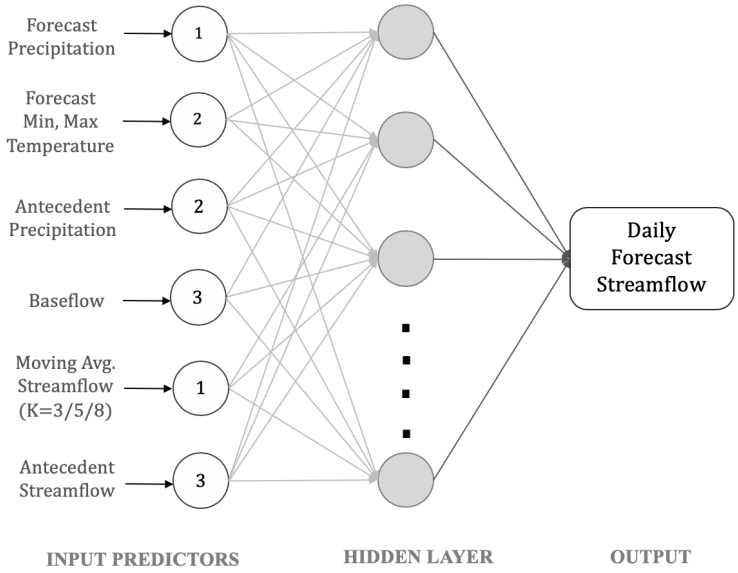

Figure 4.4 ANN model configuration with selected input predictors for daily streamflow forecasting over Blue Mesa dam. Log sigmoid and linear transfer functions were used for hidden and output layers, respectively. The number of antecedent/forecast days for each node are also shown. K is the window length for moving average streamflow that varies with the forecast lead time.

4.3.1.2 Linear Regression Model for Downstream dams

Using the modeled inflow into the most upstream dam, a linear regression model was developed to route the release from upstream dams to inflow into the downstream reservoirs. The linear regression model was deemed fit for the purpose as the two downstream dams, Morrow Point and Crystal, mostly receive regulated flow with minimal contribution from the

intermediate tributaries. The two sets of linear regression models were developed: (a) between Blue Mesa release and Morrow Point inflow, and (b) between Morrow Point release and Crystal inflow. The linear relationships and the respective correlations are shown in Figure 4.5.

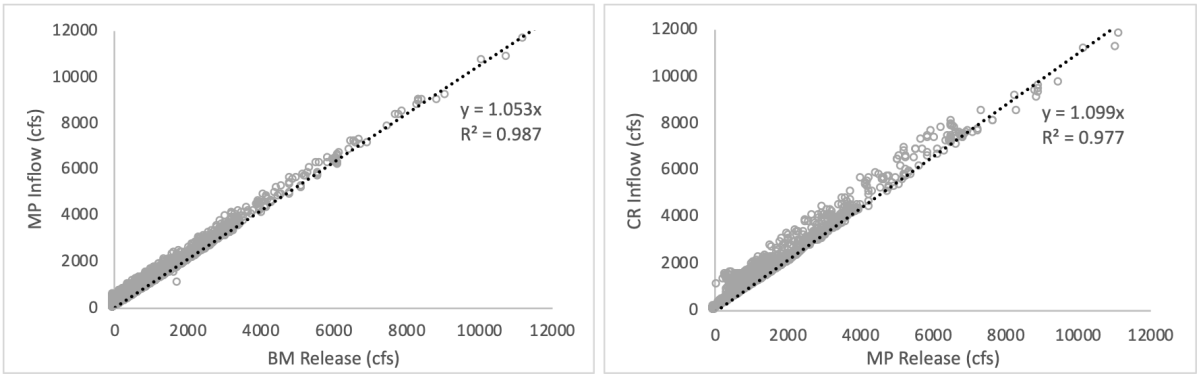

(a) (b)

Figure 4.5 Scatter plots showing linear regression between release and inflow of the upstream-downstream dam pairs of (a) Blue Mesa (BM) – Morrow Point (MP) and (b) Morrow Point (MP) – Crystal (CR) dams.

4.3.1.3 Ensemble flow processing

After the base reservoir inflow models (ANN-based for Blue Mesa and linear regression-based for other two dams) were developed to obtain deterministic inflow forecasts for 1-7 days lead time, the uncertainty in forecasts was modeled next for the Blue Mesa dam inflow. The trained ANN model was fed with 11 ensemble scenarios of the forecast forcings from GEFS model to result in the ensemble inflow forecast. Given that the reservoir operations model was designed to use a deterministic optimization technique, the average scenario of the ensemble forecast members was used in the optimization model (see section 3.3). The average of the ensemble flow forecasts showed higher skill compared to the deterministic forecasts obtained using GFS forcings (see Table 4.5). The higher skill in the average scenario of GEFS-based ensemble forecast flow as compared to the deterministic daily forecasts from GFS was also confirmed in a study by Ahmad et al. (2019) for multiple dams in US.

4.3.2 *Long-term ensemble flow forecasting*

For nesting the short-term optimization model with long-term operations, long-term flow forecast model was developed to result into monthly inflow forecasts for up to 7-months in future. Similar to the short-term forecasting, a feedforward ANN model with one hidden layer was designed to forecast the inflow into the most upstream Blue Mesa dam. However, an entirely different set of input predictors from the NMME climate model outputs suitable to capture seasonal variations in seasonal runoff was developed. Based on a predictor selection analysis similar to that for short-term ANN model, the input predictors were forecast precipitation (1 month; from CFSv2 model), forecast sea surface temperature (1 month; from GFDL CM2.1 model), antecedent inflow (1/2/3 months based on lead time), antecedent baseflow (3 months), antecedent moving average flow (3/5/8-month window based on lead time), and Niño 3.4 index (1 month). The climate models in NMME contain 12 ensemble members (realizations) for each variable, which were used to train the ANN model. The average trace of the forecast flow was used for optimization. For the other two downstream dams, the linear regression model for daily forecasting was used under the assumption that inflow contributions from tributaries at monthly scale is insignificant. The available dataset was divided into *training*, *validation* and *test* sets extending from 1981-2007, 2008-2011 and 2012-2018, respectively.

4.3.3 *Reservoir Operations Optimization*

The forecast flow information obtained from short and long-term forecasting models was used as input to the optimization model for obtaining optimal release decisions. The focus of this study was on hydropower maximization which was formulated as the major objective. Other constraints were incorporated into the model representing flood control, environmental flow concerns, and dam safety. The short-term optimization model was set up with daily

temporal scale over 7-day horizon, while the long-term model was developed to output optimal release decisions at monthly scale with optimization horizon of 7 months. The nesting of the two optimization models was carried out by using long-term optimal reservoir state to formulate a complementary objective function into the short-term model at every time step of the horizon. Different operation strategies were devised to evaluate the value in co-optimization. The long-term optimization model is described next which is the basis for the nesting procedure, followed by short-term optimization and the evaluation strategies.

4.3.3.1 Long-term ensemble flow forecasting

The optimization model for monthly release decisions is based on two objective functions – maximizing the total hydropower generation from all powerplants in the system and minimizing the deviation of elevation of Blue Mesa dam at the end of year from a required target level. As the skill in long-term forecasts degrades with the increasing lead time, the model predictive scheme (MPC) was employed at the monthly scale that updates the flow forecasts at every step of the optimization horizon (Turner et al., 2017; Ahmad and Hossain, 2020). The spread of the ensemble flow forecasts was ignored in the deterministic optimization procedure so that it can provide a clear indication of the contribution of forecasts to the optimal operation performance (Turner et al., 2017).

The two objectives are formulated below.

1. Maximizing hydroelectric power production (MW) from the system's three powerplants,

$$\max f_1(MW) = \sum_n \sum_t \epsilon^n \cdot \Delta t^n_{turb} \cdot (HF^n_t - HT^n_t) \cdot R^n_{p,t} \quad (4.1)$$

where, t is optimization horizon of 7 months, n is the index for reservoir in consideration, n = 1, 2, 3, HF and HT are reservoir forebay and tailrace water levels

(ft), ϵ is turbine efficiency, Δt_{turb} denotes turbine operating hours and R_p is power release from turbines (cfs).

2. Minimize the absolute value of deviation of reservoir elevation from the target level (T) in the month of December (H_{Dec}) for Blue Mesa dam. This is to satisfy the requirement for Blue Mesa dam to return to 7,490 ft on December 31st to provide storage for next spring's runoff and minimize upstream icing. Under the MPC scheme of optimization, the objective is only implemented for horizons containing the month of December.

$$\min f_2(ft) = |\mathrm{H_{Dec}} - T| \tag{4.2}$$

The energy production function in equation 4.1 requires the knowledge of turbine efficiency and number of operating hours for everyday operations. Because the turbine operating characteristics usually vary over the year and within any day of operations, a regression model was developed for estimating energy generation. Linear regression was performed between the observed hydropower (in MWh) and the product of hydraulic head ΔH and power release R_p based on the historical data. The obtained regression constant captures the unknown turbine efficiency ϵ and operating hours Δt_{turb}. The constants were obtained as 17.02 hours, 18.64 hours, and 12.22 hours for Blue Mesa, Morrow Point and Crystal dams, respectively. Multiple constraints were imposed on the long-term optimization model considering flood control, dam safety, environmental flow requirements, and operational restrictions for Aspinall reservoirs specified in the control manuals. Various operational restrictions specified by the control manuals (USBR, 2004; USBR, 2012a; USBR, 2012b) (see section 2.1) were considered for setting up the constraints as summarized in Table 4.2.

Table 4.2**.** Dam-specific and general constraints imposed on the monthly optimization model

Dam-specific constraints	**Value**
Blue Mesa Dam	
Minimum elevation	7393.0 ft
Maximum elevation (Jan-Mar)	7490.0 ft

Maximum elevation (Apr-Dec)	7519.4 ft
Elevation on Dec 31	7490.0 ft
Morrow Point Dam	
Minimum elevation (Jun-Sep)	7151.0 ft
Minimum elevation (Oct-May)	7143.0 ft
Maximum elevation	7160.0 ft
Crystal Dam	
Minimum elevation	6725.0 ft
Maximum elevation	6772.0 ft
General constraints	
Minimum monthly release	2500 cfs
Maximum monthly release	64,500 cfs
Maximum monthly release (May 10 – Jun 1)	220,000 cfs

4.3.3.2 Short-term daily optimization model

Daily-scale multi-objective optimization model using the MPC scheme was set up to generate optimal release decisions for one week ahead in future. The primary and secondary objectives varied with the strategy of optimization (see Table 4.4). The ensemble forecast spread was ignored during the optimization for reasons mentioned under long-term optimization model. The constraints for optimization were tailored to account for the daily-scale reservoir operations of the three dams. In addition to the constraints for long-term optimization model, the daily ramping rates for Crystal dam release and daily maximum change in the Crystal reservoir forebay elevations were constrained by the values specified in the control manuals and are summarized in Table 4.3.

Table 4.3**.** Additional constraints imposed on daily scale short-term optimization model

Dam-specific constraints	**Value**
Crystal Dam	
Maximum elevation change (Apr-Jun)	4 ft per day
Maximum elevation change (Jul-Mar)	10 ft per day
Daily ramping rate - increase	500 acre-ft per day
Daily ramping rate - decrease	400 acre-ft per day
Morrow Point Dam	
Daily ramping rate – increase/decrease	2000 acre-ft per day
Blue Mesa Dam	
Daily ramping rate – increase/decrease	2000 acre-ft per day
General constraints	

Minimum daily release	300 cfs
Maximum daily release	2150 cfs
Maximum daily release (May 10 – Jun 1)	12500 cfs

4.3.3.3 Optimization Algorithm

The multi-objective optimization problem was solved using the deterministic genetic algorithm-based optimization. Due to the conflicting nature of objective functions, a non-dominated or Pareto set of solutions is needed where one objective function cannot be improved further without violating the other. To implement the Pareto optimality, the Non-dominated Sorting Genetic Algorithm (NSGA-II; Deb et al., 2000) was used. Open-source library *platypus* (https://platypus.readthedocs.io) was incorporated to formulate the multi-dam optimization problem. The algorithm produces a set of Pareto optimal solutions (with the user-defined size of Pareto optimal set), from which the dam operator can choose the preferred solution based on which objective function receives priority according to the situation at hand. For the sake of this study, a balanced optimal solution was selected on the Pareto front that gives equal weightage to both the objectives. Pareto optimization allows for different units of objective functions without the need to transform to consistent units which is often difficult to achieve (Madsen et al., 2009).

4.3.4 *Co-optimization at Long-term and Short-term scales*

The proposed strategy optimizes the operations of the cascade of dams in tandem while considering the long-term benefits for short-term optimality. We coin this co-optimization as *temporal nesting with spatial coupling* (TeNeSC). The TeNeSC-based optimization is carried out in two steps, first the long-term model, as described in section 3.3.1, is used to obtain monthly optimal release decisions over an optimization horizon of seven months into the future. The monthly optimal operations yield the optimal reservoir states at the end of each month. The end-of-month reservoir storages over the 7-month horizon are linearly interpolated to result into the daily levels that form the boundary conditions or constraints for the short-term

daily scale optimization model. The small storage of dams in consideration (capacity to annual inflow ratio close to one) results in variability in the reservoir state at daily scale and justifies the daily timestep for short-term optimization (Anghileri et al., 2016). Furthermore, the 'coupled' component in TeNeSC scheme signifies the joint operation of the dam network, where the co-optimization is carried out by simultaneously considering releases from all the dams. The water released from the upstream dam reaches the downstream reservoir with a certain delay equal to the flow travel time along the reach. The delay time usually ranges from several hours and extends to days only when the flow travel time is long enough in large multi-reservoir systems (Souza and Diniz, 2012; Ge at al., 2014). Given that the present study considers daily scale operations over medium scale inter-reservoir reaches, the delay time was neglected in the routing of streamflow. A schematic illustrating the temporal nesting of the optimization models is shown in Figure 4.6.

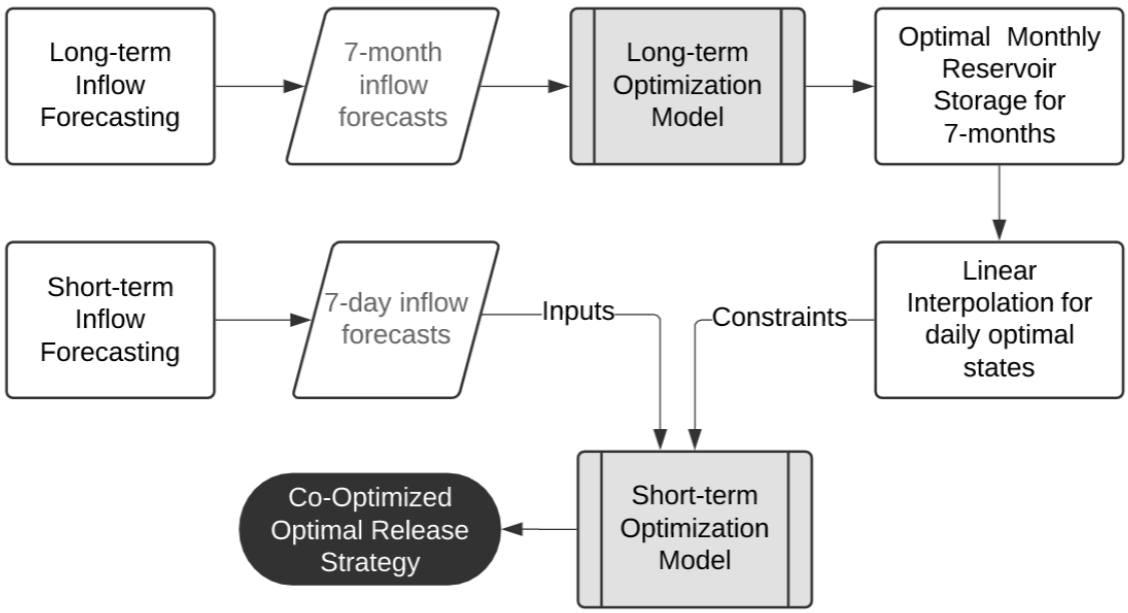

Figure 4.6 Schematic explaining the procedure of co-optimization with the long- and short-term objectives.

The boundary conditions were used to formulate the secondary objective for the short-term optimization model where the primary goal is hydropower maximization across all the

dams in the network. The objective was set to minimize the deviation of elevation from the boundary conditions (or target elevation) reflecting the long-term optimal conditions over the short-term optimization horizon. Because the main purpose of Crystal dam is to act as a regulator of the upstream releases, there is a lesser flexibility left for the optimal reservoir level for hydropower maximization. This was taken into consideration by obtaining the deviation of reservoir levels only on the first day of the optimization horizon. Higher weight is indirectly assigned to the secondary objective as the MPC scheme only considers the first day's optimal release and discards the rest. However, for Blue Mesa and Morrow Point dams, the deviation was obtained at the last (seventh) day of the horizon as they are operated for peaking power and permit higher flexibility in operations. Mathematically, the secondary objective is formulated as:

$$\min f_2(ft) = |H_7^1 - T_7^1| + |H_7^2 - T_7^2| + |H_1^3 - T_1^3| \tag{4.3}$$

where, H_t^n is the n^{th} reservoir's storage (numbered from upstream to downstream dam) at time step t. The optimization problem was bounded by the fundamental long-and short-term constraints on reservoir storages and releases described in the sections 3.3.1 and 3.3.2. Apart from those, the continuity constraints for the three reservoirs over each time step t of the optimization horizon can be mathematically stated in vector form as:

$$\boldsymbol{S_i}(t+1) = \boldsymbol{S_i}(t) + \boldsymbol{I_i}(t) + \boldsymbol{M}.\boldsymbol{R_i}(t) \tag{4.4}$$

where $\boldsymbol{S_i}(t)$ is the vector of storages in reservoirs $i = 1, \dots n$; $\boldsymbol{I_i}(t)$ and $\boldsymbol{R_i}(t)$ are vectors of inflows into and release from each reservoir, and $\boldsymbol{M}$ is a $n * n$ square matrix representing the indices of reservoir connections,

$$\boldsymbol{M} = \begin{bmatrix} -1 & 0 & 0 \\ 1 & -1 & 0 \\ 0 & 1 & -1 \end{bmatrix}$$

For the continuity constraints, storage-elevation relations were obtained as second-order polynomial equations for each reservoir using 15 years of historical data (2004-18) using

which the storage at each time step was converted to respective reservoir level. The coupled optimization model solves a giant matrix for all the reservoirs to derive the optimal reservoir release decisions and their respective states at each time step.

4.3.5 *Evaluation framework for co-optimization*

To answer the first research question of this study and establish the efficacy of co-optimization, several strategies of optimization were implemented under an evaluation framework. The objective is to separately underscore the value in two different facets of co-optimization for maximizing hydropower: (a) nesting of short- and long-term objectives in time, and (b) coupling of reservoirs in space. Table 4.4(a) and Table 4.4(b) summarize the specifics of each strategy for evaluating temporal nesting and spatial coupling.

Table 4.4 (a) Specifics of strategies under the framework to evaluate value in temporal nesting, formulated as multi-objective problem.

Strategy	**Formulation**	**Description (all spatially coupled)**	**Objective**
TeNeSC	Short + Long	• Uses nested co-optimization at long and short-term scales • Continuity constraints formulated as one giant matrix (equation 4.4)	***Primary***: Maximize hydropower ***Secondary***: Minimize deviation of reservoir elevation from target levels based on long-term optimality (equation 4.3)
T1	Short-only	• No use of nested co-optimization • Continuity constraints same as TeNeSC	***Primary***: Maximize hydropower ***Secondary***: Minimize absolute deviation between reservoir release and turbine capacity: min $f_2(cfs) = \sum_{i=1}^{n} \sum_{t=1}^{T} \lvert R_t^i - T_{cap}^i \rvert$ (n: number of reservoirs; T: short-term horizon of 7 days).
T2	Long-only	• No use of nested co-optimization • Considers long-term optimality only during daily optimization	***Primary***: Minimize absolute deviation of reservoir elevation H from target levels based on long-term optimality T for the first day of horizon min $f_1(ft) = \sum_{i=1}^{n} \lvert H_1^i - T_1^i \rvert$

	• Continuity constraints same as TeNeSC	(n: number of reservoirs) ***Secondary***: Same as secondary objective in T1

Table 4.4 (b) Specifics of strategies under the framework to evaluate value in spatial coupling.

Strategy	**Formulation**	**Description (both temporally nested)**	**Objective**
TeNeSC C1	Coupling No Coupling	• Same as in Table 4.4(a) • No coordination amongst reservoir release decisions. • Separate optimization models developed for each reservoir; regression model converts upstream release into downstream inflow	Same as in Table 4.4(a) ***Primary***: Maximize hydropower ***Secondary***: Same as TeNeSC, deviation calculated individually for each reservoir in the respective optimization model

An additional aspect that needs consideration for demonstrating the robustness of this concept is the value of real-time forecasting model in improving the operational benefits of the dam network. Our study accomplishes this by considering two different scenarios of obtaining the inflow forecasts –

a) *perfect forecast scenario* that stands as a hypothetical benchmark of maximum attainable benefits using the different strategies described above. Here the observed inflow is used as a proxy to the forecasts over the desired optimization horizon to simulate the perfect forecast scenario.

b) *operational forecast scenario* where the reservoir inflow forecasts are obtained using the short- and long-term forecasting models developed in sections 3.1 and 3.2. This scenario is representative of the practically possible benefits using an operational flow forecasting (Ahmad and Hossain, 2020a). The technique is operational for real-time reservoir inflow forecasts for Ganges and Brahmaputra river basins (http://depts.washington.edu/saswe/datavis_Timeseries.html).

4.3.6 *Benchmark Scheme*

To obtain the actual value in using forecast information for realizing optimal operations, a benchmark operating scheme is necessary that by itself neither uses any forecast information nor is based upon any co-optimization at different timescales. Rather, the benchmark scheme should be reflective of control rules designed with respect to certain operating objectives, that the dam operator follows in practice. Thus, to set up a fair benchmark, a customized control-rules based operation scheme was designed to specifically address the hydropower maximization objective (Turner et al. 2017), which is also the basis of strategies described under the evaluation framework. The control rules were designed in the form of look-up table where the optimal release is specified as a function of two state variables – reservoir storage and season of year, as proposed by Turner et al. (2017). The stochastic dynamic programming (SDP)-based optimization procedure coded in the R package *'reservoir'* (Turner and Galelli, 2016) was incorporated to optimize for these rules. The observed inflows for 15-year period (2004-2018) were used for each dam as input to the SDP model, including the reservoir and objective function specifications. Three separate set of control rules were obtained for each reservoir at monthly time step, with no coupling between the operations of adjacent reservoirs. To assess the benefits against this benchmark, a metric called *percent improvement over benchmark* (IB) was formulated as,

$$IB\ (\%) = \frac{HP_{optim} - HP_{bm}}{HP_{bm}} * 100 \tag{4.5}$$

where, HP_{optim} and HP_{bm} are the total hydropower production from the three dams of the Aspinall Unit using optimized and benchmark reservoir operating schemes.

4.3.7 *Effect of skill in long-term forecasts*

The skill in long-term monthly flow forecasts usually degrades rapidly as compared to that in the short-term daily-scale forecasts. As the temporal nesting uses long-term forecasts as

boundary condition for the daily-scale optimization model, the performance is primarily driven by the skill in the long-term forecasts. For instance, any major error in predicting the onset of flood or drought season can cause the short-term release decisions to be optimized towards an objective function that does not reflect long-term optimality. This can potentially result into sub-optimal operations both in the short and long terms. Hence, it is imperative to assess how the skill in monthly ANN-based forecasts affects the resulting optimal reservoir operation policy.

The observed monthly inflow data was synthetically corrupted to simulate underestimation and overestimation in the flow forecasts. Six perturbed monthly inflow timeseries were generated by adding multiplicative bias with six different constants, three of which simulated underestimation (multiplicative constant < 1) while the rest simulated overestimation in the predicted inflow (multiplicative constant > 1). The multiplicative factors simulate the worst-case scenarios of consistent over- or under-prediction of the flows across the period of analysis. Also, as the forecast error is more likely to increase for higher river flows (Montanari and Grossi, 2008), the proposed factors were able to replicate increasing bias in forecasts for higher inflow. Perturbed monthly inflow timeseries were used to carry out the co-optimization (TeNeSC) using the perfect short-term inflow forecasts. The resulting reservoir elevations and hydropower benefits were compared across the different perturbed scenarios to assess the effect of degrading skill in long-term predictions.

4.4 Case Study Results

4.4.1 *Reservoir Operations Optimization*

The proposed concept of co-optimization and strategies for evaluation were implemented over the selected multi-dam network of Aspinall Unit of Blue Mesa, Morrow Point and Crystal dams. Three years (2016-18) with different inflow characteristics were selected for the

analysis. While 2016 was a moderately wet year with 441,535 cfs of annual inflow into the system, 2017 and 2018 experienced anomalously wet and dry conditions with 629,083 cfs and 211,853 cfs of annual inflow, respectively. The different flow conditions were chosen to further underscore the robustness of this technique under different seasons of dam operations. The detailed results are described in the following sections. Assessment of the forecast skill in short and long-term ANN flow forecasting models is described in detail in Appendix C for the interested readers.

4.4.1.1 Evaluation framework

The long-term optimal policy derived from the monthly scale optimization model were used for the strategies that nest long-term benefits with short-term optimization (i.e. TeNeSC and C1). For the other strategies used for evaluation, either only the short-term forecasts (T1) or long-term forecasts (T2) were used for the optimization. Figure 4.7 shows the optimal reservoir elevations using these strategies using perfect forecasts for the three years, while Figure 4.8 shows the corresponding optimal elevations obtained using the operational forecasts (ANN-based for Blue Mesa and regression-based for the others). The long-term optimal policy of operations is also shown alongside in each plot.

When the optimization model uses temporal nesting and considers the three reservoirs as a network (TeNeSC), the reservoir levels from short-term optimization model are adjusted according to closely follow the long-term optimality. The long-term optimal policy tends to maximize the reservoir storage for the downstream two dams, where the upstream Blue Mesa dam acts as buffer for maximizing the energy generation. The resulting flexibility in the operation of upstream dams enables them to provide peaking power while Crystal dam traces the long-term optimal levels with minimal changes in reservoir levels. Considering the strategies used to evaluate TeNeSC, the short-term optimization (T1) results in lower storage levels for the downstream dams, resulting in lower hydropower benefits in the long-run due to

its myopic nature. On the contrary, long-term only strategy (T2) tends to closely trace the monthly target levels but loses additional hydropower benefits in short-term possible by tweaking the daily release decisions accordingly (Table 4.5).

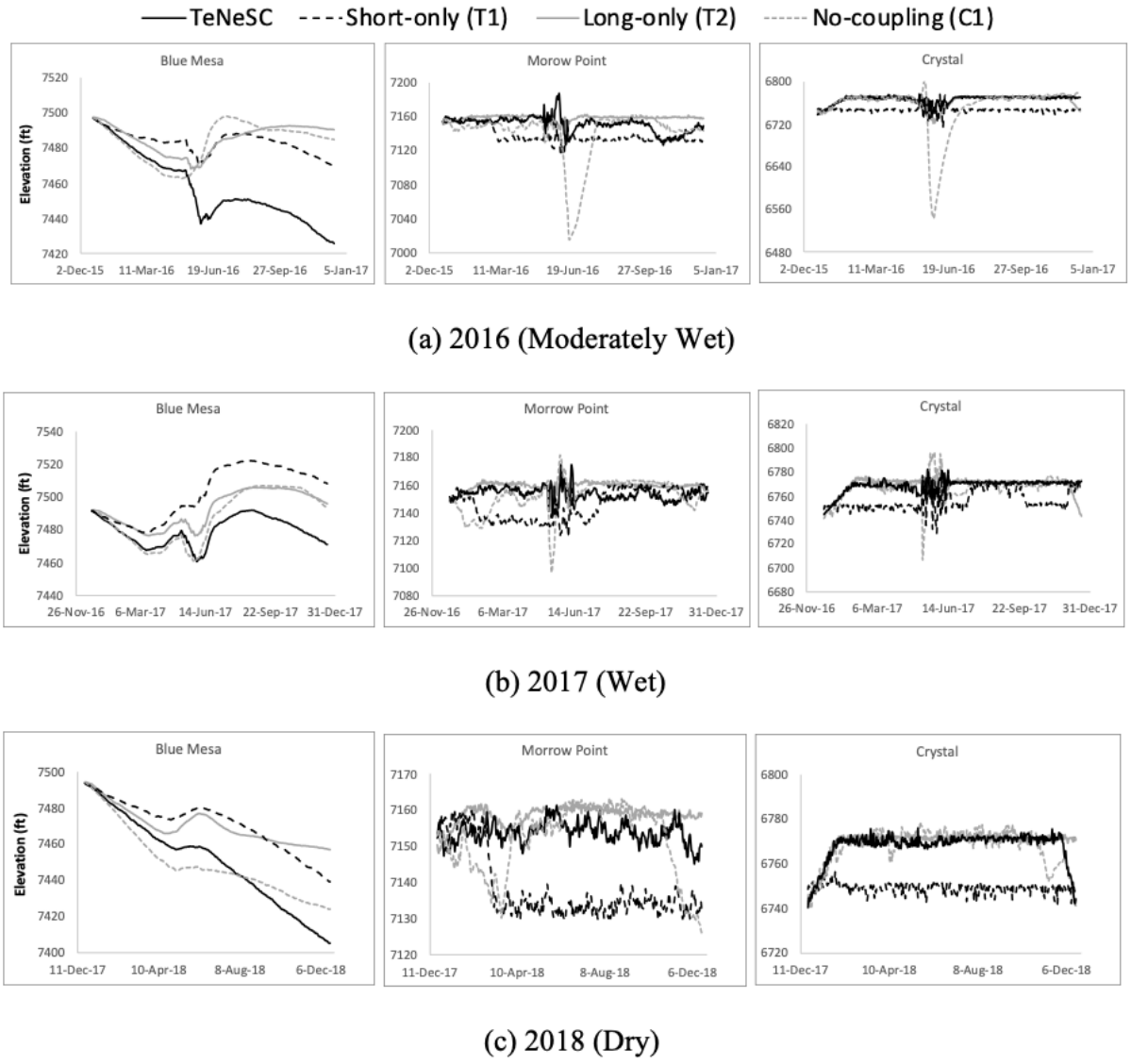

Figure 4.7 Optimal reservoir elevations from the different strategies using perfect forecast scenario for the three dams over the three years with different flow characteristics.

Further, the value in spatial coupling was assessed separately by comparing TeNeSC with no-coupling scenario (no coordination among reservoir release decisions; C1). Results from C1 suggest that one of the two downstream dams undergo major fluctuations in reservoir levels, even violating the storage constraints for a few days irrespective of co-optimization at

the long- and short-term scales. The fluctuations primarily occur during the peak flow season of wet years. In contrast, spatial coupling of dams further facilitates in keeping the reservoir levels within safe bounds and prevents violation of the storage constraints. TeNeSC helped avoid any sudden surge or steep dip in the reservoir levels during the wet and dry years. Finally, the high accuracy of operational forecasts leads to optimal policies similar to those obtained by the use of perfect forecasts (see Figure 4.8).

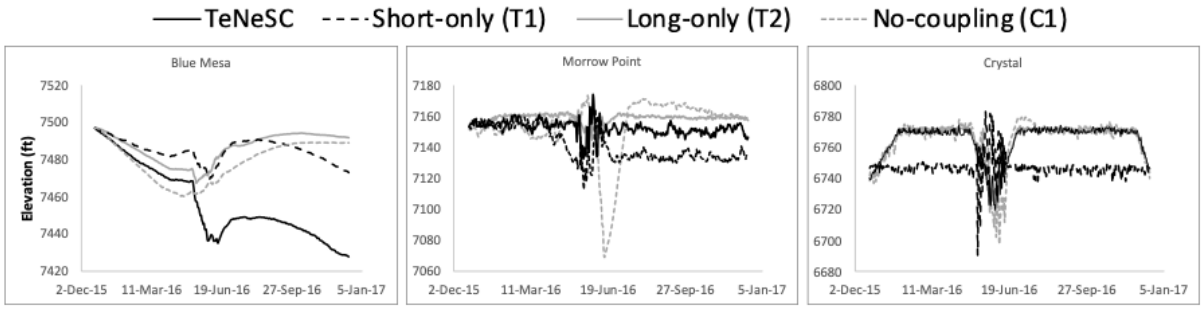

(a) 2016 (Moderately Wet)

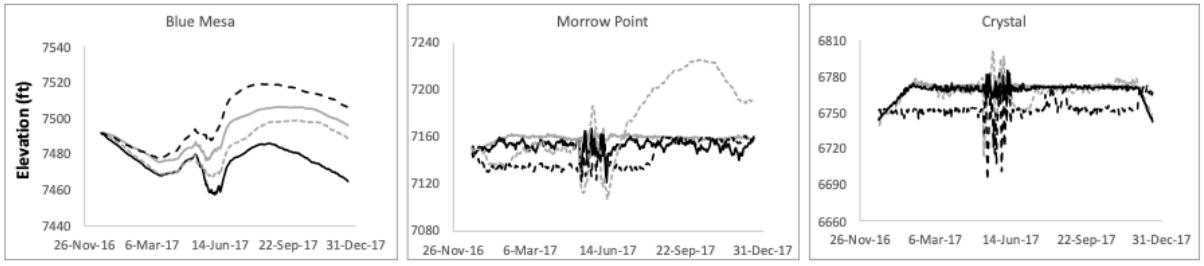

(b) 2017 (Wet)

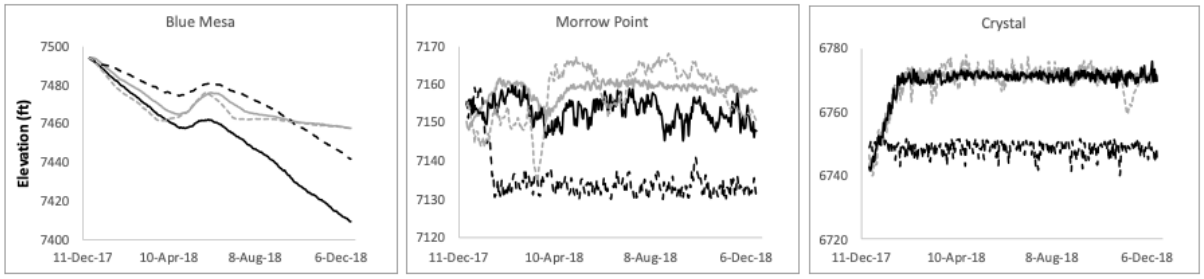

(c) 2018 (Dry)

Figure 4.8 Optimal reservoir elevations from different strategies using operational forecasts (ANN/linear regression-based) for the three dams.

4.4.1.2 Benchmark Scheme

The reservoir storage and resulting hydropower generation (MW) using the benchmark scheme are shown in Figure 4.9 for the three dams. The scheme is derived individually for each dam in the network based on the observations over 2004-2018, without using any forecast information.

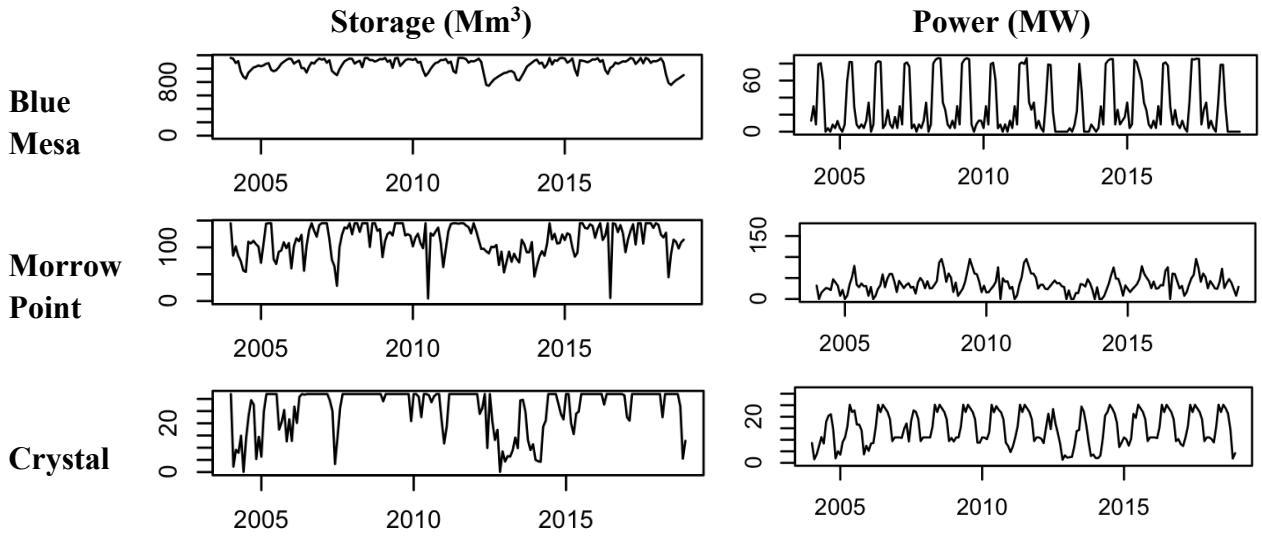

Figure 4.9 Benchmark control rules designed specifically for hydropower maximization using the R package '*reservoir'* for the dams in the Aspinall Unit during the period 2004-18 at monthly scale (after Turner and Galelli, 2016).

4.4.1.3 Hydropower Benefits Assessment

The hydropower benefits harnessed from each strategy over the three years and using the two forecast scenarios are shown in Table 4.5. The benefits from the perfect forecast scenario set bounds to maximum attainable benefits which cannot be exceeded by the optimal policy under the operational forecast scenario. Hydropower generation (MWh) using observed real-world operations (obtained from USBR) are also shown in Table 4.5 for comparison.

The high skill in ANN forecasts resulted in benefits similar and lesser to those from the perfect forecast scenario for all the strategies. Considering the different years of analysis, the proposed approach of TeNeSC, which answers the key research question of our study, is more

advantageous during the dry and moderate years (2016 and 2018) as compared to the wet year (2017).

Table 4.5. Assessment of hydropower production benefits (HP) over the Aspinall unit using different strategies compared against benchmark and observed benefits over three years; IB is the improvement in production over the benchmark scheme. Comparing TeNeSC with T1 and T2 gives values in temporal nesting while comparing with C1 gives values in spatial coupling.

Year	Strategy	Formulation	HP (GWh-perfect forecast)	IB (%)	HP (GWh-operational forecast)	IB (%)
2017 (wet)	TeNeSC	Short + Long + Coupled	1028	14.8	1021	14.1
	T1	Short-only	893	-0.3	877	-2.0
	T2	Long-only	934	4.3	929	3.8
	C1	Uncoupled	921	2.8	915	2.2
	Benchmark		*895*		–	
	Observed		*812*		–	
2016 (moderate wet)	TeNeSC	Short + Long + Coupled	974	26.9	948	23.5
	T1	Short-only	837	9.0	821	7.0
	T2	Long-only	759	-1.1	750	-2.3
	C1	Uncoupled	807	5.2	780	1.7
	Benchmark		*767*		–	
	Observed		*761*		–	
2018 (dry)	TeNeSC	Short + Long + Coupled	847	41.5	829	38.5
	T1	Short-only	684	14.3	669	11.8
	T2	Long-only	603	0.6	599	0.1
	C1	Uncoupled	702	17.2	652	8.9
	Benchmark		*599*		–	
	Observed		*609*		–	

Within the strategies evaluating value in temporal nesting, both the short-term-only (T1) and long-term-only (T2) optimization result in lower benefits in hydropower when compared against the proposed benchmark. TeNeSC, on the other hand, generates benefits of 14% to 41% over the different seasons for perfect forecast scenario. Further, using the short-only optimization (T1) was most beneficial for drier year while the long-term only optimization (T2) produced more benefits for the wetter year. This stresses the value in incorporating both the strategic and tactical planning for robustly efficient operations across different years. Next, the

value in spatial coupling is underscored by comparing TeNeSC against strategy C1 with no coupling. The latter again falls short of the hydropower benefits compared to the former. This is because when the optimization considers only the individual reservoirs without any coordination in release decisions, the optimal policy for one dam leads to other dams perform sub-optimally, leading to an overall reduced performance of the system. The hydropower generation from real-world observed operations, although not used for assessment as mentioned in section 3.6, was comparable to those from the benchmark scheme.

4.4.2 *Effect of skill in long-term forecasts*

The perturbed inflow forecasts for Blue Mesa dam were obtained for the moderately wet year of 2016 to study the effect of skill in monthly forecasts on the optimal operations. Figure 4.10(a) shows the perturbed inflow time series using six different constants of multiplicative bias. The long-term optimization model was first used to obtain monthly optimal policies for the three dams. Figure 4.10(b) shows the optimal long-term policy for Blue Mesa dam for the corresponding perturbed inflow time series.

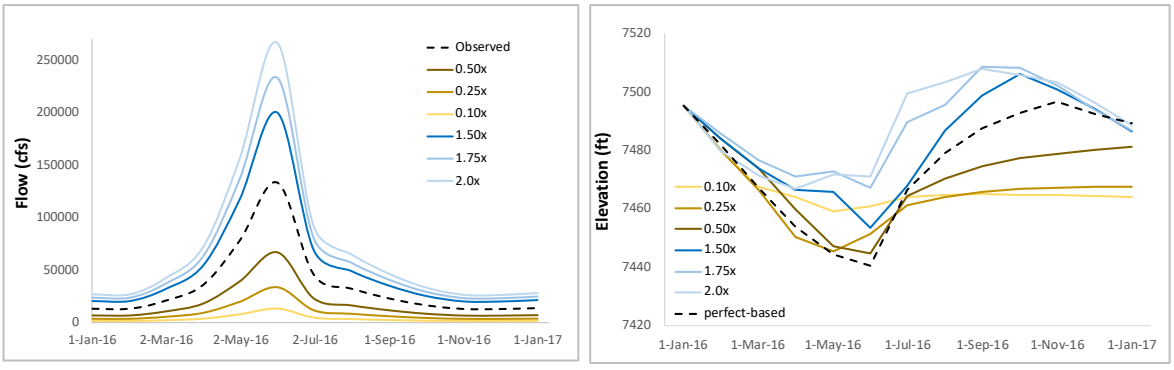

(a) (b)

Figure 4.10 (a) Perturbed inflow timeseries for Blue Mesa dam over 2016 to be used for the TeNeSC scheme; (b) Optimal monthly elevations for Blue Mesa dam using long-term optimization model based on the different perturbed forecast inflow timeseries – black dashed line is based on perfect forecasts (i.e. observed inflow).

Table 4.6 Hydropower benefits obtained with TeNeSC using different perturbed inflow scenarios, 'Nx' represents the perturbed inflow scenario obtained by multiplying the observed inflow timeseries by constant 'N'

Underestimation Scenario	Hydropower (GWh)	**Overestimation Scenario**	Hydropower (GWh)
0.10x	968.1	**1.50x**	949.4
0.25x	973.4	**1.75x**	949.9
0.50x	960.8	**2.0x**	937.9
Perfect forecast	*973.8*		

The long-term optimal elevations were then used to constrain the short-term optimization under the TeNeSC scheme. The hydropower benefits using the optimal operating policy from different underestimation and overestimation scenarios are summarized in Table 4.6. Comparing the outputs from different scenarios of perturbation, a higher bias of the inflow forecasts towards over- or underestimation generally results in lower energy benefits relative to the perfect forecast benefits. The effect of degrading skill is more prominent for the overestimation scenarios where the optimization strategy results in over-conservative release policy leading to lower energy production. The underestimation scenarios, on the other hand, yield relatively higher releases and generate more energy when assessed over the entire year. However, the overall difference among resulting optimal policies and respective hydropower benefits was insignificant. This is partly because the long-term forecasts are not directly utilized for arriving at the final optimized releases, rather, the first step of long-term optimization leads to monthly optimal release policy which then feeds the daily optimization. Thus, the effect of poor skill in monthly forecasts is, to some extent, compensated for by the more accurate short-term forecasts while deriving the final daily optimal releases. This is advantageous in the case when long-term forecasts are not very skillful as demonstrated here with heavy over/underestimation, further underscoring the value of co-optimization at long- and short-time scales.

4.5 DISCUSSION

Smart use of skillful forecasts at weather and climate scales can potentially make the operation of existing dams more efficient. As forecast systems require much less resources and manpower than building new energy infrastructure (Turner et al., 2017), a major implication of using the forecasts is the improved efficiency of operations instead of building new hydropower dams for satisfying same energy demands. To realize this potential towards energy generation, we have demonstrated a scheme that integrates the long-term benefits with short-term optimization model to achieve optimality at both the times scales for a multiple dam network. The findings presented here are globally applicable, where energy demands and the need for greener and cleaner energy production are simultaneously escalating.

As a first step, to model the reservoir short-term (daily) and long-term (monthly) inflow forecasts, we used a numerically efficient and skillful data-based technique of ANN for the upstream-most dam that receives unregulated natural flow. The publicly available NWP forecast forcings at the weather scale and the climate model outputs at the climate scale currently represent an underutilized resource for the energy and water resources community. The data-intensive and skillful ANN modelling technique was only employed for the most upstream dam of the three-dam network that brings natural inflow into the system. However, for the downstream reservoirs whose inflow is serially correlated with releases from the respective upstream dams, a linear regression model was found to be suitable for modeling the cascading inflow. This concept can be useful even for more complex multi-dam networks such as a parallel or combination of series-parallel network, where only the most upstream reservoirs (one or more) need skillful forecasting technique.

Our study shows that using the long-term optimal policy as a guide to short-term optimization model aids the reservoir in avoiding any sudden surge or dip in the levels that might occur in the extreme seasons. In particular, this is valuable for the wet season when an

inflow peak with high uncertainty can leave the dam operator with a small temporal window to pre-release and adjust the reservoir levels when using short-term forecasts. With a skillful monthly forecast of the inflow volume from climate models, the temporal window of operations extends manifold giving the operator enough room to adjust the levels with minimal spells of heavy spillway release. Similarly, during the extremely dry seasons, long-term forecasts of drier years can keep the storage levels within safe bounds for a relatively unvarying energy supply (satisfying the baseload demands). The Pareto optimality in multi-objective optimization provides flexibility to the dam operator to choose an appropriate solution based on the prevailing circumstances and tradeoffs between the two conflicting objectives.

The other component of co-optimized operations is the spatial coupling of reservoirs where the connected dams are operated and optimized for in tandem. The results suggest that benefits to the dam operator offered by coordination in release decisions depends on the characteristics of the reservoirs in the network. A diverse network comprising reservoirs and powerplants with varying characteristics can potentially use the spatial coupling for release policy tailored to each dam. Thus, if a dam is assigned to meet base load demands, its optimal release policy should allow for minimum changes in reservoir levels. While, for the dams whose purpose is to provide peaking power during certain operational hours/days, the release policy can be adjusted accordingly to maintain the requirements for other baseload-providing reservoirs. This when integrated with temporal nesting has far-reaching implications for the numerous small and large multi-dam networks which were constructed in the previous centuries with long service lives but are suffering from fading efficiencies. Our proof-of-concept implies that a smart use of seasonal and short-term forecasts can compensate for the losses in performance and generate more energy.

The quantification of benefits under evaluation framework was performed by comparing them against a benchmark scheme that completely neglects the forecasts. The study

showed 14% to 41% of improvements in energy benefits from the co-optimized scheme against the benchmark over years with different flow characteristics. In general, the dry and medium years showed higher energy improvements than the considered wet year. A similar conclusion was also reported by Xu et al. (2014) who obtained long-term energy generation as a function of short-term operations. As Xu et al. (2014) suggest, the objective of maximizing the hydropower or stored energy favors the long-term energy production under drier conditions by maintaining higher storage levels. This leads to relatively higher overall improvements on nesting the short and long-term optimality. However, wetter conditions demand higher release leading to a loss to the storage maximization objective in the long term and hence comparatively lesser improvements to hydropower.

The study specifically focused on the application of forecast-based reservoir operations at different temporal scales for improving upon the hydropower generation. The technique involves components of flow forecasting and optimization that require in-situ data on reservoir operations and inflow for setting up the models. For operationalizing the concept over other dam networks across the globe, the forecasting models can rely on inputs from global NWP model and satellite remote sensing. However, the optimization model needs to be set up in conditions of scarce in-situ data on dam operations. We hope to consider this in a future study. Moreover, with improved efficiency of reservoir operations, any excess energy generation can be wasted if there is not enough demand for dispatching the power to the grid or in case there is no provision for excess energy storage. Thus, another logical future extension of this work is to integrate energy demand forecasting and excess energy storage with the co-optimized reservoir operations. The utility of nesting the weather forecasts within the climate forecasts-based operations is not only limited to hydropower but can also benefit other renewables such as solar and wind energy generation. Future endeavors on fostering the clean energy generation should aim towards an integrated hydro-wind-solar based energy framework.

4.6 CONCLUSIONS

This study presents a scheme for co-optimizing the long-term (seasonal) reservoir operating objectives with the short-term (daily) objectives for multi-dam networks to maximize hydropower generation. Multi-objective optimization problem at both the temporal scales was simultaneously solved considering Pareto optimality between conflicting objectives. Constraints pertaining to flood control, dam safety and environmental flow were imposed. The proposed scheme was implemented over a network of Blue Mesa, Morrow Point, and Crystal dams in the Upper Colorado Basin. Results show an improvement of 41%, 27% and 15% in hydropower generation using the co-optimization during wet, moderate and dry years, respectively, against a benchmark that neglects inflow forecasts. The study demonstrates the additional benefit of co-optimizing the operations for hydropower generation based on short- and long-term forecasted reservoir inflow. Given that most dams today operate as a network in a river basin, we recommend moving away from single dam and single timescale optimization to a multiple-dam with long- and short-term scale co-optimization-based operations to make renewable energy generation more efficient.

We have shown by now that co-optimizing the release decisions using both weather and climate scale forecasts can benefit operating objectives pertinent to both the temporal scales. However, the demand to generate more energy also has detrimental effects on the ecology which needs due consideration for a fully sustainable hydropower operation. This will be considered in Chapter 5 with a case study demonstrated on Detroit dam, OR.

Chapter 5. REALIZING ECOSYSTEM-SAFE HYDROPOWER FROM DAMS

Note: This chapter has been published mostly in its current form in the journal, Renewables: Wind, Water, and Solar (Ahmad and Hossain, 2020c). This is an open access article distributed under the terms of the Creative Commons CC BY license.

Ahmad, S.K., Hossain, F., 2020c. Realizing ecosystem-safe hydropower from dams. Renewables: Wind, Water, and Solar, 7(1), pp.1-23. doi:10.1186/ s40807-020-00060-9

ABSTRACT

For clean hydropower generation while sustaining ecosystems, minimizing harmful impacts and balancing multiple water needs is an integral component. One particularly harmful effect not managed explicitly by hydropower operations is thermal destablization of downstream waters. To demonstrate that the thermal destabilization by hydropower dams can be managed while maximizing energy production, we modelled thermal change in downstream waters as a function of decision variables for hydropower operation (reservoir level, powered/spillway release, storage), forecast reservoir inflow and air temperature for a dam site with in-situ thermal measurements. For data-limited regions, remote sensing-based temperature estimation algorithm was established using thermal infrared band of Landsat ETM+ over multiple dams. The model for water temperature change was used to impose additional constraints of tolerable downstream cooling or warming (1-6˚C of change) on multi-objective optimization to maximize hydropower. A reservoir release policy adaptive to thermally optimum levels for aquatic species was derived. The novel concept was implemented for Detroit dam in Oregon (USA). Resulting benefits to hydropower generation strongly correlated with allowable flexibility in temperature constraints. Wet years were able to satisfy stringent temperature

constraints and produce substantial hydropower benefits, while dry years, in contrast, were challenging to adhere to the upstream thermal regime.

5.1 INTRODUCTION

Previous chapter highlighted the need to co-optimize dam operations by nesting long- and short-term forecasts over multi-dam networks. The third component for efficient hydropower generation system is to address the detrimental impacts on ecology due to dam operations and restore ecological sustainability. This will be the focus of this chapter.

The need to satisfy energy demand of a growing planet while simultaneously meeting sustainability standards with clean energy generation has resulted in a growing hydropower infrastructure, especially in the developing regions (Moran et al., 2018). The design and management of such infrastructure has traditionally focused on flood control, hydropower, water supply, and irrigation (Carron and Rajaram, 2001). Hydropower, once perceived as clean and renewable, has now become a contributor of negative ecological impacts to the reservoir and aquatic and riparian ecosystem (Abbasi and Abbasi, 2000). Hereafter ‘reservoir’ and ‘dam’ are used interchangeably to imply the reservoir-dam system.

Coldwater fishes such as salmon and trout are sensitive to changes in water temperature. Extreme temperature deviations can be lethal to their population (Handcock et al., 2012). Warm water tends to hold less dissolved oxygen which is critical to the health of aquatic habitat (Li et al., 2014). Such adverse thermal impacts of hydropower dam operation demand a reevaluation of dams’ operational objectives from an ecosystem standpoint (U.S. Department of Interior, 1995; McCartney, 2009). In the past, recommendations have usually specified minimum flow release from reservoirs for habitat maintenance, water quality, and temperature control (Carron and Rajaram, 2001; Chen and Olden, 2017). However, little or no recommendation exists in the form of operational strategy to minimize the negative eco system

impacts from a thermal standpoint. Thus, one of the formidable challenges that exist today and will only intensify in the future with changing climate and increasing hydropower dam construction (Moran et al., 2018; Zarfl et al., 2015) is the alteration of river's natural thermal regime by the hydropower operations (Olden and Naiman, 2010).

5.1.1 *Thermal Pollution from hydropower operations*

The natural temperature of regulated rivers, apart from responding to changes in hydrologic and hydraulic conditions, is largely impacted by the operations of regulating reservoirs in the upstream (Gu et al., 1999). During the seasons of maximum heat exchange between reservoir surface and atmosphere, the surface warms rapidly lowering its density. The lower density surface rests on top of water column that becomes colder and denser with depth. This inhibits the vertical mixing of reservoir and causes seasonal thermal stratification with low diffusion rates between the top and bottom reservoir layers, also termed as epilimnion and hypolimnion, respectively (Niemeyer et al., 2018; Xie et al., 2017). The surface warming is also enhanced by the large reservoir surface area and resulting longer residence time of the rivers (Vörösmarty et al., 1997). During hydropower operations, penstocks, usually located at the bottom layers (hypolimnion), tend to release cold water and lower the downstream peak temperature (Carpentier et al., 2017). In late summer and autumn, the stratification breaks as the reservoirs are drawn down through the spillway to provide flood storage capacity for the coming winter and spring precipitation. This leads to a well-mixed reservoir with downstream temperatures warmer than the natural regime. Such alterations in temperature regime, also termed as thermal pollution create challenging conditions for spawning and rearing of certain fish species and can be lethal for aquatic life (Old and Naiman, 2010).

The persistent thermal pollution from hydropower infrastructure worldwide, if left unaddressed, can potentially dwarf the benefits harnessed for renewable energy. According to the prediction from U.S. Energy Information Administration, world's energy demands will grow up by 50% from 2018 to 2050, mostly driven by steep rise in developing nations (U.S. Energy Information Administration, 2019). This is proportionally increasing the installation of newer hydropower capacity in these countries. One of the striking examples is that of Laos which is aiming to become the "battery of Southeast Asia" by investing heavily in the hydropower dams across the nation (Rujivanarom, 2019). While such a rise of new hydropower dams in emerging economies is inevitable, the only way to sustain the ecosystem while still generate clean energy is to improve their operational efficiency in terms of minimal impacts to the ecosystem.

5.1.2 *Need to improve hydropower efficiency from ecological standpoint*

In contrast to developing nations, developed nations have saturated their dam installation capacity (Labadie, 2004). As the escalating environmental impacts are being identified, the efforts have started shifting towards mitigation. The Federal Energy Regulatory Commission (FERC) in United States examines the environmental impacts and issues operational changes through 30- to 50-year licenses (Bednarek, 2001). There have also been efforts to undam the rivers when the mitigation tolls are not enough. More than 1200 dams have been removed in the United States, especially in the past two decades (Bellmore et al., 2017). While dam removal has become commonplace to deal with aging and uneconomical dams, the resulting loss of reservoir habitat and movement of sediments can incur heavy costs to the ecology and environment (Stanley and Doyle, 2003). Given the increasing need for clean and stable supply of baseload (Matek and Gawell, 2015), removing the infrastructure would also be unfavorable for sustainable energy goals. From a logistical standpoint, the time and accrued cost of each dam removal would demand immense resources and a few centuries to remove all the dams the

right way. As dams have become pervasive features of the river systems, continued improvement in the efficiency of dam operations is therefore the more pragmatic approach to maximize their benefits to humans and ecosystem.

Despite the recognized impact of dams on river's thermal regime (Olden and Naiman, 2010; Gu et al., 1999; Niemeyer et al., 2018; Rheinheimer et al., 2014), the quantitative effect of hydropower operations on downstream water temperature and the subsequent consequences on ecosystem have received little attention (Bonnema et al., 2019). Mitigation efforts to reduce thermal pollution from hydropower dams either focus on structural measures such as construction of selective withdrawal structures (Rheinheimer et al., 2014) or, by specifying required instream or minimum spillway flow downstream of the reservoir (Tharme, 2003) based on an environmental flow assessment (King et al., 1999). The selective withdrawal outlets require additional construction and can be unviable for a reservoir due to the involved logistics and monetary constraints. Relying on environmental flows for controlling the downstream temperatures is prone to result in suboptimal conditions for the aquatic habitat particularly in conditions when inflow regime deviates from the climatology. Instead, a more dynamic scheme that considers inflow forecast information at short-term weather scale can guide the dam operator ahead of time on optimal operations for realizing ecologically safer downstream conditions (Ahmad and Hossain, 2020a).

Optimization of reservoir operations has been extensively studied for various operating objectives at short- and long-term operation scales (Yeh and Becker, 1982; Barros et al., 2003; Ahmad et al., 2014). Multi-objective optimization for hydropower has been performed to satisfy other stakeholder benefits of flood control, water supply, irrigation and water quality (Le Ngo et al., 2007; Yazicigil et al., 1983; Shaw et al., 2017; Asadeieh and Afshar, 2019). Ahmad and Hossain (2020a) optimized daily operations of two dams in U.S. to maximize hydropower without compromising flood control. Jordan et al. (2012) presented optimization

of turbine and bottom outlet operations for flood protection in a hydropower multi-reservoir system in Switzerland. Similar to flood control, maintaining a stable thermal regime also competes against the energy maximization objective as higher release or storage can significantly change downstream temperature. However, the inclusion of downstream river temperature as a constraint has not yet been explored or reported in published literature to the best of our knowledge.

5.1.3 *Need to model reservoir temperature*

Incorporating water temperature as a constraint within an optimization scheme for hydropower generation requires quantitative relationship between the reservoir operations and changes in downstream thermal regime. There have been efforts to model the river temperature using deterministic and statistical models. Deterministic models, based on governing equations for heat transport, flow, and climatic conditions, do not explicitly include the reservoir operations as parameters for modeling temperature (Benyahya et al., 2007). Also, they typically require intensive hydrological and meteorological data input and computational effort in model building and calibration. Distributed river temperature models also exist that simulate river network by discretizing the river cell (Li et al., 2015; Yearsley, 2012). Some of them often explicitly simulate reservoir's thermal stratification by integrating land surface models (LSMs) with hydrodynamic models (Niemeyer et al., 2018; Buccola et al., 2016). Even complex three-dimensional models have been used such as by Jiang et al. (2018) to study thermal pollution in Lancang River using Delft3D-FLOW model. However, a major limitation with these complex models is the inability to integrate them with the hydropower optimization framework.

Another challenge towards temperature-constrained optimization is the dearth of in-situ temperature measurements. The water temperatures in rivers are limited by sparse sampling in both space and time. The scarcity of in-situ temperature measurements is even more prominent

in the developing nations that present major hurdles in building and validating the temperature models. Recent advancements in thermal infrared (TIR) remote sensing can quantify spatial and temporal patterns of surface water temperature at multiple spatial scales (Ling et al., 2017). This has been demonstrated by Bonnema et al. (2019) where dry season water temperature cooling trends correlated with dam development in the Mekong basin, analyzed using 30 years of Landsat TIR observations. Thus, applications for ecologically sensitive hydropower optimization are better served by simpler river temperature model that can relate downstream temperature against decision variables for dam operations and global-scale satellite-derived temperature (where in-situ data is scarce).

Only a few studies have explored simple regression models for stream temperature changes. Neumann et al. (2003) presented empirical model for daily maximum stream temperature in summers using average daily flow and air temperature as predictors. Mohseni et al. (Mohseni et al., 1998) predicted weekly temperatures for fish habitat evaluation using nonlinear function of weekly air temperatures. The heat storage effects were considered by developing separate models for warming and cooling season. Benyahya et al. (2007) reviewed different regression models used for stream temperature. However, inclusion of reservoir operations in the regression model at daily time step has not yet been investigated in the literature. Because ecological impacts are more sensitive to changes in downstream temperature from natural thermal regime and not their absolute values, regression model offers an attractive alternative for the purpose.

The pertinent issues with the current state of hydropower operations, brief summary of the existing literature and proposed solutions leading to the objectives of this study are shown in Figure 5.1.

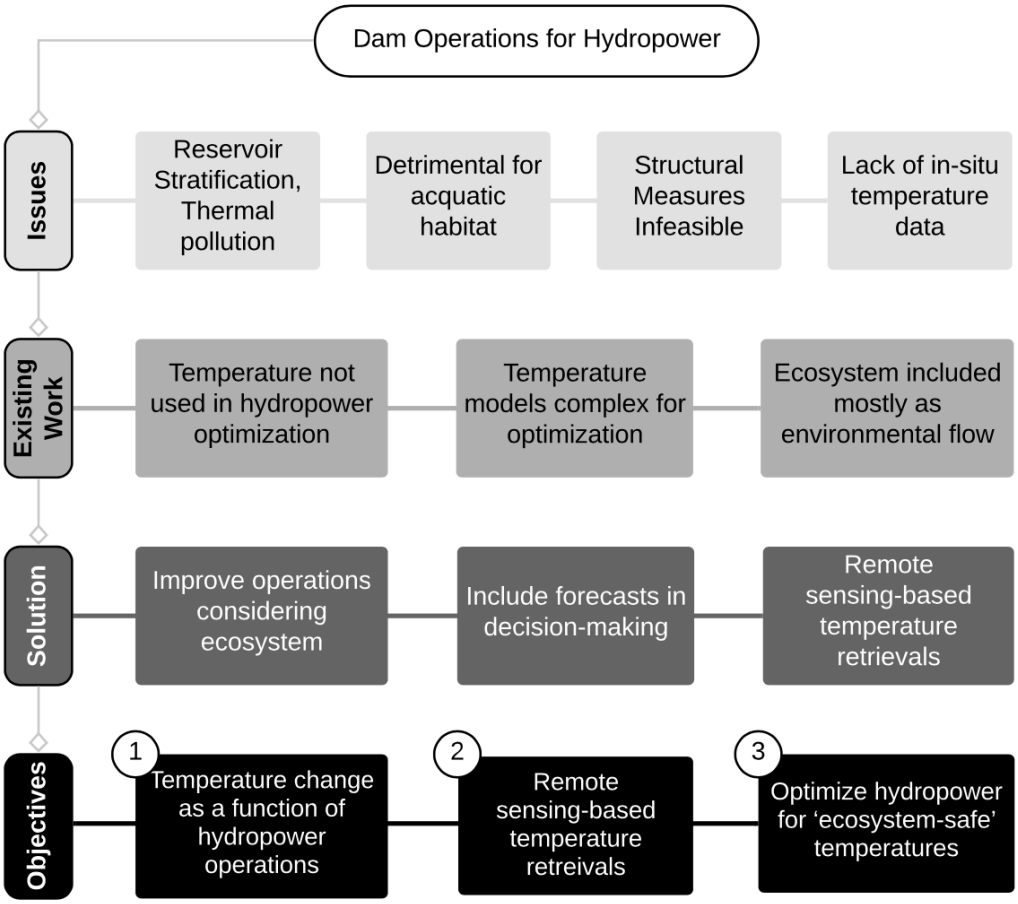

Figure 5.1 Pertinent issues with the current state of hydropower operations, brief summary of the existing literature and proposed solutions leading to the study objectives

5.1.4 *Study Objectives*

The goal of this study is first to tackle the challenges presented so far using the low hanging fruit of global weather forecasts from Numerical Weather Prediction (NWP) model (Ahmad and Hossain, 2020c). The use of NWP models for benefits to hydropower is well established (Ahmad and Hossain, 2019b) and running operationally (http://depts.washington.edu/saswe/damdss/) for Detroit dam in Oregon, U.S. The hydropower optimization is refined in this study by imposing temperature-based constraints to explore if hydropower benefits can still be realized while maintaining ecosystem thermal stability. The overarching question addressed here is: *can we generate more hydropower using weather*

forecasts while balancing ecosystem needs from a thermally stable regime standpoint? The question is further broken down into tangible research objectives: (1) to understand downstream temperature change as a function of hydropower operations, (2) to develop a remote sensing-based approach for temperature modeling that can be used in developing nations, and (3) to optimize hydropower operations while ensuring 'ecosystem-safe' downstream water temperatures. The rest of the study is organized as follows. In section 5.2, the selected site and necessary datasets are described. This is followed by a description of the various methods used in Section 5.3. The case study results on demonstrating the eco-safe hydropower generation are presented in Section 5.4, followed by discussion and concluding remarks in Section 5.5.

5.2 TOOLS AND DATASETS

5.2.1 *Study Site*

The Detroit Dam on the North Santiam River, Oregon (Figure 5.2), controlled by U.S. Army Corps of Engineers (USACE), is authorized to provide flood control, hydroelectric power, navigation, and water in summer for irrigation and recreation. The reservoir is relatively small with a storage capacity of 455,000 ac-ft and storage to annual inflow ratio of 0.28. The powerhouse is designed for nameplate capacity of 100 megawatts (MW) with a hydraulic capacity of 5,340 cfs. Located around three miles downstream of Detroit dam is the Big Cliff re-regulating dam with a small reservoir. The purpose is usually to smooth out the power generation release from the upstream Detroit dam and control fluctuations in downstream river level (Oregon Water Resources Department, 2012).

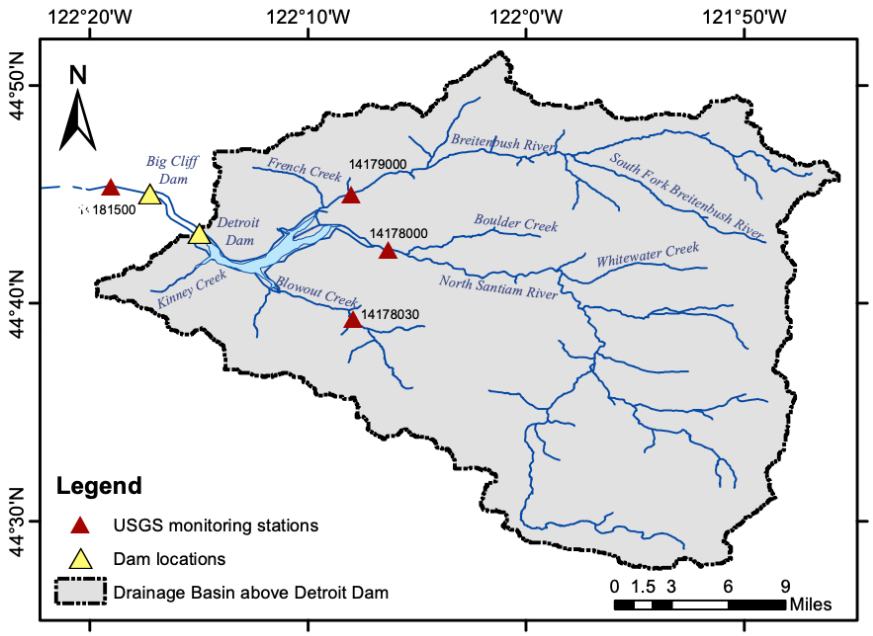

Figure 5.2 Drainage basin above Detroit dam (OR) and pertinent USGS monitoring stations used in the study

Since the commissioning of dam in 1953, the dam operations have changed the natural flow patterns in the basin to meet the authorized objectives. The changed flow patterns have also led to unintended consequences for the ecosystem and aquatic life (Oregon Department of Environmental Quality, 2006). The variation in reservoir temperatures is shown in Figure 5.3a where downstream temperatures usually correspond to the temperature of one of the pools in hypolimnion, depending on the penstock release. The reservoir stratification and bottom release of stored water have not only led to alterations in the downstream river temperature magnitudes but also in the timing of low and high temperature occurrences. As shown in Figure 5.3b, higher stream temperatures that normally occur in July and August have been shifted towards September and October.

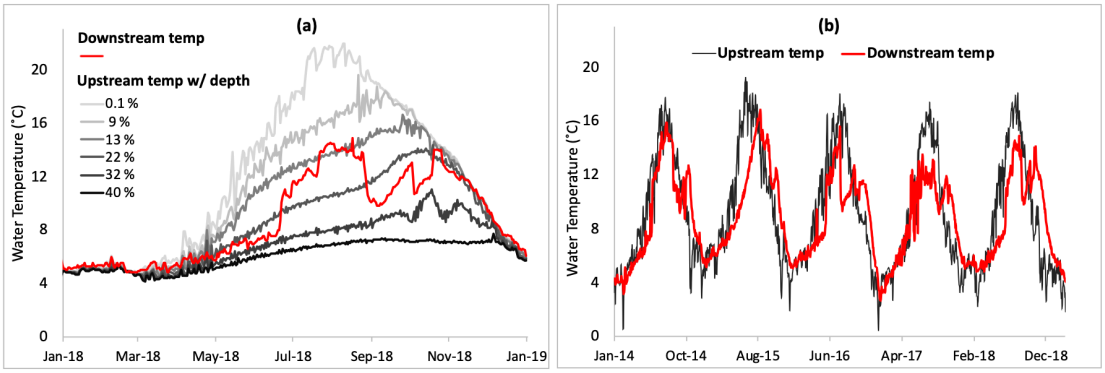

Figure 5.3 (a) Variation of upstream reservoir temperature with depth from spillway crest plotted as a percentage of maximum reservoir depth (440 ft) for Detroit dam (OR) in 2018. Downstream temperature is also plotted alongside; (b) Timeseries of stream temperatures upstream and downstream of dam showing alteration in downstream thermal regime, where flow averaged temperature of upstream tributaries from USGS gages are used for upstream temperature (Source: USGS; USACE).

5.2.2 *Datasets – Observed and Forecast*

To understand how the downstream temperature changes as a function of hydropower operations, in-situ measured temperatures were obtained from U.S. Geological Survey (USGS) stations located on both the upstream tributaries and downstream river channel (Figure 5.2). Flow-averaged temperatures were obtained from USGS stations on three rivers upstream of Detroit reservoir (44°43’N, 122°15'W). The downstream temperature station is located below the Big Cliff dam and accounts for regulation effects from both the dams. The upstream stations measure temperature of the top surface or epilimnion of the reservoir while the downstream stations represent average temperature of the downstream water column due to reduced tailwater stratification. The forecast meteorological fields were acquired from the NWP model of Global Forecast System (GFS) for forecasting reservoir inflow. The GFS fields were acquired at 0.5° resolution for 1–7 days lead-time with a 3-hourly temporal resolution. Air temperature was obtained from CPC Global Temperature data provided by the

NOAA/OAR/ESRL PSD, Boulder (https://www.esrl.noaa.gov/psd/). The observed reservoir inflow and operations data were obtained from USACE.

5.2.3 *Datasets – Remote Sensing*

The primary data source for remote sensing-based water temperature estimation was a series of Landsat-7 ETM+ (Tier 1) satellite images. The TIR band (10.45 to 12.5µm) is acquired at a resolution of 60 m. The image processing and temperature estimation analysis was performed in the cloud computing environment provided by Google Earth Engine (Gorelick et al., 2016).

As the river channel downstream of Detroit dam is quite narrow, the pixels in TIR band acquired over water at 60m possibly represent mixed pixels with a portion of reflectance contributed by surrounding land cover. Thus, ten dam sites with varying reservoir depths and downstream river width were chosen to explore the effect of pure water pixels in temperature extraction. The locations of selected dams and their average reservoir depths are shown in Figure 5.4. Table D1 (Appendix D) summarizes the selected dams, their coordinates, approximate downstream river channel widths, respective Landsat-7 ETM+ scene path and row numbers, and USGS stations for upstream and downstream in-situ temperature measurements.

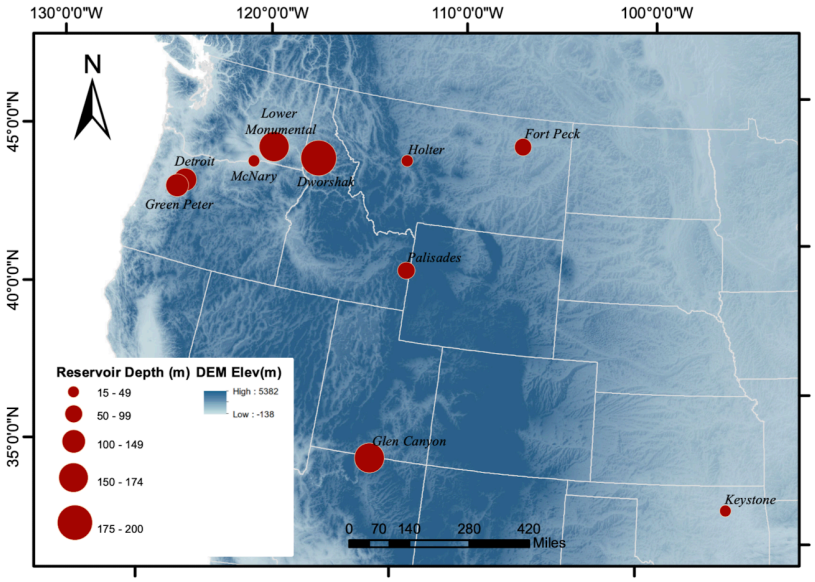

Figure 5.4 Selected dams for establishing the remote sensing-based temperature estimation. Markers are sized with their respective average reservoir depths.

5.3 METHODS

The study first establishes relationship between hydropower operations and temperature to be used for constraining the optimization problem. Remote sensing-based temperature estimation algorithm was established for validating the relationship in data-limited regions. Figure 5.5 summarizes the experimental approach followed to address the objectives.

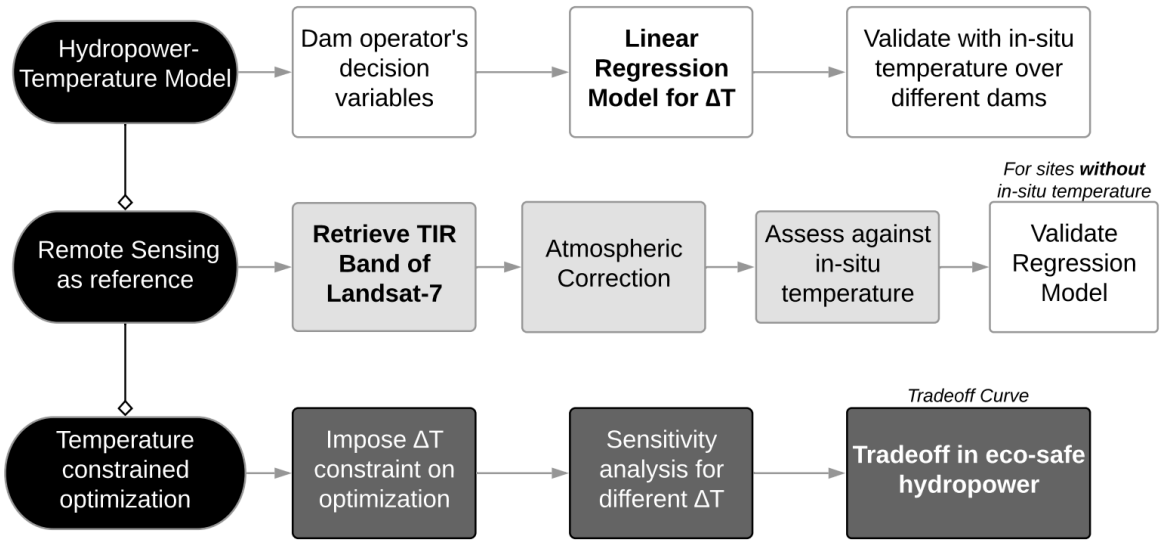

Figure 5.5 Experimental approach showing development of the temperature model, validation using remote sensing and its integration with the reservoir operations optimization to realize tradeoffs in ecosystem-safe hydropower generation.

5.3.1 *Modeling temperature-hydropower operations relationship*

In order to understand the role of dam's hydropower operations in modifying downstream river temperatures, we opted for a statistically based model that characterizes the statistical relationships between river temperature and decision variables for the dam operator. A simple statistical relationship between the reservoir operations and water temperatures also facilitates

integration with the optimization model. We use the functional linear regression model relationship for this purpose.

For the linear regression relationship, daily difference between the upstream and downstream water temperatures was selected as the dependent variable. This is adequate because, firstly, the aquatic habitat is more susceptible to the relative difference between the downstream thermal regime and natural (upstream) conditions compared to their absolute values. Secondly, the statistical relationship is usually suited for comparative analysis and in predicting relative difference in modeled variable instead of its absolute value, which would require a more complex model (Yuba County Water Agency, 2007). A set of candidate decision variables were selected as: (i) total release rate from reservoir, R_t, (ii) penstock release, R_p, (iii) turbine operating hours (captured in total hydropower generation, HP), (iv) reservoir forebay elevation, E, (v) inflow into reservoir, I, and (vi) air temperature, T_a. As tailwater elevation of the reservoir does not vary much with the tailrace discharge to significantly alter hydropower production, a constant value of 1200 ft was assumed based on the average value over past 10 years. The spillway release was obtained by subtracting the penstock release from the total discharge. The relationship between water and air temperature deviates from linearity for low (sub-zero) and high air temperatures (Mohseni et al., 1998) that necessitates a transformation function for air temperature to accurately capture the full variability. A logistic function was proposed by Mohseni et al. (1998) to describe the S-shaped air-water temperature relationship at weekly scale. We employ this function to transform the air temperature before feeding into the regression model.

$$T_a' = \frac{\alpha}{1+e^{\gamma(\beta-T_a)}} \tag{5.1}$$

where, T_a' is the transformed temperature, the coefficient α represents the estimated maximum stream temperature, T_a is the air temperature, γ is a measure of the steepest slope of the

function, and β represents air temperature at inflection point of the S-shaped relationship. Buccola et al. (2016) implemented this approach for Detroit dam and obtained the fitting parameters for daily water temperature. The present study borrowed fitting parameter values, $\alpha = 18.08, \gamma = 0.10$ and $\beta = 20.42$ for North Santiam River at Boulder (USGS ID 1718000) from Buccola et al. (2016).

The decision variables were chosen such that the regression model can be used for predicting future temperature changes. The release rates, hydropower generation and elevation are outputs from reservoir operation model, reservoir inflow is derived from flow forecasting model (section 3.3.1) and air temperature can be obtained from NWP model forcings.

5.3.1.1 Seasonality in water temperature

In using the inherent relationships of different decision variables with the temperature change, seasonal variation in reservoir's behaviour is not modeled explicitly. The reservoir usually exhibits varying temperature signals based on changes in the stratification with seasonal temperature. Not accounting for seasonal stratification in the temperature model can induce seasonal bias in modeled temperature and poorer model performance. One way to indirectly account for the characteristic behavior across different seasons is to use a piecewise linear regression, fitting different relationships for different periods of the year. However, temperature data needs to be divided into separate chunks where the piecewise model might not result in representative slopes at the upper or lower ends of individual chunks (Mohseni et al., 1998). Time-varying coefficients can capture the variability over time (Li et al., 2014), however one drawback is the difficulty in interpreting the parameters in case of a multiple regression model.

The problem of seasonal variation and in particular, distinguishing the trend and cyclical movement components, has been dealt by economic analysts by performing

adjustment for seasonal patterns within the regression model (Thomas and Wallis, 1971). To perform this adjustment and capture the seasonal variation in water temperatures in addition to daily trends, we include additional seasonal dummy variables in the model. The seasonal dummies are a function of frequency at which seasonal behavior is prominent for the reservoir in consideration. The seasonality that is explicitly modeled here captures the deterministic seasonal processes and is usually termed as deterministic seasonality. Mathematically, let s be the seasonal frequency (dividing year into s different periods) and let $D_{1t}, D_{2t}, \ldots D_{st}$ be seasonal dummy variables for any particular day t, corresponding to periods $1, 2 \ \ldots, s$. For a selected day t, one of the seasonal dummies D_{it} equal one, while all the others equal zero,

$$D_{it} = \begin{cases} 1, & \text{if observation at time } t \text{ is in } i^{th} \text{ period} \\ 0, & \text{otherwise} \end{cases} \tag{5.2}$$

Monthly timestep was chosen here as the seasonal frequency for modeling reservoir's seasonal behavior. Hence, the deterministic seasonality, S_t, can be expressed as a linear function of dummy variables,

$$S_t = \begin{cases} \theta_1, & \text{if } t = Jan \\ \theta_2, & \text{if } t = Feb \\ \vdots & \\ \theta_{12}, & \text{if } t = Dec \end{cases} \tag{5.3a}$$

$$S_t = \sum_{i=1}^{s} \theta_i D_{it} \tag{5.3b}$$

where, θ_i are the regression coefficients for each dummy variable and s=12 for the monthly frequency.

5.3.1.2 Formulation of regression model

Apart from the seasonal components, optimal set of decision variables to capture the daily trends were selected based on a sensitivity analysis. The analysis was based on indicator metrics of correlation coefficient, Akaike's Information Criteria (AIC) and mean absolute error

(MAE) of the model. AIC tries to maximize the explained variance in predictors while also minimizing the variance of the resulting estimates by limiting the number of coefficients (Neumann et al., 2003).The least squares regression model can then be formulated as,

$$y_t = \alpha + \sum_{k=1}^{n} \beta_k P_k + \sum_{i=1}^{s-1} \theta_i D_{it} + \epsilon_t \quad (5.4)$$

where, t spans the days of year, y_t is the modeled temperature difference between upstream and downstream, α is the intercept, β_k is the regression coefficient for the k^{th} predictor variable P_k $(k = 1,2 \dots n)$ where n is the total number of selected predictors, seasonal frequency $s = 12$, and ϵ_t accounts for unexplained variation in modeled temperature for time t. It should be noted that the regression is performed by omitting one of the monthly dummy variables (e.g. December), for they would be collinear and redundant.

5.3.2 *Water temperature from remote sensing*

Remote sensing was used to obtain water temperature so that the technique can serve as a potential reference when in-situ temperature data is scarce or absent. From the decade-long record provided by Landsat-7 mission, the thermal infrared (TIR) band was used to extract the water temperature using single channel (SC) algorithm (Jiménez-Muñoz and Sobrino, 2003; Jiménez-Muñoz et al., 2008) both upstream and downstream of the dam. The temperature estimation algorithm is shown schematically in Figure 5.6.

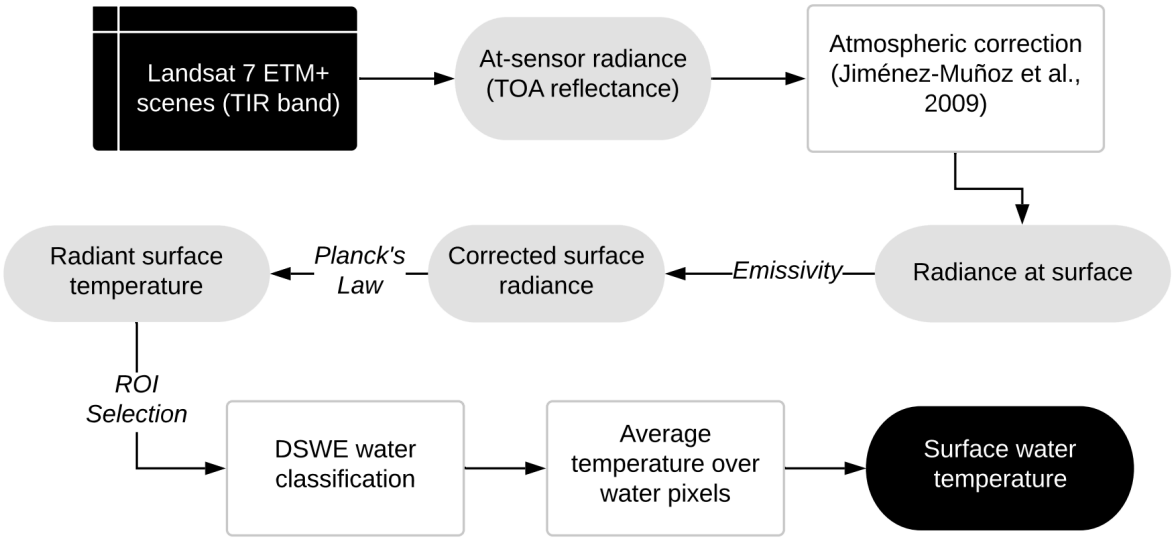

Figure 5.6 Single Channel (SC) algorithm using Landsat ETM+ for estimating water temperature upstream and downstream of dams.

Top-of-atmosphere (TOA) reflectance from TIR band of cloud-free Landsat 7 scenes was atmospherically corrected. The correction procedure used information about upwelling and downwelling radiances and atmospheric transmissivity, estimated using atmospheric functions (AFs). We used coefficients derived by Jiménez-Muñoz et al. (2008) to relate AFs and water vapor content for the operative SC algorithm. The ground leaving TIR radiance was corrected with an emissivity of 0.99 for distilled water (Handcock et al., 2006). The resulting corrected radiance led to the calculation of radiant surface temperature using Planck's Law. Water pixels were classified using Dynamic Surface Water Extent (DSWE) algorithm within regions of interest (ROIs) containing USGS measurement stations (Jones, 2015). Pixels with high confidence were retained for averaging surface temperature estimate from low-gain TIR Band (B6 VCID 1) of the processed Landsat 7 image. Averaging the temperature retrievals also help minimize the effect of any possible contamination of reflectance from the surface due to factors such as eutrophication or presence of vegetation on the water surface.

5.3.3 *Eco-system sensitive hydropower via multi-objective optimization*

We modeled dam operations at daily time step using water balance approach to optimize for reservoir releases leading to optimal flow designs (see Figure 5.5). The reservoir's actual bathymetry was factored in the model using a storage-elevation relationship derived for the reservoir. Release decisions were optimized using a multi-objective optimization model. The primary objective was to maximize hydropower generation from powerplant over an optimization horizon of seven days.

$$\max f_1(MW) = \sum_t \epsilon \cdot \Delta t_{turb} \cdot (HF_t - HT_t) \cdot R_{p,t} \tag{5.5}$$

The secondary objective was set to minimize a penalty cost function that accounts for the long-term effects of the release decisions over the short-term optimization horizon. The penalty function is quantified based on the deviation of reservoir storage S from the rule curve-specified level RC, which is representative of the long-term optimal state of reservoir under climatological flow regime.

$$\min f_2(acft) = \sum_{t=T}^{7} |S_t - RC_t| \tag{5.6}$$

where deviation is considered starting T^{th} day of the 7-day optimization horizon. Under normal flow circumstances, T was set to two to consider last six days of the horizon for calculating the deviation. During high inflow periods, where the forecasted inflow exceeds the turbine capacity, deviation was calculated only over the last two days to slacken the penalty function and give more room for controlling the high inflow event.

The optimization problem involves mutually conflicting objectives where it would be impossible to realize a single release schedule that satisfied both of them perfectly. Thus, a balance in tradeoff solutions was achieved using Pareto optimality. An optimal solution that gives equal weightage to both the objectives was selected on non-dominated set of solutions of

a Pareto front. The cost to ecosystem was considered in terms of change in riverine thermal regime while designing the optimal releases. The hydropower-temperature relationship was incorporated to impose additional constraint on the optimization model to guide the release decisions. The modeled temperature difference between upstream and downstream reaches was limited to a selected minimum and maximum threshold,

$$\Delta T_{min} \leq \Delta T \leq \Delta T_{max} \tag{5.7}$$

The temperature-driven constraints in equation (5.7) form the essence of realizing ecosystem-safe hydropower using weather forecasts from thermally stable regime viewpoint. The prescribed window between ΔT_{min} and ΔT_{max} determines the level of 'safety' that the optimization aims to attain. Other constraints pertaining to dam safety, reservoir storage, and release rates were imposed based on the physical and operational limits of the reservoir. Readers are referred to Ahmad and Hossain (2020a) for detailed formulation of the constraints. The reservoir operations were modeled using a water balance approach, where the amount of water in reservoir S_t on day t of the optimization horizon is a function of storage on the previous day $(t - 1)$ and the inflows, losses and releases on the current day:

$$S_t = S_{t-1} + \delta(I_t - L_t - R_t) \tag{5.8}$$

where, δ is a constant to extrapolate flow rates into daily volume units while assuming a constant flow within each day. As the optimization is performed at daily time steps, storage losses L_t due to evaporation and seepage were ignored. The optimization was carried out using the Non-dominated Sorting Genetic Algorithm (NSGA-II) (Deb et al., 2002).

5.3.3.1 Forecasting reservoir inflow

For the inputs to the reservoir optimization model, weather-scale inflow forecasts were modeled using a machine learning technique to ensure high skill with computational efficiency

in processing. The forecasting was based on a feedforward artificial neural network (ANN) involving input, hidden and output layers, as established in our earlier work (Ahmad and Hossain, 2019a) to be valuable and skillful over muliple reservoirs in U.S. Forecast fields from GFS model were inputs to a three-layered ANN model along with antecedent hydrometeorological conditions of precipitation, temperature, basin's runoff and baseflow. Consecutive daily ANN models were used to result forecast streamflow for seven days in future. Ahmad and Hossain (2019a) describe the model development and predictor selection in more details. Training was performed using Levenberg-Marquardt method and early stopped training (STA) was incorporated to avoid overfitting and lack of generalization.

5.3.3.2 Sensitivity to allowable change in temperature

The objective concerning hydropower generation demands larger storage and higher releases through the penstocks. This is likely in conflict with the goal of attaining a stable thermal regime, as larger reservoir storage intensifies stratification leading to larger temperature differences. Also, higher penstock releases end up cooling downstream reaches. We performed a sensitivity analysis to investigate the amount of hydropower benefit realized by imposing constraints of varying degrees of allowable change in temperature between upstream and downstream rivers. Allowable temperature-difference (ΔT_{allow}) windows ranging from 1 to 6˚C of change were imposed as constraint to the objective of hydropower maximization for multiple years. Oregon Department of Environmental Quality (ODEQ) has prescribed Total Maximum Daily Loads (TMDLs) for temperature to ensure river does not exceed water quality criteria considering pertinent fish uses (Oregon Department of Environmental Quality, 2006). The choice for ΔT_{allow} windows was driven by the observed deviations in downstream thermal regime from the prescribed ODEQ limits over the past decade. The selected windows signify resilience of the downstream ecosystem in response to hydropower operations. Moreover, the

approach, by considering different ΔT_{allow} possibilities, is also able to study system's resilience against future alterations in stream temperature due to climate change impacts.

5.3.3.3 Designing adaptive release policy

The sensitivity analysis focused on adhering to the natural thermal regime upstream of the dam. With changes in climate leading to larger temperature anomalies from the historical average, the upstream temperatures can render suboptimal for the habitat downstream of the dam. Here, we explore a more holistic approach to designing operations by considering specific ecosystem's biodiversity and tolerance level of aquatic species to thermal instability, as informed by dam's pre-existing biology. For the North Santiam River, regulated by Detroit dam, the most sensitive beneficial uses of the river include Salmonid fish spawning and rearing, and anadromous fish passage. Biologically based numeric criteria have been prescribed under TMDL for each season to meet the critical downstream uses (National Marine Fisheries Service, 2008) The criteria, summarized in Table 5.1, are expressed as a seven-day moving average of daily maximum temperature.

Table 5.1 Biologically based numeric criteria prescribed under TMDL for North Santiam Subbasin of Detroit dam

Season	**Downstream use**	**7-day average temperature criteria**
September 1 – June 30	Salmon spawning	12.8 ˚C
Summer (July 1 -August 31)	Salmon and Steelhead rearing	17.8 ˚C

We used these criteria to frame the multi-objective optimization for release decisions that adapt to the downstream habitat uses while still maximizing hydropower. Instead of temperature difference, the optimization framework now constrains the average of absolute downstream temperature over seven-day horizon within the required criteria for the respective season. Thus, the constraint in equation (5.7) is modified as,

$$average\ (T_{dn,t}) \leq T_{target} \tag{5.9}$$

where $T_{dn,t}$ is the downstream temperature for $t = 1, 2 \ldots 7$ days and T_{target} represents the biological criteria.

5.3.3.4 Evaluation of optimal decisions

We evaluated the results of ecosystem-safe reservoir releases that concurrently improve hydropower generation by comparing with benchmark operations for multiple years. Two benchmark scenarios were incorporated: (i) *business-as-usual (BAU)* based on the actual operations of reservoir under observed conditions, (ii) *climatological baseline* (CLB) that uses climatological flow instead of ANN-based forecasts to perform the multi-objective optimization and derive optimal reservoir release. No temperature constraint is imposed on optimization with climatological flows. BAU allows assessment of the degree of improvement possible with the proposed eco-safe optimization concept over the real-world operations. On the other hand, CLB provides a realistic and fair benchmark where the rules are derived under the same framework as used for inflow forecast-based optimization, which might not hold for BAU. Comparison with CLB explains significance of using forecast information and imposing temperature constraints on the optimization model.

We used 50 years of reservoir inflow to derive the climatology which was then used to perform the hydropower optimization over five years of different inflow regimes without imposing any temperature constraint (Figure D1). The daily and annual inflow variations over the selected years are shown in Figure D2. Improvement in energy over the two benchmark scenarios in different years led to derivation of a tradeoff curve. The curve signifies mutual conflict between the possible hydropower improvement using weather forecasts and degree of thermal stability in downstream waters.

5.4 RESULTS

5.4.1 *Quantifying hydropower-temperature relationship*

To quantify associations between change in thermal regime downstream of dam and hydropower operations, functional linear regression model was developed for Detroit dam. A stepwise procedure was followed for selecting the most optimal set of inputs to the model. The dependent variable was regressed against sequential combination of input variables over five years of daily data (2011-15). Table 5.2 summarizes the indicator metrics of correlation coefficient, AIC and MAE for different models used in the stepwise regression procedure, underscoring the predictive skill in each of the inputs.

Table 5.2 Indicator metrics for models with different candidate predictors in the stepwise regression procedure (refer to section 5.3.1 for notations)

Model Predictors	**Correlation Coeff. (R)**	**MAE (˚C)**	**AIC**
R_p	0.19	1.58	7624
R_p, HP	0.45	1.41	7282
R_p, HP, R_t	0.47	1.41	7252
R_p, HP, R_t, E, I	0.51	1.39	7179
R_p, HP, R_t, T_a'	0.58	1.37	6983
T_a'	0.49	1.48	7204
R_p, HP, R_t, E, I, T_a'	0.59	1.36	6937
D_i (i=1, 2, …12)	0.71	1.12	6476
$R_p, HP, R_t, E, I, T_a', D_i$	0.82	0.93	5737

The effect of including seasonality in the regression model via seasonal dummy variables is shown in Table 5.2 by the significant reduction in MAE and AIC of the resulting model. Air temperature, T_a' is transformed using the logistic function as described in section 3.1. The statistical significance of each predictor was ensured with their P values consistently less than the 95% confidence α level of 0.05, except for the inflow. The resulting coefficients in the final regression model and their respective P values are shown in Table 5.3.

Table 5.3 Regression coefficients and statistical significance (P values) of the selected predictors.

Predictor	$\boldsymbol{R_p}$	$\boldsymbol{HP}$	$\boldsymbol{R_t}$	$\boldsymbol{E}$	$\boldsymbol{I}$	$\boldsymbol{T'_a}$
Coefficient	-0.0017	0.0041	-2.2e-4	-0.0038	-2.9e-5	0.82
P value	2.1e-8	3.7e-13	4.0e-11	0.02	0.06	0.00

The coefficients of the regression model indicate the sensitivity of downstream temperature change to each of the independent predictors. For instance, difference between upstream and downstream water temperatures can go down by one degree decrease on a penstock release of ~600 cfs and can increase by one degree on an increase in air temperature of 1.3˚C. The positive sign on the coefficient for hydropower (owing to negative signs on penstock release and reservoir level coefficients) depicts the contrasting effect where a larger generation leads to higher difference between upstream and downstream water temperatures.

The selected model was then validated over three years (2016-18). Observed and modeled change in temperatures are compa**re**d in Figure 5.7a and Figure 5.7b. Timeseries plot of the residuals and their probability distribution function (PDF) are shown in Figure 5.7c and Figure 5.7d. The model is able to capture peaks and lows in temperature change and the residuals are mostly centered around 0˚C. The functional regression is able to explain 64% variance in temperature change as a function dam operations and seasonal dummy variables. Predictions from this temperature-hydropower model formed the basis for establishing remote sensing-based temperature estimation described next as well as for the multi-objective optimization model.

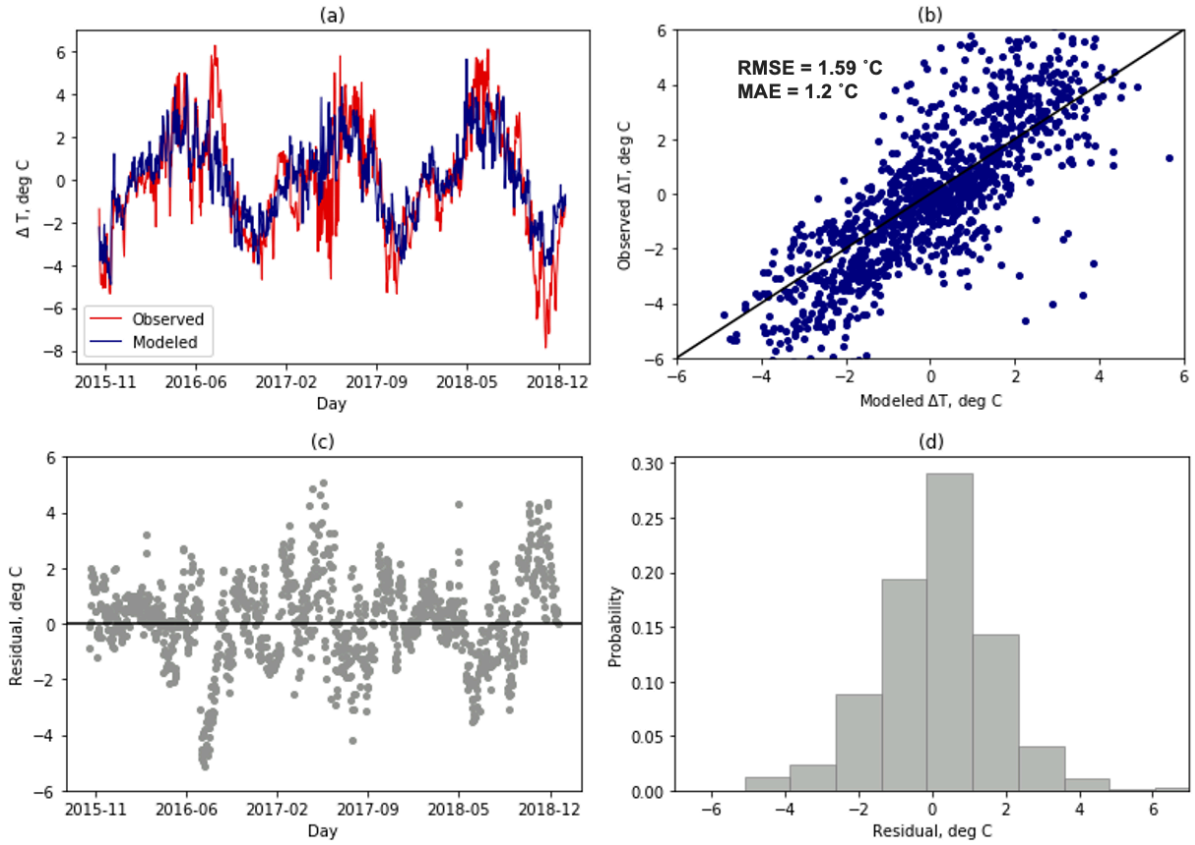

Figure 5.7 Performance assessment of the regression model for temperature change between upstream and downstream reaches: (a) timeseries of observed and modeled variable, (b) scatter plot for the same, (c) timeseries of the residuals in the modeled variable and (d) PDF of the residuals.

5.4.2 *Reservoir temperature from satellite remote sensing*

The Landsat-7 satellite imagery was utilized to extract the water surface temperature along the reaches upstream and downstream of the dam. As the channel width downstream of the dam is critical in acquiring pure water pixels for temperature extraction, the SC algorithm was applied to multiple dams with varying river widths. Figure 5.8 shows the extracted remote sensing-based temperatures and qualitatively compared with the USGS in-situ measurements both upstream and downstream of the dams.

The results suggest that for downstream reaches of rivers with depth to width ratio of less than or close to one and a width (W) of atleast 150m, both the upstream and downstream

temperature estimates from remote sensing match well in terms of capturing variations and peaks when compared with in-situ measurements.

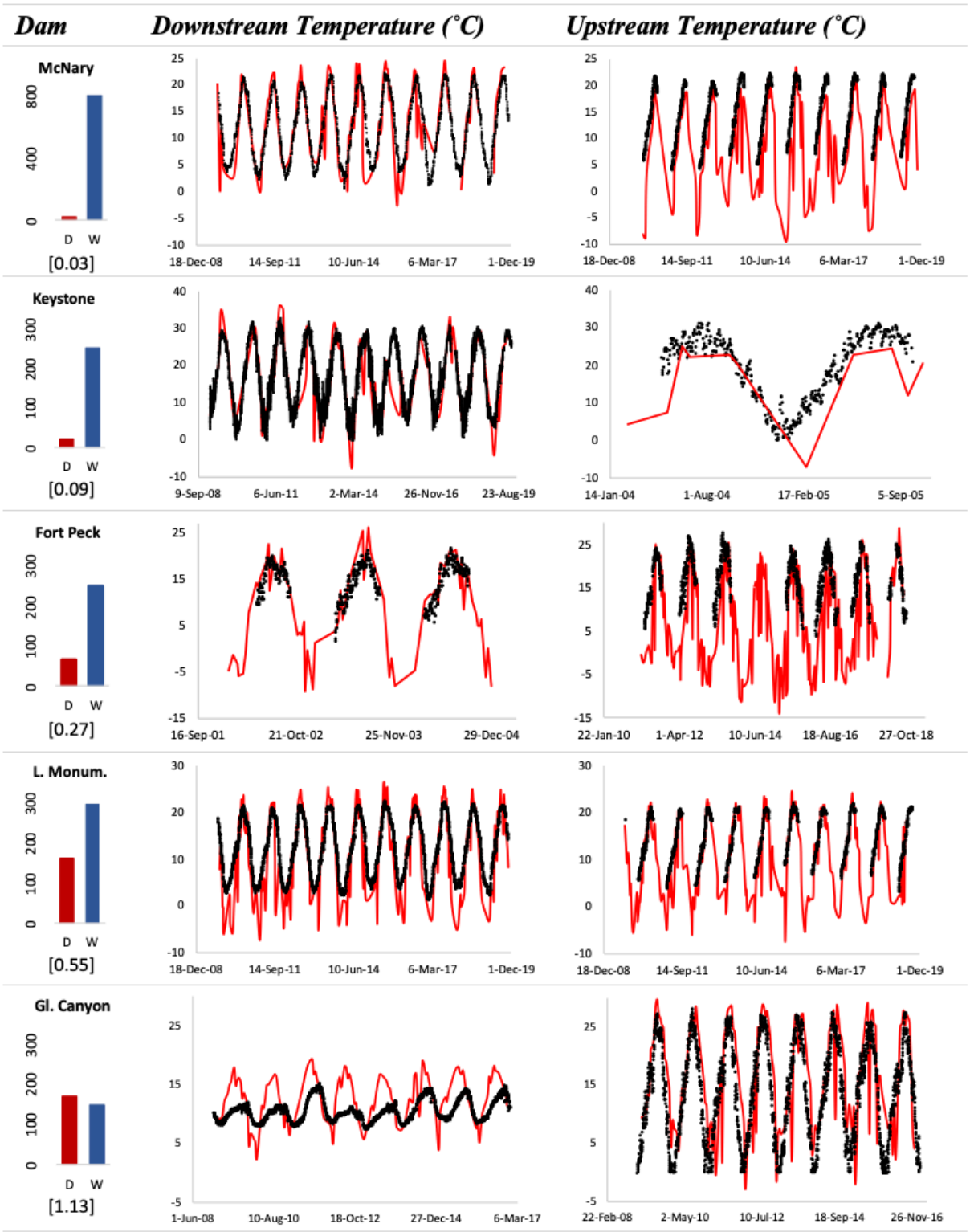

(b) Downstream river width ≥ 150m

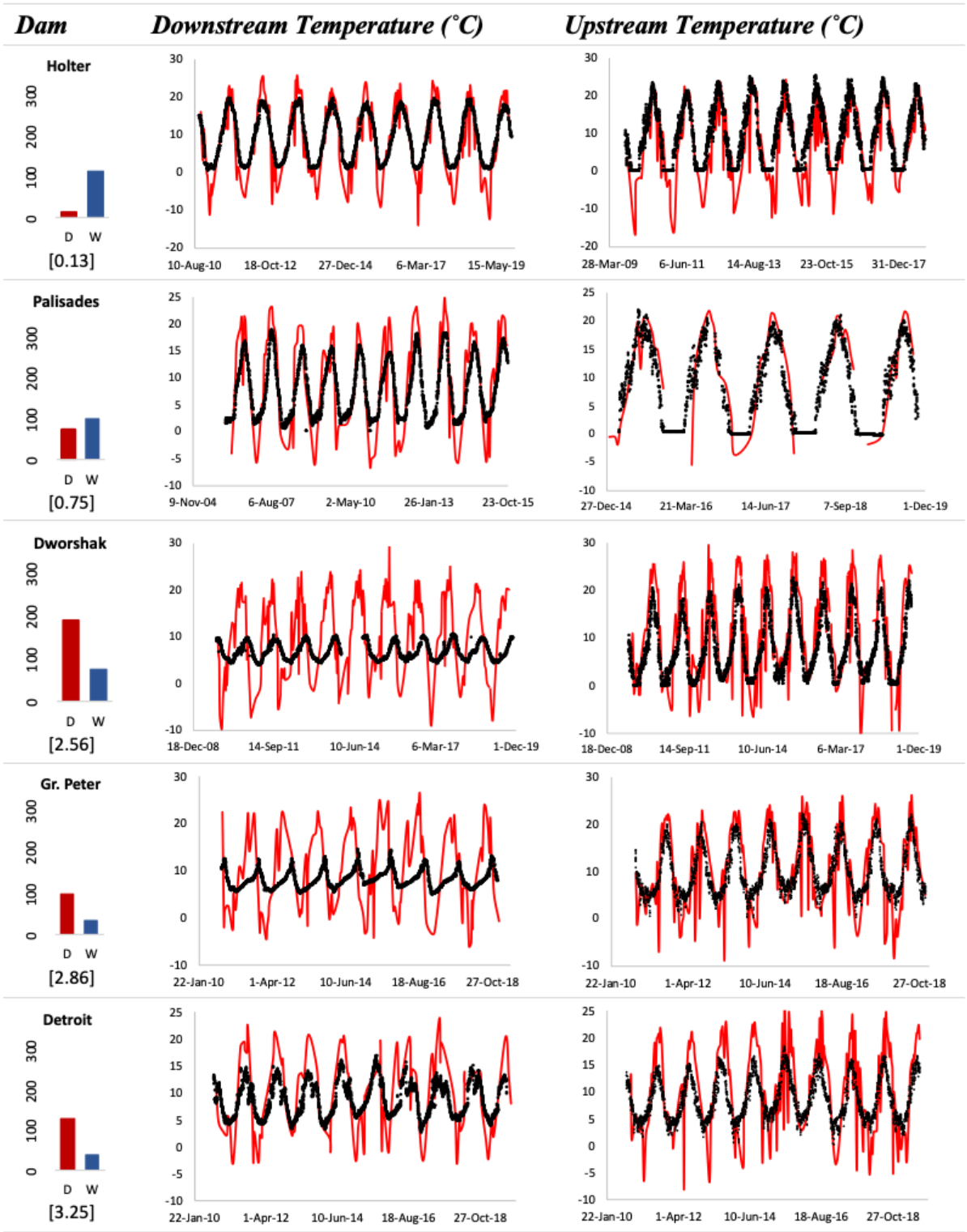

(c) Downstream river width < 150m

Figure 5.8 Timeseries of remote sensing-based temperatures (red), compared with USGS in-situ measurements (black) upstream and downstream of dams with (a) W ≥ 150m, and (b) W < 150m. The average reservoir depth (D) and downstream river width (W) in meters as well as D/W ratio (in square brackets) for each dam are shown alongside.

In general, when downstream channels entail more than two water-only pixels in TIR band (W≥120m), averaging over them results in improved estimates. Shallower reservoirs, on the other hand, have weaker stratification where surface closely represents the temperature of released water from deeper pools. The extracted temperatures were usually lower than the observed values across all the dams during winter season. As the TIR band provides measurement of radiant temperature at the surface or 'skin' layer of water (approximately top 10 cm), it is not representative of the kinetic or bulk temperature along the water column as measured by in-situ sensor. The difference in the two temperatures especially escalates during winter regimes where a sheet of ice forms on the surface, shielding the water below from dropping to sub-zero temperatures. Cloud interference was also a prominent issue during winters causing discrepancies therein. An example is shown in Figure 5.9 for two dams.

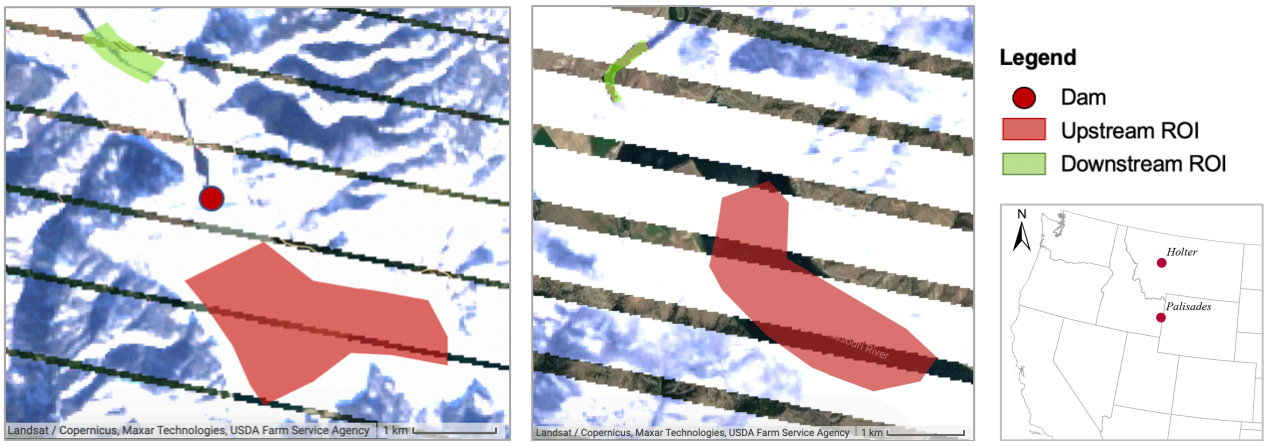

(a) Jan 1, 2016: Palisades dam (b) Jan 8, 2016: Holter dam

Figure 5.9 Scenes from Landsat -7 (ETM+) showing a sheet of ice forming on top of reservoir surface during winter season, resulting in sub-zero surface radiant temperatures for two dams. Green and red polygons (regions of interest; ROI) were used for obtaining average temperatures downstream and upstream respectively.

For dams such as Detroit, Dworshak and Green Peter with narrower river channels and less than a couple pixels covering the river width, overestimation in peak temperatures was observed due to the issue of mixed pixels. For deeper reservoirs of Green Peter, Dworshak and Glen Canyon dams, remote sensing-based estimations exhibit rapid warming during pre-peak

periods, reaching the peaks earlier than in-situ measurements. This, in fact, is an artefact of the intensified stratification across the deeper reservoir pools, leading to warmer radiant surface temperature as compared to colder kinetic temperatures represented by in-situ gages. The upstream reaches revealed better performance than their downstream counterparts across all the dams due to larger water area for averaging and a greater number of 'pure' pixels.

5.4.3 *Tradeoffs in hydropower generation while maintaining thermally stable regime*

Based on the short-term inflow forecasts obtained from ANN model, the hydropower operations were optimized with varying temperature change constraints. The analysis was first performed over two years with different climate regimes: (i) dry year (below-average annual river discharge) and, (ii) wet year (above-average annual river discharge). The Pareto frontier from the multi-objective optimization between hydropower maximization and storage deviation minimization during two different seasons is shown in Figure 5.10. A sample solution, shown with blue triangle, is selected on the front to perform the sensitivity analysis and obtain the tradeoffs.

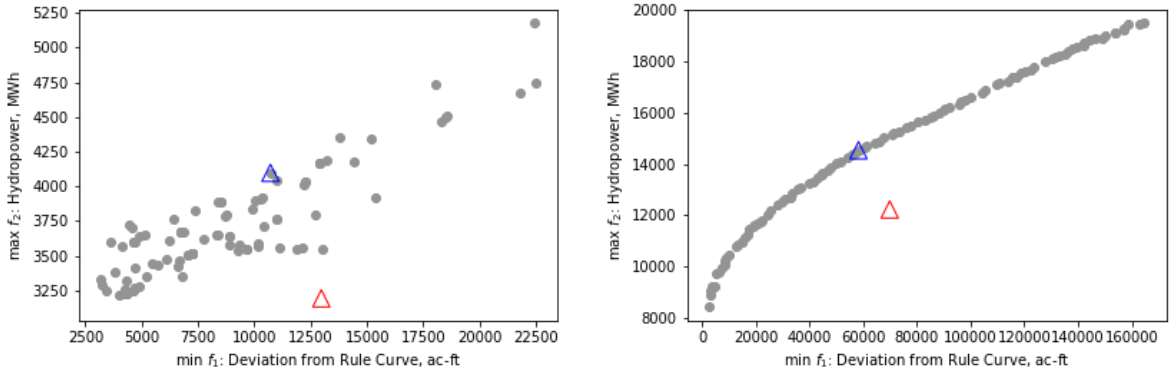

(a) (b)

Figure 5.10 Sample Pareto frontiers between hydropower generations and storage deviation from rule curve, depicting the optimal release decisions for (a) 5 Jan 2014 (wet year) and (b) 4 March 2016 (relatively drier year). Blue triangle represents the selected solution for carrying out sensitivity analysis while red triangle is the location of respective objectives from BAU scenario.

The resulting pareto optimal solutions consistently overperformed BAU scenario in terms of the considered objectives over different seasons. The selected solution on this front seeks to concurrently balance the objective of hydropower generation and penalty for deviation from the rule curve. The optimal reservoir states and corresponding downstream temperatures for different allowable temperature change scenarios are shown in Figure 5.11.

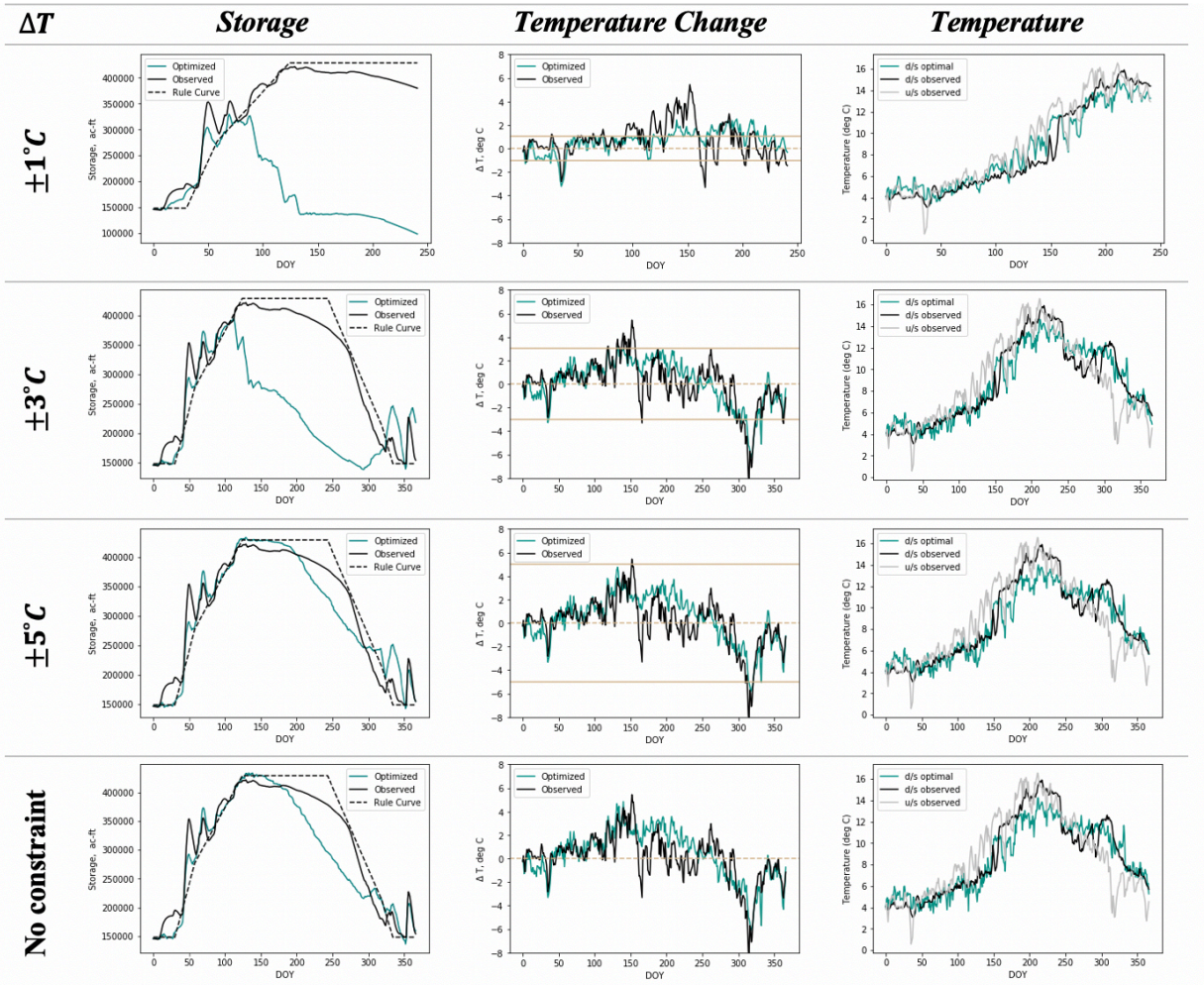

(a) Wet Year (2014)

Figure 5.11 (a) Optimal reservoir states and downstream temperatures for different allowable temperature change scenarios over wet (high flow) year. Optimal downstream temperatures (third column) are derived from the respective optimal temperature changes (second column).

To constrain the downstream temperature change within the allowable range, the reservoir has to be lowered based on the hydropower-temperature relationship. This leads to lower

storage levels compared to the observed scenario as constraints became more stringent. Over the wetter year of 2014, the optimal downstream temperatures mimicked the upstream regime for almost all the allowable ΔT constraints. In the most stringent constraint scenario of 1˚C of allowable change (for a very sensitive or weak downstream ecosystem), the prescribed release policy led to rapid drawdown of the reservoir with levels reaching the minimum storage bound. This resulted in no feasible solution by the month of September (Figure 5.11a). For the drought year of 2015, optimization ceased with infeasible solutions by July and August for all the scenarios as the reservoir was not able to recover due to low inflow volumes (Figure 5.11b).

The hydropower benefits for each scenario, obtained in terms of improvement in energy generation over the benchmark of CLB, are shown in Table 5.4 for the year 2014. The benefits for the dry year 2015 were not quantified here for assessment as only a portion of the year was optimized. The analysis highlights the tradeoff between benefits that short-term weather forecasts can provide for improving hydropower generation and the acceptable change in downstream temperatures from the upstream thermal regime.

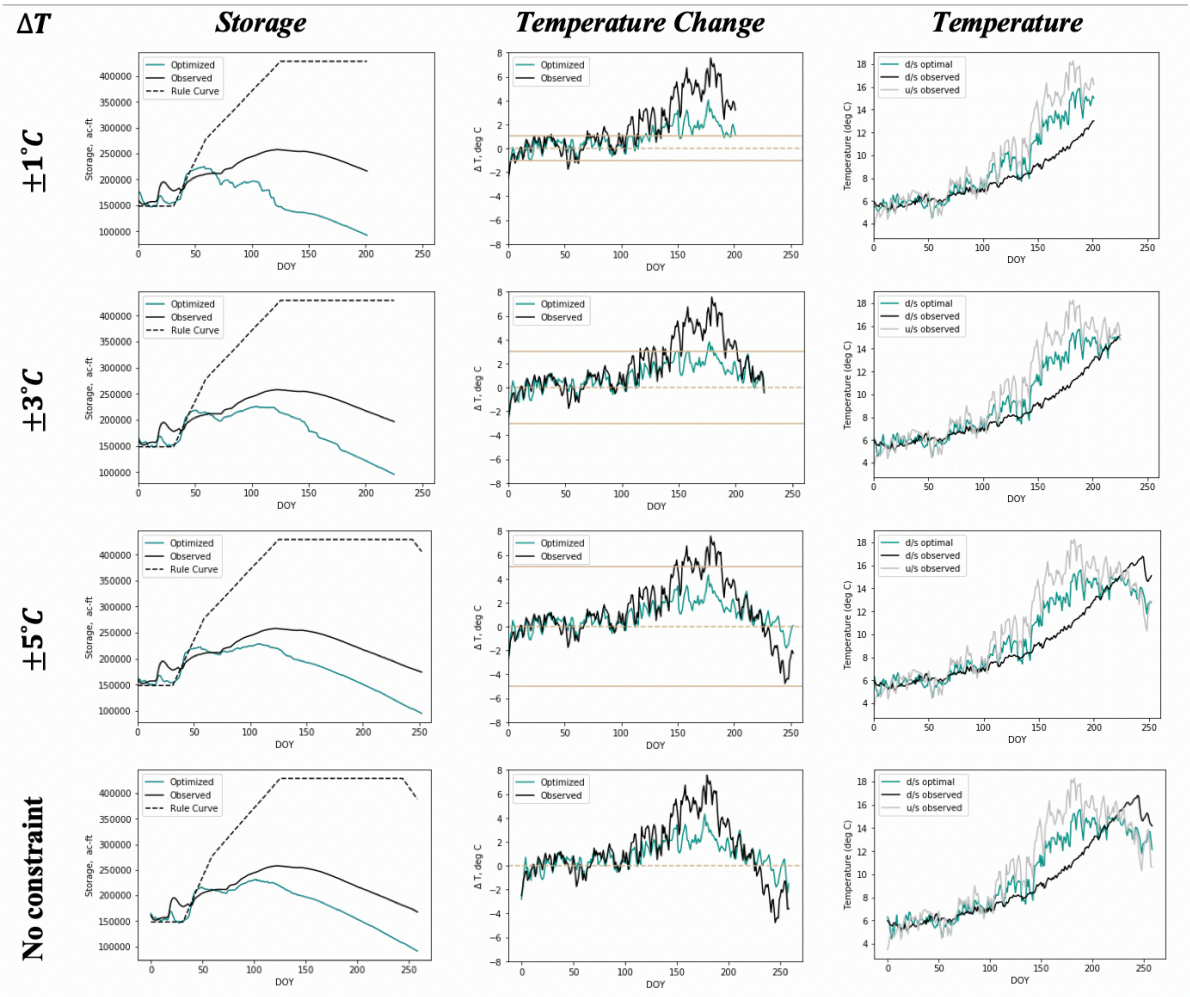

(b) Dry Year (2015)

Figure 5.11(b) Same as Figure 5.11a but for dry (low flow) year of 2015.

Table 5.4 Tradeoffs in hydropower generation for a set of constraints of allowable change in temperature. The benefits are compared in terms of percent increase in generation over the benchmark of CLB scenario for the year 2014.

ΔT (˚C) constraint	**Hydropower (GWh)**	**% Increase from CLB**	**ΔT (˚C) constraint**	**Hydropower (GWh)**	**% Increase from CLB**
±3	401.7	-3.6	±6	472.2	9.3
±3.4	450.8	4.3	No constraint	471.7	9.2
±4	466.3	7.9	BAU	445.1	3.0
±5	471.5	9.1	*CLB*	*459.4*	–

As the temperature constraint becomes more stringent, the potential of generating additional hydropower drops. However, the tradeoff does not follow straightforward linear trend. Comparatively lower hydropower was generated for tighter windows of ±3.5˚C and lower. As the constraints were relaxed, a sudden increase in benefits is realized with the trend stabilizing on further increasing the allowable temperature change window until ±6˚C. When no temperature constraints were imposed, the benefits were comparable to that obtained using constraints of ±5 and ±6˚C. This signifies an upper limit on energy benefit using flow forecasts, under hydrometeorological conditions of the considered year.

Based on the sensitivity analysis, a tradeoff curve was obtained for Detroit Dam to underscore the obtained improvements in energy generation with varying degrees of allowable temperature change. The multi-objective optimization was performed individually with different constraints of allowable temperature change over five years. Years with a blend of dry and wet inflow regimes were selected to arrive at the spread in possible tradeoffs (see Figure D2). Figure 5.12 shows the spread with mean, maximum and minimum of the obtained improvements in hydropower across the selected years. Improvements were calculated against the two benchmark scenarios of CLB and BAU. Hydropower generation (in GWh) for each scenario is shown for each year in detail in Figure D3.

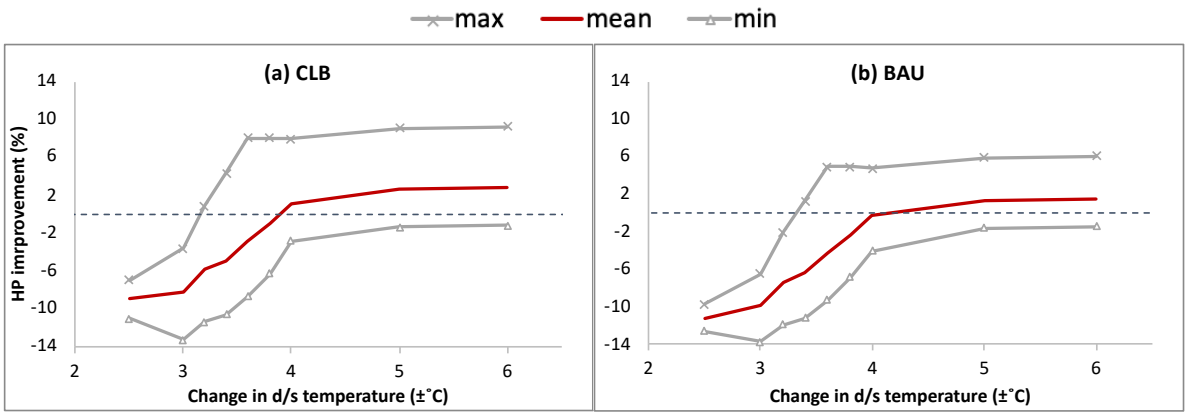

Figure 5.12 Tradeoff curve for improvement in hydropower generation (HP) over benchmarks of (a) CLB and (b) BAU scenario, with varying temperature constraints. The curve is derived from five years of optimization runs performed for Detroit dam involving a series of dry and wet flow regimes

The improvement in hydropower benefits generally follows a steep trend in the range of ± 3 to $\pm 4^{\circ}C$, beyond which the rate of improvement slows down. Comparison against CLB scenario revealed larger improvements as compared to those over BAU scenario. This highlights the value in using real-time inflow forecasts for optimizing reservoir operations against a historical climatology of inflows. The benefits from BAU could also be attributed to other objectives and constraints that operations consider instead of, or in addition to, hydropower and temperature objectives. The loss in hydropower is noticeable with more stringent constraints. The spread in benefits captures the variability in hydrological regime of operations where wetter periods led to larger energy benefits even with stringent constraints. The analysis suggests that beyond a threshold ΔT window (around $\pm 4^{\circ}C$ for Detroit dam), the amount of additional hydropower benefits is controlled primarily by the skill of weather forecasts and ambient hydrologic conditions. In other words, the dam operators might not benefit much from a wider ΔT range as the weather forecasts cannot leverage that high flexibility for improving energy generation. This has far-reaching consequences as even the sensitive ecosystems, where slight alterations to thermal regime can disturb the habitat, can also benefit from weather forecasts while keeping narrow ΔT during optimization, depending on the hydrologic conditions.

5.4.4 *Adaptive policy for ecosystem-safe hydropower*

Building on from the findings of sensitivity analysis, mimicking natural thermal regime during low water availability is remarkably challenging. In such challenging low flow scenarios,

natural temperature is not ensured to produce the best conditions for downstream habitat. We demonstrate an adaptive release policy by moving away from following the upstream temperatures. Over the drought year of 2015 (see Figure D2), the multi-objective optimization was performed by embedding biologically based criteria to result in downstream temperatures as shown in Figure 5.13.

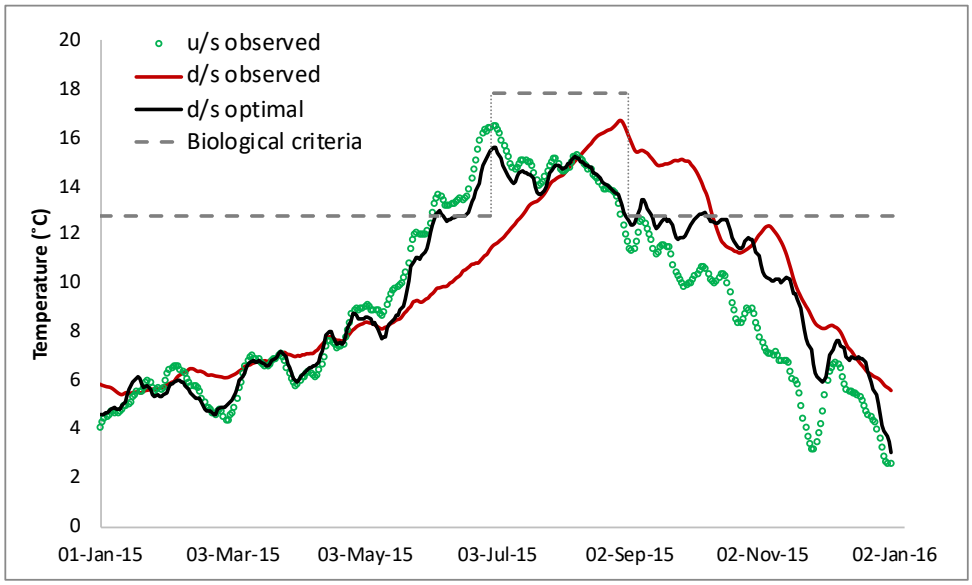

Figure 5.13 Optimal downstream temperatures during the year 2015 based on the adaptive release policy for Detroit dam. The policy was able to contain downstream temperatures within the required biological criteria to meet spawning and rearing uses, in contrast to the observed scenario exceeding the criteria.

Under the observed scenario (BAU), temperatures at North Santiam River downstream of Detroit dam exceeded salmon spawning use temperatures from September and into early October. Figure 5.13 suggests that the adaptive release policy outperformed observed operations and achieved downstream temperatures satisfying the specified biological criteria. Hydropower production over the selected dry year based on adaptive policy amounted to 236.4 GWh, which does not differ significantly in comparison to 235.7 GWh and 240.0 GWh from CLB and BAU scenarios, respectively. This further explains that while it might be challenging to generate

additional energy during anomalously dry years, it is indeed possible to meet the biological requirements with proposed adaptive policy.

5.5 DISCUSSION

Our study has found that the objective of hydropower maximization has an aggravating effect on downstream temperatures leading to higher deviation from natural thermal regime upstream. This has implications especially during the peaking power operations when large penstock releases are required while maintaining higher storage levels. During the spawning and rearing periods for certain fish species present in the downstream river reaches, the temperatures have to be maintained within a narrow window which can be challenging to achieve. The multi-objective optimization proposed here provides a framework to incorporate temperature targets while meeting hydropower demands. The tradeoff curves (Figure 5.12) facilitate broadening the perspective in comparing different operating policies by informing the dam operator on consequences to ecology and energy generation. Different scenarios can be chosen based on the time of year and optimal conditions for the downstream habitat. The analysis characterizes a reservoir system's resilience against hydropower operations as well as alterations in river temperature due to climate change impacts.

The functional regression model for modeling the change in thermal regime was found to perform well in capturing the peaks and daily trends over multiple years of data. The simple yet effective regression model allows for its generalized use over any other dam site, with minimal in-situ data requirements. The model can be simulated using the global scale NWP weather forecast fileds, while other decision variables of release rates, hydropower generation and elevation are outputs of the reservoir operation model and inflow derived from the flow forecasting model. The

performance was comparable to results from other studies using more complex models. A two-layer stratified reservoir model used by Niemeyer et al. (2018) to model absolute river temperatures resulted in RMSE of 1˚ to 3˚C. Buccola et al (2016) used a previously calibrated hydrodynamic and water-quality model CE-QUAL-W2 over Detroit dam and reported MAE of 0.34˚C in daily downstream temperatures. Neumann et al. (2003) used a regression model for daily maximum temperature, producing R^2 values of 0.57 to 0.74 over Truckee River. As the aquatic habitat is more sensitive to the changes in temperature instead of the absolute values, simpler regression models present a viable preference for predicting relative changes and integrating with the multi-objective optimization framework. Given that the available temperature models require intensive hydrological and meteorological data and computational effort in model building and calibration, our proposed solution can solve the logistical constraints for data- and resource-constrained settings, especially in the developing nations.

The release decisions ensued from the proposed optimization strategy were in accordance with the downstream flow needed for the specified temperature change constraint. Most of the past studies considered an explicit goal of releasing only environmental flows to imitate the natural flow regime and benefit the native fishes. However, as shown by Chen and Olden[8], mimicking the natural flow paradigm does not necessarily result in highest benefits. In contrast, our coupled hydropower-temperature based optimization goes beyond the notion of explicitly matching certain flows. It prescribes releases that not only adhere to the best suited environmental flows but is also optimal for hydropower objective. As the water availability continues to shrink, strict objective to meet a pre-specified flow can inherently preclude ability to tailor the downstream conditions on a short-term (e.g. day-to-day) basis. Our results suggest that integrating the ecologically driven

objectives (or constraints) within the dam operation module where one has a direct bearing on the other can potentially overcome dam's detrimental impacts on ecology.

The remote sensing-based results for extracting water surface temperature were encouraging especially for data-constrained regions. The sheer prevalence of planned and under construction hydropower dams in the developing nations[9] creates a significant opportunity for implementing the concept. Using remotely sensed TIR images for stream temperatures provides an alternative to scarce in-situ sensors in such regions for establishing the functional regression models. The technique is not limited to validating regression relations for a particular dam. It can also be incorporated for prior reconnaissance of existing and numerous future dams facing highest degrees of thermal pollution to guide and improve the policy development. It is noteworthy of mention that the approach is limited when mixed water pixels are present in the TIR band. Our results underscored reliable performance for river channels with smaller depth to width ratio and where the width covers atleast two to three pixels of Landsat ETM+. Similar findings on minimum number of pixels were reported by Handcock et al. (2012) who tested with airborne and satellite TIR images of varying pixel sizes.

In light of the findings from sensitivity analysis, drier years posed challenges in mimicking natural temperature regime. Embedding prescribed biological criteria in the optimization framework with skillful flow forecasts aided in realizing temperatures suitable for relevant downstream aquatic habitat and potentially benefitting energy and ecosystem objectives. USACE recently proposed a temperature control tower for Detroit dam to improve fish passage and temperatures for endangered salmon and steelhead, costing more than USD $350 million (Harrison, 2019). Our daily forecast-based optimization demonstrated here can help avoid such

expensive measures for other existing and planned dams by minimizing the adverse impacts of dam operations.

5.6 CONCLUSIONS

The advancements in flow and reservoir operations modeling have resulted in considerable understanding of the ecological effects of flow regime alteration. This study specifically focused on the thermal impacts of hydropower dams and explored them in context of operations for improving hydropower generation. Studying the relation between hydropower and changes in thermal regime between dam's upstream and downstream reaches was facilitated by a simple functional regression model. A multi-objective optimization framework was designed to utilize short-term NWP weather forecasts. The model for water temperature change was used to impose additional constraints of tolerable downstream cooling or warming on multi-objective optimization to maximize hydropower. Remote sensing-based temperature estimation algorithm, valuable for regions with scarce in-situ data, was established using thermal infrared band of Landsat ETM+ over multiple dams. The hydropower benefits correlated strongly with the allowable flexibility in temperature constraints. Across the different years with varying climatological conditions, wet years showed maximum hydropower benefits while still satisfying stringent temperature constraints.

It is worth noticing that confidence in the presented tradeoffs in ecosystem-safe hydropower is bounded by the validity of developed hydropower-temperature relationships and flow forecasting model. The performance is affected by how well the temperature changes are modeled as a function of dam operations or if there were any spurious correlations driving the performance (Chen and Olden, 2017). Accounting for non-linear variable relationships in hydro-

climatic processes and reservoir's thermal response is warranted for further improvement. Long term forecasts (Ahmad and Hossain, 2020b) can be incorporated to broaden the temporal foresight and operating horizon under climatologically dry/wet years. Finally, for a more holistic ecosystem-safe hydropower optimization, other water quality constituents of concern such as dissolved oxygen levels, total dissolved solids, and bubbling of carbon dioxide or methane from reservoirs also need consideration.

While the cost to environment can never be completely eliminated, we have demonstrated a practicable solution to navigate the tradeoffs in hydropower and thermal stability for exisitng dams. The challenge is now to realize this as an operating standard for future dams and thus foster the goal of sustainable energy generation. Chapter 6 follows next to study the thermal impact of future hydropower dams.

Chapter 6. HOW MIGHT PLANNED HYDROPOWER DAMS ALTER RIVER TEMPERATURES AROUND THE WORLD?

Note: This chapter has been adapted from an article submitted to Earth's Future. At the time of writing, this article is under review.

Ahmad, S.K., Hossain, F., Holt, G., Galleli, S., Pavelsky, T. 2020d. How might Planned Hydropower Dams Modify Temperature of Rivers around the World? Earth's Future (*in review*)

ABSTRACT

Selective water release from the deeper pools of reservoirs for energy generation alters the temperature of downstream rivers. Thermal destabilization of downstream rivers can be detrimental to riverine ecosystem by potentially disturbing the growth stages of various aquatic species. To predict this impact of planned hydropower dams worldwide, we developed, tested and implemented a framework called '*FUture Temperatures Using River hISTory*' *(FUTURIST*). The framework used historical records of in-situ river temperatures from 107 dams in the U.S. to train an artificial neural network (ANN) model to predict temperature change between upstream and downstream rivers. The model was then independently validated over multiple existing hydropower dams in Southeast Asia. Application of the model over 216 planned dam sites afforded the prediction of their likely thermal impacts. Results suggested a consistent trend of thermal cooling of downstream regime during summers and warming during winters. During Jun-Aug, 73% of dams planned in the Northern Hemisphere are likely to cool downstream rivers, with 16% dams that experience strong thermal stratification expected to reduce temperatures by more than 6˚C. Winter season operations were predicted to consistently warm downstream by temperatures

of up to 6˚C. Reversed seasonal trends were predicted for dams planned in the Southern Hemisphere. Such impacts, homogenized over time, raise concerns for the ecological biodiversity and native species. The presented outlook to future thermal pollution will help design sustainable hydropower expansion plans so that the upcoming dams do not face and cause the same problems identified with the existing ones.

6.1 INTRODUCTION

The preceding chapters two to five have proposed solutions to improve the efficiency of hydopower operations on the three fronts outlined in chapter one. However, as the near future is going to witness a large expansion of hydropower infrastructure, especially in the Global South, this chapter addresses the energy efficiency from sustainability standpoint for the future dams. The goal here is to facilitate expansion of hydropower infrastructure in an environmentally sustainable way and thus foster the goal of sustainable energy generation.

The arguments for or against building dams, particularly hydropower dams, are many. Hydropower dams serve as a source of relatively low-carbon energy, guard against extreme floods and meet a steadily increasing water demand. Many countries have included the expansion of hydropower infrastructure as part of their climate mitigation strategy, following the United Nations Climate Change Conference in Paris in 2015 (Zarfl et al., 2019). To date, about 3600 medium and large hydropower dams are either under construction or planned, predominantly in South America, Africa, and South/East Asia, an area with relatively untapped hydropower potential (Zarfl et al., 2015). Laos, for example, has pursued an ambitious initiative to become the ‘Battery of Southeast Asia’ by building an unprecedented number of dams in the Mekong River Basin (Schmitt et al., 2019; Chowdhury et al., 2020). However, hydropower dams also substantially affect surrounding

ecosystems, and these long-term ecological impacts are often discounted in decision-making processes (Winemiller et al., 2016). In addition to fragmenting almost two-thirds of the world's free-flowing large rivers (Nilsson et al., 2005), dams in general have modified natural sediment transport (Zarfl and Lucía, 2018; Yang et al., 2005), disrupted natural hydrologic variability (FitzHugh and Vogel, 2011), contributed to greenhouse gas emissions (Deemer, 2016), and led to resettlement of local communities and loss of culture and heritage (Hecht et al., 2019). Such impacts have threatened freshwater biodiversity and harmed fisheries (Barbarossa et al., 2020).

Amongst the many negative consequences of hydropower dam operations, dramatic alteration of river's thermal regime is amongst the most adverse impacts (Bonnema et al., 2020). In the storage dams used for extensive hydropower generation, reservoirs are designed for higher hydraulic head and a large storage capacity. This relatively stagnant and deep body of water tends to thermally stratify into multiple horizontal layers or pools (Imboden and Wuest, 1995). Water for flood control tends to be released from the uppermost pool via the spillway, while water for irrigation or other downstream users is mostly released from the uppermost and middle pools (often called 'conservation' pool). However, it is the water for hydropower production that causes the most drastic difference in temperature to downstream water, as it is drawn from the bottom pool. This pool is often colder than the rest of the pool and the downstream river, especially during summer seasons. The selective release of water from the deeper pools is the main cause of river's thermal pollution, that is the modification of the natural thermal regime of downstream river segments (Niemeyer et al., 2018; Olden and Naiman, 2010). Because river temperature plays a vital role in sustaining aquatic habitat (Angilletta, 2008), thermal pollution can damage aquatic biodiversity, potentially disturbing the growth stages of various fish and other aquatic species.

The significance of riverine thermal pollution caused by existing dams has been acknowledged but only partially addressed in the literature (Bonnema et al., 2020, Caissie, 2006; Poole and Berman, 2001). Current approaches for estimating dam-driven thermal pollution rely on either statistical approach such as regression (Benyahya et al., 2007; Ahmad and Hossain, 2020b) or more complex and physically distributed river temperature (Yearsley, 2012) and hydrodynamic models (Cheng et al., 2020a, Cheng et al. 2020b, Niemeyer et al., 2018, Buccola et al., 2016; Cole and Wells, 2015). While some of these models use ambient conditions and flow variables to predict downstream river temperatures (Mohseni et al., 1998; Neumann et al., 2003), others solve thermal energy budget and heat advection-dispersion equations (Cole and Wells, 2015; Yearsley, 2012). However, current models have multiple limitations when it comes to studying the impact of planned hydropower dams. On one hand, hydrodynamic and thermodynamic models are complex and require inputs on quantities difficult to measure or estimate such as for non-radiative fluxes (Mohseni et al., 1998, Toffolon and Piccolroaz, 2015; Van Vliet et al., 2011). For instance, there may be no boundary condition data for flow and temperature to initialize such models when a dam has not been built yet. On the other hand, simpler statistical models cannot be extrapolated to predict thermal response of dams with unobserved hydro-climatological and geophysical characteristics (Toffolon and Piccolroaz, 2015). Both classes of models, however, suffer from the inability to be set up for large number of future dams, which instead require a rapidly transferrable yet skillful technique of modeling dam's thermal response.

Given the pace at which future hydropower dams are being built, it is imperative to identify development pathways where the proposed infrastructure can serve its purpose while maintaining a sustainable and productive river system (Grill et al., 2015). As predicted by Zarfl et al. (2019), the majority of future hydropower development is planned in catchments with a high share of

threatened megafauna species. This requires a study of future dams in the context of their potential impacts on the ecosystem. Towards that end goal, we outline three key traits for a modeling framework to 'predict', or infer, the thermal modification impact of planned dams. As the aquatic biodiversity is more sensitive to alterations in thermal regime than the absolute water temperature (Haxton and Findlay, 2008), we need a technique that is reliably accurate in providing the qualitative understanding of thermal regime change. Second, the technique should be transferrable for use over any planned dam site around the world. Finally, there should be minimal input data requirement, a fundamental prerequisite for working on the data-scarce conditions characterizing the Global South, where the majority of hydropower dams are planned. Thermal infrared (TIR) remote sensing from the vantage of space offers the only feasible method over data-limited regions to monitor spatial and temporal patterns of surface water temperature due to hydropower development (Ling et al., 2017). The potential of TIR data has recently been demonstrated by Bonnema et al. (2020) using the 3S (Sekong, Sesan, and Sre Pok) river basins as a microcosm of hydropower development for the rest of the Mekong basin.

Here, we predict the thermal impact of 216 planned hydropower dams around the world on their likely change to downstream river temperatures. The dams were selected to represent a diverse range of dams with different structural characteristics, types (storage or run-of-river), hydrology, and climates. Also, most of these dams are planned at. locations far apart to avoid the thermal pollution of upstream dams from impacting the downstream ones. Our predictions are based on a novel framework for planned hydropower dams called '*FUture Temperatures Using River hISTory*' *(FUTURIST).* The *FUTURIST* framework is based on the key premise that a long record of the past thermal impact is a reasonable representation of the near-future impact due to planned hydropower dams. More specifically, we use *FUTURIST* framework to answer the

following questions: (i) can we learn patterns of thermal impact on downstream rivers caused by the existing dams based on known climate, hydrology, and dam characteristics? (ii) having identified, or learnt, such a relationship over existing dams, can we predict the thermal impact of the future (planned or under construction) dams?

To answer these questions, we employed a historical record of in-situ river temperature changes from 107 dams in the U.S. to train an artificial neural network (ANN) model (Ahmad et al., 2020d). This data-based ANN approach predicted temperature change between upstream and downstream rivers. The ANN model was able to capture nonlinearities in predicting dam's thermal impacts that makes the technique transferrable to other dams with unobserved conditions. This was demonstrated by the high predictive skill over tropical climate of Southeast Asian dams during model validation. Also, the challenges with existing data-intensive models were tackled by FUTURIST for which the required inputs were either one of the dam's structural properties or variables derived from remote sensing products. TIR remote sensing-based thermal change was used for model training and validation where in-situ monitored values were absent or scarce. The ANN model was then applied at planned hydropower sites worldwide to predict the likely thermal impacts and elucidate the need to include thermal pollution within dam planning to ensure safety and sustainability of the ecosystem. Finally, we explored the effect of climate change on riverine thermal regime change using our framework by forcing the ANN model with different warming scenarios towards the end of the century.

6.2 MATERIALS AND METHODS

6.2.1 *Dam Sites and Temperature Data Preparation*

For establishing the *FUTURIST* framework, we first selected dam sites in the U.S where in-situ temperature measurements are available both upstream and downstream of the hydropower dams. For in-situ temperature data, we used the network of stream temperature monitoring stations from the United States Geological Survey (USGS). A total of 4,186 sites were first filtered out from the USGS gage database based on the availability of temperature measurements. To filter out stations that are located upstream and downstream of the existing dam sites, we used the Global Reservoir and Dams (GRanD) database (Lehner et al., 2011). This resulted in 87 hydropower dams, out of which 68 locations had at least a year of overlapping temperature records on upstream and downstream stations. We selected the USGS gauges closest to dam and at a maximum distance of 50 km from the dam for both upstream and downstream temperatures. The temporal record length exceeded more than 10 years for most of the selected sites.

To expand the database of hydropower dams with information on thermal impacts in the past, we used remote sensing observations of surface water temperature from TIR data. Because the remote sensing-based temperature extraction is limited by the spatial resolution of the satellite (see Section 6.2.2), it is challenging to obtain pure water pixels over narrower rivers, unless the river is wide enough to reflect pure water signal. Upstream of a dam, however, with the larger expanse of reservoir, the spatial resolution of TIR remote sensing is not an issue. We therefore filtered out 39 additional sites with USGS station located downstream for which the upstream reservoir temperatures were obtained from remote sensing, sampled over the reservoir. Thus, the selected set of 107 dams consisted of a diverse range of climates, dam types (storage and run-of-

river), sizes (with reservoir capacities varying from 10 to ~6500 mcm), and topography, so that the model trained on these sites can capture the variability across other dam sites with unobserved conditions (see Appendix E, Figure E1).

Developing a thermal change model that can be scaled globally requires validation over sites that are devoid of in-situ measurements. Thus, for a robust validation of our approach, we selected existing dam sites in Southeast Asia (MRB and India), where a large number of hydropower dams have recently been built with more dams at different planning stages. Location and relevant information for dams in the MRB were obtained from CGIAR WLE Database (Mekong Dam Database, 2011), the Mekong River Commission (MRC, 2009), Räsänen et al. (2017), Piman et al. (2013), and other reports from dam authorizing agencies. Data for existing dams in India were retrieved from the National Register of Large Dams (NRLD, 2012). Only the dams with river channels (upstream or downstream) wider than 120 m (see Section 6.2.2) were used, so as to avoid the impure non-water pixels during retrieval.

Information on planned hydropower dams was retrieved from multiple sources, as no global scale database exists yet with information on dam design features. Some of the sources used here include Georeferenced Information System of the Electric Sector (SIGEL – https://sigel.aneel.gov.br/portal/home/) of the Brazilian National Hydroelectric Agency (ANEEL) and Anderson et al. (2018) for Brazilian dams, Finer and Jenkins (2012) and Forsberg et al. (2017) for Andean dams, Hydropower Project Database from MRC (Hydropower Project Database, 2012), Piman et al. (2016), and Wild and Loucks (2014) for dams in MRB, and AQUASTAT (FAO AQUASTAT Main Database, 2016) for the dams in the remaining countries. Individual reports from dam authorities were also consulted to fill in the missing data and to cross-validate the retrieved information. The selected planned dams also represented a wide variety in

characteristics, types (storage and run-of-river), hydrology, and climates. Also, most of these dams are planned at locations far apart to avoid the thermal pollution of upstream dams from impacting the downstream ones. A distribution of selected planned dams and their characteristics are shown in Figure E5 (Appendix E).

6.2.2 *Monitoring Thermal Impacts from Space*

Despite the advantage of a robust temperature monitoring network in U.S., developing nations still lack in-situ measurements. We therefore used Landsat-7 ETM+ TIR band observations (available 1999 onwards) to obtain estimates of surface water temperature for upstream reservoir (for selected dams within U.S., where upstream USGS stations were absent) and both upstream and downstream for dams in Southeast Asia (used for validation). Landsat-5 TM TIR band was also employed for dams (specifically in the MRB) that required temperature estimates before 1999 for pre-dam thermal regime. The TIR band from Landsat-7 band is acquired at 60 m and that from Landsat-5 at 120 m, due to which we restricted the selection to dams with rivers wider than 120 m (to avoid impure water pixels). The single algorithm (Jiménez-Muñoz et al., 2008; Jiménez-Muñoz and Sobrino, 2003) for temperature extraction was used, with atmospheric correction for top-of-atmosphere (TOA) reflectance. The procedure is described in detail by Ahmad and Hossain (2019c).

A comparison of Landsat-derived surface temperature and in-situ observations from USGS stations upstream of a few dams in the U.S. was performed (see Appendix E, Figure E2). An extensive validation of upstream and downstream temperatures from Landsat has been presented for multiple dams in U.S. against USGS records in our previous study (Ahmad and Hossain, 2020c). Temporally synchronous measurements of in-situ and Landsat-derived temperatures for the upstream and downstream waters were used to quantify the change in thermal regime.

Exception to this were the dams in MRB, where pre-dam temperatures were acquired from Landsat due to recent dam construction in the past two decades. Thus, for MRB dams, temperatures before the start of dam construction were used instead of the upstream reservoir temperatures for calculating thermal regime change.

6.2.3 *Dam Operation-Induced Thermal Regime Change*

Dam operations affect downstream temperature regime in multiple aspects (see Appendix E, Figure E3). Marked changes occur in the timing, magnitude and duration of peaks and lows of the temperature distribution over the year relative to the thermal regime (Olden and Naiman, 2010). Here, the variable of interest is the change in thermal regime of rivers caused by dam operations with respect to the natural thermal regime. Because of the early construction of dams in the U.S., pre-dam temperatures were challenging to obtain from USGS gauges or any other source. Thus, the temperature of upstream river flowing into the reservoir was considered as proxy to the natural riverine thermal regime when pre-dam temperature was absent. We considered the mean difference between upstream and downstream temperatures over multiple years on record to capture the key aspects of thermal impact, homogenized over time. Thus, the temperature of upstream river flowing into the reservoir was considered as proxy to natural riverine thermal regime when the pre-dam data are absent. We considered the mean difference between upstream and downstream temperatures over multiple years on record to capture the change in thermal regime, homogenized over time. To this end, we defined thermal regime change, ΔT as,

$$\Delta T_{warm} = \overline{T_{up} - T_{down}} \tag{6.1}$$

where, ΔT_{warm} is the thermal change over warm season (months of JJA) calculated as difference between the upstream (T_{up}) and downstream water temperatures (T_{down}) over those months. A

similar equation is used for the cold season (ΔT_{cold}) where the averaging is performed over the months of DJF.

In light of the previous efforts to assess dam impacts on different ecosystem aspects using qualitative categories (Zarfl et al., 2019; Barbarossa et al., 2020; Grill et al., 2015), we introduced the Thermal Change Class (TCC) for categorizing and assessing the thermal impact. We used the cumulative distribution function (CDF) plots of thermal change for existing dams as a guide (Figure 6.1) to formulate TCC. The thermal change values were first classified into two basic categories of cooling and warming, which were then broken down into four sub-categories: moderate cooling (between -6 ˚C and 0 ˚C), severe cooling (less than -6 ˚C), moderate warming (between 0 ˚C and +5 ˚C), and severe warming (more than + 5 ˚C). It should be noted that the FUTURIST framework is independent of the choice of thermal thresholds, and the output classes can be adapted based on the needs of the stakeholder.

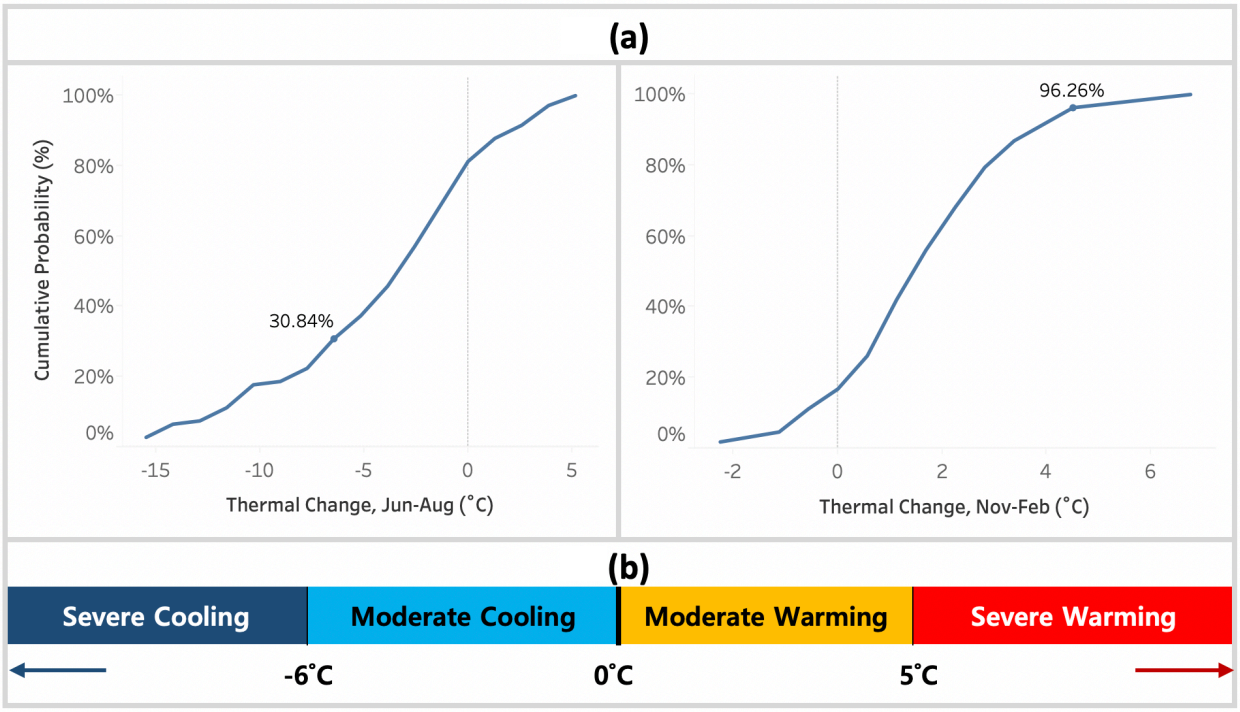

Figure 6.1 (a) Cumulative Distribution Functions (CDF) for thermal regime changes during cold and warm season across the existing 107 dams in U.S. (b) Thermal Change Class (TCC) based on the selected thresholds of -6˚C and 5˚C for subclassifying the cooling and warming regimes, respectively.

6.2.4 *FUTURIST Framework*

Our proposed framework, *FUTURIST*, is designed to predict the qualitative category of thermal regime change caused by a planned dam. The procedure begins with developing a data-based model to learn historical patterns of the impact on rivers due to dam operations. Various dam characteristics, hydrology, topography and climate of the reservoir basin were used for training. A multilayer perceptron feedforward ANN model was selected, and hyperparameter tuning was performed for designing the network architecture to predict the temperature change which was subsequently converted to classes of thermal change. The architecture, designed based on hyperparameter tuning, consisted of two hidden layers with 16 and 8 nodes, where the input layer comprised of 7 nodes (see Appendix E, Figure E4). The training was performed over dams in U.S. and then validated over selected sites in Southeast Asia (MRB and India).

Predictor variables were selected that (a) directly impact reservoir stratification and river temperature, and (b) can be acquired either from the dam operating agency or derived from globally available remote sensing or atmospheric products. The second criterion was used to ensure our framework is transferable in data-constrained regions. The selected input nodes thus comprised of dam height (in meters), reservoir area (in km^2), storage capacity (in million m^3), Köppen-Geiger climate class (Peel et al., 2007) , terrain elevation (in meters, retrieved from the Digital Elevation Model (DEM) from Shuttle Radar Topography Mission (SRTM), ambient air temperature (in ˚C, extracted from the ECMWF's ERA5 reanalysis product from

https://developers.google.com/earth-engine/datasets/catalog/ECMWF_ERA5_DAILY), and a dimensionless bathymetry coefficient (see Appendix E, Table E2). Air temperature is input as an average of the daily time series during the respective season (JJA or DJF) over the period of record. The Köppen-Geiger climate classes represent a categorical variable that was pre-processed using ordinal encoding (with integers from 1 to 27), and further normalized between 0-1 like all other predictors. The bathymetry coefficient is a measure of similarity between reservoir's bathymetry and a rectangular cross-section, calculated as the ratio of storage capacity with the product of reservoir's maximum area and depth. A similar dimensionless ratio called reservoir coefficient was proposed by Mohammadzadeh-Habili et al. (2009) where lower values correspond to reservoirs with gorge-like bathymetry. The modeling framework is open-source and available on the GitHub repository at: https://github.com/shahryaramd/futurist.

6.2.5 *Climate Change Impact Assessment*

By the end of the 21st century, air temperatures are projected to increase due to global warming according to all the climate models under the Coupled Model Inter-comparison Project Phase 5 (CMIP5) (Taylor et al., 2012). The ANN model developed for the prediction of thermal impact includes ambient air temperature as one of the predictors (see section 6.2.4). Therefore, we used different air temperature scenarios as forcings to the FUTURIST framework for studying the effect of climate change on riverine thermal regime change. Specifically, we used two Representative Concentration Pathway (RCP) scenarios, RCP4.5 and RCP8.5, and a retrospective (historical) run from globally downscaled Coupled Model Intercomparison Project Phase 5 (CMIP5) climate projections (Collins et al., 2013). The climate scenarios were acquired from 21 different runs of General Circulation Models (GCM) conducted under CMIP5, available in Google Earth Engine data catalog as NASA Earth Exchange (NEX) GDDP dataset

(https://developers.google.com/earth-engine/datasets/catalog/NASA_NEX-GDDP). The details on the selected CMIP5 models are provided in the supplementary information. The analysis of predicted thermal changes under climate change was carried out using the ensemble mean of all the 21 models and averaged around the dam location over a period of 25 years (1980-2005 for the baseline scenario and 2075-2099 for the two RCP scenarios).

6.3 RESULTS

6.3.1 *Thermal Impact of Existing Dams in the U.S.*

The large number of U.S. dams with long temperature records form an ideal testbed for studying thermal impact of planned hydropower dams. Using data from temperature gauges located upstream and downstream of 107 dams (see Figure E1, Appendix E), we obtained mean change in temperature over the period of record during warm and cold season months in Northern Hemisphere of Jun-Aug (JJA) and Dec-Feb (DJF) respectively. For upstream stations with no in-situ gages, we used satellite TIR remote sensing for reservoir temperature estimates. Because for some reservoirs, ice formation on the lake surface during winters resulted in sub-zero temperatures when using remote sensing, those values were excluded from the analysis.

We found that most dams in general tend to cool downstream rivers during the warm season and warm during the cold season. These impacts reflect homogenized changes over the available data during the past two decades. During months of JJA, 74 (69%) hydropower dams in the U.S have cooled downstream rivers when compared to their upstream (used as the proxy to natural baseline) thermal regime (Figure 6.2a). Sub-categorizing this impact further, 27 of the dams (25%) caused severe cooling to the downstream rivers. Interestingly, only five hydropower dams (5%) severely warmed the tailwaters (defined as an increase of 5˚C or more in the downstream river

temperature). In contrast, during the cold season (DJF), most hydropower dams (85%) caused moderate warming, while only 11% led to moderate cooling and 4% led to severe downstream cooling (Figure 6.2b).

These results can be explained based on the characteristics of reservoirs and the ambient conditions. The primary cause of cooling is the stratification of reservoirs with significant difference between the temperatures of surface water and that of deeper pools from which the water is released. Dams with larger storage of reservoirs and smaller area experience strong thermal stratification and such dams tend to have a severe cooling impact. In contrast, small storage reservoirs with large area have relatively uniform water pool leading to comparatively warmer release downstream. A detailed description of other factors affecting the observed trends in thermal impacts is given in Section E1 and Figure E6 (Appendix E).

6.3.2 *FUTURIST Thermal Change Model Development*

Using in-situ data, we trained an ANN model that predicts the mean temperature difference between upstream and downstream of a dam for each season. For most reservoirs, the stations that provided upstream temperatures were located on rivers flowing into the reservoir. This minimized the impact of reservoir's surface area on water temperature. However, the dams for which upstream in-situ stations were unavailable and the upstream rivers were narrow (see Methods section), remote sensing was used to observe the skin temperature of the reservoirs. Predictors to the model included dam height, reservoir area and storage, climate class, topography and ambient air temperature. Model validation was performed over 27 existing dams in Southeast Asia located in Mekong River Basin (MRB) and India.

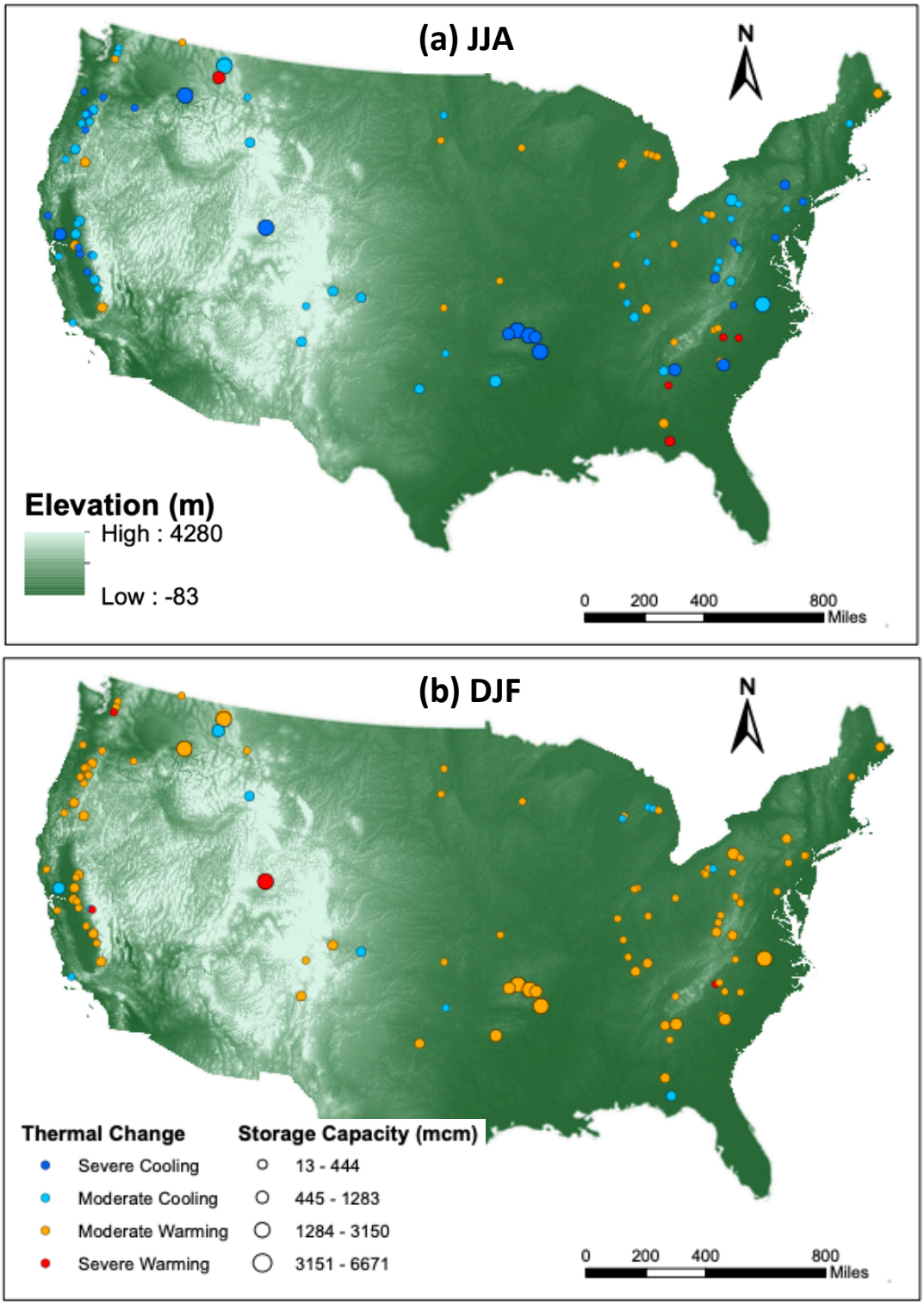

Figure 6.2 Dams used for training ANN model to learn the thermal regime change (mean difference of upstream and downstream temperatures) over months of (a) JJA and (b) DJF.

Classes of the thermal change are defined using quantiles of temperature distribution, see Methods section.

During JJA, when observed temperature changes ranged between -6.7 ˚C to 5.6 ˚C, 21 out of the 27 validation sites in Southeast Asia were predicted correctly (78% accuracy) in terms of the nature of thermal regime change (warming/cooling) as well as in severity (severe/moderate). When considering only the nature of thermal change, however, the model was able to predict thermal regime changes with even higher accuracy (89%) and just two cases of warming misclassified as cooling (Figure 6.3). The model was relatively less sensitive during the cold season (DJF), with observed temperature changes ranging between -1.8 ˚C to 3.8˚C (moderate cooling/warming), predicted categorically with an accuracy of 81%. The ability of FUTURIST model to accurately predict the direction and general magnitude of thermal change for 78% and 81% of the sites is encouraging, despite the geographic differences between training and validation datasets. We also performed a validation exercise based on the continuous variable of thermal change in degrees. The mean absolute error in predicted temperature change over the selected dams was 2.2 ˚C and 2.0 ˚C during months of JJA and DJF, respectively.

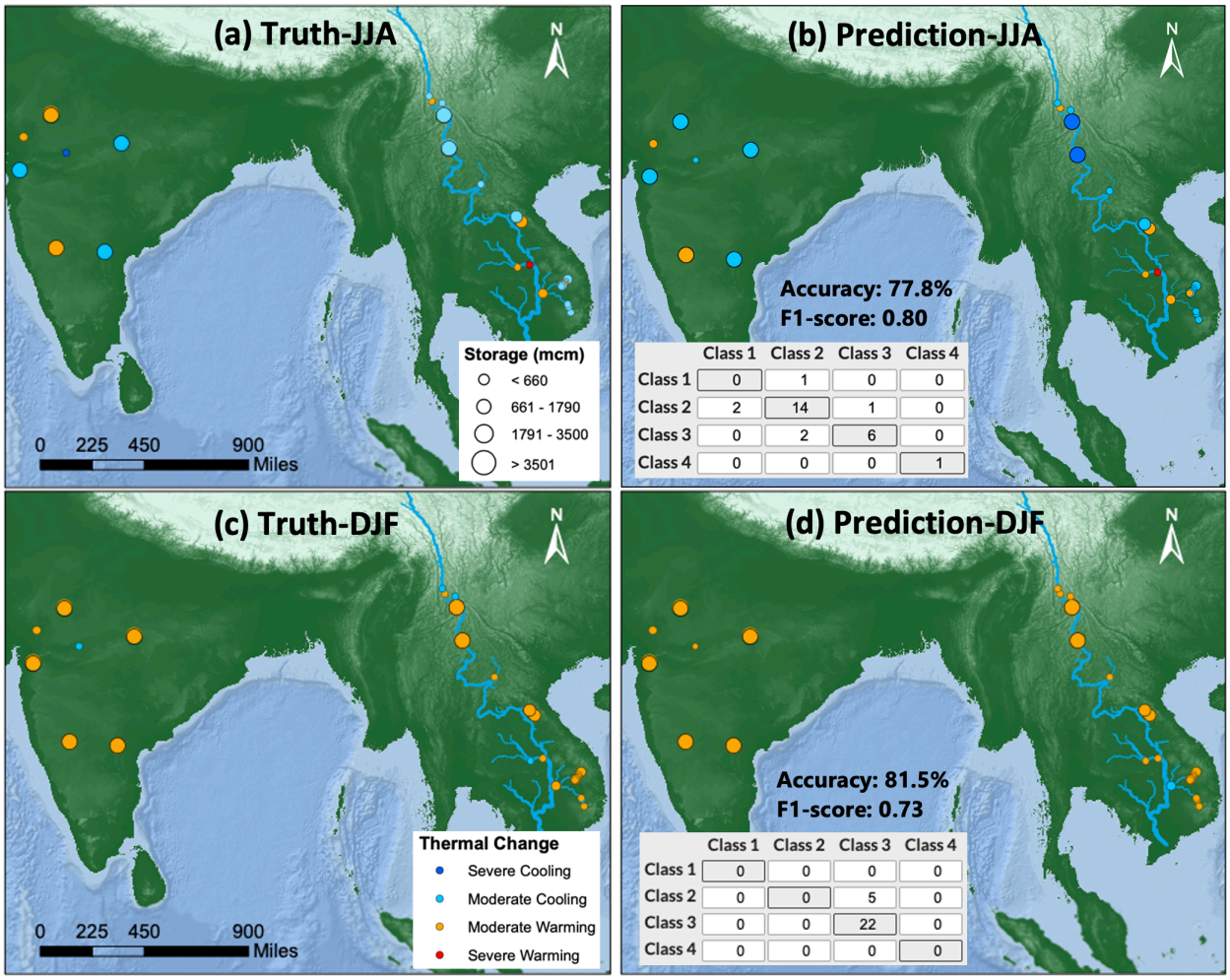

Figure 6.3 Validation results for existing dams in Southeast Asia during the months of JJA (top panel) and DJF (bottom panel). Reference thermal change classes are shown on the left (a and c) while corresponding model predictions are shown on the right panel (b and d). Confusion matrices, accuracy (ratio of correct predictions and total sample dams) and F1-scores for the respective classifications are shown in the right panel.

6.3.3 *How will Planned Hydropower Dams Alter River Temperatures Around the World?*

Using the model trained and validated on a variety of existing dams in the U.S. and Southeast Asia, we applied the FUTURIST framework to 216 planned hydropower dam sites around the world (including those under construction). Amongst the selected sites, 100 are planned in Northern Hemisphere and the rest in Southern Hemisphere. It is worth noticing here that the predictions are

an estimate of the likely changes in thermal regime due to future hydropower dam operations if the plans are executed under the current temperature scenario.

Figure 6.4(a) shows the results of FUTURIST predictions across the selected dams. During the months of JJA (summer season in the Northern Hemisphere), 73 of 100 hydropower dams planned in the northern hemisphere are likely to cool downstream rivers, with 16 of those expected to exhibit severe cooling. The majority of dams that cause downstream rivers to cool during summers experience strong reservoir stratification. As such, these have either large storage pool or smaller reservoir area. In contrast, for the dams planned in Southern Hemisphere that experience winter during JJA, all the dams are predicted to cause warming of the tailwaters with thermal changes varying between 1.2 ˚C to 5.5 ˚C.

During the months of DJF (Figure 6.4(b)), a reverse trend was suggested by the FUTURIST predictions. Consistent downstream warming is predicted due to all the dams in Northern Hemisphere, with a likely thermal change of 1.2 ˚C to 6.0 ˚C. While for the Southern Hemisphere, 100 of 116 dams (86%) are likely to cool downstream rivers during their summer season, amongst which 13 have the potential of causing severe cooling to the tailwaters. Again, the reservoirs with strongest stratification were the ones predicted to impact the downstream rivers most severely.

These results are consistent with the thermal impact due to dams used for validation in Southeast Asia, where most dams have resulted in summer cooling and winter warming of the tailwaters. A similar pattern was also observed for existing U.S. dams used for training (used for training, Figure E6 of Appendix E), although other factors like climate and dam bathymetry resulted in apparent differences between the dams in U.S. and those planned across the world.

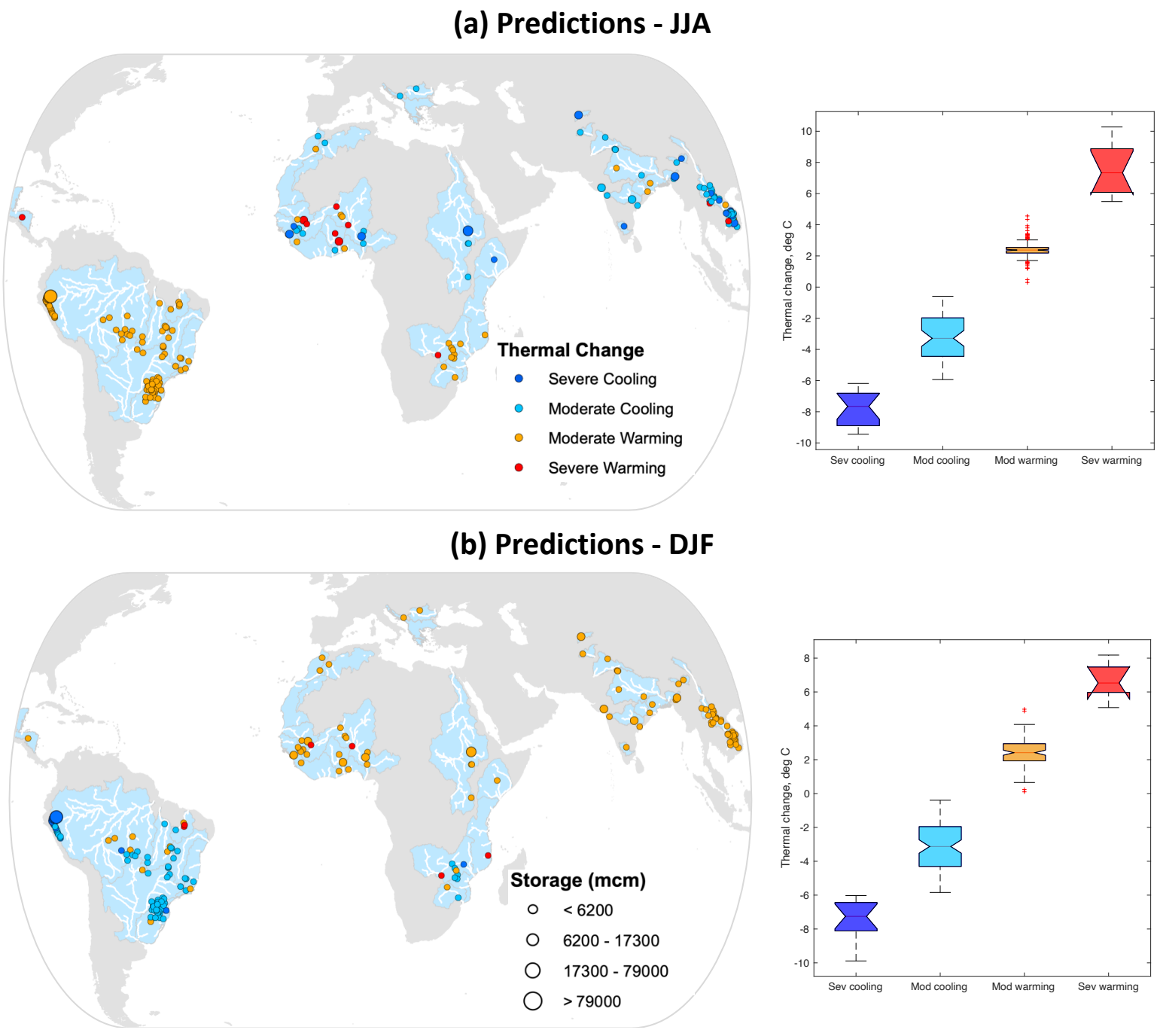

Figure 6.4 Thermal regime predictions for planned hydropower dams during the months of (a) JJA and (b) DJF. Variability in each class of thermal change is shown as boxplots for the respective seasons. River and basin shapefiles are obtained from HydroSHEDS and HydroBASINS databases respectively (Lehner et al., 2013).

It is worth mentioning that the predictions on planned dams are dependent on the diversity and variability represented by the training set of the *FUTURIST* framework. As only dams in U.S. were used for training due to limitations of data availability in other regions, uncertainty can increase in the predictions over significantly different climates such as in Southern Hemisphere. The same class of thermal change predicted across all the dams during winters could possibly be affected by this uncertainty.

6.3.4 *Explaining Model Predictions*

Neural networks have been criticized for being black-box type models with little insight into the physical processes driving the outputs. However, in order to build a trustworthy model, an explanation of the predictions made by the model is fundamental. Here, we used a technique called Local Interpretable Model-Agnostic Explanations (LIME) (Ribeiro et al., 2016). The technique provides prediction of any classifier in an interpretable manner presenting contributions (set of coefficients) of the individual predictors towards the final model outcome.

Using the LIME model, we analyzed our trained NN model for the contributions from selected input nodes for modeling the thermal change. Figure E7 (Appendix E) shows these contributions for a sample of existing and future dams. The magnitude of individual contributions suggest that the top contributors are, in general, the parameters that control reservoir's stratification such as reservoir area and storage capacity. Also, ambient air temperature plays a significant role for the majority of dams. These findings build confidence in the model and allow the planner or manager to decide if the predictions should be trusted depending on which predictors are deriving the outcomes.

6.3.5 *Impact of Climate Change on Predicted Thermal Pollution*

The ensemble mean of climate scenarios from 21 models under GCM runs were used to force the FUTURIST ANN model and study the effect of climate change on riverine thermal regime (average difference between upstream and downstream temperatures). Resulting predictions of thermal changes were compared across the three scenarios of baseline, RCP4.5, and RCP8.5. Figure 6.5 shows the empirical distribution of predicted temperatures and respective thermal changes over the 216 planned sites for both the winter and summer seasons.

The greenhouse gas emissions scenarios of RCP4.5 and RCP8.5 cause the temperature distribution to shift towards right with a higher amplitude of thermal change. The resulting thermal regimes also experience changes under the projections of changing climate. During JJA, the dams that are predicted to cause warming under current temperatures (dams with positive thermal change in Figure 6.5, right panels) will slightly intensify their impact, with an increased downstream warming over the baseline scenario by 0.7% (1.2%) under RCP4.5 (RCP8.5) scenario, with an uncertainty of 0.01 ˚C (0.02 ˚C). However, the dams causing downstream cooling (negative thermal change), on experiencing warmer air temperatures, will have a curtailed cooling impact by 2.3% (4.5%) under RCP4.5 (RCP8.5) scenario with uncertainty bounds of 0.03 ˚C (0.05 ˚C). During DJF, these values are predicted to be 1.1% (2.0%) for dams causing warming and 3.5% (6.9%) for dams causing cooling under RCP4.5 (RCP8.5) scenario.

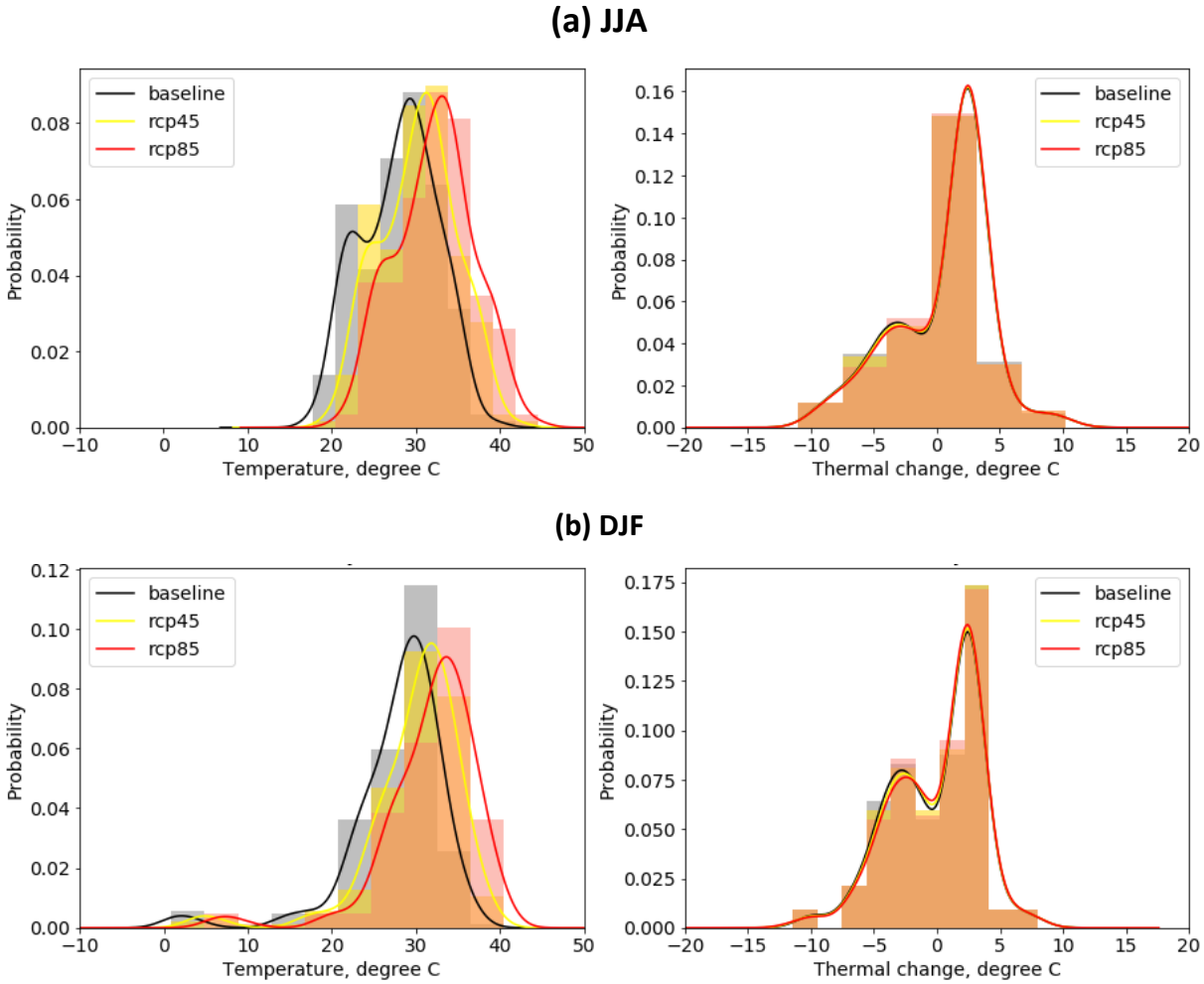

Figure 6.5 Probability distributions of air temperature as histogram and smoothed curves (left panel) and those for respective thermal regime changes (right panel) over 216 planned dams for three scenarios of baseline (historical temperatures during 1980-2005), RCP4.5 (2075-2099), and RCP8.5 (2075-2099) during months of **(a)** JJA and **(b)** DJF.

6.4 DISCUSSION

We have shown here that the past historical records of dams in the U.S can be leveraged to predict the likely impact of future hydropower dams on river temperature in a variety of climates and basins around the world. The *FUTURIST* modeling framework provides an unprecedented advantage in terms of efficiently learning how future dams might affect ecosystems by altering the

natural thermal regimes of rivers. It also allows for the assessment of climate drivers of water temperature in addition to dam operations. By providing a preliminary estimate of likely thermal impacts due to dam operations, our *FUTURIST* framework also helps prioritize the planned sites where more detailed and expensive physical studies need to be carried out.

6.4.1 *Global Overlook of Thermal Impacts in the Future*

Existing studies on dams have demonstrated the potential impacts on freshwater megafauna species (Zarfl et al., 2019), fragmentation of the fish occurrence ranges (Barbarossa et al., 2012), flow regulation and fragmentation of large rivers (Nilsson et al., 2005, Grill et al., 2015). A global overlook of thermal impacts due to future dams adds another dimension to our understanding of human-induced changes to riverine ecosystems and the services they provide.

Our results reveal interesting and varying patterns of thermal impacts across the selected planned dams. A general trend of lower highs (reduced temperatures during summers) and higher lows (warmer temperatures during winters) is predicted. The predictions reflect homogenized changes in the thermal regime of downstream rivers over a long period of time. Dams with strong thermal stratification tend to cool downstream rivers during warm seasons. The effects of change in thermal regime are not only limited to the local river channel but may also translate into basin-wide impacts, in many cases over longer period of times, as reported by Bonnema et al. (2020). A number of potential hotspots appear that may lead to severe changes of warming or cooling for the native biodiversity. Noteworthy conclusions can be inferred using the index of dam impact matrix (DIM) presented by Grill et al. (2015) for dam development. Basins like Amazon which have been labeled as relatively pristine in terms of fragmentation and flow regulation will be experiencing dam development that can lead to moderate cooling and, in some cases, moderate warming (Figure 6.4). There are also basins such as the Parana in South America and the Niger in Africa that have

undergone significant fragmentation in the past due to hydropower dams. These two basins are projected to experience further hydropower dam developments in the near future. While the hydropower dams in the Niger basin will likely be causing a severe warming impact on the tailwaters, those in Parana basin are predicted to cause moderate cooling during summers. This suggests that basins already fragmented due to hydropower dam operations are also susceptible to serious thermal impacts. Such basins demand reconsideration of hydropower generation plans or design of adaptive operation procedures to protect the ecosystem from long-term ecological impacts due to thermal regime change.

Climate change is a major challenge, especially for developing countries in their efforts to install more hydropower capacity (Ali et al., 2018). While the impacts of climate change on the hydropower potential have been studied globally (Liu et al., 2016; Turner et al., 2017; Ali et al., 2018), our FUTURIST framework also allows quantifying and assessing the thermal response of downstream rivers due to dam operations under long-term changes in climate. This is pertinent for performing more holistic environmental impact assessment studies with insights into thermal modifications due to hydropower generation and its variability. The impact of increased warming by the end of the century on thermal regime changes revealed that not all dams will respond the same to changing climate. Figure 6.5 shows that, under increased global warming, dams that have a cooling impact on the tailwaters (negative thermal change) will get weaker in their impact, with decreasing amplitude of thermal cooling during summers. However, the dams that led to downstream warming will likely intensify in their warming impact with higher amplitude of thermal change. It is also noteworthy that the projected increase in air temperature by the end of this century do not translate into thermal regime changes of the same magnitude. A possible reason could be the aggregation of all the dams for analyzing the changes. Also, from the predictive

abilities of different inputs (Figure E7 of Appendix E), there are other factors with higher contribution in deriving thermal regime change such as reservoir capacity or area, which can suppress the effect of air temperature.

Our *FUTURIST* modeling framework can be easily transferred to any other hydropower dam site of interest with minimal data requirements. The framework is also applicable for dams operated for other purposes, such as water supply or irrigation, which use water released from the penstocks and alter the thermal regime. Because the framework is trained on temperature change values and not on qualitative classes, the technique provides flexibility in the choice of output classes of moderate/severe change. Depending on the focus of stakeholders (fisheries, resource management, water management), the thermal class definitions can be tweaked and trained accordingly. Each community can assign its own priorities of the acceptable as moderate and unacceptable as severe to understand the impacts of a planned hydropower dam.

6.4.2 *Sources of Uncertainty in Thermal Impact Predictions*

The predictions of thermal regime change from the FUTURIST framework are influenced by uncertainty from multiple sources. First, for around 35% of the training sites that used a combination of remote sensing (upstream) and in-situ measurements (downstream), satellite-derived upstream temperatures were sampled over the reservoir extent. This was done in order to avoid narrower upstream river channels that potentially suffer from mixed pixels. However, as the USGS stations are located on the upstream river channels, comparing the two for thermal changes can lead to biases due to mixing and stratification within the reservoir.

While the in-situ gauges upstream and downstream of the dams were selected to be as close as possible to the dam, their distance from the dam location also contributes to the overall

uncertainty in predictions. The possible discrepancies between water surface temperature sensed by satellite and that averaged over the water column from in-situ sensors also introduce potential uncertainty—although such biases were avoided for Southeast Asian sites (used for validation), where both the upstream and downstream temperatures were derived using remote sensing. Further, the availability of pre-dam era temperatures in the MRB due to recent dam construction in the past two decades provided a reliable estimate of natural thermal regime.

The satellite-derived temperature estimates were encouraging especially for use in data-constrained regions. However, even after filtering out for narrow rivers to avoid mixed pixels, the estimates might have retrieval errors, caused by clouds, ice sheet or subzero water temperatures, shadow caused by terrain or dense vegetation, etc. The in-situ temperature stations from USGS can also affect the estimates of thermal regime changes owing to the distance of gauges from dams, although the 50 km proximity threshold was used to minimize the bias. Also, the temperature retrievals during winter season are prone to higher occurrences of dense cloud cover as well as icing conditions over the lake. This subsequently causes higher uncertainties in thermal impact predictions during the winter season. Further, as only dams in the U.S. were used for training due to constraints on data availability in other regions, predictions over different climates can also result in increased uncertainty. Due to a strong seasonal temperature amplitude in North America, the reservoir thermal stratification is driven by the storage of and release from the dams during summer and winter seasons. Subsequently, in more tropical environments where the seasonal temperature signal is not strong to the same extent or significantly different from the U.S., the predictions of thermal impact on downstream rivers based on our trained model can suffer potential

biases. The performance of the predictions can be further improved by training the ANN model on more dams that holistically capture the variability in climate and dam characteristics.

6.4.3 *Ecological Consequences of Thermal Pollution*

The established thermal impacts of the existing dams have already raised concerns for ecological processes and biodiversity (Olden and Naiman, 2010). With the understanding of the potential thermal alterations due to planned dams from *FUTURIST* framework, it is imperative to study how the ecology will respond to these predictions. We present here a few case examples that highlight the trade-offs and provide insight into the potential ecological response if the dam development plans are to be executed.

The operations of Xinanjiang and Danjiangkou hydroelectric dams in China, that began in 1960s, have been causing serious environmental impacts on the downstream reaches of Qiantang and Han rivers, respectively. Zhong and Power (1996) showed that these dams caused peak summer temperatures to decrease by 4-6°C and winter temperatures to increase by 4-6°C. As a result of cooler summer discharge, fish spawning was retarded by three to eight weeks, causing extirpation of a majority of warmwater fishes.

In the alpine climate of the Colorado River basin, operations of Flaming Gorge dam contributed to local extinction of multiple endangered fish species in the downstream Green River. Again, this was a consequence of the significant cooling of downstream channels where peak temperatures depressed to 6 °C from a previous range of 7–21 °C (Clarkson and Childs, 2000). Also, in Australia, Preece and Jones (2002) concluded that the cooler and delayed peak temperatures hamper the spawning success of several native fish species.

Fluctuations in winter temperature have also caused damage to the biodiversity. For example, consistent warming during winters was observed downstream of a dam on the

Saskatchewan River in Canada. This caused complete loss of insect fauna due to the elimination of stimuli essential for the completion of their life cycles (Lehmkuhl, 1974). Another such impact was observed by Stevens et al. (1997) where macroinvertebrate fauna of the Colorado River downstream of Glen Canyon Dam was highly depauperate compared with other unregulated rivers of the basin (Olden and Naiman, 2010).

6.5 CONCLUSIONS

Temperature variation of rivers is a natural phenomenon, and the ecosystem is, in general, resilient to adapt to natural fluctuations. However, the intensive damming of those natural river systems has not only also caused net shifting of temperature profiles but also led to the homogenization of those temperatures over longer periods. Such homogenized changes as predicted by the FUTURIST framework (warmer cool water periods and colder warm water periods) are the drivers of negative biological responses. The framework is designed to predict the changes in thermal regime defined on a wide temperature range, instead of precision temperatures changes. The advantages of such a framework are (a) its wide adaptability, where the definition of thermal regime can be modified based on user's perception without affecting the model performance, and (b) reproducibility, where the framework can be reproduced with users' self-perceived thermal regime and further accompanied with a more detailed model and localized understanding of thermal regimes. Our study clearly elucidates the need of frameworks like FUTURIST using which thermal pollution can be included within the dam planning to ensure sustainable river systems.

Chapter 7. CONCLUSIONS AND FUTURE RECOMMENDATIONS

7.1 CONCLUSIONS

This dissertation sets the path forward to realize hydropower operations that are efficient not only in terms of maximizing energy generation, but also in terms of sustaining our environment and attaining an eco-system resilient system that benefits different stakeholders. As elucidated in Chapter 1, for hydropower operations to be efficient, the efficiency has to address three different aspects – (i) environmental sustainability, (ii) maximization of energy generation without compromising other objectives, and (iii) resource feasibility of dam operation framework. Chapters 2 and 4 focused on maximizing the hydropower benefits for single and multi-dam networks. Chapter 3 developed a fast, skillful, and transferable approach to forecast reservoir inflow to address resource feasibility of the framework. Finally, chapters 5 and 6 proposed solutions to ensure thermal stability of river and satisfy ecological needs during hydropower operations. Key takeaways from each chapter are summarized below.

7.1.1 *Value of short-term weather forecasts*

Informing dam operations with short-term forecasts of reservoir inflow not only generated more hydropower, but also helped satisfy the competing goals of flood control, water security, and dam safety. The benefits of short-term forecasts were highest during the peak flow (wet) period when uncertainty in the reservoir inflow is generally high causing over-conservative operations. Using an ANN model fed with hydrologically relevant inputs, we efficiently forecasted inflow into reservoir for lead times of up to one week with high skill. Pareto optimal solutions to the multi-objective optimization problem can provide the dam operator enough leverage in choosing optimal solution based on situation-specific needs.

7.1.2 *Co-optimization using long- and short-term forecasts*

Application of forecasts at different temporal scales for multi-dam networks also showed significant value in achieving optimality for both long term (seasonal) and short-term (weekly) scale objectives. By incorporating long-term optimal policy (derived using climate forecasts) as a guide to short-term optimization aids the reservoir in avoiding any sudden surge or dip in the levels that might occur in the extreme seasons. The utility of nesting the weather forecasts within the climate forecasts-based operations is not only limited to hydropower but can also benefit other renewables such as solar and wind energy generation.

7.1.3 *Realizing ecosystem-safe hydropower*

The work presented here also addressed environmental sustainability in hydropower operations by imposing additional constraints on the optimization, pertinent to maintaining safe thermal regime for river's aquatic biodiversity. The hydropower benefits correlated strongly with the allowable flexibility in temperature constraints. Wet years had higher potential of benefitting hydropower generation while adhering to stringent temperature constraints. Also, remote sensing-based temperature estimation algorithm proved valuable for regions with scarce in-situ temperature measurements.

7.1.4 *Sustainable operations of future hydropower dams*

Further, because a large number of developing nations have planned hydropower installed capacity in the coming decades, policies for sustainable dam operations are necessary that do not discount the ecological safety. The *FUTURIST* framework provided an unprecedented advantage in terms of efficiently learning how future dams might affect ecosystems by altering the natural thermal regimes of rivers. Model suggests a general trend of lower highs (reduced temperatures

during summers) and higher lows (warmer temperatures during winters). Such a change homogenized over longer periods can be detrimental to various native population of fisheries as evidenced by case studies of dams in a variety of different conditions. The study elucidated the need to revisit dam planning and include thermal pollution within the decision making to ensure optimal strategies for expanding hydropower infrastructure in a sustainable manner.

7.1.5 *Bridging research-application gap*

One of the pivotal contributions of this dissertation is to bridge the gap between the theoretical proof-of-concepts presented as case studies and their application in real-life scenarios. The first step to achieve this is the use of publicly available global scale forecasts from NWP models. These forecasts still represent an underutilized low-hanging fruit for the hydropower community. Currently, the integration of such forecasts into existing water management decision processes at weather scale is not yet popular or mainstream in the dam operations. Primary reasons include the traditional risk averse nature of water managers or their coarse resolution that necessitated computationally prohibitive dynamic downscaling. By demonstrating the value in using native scale NWP forecasts as inputs to the ANN model for skillful inflow forecasts, we have not only avoided computational burden but also set the path forward to mainstream their use in the application domain.

Secondly, the use of freely available and global extent satellite remote sensing products for various hydrometeorological parameters, reservoir states, and river's thermal conditions allow the approaches presented here to transferrable to locations with scarce or no network of in-situ gauges. Moreover, with the advent of cloud computing platforms such as Google Earth Engine, comprehensive collection of remote sensing data along with the computing power needed to process those data are more accessible than ever. This facilitates adoption of the proposed approach

by water management agencies and stakeholders around the world, providing them with information on variables that would be otherwise inaccessible. Of particular significance are the transboundary dam networks such as in Mekong River Basin where upstream dam development directly impacts downstream operations. In such scenarios, global vantage of satellite datasets provide access to information irrespective of regional boundaries, thus promoting the democratization of water management decisions.

The last mile to facilitate real-world engagement with dam-operating agencies in the decision-making process was to develop a web-based open-source DSS called iDDEA (http://depts.washington.edu/saswe/damdss/). This system provides daily advisory on release decisions informed with dynamically updated forecasts and helps the dam operator assess how much more 'smarter' operations can be if weather forecasts and open-source technology are used. More importantly, this generic DSS acts as a robust template, free and open-source that can be used for the vast number of powered dams to benefit from the forecast-based optimization and improve the hydropower generation scenario.

Because hydropower dams that already exist are not getting phased out globally anytime soon, efficiently managing such a resource has the potential to not only expand clean (i.e., non-fossil fuel) energy generation but also provide resilience against extreme hazards. The long-term benefits of maximizing the hydropower every day, even in small amounts, is a low-hanging fruit that should not be overlooked. The challenge is now to realize this approach of forecast informed energy operations as an operating standard for existing and future dams and thus foster the goal of clean energy without sacrificing the societal and ecosystem benefits.

7.2 RECOMMENDATIONS

We recommend here few follow-up studies that can help transition current dam operations to a more informed state using dynamic forecast information and intelligent optimization algorithms.

(1) *Energy Storage*: Complete transition to 100% renewable energy-based generation will necessitate investigation into innovative solutions to improve the current energy storage capacities. The more intermittent sources of wind and solar energy need significant storage at times of windy/sunny days to meet peak energy demands during other less conducive hours. Avenues to integrate pumped storage hydropower with wind and solar needs to be explored. Efforts such as those from RE100 group to identify around 616,000 potentially feasible pumped hydropower storage sites (Global PHES Atlas, 2020) can serve as a great resource to plan for optimal sites where wind and solar can be installed for synergistic smart grid operations. Studies are necessary to investigate optimal periods and amount of storage required towards smart grid operations where intermittent sources of wind and solar will be complemented by more stable hydropower satisfying the baseload demands.

(2) *Energy demand forecasting*: With improved efficiency of reservoir operations to generate hydropower, any excess energy can be wasted if there is not enough demand for dispatching the power to the grid or in case there is no provision for excess energy storage. Thus, a logical future extension of this work is to integrate energy demand forecasting and excess energy storage with the reservoir operations.

(3) *Integration with energy pricing model*: Further endeavors are also required to consider variations in energy prices and integrating within the optimization framework. Based on the predicted energy pricing, its demand, and inflow into the reservoir at weather scale, more holistic decision-making can be achieved concerning various stakeholders and

operating agencies. The limitations and capabilities of the power grid also need due consideration.

(4) *Informing other renewables with forecasts*: As the NWP models also provide forecast fields of the weather conditions (such as temperature and wind speed), other renewable sources of energy such as wind and solar, also stand to benefit from forecast-informed operations. Future endeavors on fostering the clean energy generation should aim towards an integrated hydro-wind-solar based energy framework. This effort could be a part of larger initiative of achieving smart grid operations, synergizing the operations of water, wind and solar (WWS) power operations.

(5) *Other parameters of environmental sustainability*: In this dissertation, only a single but important factor of river's thermal stability was considered to address ecological sustainability in operating hydropower dams. Other aspects of dam's impact on environment also needs consideration such as greenhouse gas emissions, modification of natural sediment transport, dissolved oxygen levels, total dissolved solids, and bubbling of carbon dioxide or methane from reservoirs also need consideration. Frameworks should be designed to incorporate these impacts while optimizing for hydropower generation and other competing dam operation objectives.

Successful completion of these endeavors will make our energy systems robust and efficient in terms of energy generation, sustainability, and accessibility. The system will also evolve to become more resilient against increasingly likely high-impact external events such as extreme weather events or sudden fluctuations in peak energy demands. Above all, this will bring us several steps closer to the dream of a future powered with clean and renewable energy.

BIBLIOGRAPHY

Abbasi, S.A., Abbasi, N., 2000. The likely adverse environmental impacts of renewable energy sources. Applied Energy, 2000, 65(1-4), 121-144.

Ahmad S.K., Hossain, F., 2019a. A Globally Scalable Data-driven Technique for Forecasting of Reservoir Inflow for Hydropower Maximization. Environ. Model. Softw., 119, pp.147-165. doi:10.1016/j.envsoft.2019.06.008.

Ahmad S.K., Hossain, F., 2019b. A Web-based Decision Support System for Smart Dam Operations using Weather Forecasts. Journal of Hydroinformatics, 21(5), pp. 687-707. doi:10.2166/hydro.2019.116

Ahmad, S.K., Hossain, F., Eldardiry, H., Pavelsky, T.M., 2019c. A Fusion Approach for Water Area Classification Using Visible, Near Infrared and Synthetic Aperture Radar for South Asian Conditions. *IEEE Transactions on Geoscience and Remote Sensing*, *58*(4), pp.2471-2480.

Ahmad, S.K., Hossain, F., 2020a. Maximizing Energy Production from Hydropower Dams using Short-Term Weather Forecasts. Renewable Energy, 146, pp.1560-1577. doi:10.1016/j.renene.2019.07.126

Ahmad, S.K., Hossain, F. 2020b. Forecast-Informed Hydropower Optimization at Long and Short-time scales for a Multiple Dam Network. Journal of Renewable and Sustainable Energy 12. doi:10.1063/1.5124097

Ahmad, S.K., Hossain, F., 2020c. Realizing ecosystem-safe hydropower from dams. Renewables: Wind, Water, and Solar, 7(1), pp.1-23. doi:10.1186/ s40807-020-00060-9

Ahmad, S.K., Hossain, F., Holt, G., Galleli, S., Pavelsky, T. 2020d. How will Future Dams Modify Temperature of Rivers around the World? Earth's Future (*under review*)

Ahmad, A., El-Shafie, A., Razali, S.F.M., Mohamad, Z.S., 2014. Reservoir Optimization in Water Resources: A Review. Water Resour. Manag. 28, 3391–3405. doi:10.1007/s11269-014-0700-5.

Ahmadi, M., Bozorg Haddad, O., Mariño, M.A., 2014. Extraction of Flexible Multi-Objective Real-Time Reservoir Operation Rules. Water Resour. Manag. 28, 131–147. doi:10.1007/s11269-013-0476-z.

Akhtar, M.K., Corzo, G.A., Van Andel, S.J., Jonoski, A., 2009. River flow forecasting with artificial neural networks using satellite observed precipitation pre-processed with flow length and travel time information: case study of the Ganges river basin. Hydrol. Earth Syst. Sci. 13(9),1607-1618. https://doi.org/10.5194/hess-13-1607-2009

Alemu, E.T., Palmer, R.N., Polebitski, A., Meaker, B., 2011. Decision Support System for Optimizing Reservoir Operations Using Ensemble Streamflow Predictions. J. Water Resour. Plan. Manag. 137, 72–82. doi:10.1061/(ASCE)WR.1943-5452.0000088.

Anctil, F., Perrin, C., Andréassian, V., 2004. Impact of the length of observed records on the performance of ANN and of conceptual parsimonious rainfall-runoff forecasting models. Environ. Model. Softw. 19, 357–368. https://doi.org/10.1016/S1364-8152(03)00135-X

Anderson, E.P. et al., 2018. Fragmentation of Andes-to-Amazon connectivity by hydropower dams. Science Advances 4(1), eaao1642.

Anghileri, D., Voisin, N., Castelletti, A., Pianosi, F., Nijssen, B., Lettenmaier, D. P., 2016. Value of long-term streamflow forecasts to reservoir operations for water supply in snow-dominated river catchments. Water Resour. Res. 52, 4209–4225. https://doi.org/10.1002/2015WR017864

Angilletta Jr, M.J. et al., 2008. Big dams and salmon evolution: changes in thermal regimes and their potential evolutionary consequences. Evolutionary Applications 1(2), 286-299.

Archibald, T.W., McKinnon, K.I.M., Thomas, L.C., 1997. An aggregate stochastic dynamic programming model of multi-reservoir systems. Water Resources Research, 33 (2), 333–340. http://doi.org/10.1029/96WR02859

Asadieh A., Afshar, A., 2019. Optimization of Water-Supply and Hydropower Reservoir Operation Using the Charged System Search Algorithm, Hydrology, 6(1), 5.

ASCE Task Committee on Application of Artificial Neural Networks in Hydrology, 2000. Artificial neural networks in hydrology. II: Hydrologic applications. J. Hydrol. Eng. 5(2),124-137. https://doi.org/10.5121/ijsc.2012.3203

Asif, M., Muneer, T., 2007. Energy supply, its demand and security issues for developed and emerging economies. Renew. Sustain. Energy Rev. 11, 1388–1413. https://doi.org/10.1016/J.RSER.2005.12.004

Aspinall Unit Water Operations, Bureau of Reclamation, 2019. Retrieved June 26, 2019, from https://www.usbr.gov/rsvrWater/HistoricalApp.html

Barbarossa et al., 2020. Impacts of current and future large dams on the geographic range connectivity of freshwater fish worldwide. Proceedings of the National Academy of Sciences 117(7), 3648-3655.

Barros, M.T., Tsai, F.T., Yang, S.L., et al., 2003. Optimization of large-scale hydropower system operations. Journal of Water Resources Planning and Management, 129(3), 178-188.

Bartoletti, N., Casagli, F., Marsili-Libelli, S., Nardi, A., Palandri, L., 2018. Data-driven rainfall/runoff modelling based on a neuro-fuzzy inference system. Environ. Model. Softw. 106, 35–47. https://doi.org/10.1016/j.envsoft.2017.11.026

Bauer, P., Thorpe, A., Brunet, G., 2015. The quiet revolution of numerical weather prediction. Nature, 525, 47–55. doi:10.1038/nature14956

Becker, L., Yeh, W.W.G., 1974. Optimization of real time operation of a multiple-reservoir system. Water Resources Research, 10(6), 1107-1112.

Becker, L., Yeh, W.W.G., Fults, D., Sparks, D., 1976. Operations models for central valley project. J. Water Resour. Plann. Manage. Div., 102, 101–115.

Becker, S., Frew, B.A., Andresen, G.B., Zeyer, T., et al., 2014. Features of a fully renewable US electricity system: Optimized mixes of wind and solar PV and transmission grid extensions. Energy, 72, 443–458. doi:10.1016/j.energy.2014.05.067.

Bednarek, A.T., 2001. Undamming rivers: a review of the ecological impacts of dam removal. Environmental management, 27(6), 803-814.

Bellmore, J.R., Duda, J.J., Craig, L.S. et al., 2017. Status and trends of dam removal research in the United States. Wiley Interdisciplinary Reviews: Water, 2017, 4(2), e1164.

Benyahya, L., Caissie, D., St-Hilaire, A., Ouarda, T.B., Bobée, B., 2007. A review of statistical water temperature models. Canadian Water Resources Journal, 32(3), 179-192.

Birikundavyi, S., Labib, R., Trung, H.T., Rousselle, J., 2002. Performance of Neural Networks in Daily Streamflow Forecasting. J. Hydrol. Eng. 7, 392–398. https://doi.org/10.1061/(ASCE)1084-0699(2002)7:5(392)

Block, 2011. Tailoring seasonal climate forecasts for hydropower operations. Hydrol. Earth Syst. Sci. 15, 1355–1368. doi:10.5194/hess-15-1355-2011.

Bonnema, M., Hossain, F., Nijssen, B., Holtgrieve, G., 2020. Hydropower's hidden transformation of rivers in the Mekong. Environmental Research Letters, 15(4), 044017.

Bowden, G.J., Dandy, G.C., Maier, H.R., 2005. Input determination for neural network models in water resources applications: part 1 – background and methodology. J. Hydrol. 301, 75–92. https://doi.org/10.1016/j.jhydrol.2004.06.021

Buccola, N.L., Risley, J.C., Rounds, S.A., 2016. Simulating future water temperatures in the North Santiam River. Oregon, Journal of Hydrology, 535, 318-330.

Caissie, 2006. The thermal regime of rivers: a review. Freshwater Biology 51, 1389–1406.

Campolo, M., Andreussi, P., Soldati, A., 1999. River flood forecasting with a neural network model. Water Resour. Res. 35 (4), 1191–1197. https://doi.org/10.1029/1998WR900086

Carpentier, D., Haas, J., Olivares, M., de la Fuente, A., 2017. Modeling the multi-seasonal link between the hydrodynamics of a reservoir and its hydropower plant operation. Water, 2017, 9(6), 367.

Carron, J.C., Rajaram, H., 2001. Impact of variable reservoir releases on management of downstream water temperatures. Water Resources Research, 37(6), 1733-1743.

Celeste, A.B., Suzuki, K., Kadota, A., 2008. Integrating long-and short-term reservoir operation models via stochastic and deterministic optimization: case study in Japan. Journal of Water Resources Planning and Management, 134(5), 440-448.

CGIAR WLE, Mekong Dam Database, 2011. WLE Greater Mekong, CGIAR Research Program on Water, Land and Ecosystems (WLE), Vientiane, Lao PDR. https://wle-mekong.cgiar.org/changes/our-research/greater-mekong-dams-observatory/. Accessed 13 July 2020.

Chen, D., Leon, A.S., Engle, S.P., Fuentes, C., Chen, Q., 2017. Offline training for improving online performance of a genetic algorithm based optimization model for hourly multi-reservoir operation. Environ. Model. Softw. 96, 46–57. https://doi.org/10.1016/j.envsoft.2017.06.038

Chen, W., J. D. Olden, 2017. Designing flows to resolve human and environmental water needs in a dam-regulated river, Nature communications, 8(1), 2158.

Chen, X., Hossain, F., 2016. Revisiting extreme storms of the past 100 years for future safety of large water management infrastructures. Earth's Futur. 4, 306–322. doi:10.1002/2016EF000368.

Cheng, X., Noguchi, M., 1996. Rainfall-runoff modelling by neural network approach. Proc. Int. Conf. on Water Resour. & Environ. Res. 2, 143-15.

Cheng, C., Wang, S., Chau, K.-W., Wu, X., 2014. Parallel discrete differential dynamic programming for multireservoir operation. Environ. Model. Softw. 57, 152–164.

Cheng, Y., Voisin, N., Yearsley, J.R., Nijssen, B., 2020a. Reservoirs modify river thermal regime sensitivity to climate change: a case study in the southeastern United States. Water Resources Research, 56(6), e2019WR025784.

Cheng, Y., Voisin, N., Yearsley, J.R., Nijssen, B., 2020b. Thermal extremes in regulated river systems under climate change: an application to the southeastern US rivers. Environmental Research Letters, 15(9), 094012.

Chowdhury, A.K. et al., 2020. Expected Benefits of Laos' Hydropower Development Curbed by Hydroclimatic Variability and Limited Transmission Capacity: Opportunities to Reform. Journal of Water Resources Planning and Management, 146(10), 05020019.

Clarkson, R.W., Childs, M.R., 2000. Temperature effects of hypolimnial-release dams on early life stages of Colorado River Basin big-river fishes. Copeia, 2000(2), 402-412.

Cole, T.M., Wells, A., 2015. CE-QUAL-W2: A two-dimensional, laterally averaged, hydrodynamic and water quality model, Version 4.0. Portland State University, Portland, OR, USA.

Collier, U., 2004. Hydropower and the environment: towards better decision-making. In: Proceedings of UN Symposium on Hydropower and Sustainable Development, Beijing.

Collins, M.R., et al., "Long-term Climate Change: Projections, Commitments and Irreversibility" in Climate Change 2013: The Physical Science Basis. Contribution of Working Group I to the Fifth Assessment Report of the Intergovernmental Panel on Climate Change, T. F. Stocker et al., Eds. (Cambridge University Press, Cambridge, United Kingdom and New York, NY, USA).

Corzo, G., Solomatine, D., 2007. Baseflow separation techniques for modular artificial neural network modelling in flow forecasting. Hydrol. Sci. J. 52, 491–507.

Coulibaly, P., Anctil, F., Bobée, B., 2000. Daily reservoir inflow forecasting using artificial neural networks with stopped training approach. J. Hydrol. 230, 244–257.

Croley, T.E., Raja Rao, K.N., 1979. Multiobjective risks in reservoir operation. Water Resour. Res. 15, 807–814. doi:10.1029/WR015i004p00807.

De Vos, N.J., Rientjes, T.H.M., 2005. Constraints of artificial neural networks for rainfall–runoff modelling: trade-offs in hydrological state representation and model evaluation. Hydrology and Earth System Sciences 9 (1/2), 111–126. https://doi.org/10.5194/hess-9-111-2005

Deb, K., Pratap, A., Agarwal, S., Meyarivan, T., 2002. A fast and elitist multiobjective genetic algorithm: NSGA-II. IEEE Trans. Evol. Comput. 6, 182–197.

Deemer, B.R. et al., 2016. Greenhouse gas emissions from reservoir water surfaces: a new global synthesis. BioScience, 66(11), 949-964.

Delworth, T.L., Broccoli, A.J., Rosati, A., et al., 2006. GFDL's CM2 global coupled climate models. Part I: Formulation and simulation characteristics. Journal of Climate, 19(5), 643-674.

Delucchi, M.A. Jacobson, M.Z., 2011. Providing all global energy with wind, water, and solar power, Part II: Reliability, system and transmission costs, and policies. Energy Policy, 39, 1170–1190. doi:10.1016/j.enpol.2010.11.045.

Ding, W., Zhang, C., Peng, Y., Zeng, R., Zhou, H., Cai, X., 2015. An analytical framework for flood water conservation considering forecast uncertainty and acceptable risk. Water Resour. Res. 51, 4702–4726. doi:10.1002/2015WR017127.

Do Hoai, N., Udo, K., Mano, A., 2011. Downscaling global weather forecast outputs using ANN for flood prediction. J. Appl. Math. 2011. https://doi.org/10.1155/2011/246286

Dong, X., Dohmen-Janssen, C.M., Booij, M., Hulscher, S., 2006. Effect of flow forecasting quality on benefits of reservoir operation–a case study for the Geheyan reservoir (China). Hydrology and earth system sciences discussions, 3(6), 3771-3814.

Dudhani, S., Sinha, A.K., Inamdar, S.S., 2006. Assessment of small hydropower potential using remote sensing data for sustainable development in India. Energy Policy 34, 3195–3205. https://doi.org/10.1016/j.enpol.2005.06.011

Eckhardt, K., 2005. How to construct recursive digital filters for baseflow separation. Hydrol. Process. 19, 507–515. https://doi.org/10.1002/hyp.5675

Egré, D., Milewski, J.C., 2002. The diversity of hydropower projects. Energy Policy, 30, 1225 1230.

Electricity Rates, Oklahoma City | Electricity Local [WWW Document], 2018. URL https://www.electricitylocal.com/states/oklahoma/oklahoma-city/ (accessed 8.21.18).

Ellabban, O., Abu-Rub, H., Blaabjerg, F., 2014. Renewable energy resources: current status, future prospects and their enabling technology. Renewable and Sustainable Energy Reviews 39, 748–764. doi:10.1016/J.RSER.2014.07.113.

Faber, B.A., Stedinger, J.R., 2001. Reservoir optimization using sampling SDP with ensemble streamflow prediction (ESP) forecasts. J. Hydr. 249(1-4),113-133.

Fan, F. M., Schwanenberg, D., Alvarado, R., dos Reis, A. A., Collischonn, W., Naumman, S., 2016. Performance of deterministic and probabilistic hydrological forecasts for the short-term optimization of a tropical hydropower reservoir. Water Resources Management, 30(10), 3609-3625.

Fang, H.B., Hu, T.S., Zeng, X., Wu, F.Y., 2014. Simulation-optimization model of reservoir operation based on target storage curves. Water Science and Engineering, 7(4), 433-445.

FAO, AQUASTAT Main Database, 2016. Food and Agriculture Organization of the United Nations (FAO). http://www.fao.org/aquastat/en/databases/dams. Accessed 2 Aug 2020.

Farmer, W.H., Vogel, R.M., 2016. On the deterministic and stochastic use of hydrologic models. Water Resour. Res. 52, 5619-5633. doi:10.1002/2016WR019129.

Ficchì, A., Raso, L., Dorchies, D., Pianosi, F., Malaterre, P. O., Van Overloop, P. J., Jay-Allemand, M., 2015. Optimal operation of the multireservoir system in the Seine river basin using deterministic and ensemble forecasts. J. Water Resour. Plan. Manag. 142(1), 05015005.

Finer, M., Jenkins, C. N., 2012. Proliferation of hydroelectric dams in the Andean Amazon and implications for Andes-Amazon connectivity. PloS One 7(4), e35126.

FIRO Overview – Center for Western Weather and Water Extremes [WWW Document], 2017. http://cw3e-web.ucsd.edu/firo/ (accessed 7.31.17).

FitzHugh, T.W., Vogel, R.M., 2011. The impact of dams on flood flows in the United States. River Research and Applications 27(10), 1192-1215.

Flint, L.E., Flint, A.L., 2012. Downscaling future climate scenarios to fine scales for hydrologic and ecological modeling and analysis. Ecological Processes 1(1), 2. https://doi.org/10.1186/2192-1709-1-2

Forsberg, B.R., et al., 2017. The potential impact of new Andean dams on Amazon fluvial ecosystems. PLoS One 12(8), e0182254.

Funahashi, K.I., 1989. On the approximate realization of continuous mappings by neural networks. Neural Networks 2 (3), 183–192. https://doi.org/10.1016/0893-6080(89)90003-8

Funk, C., Peterson, P., Landsfeld, M., Pedreros, D., Verdin, J., Shukla, S., Husak, G., Rowland, J., Harrison, L., Hoell, A., Michaelsen, J., 2015. The climate hazards infrared precipitation with stations - a new environmental record for monitoring extremes. Scientific data, 2, 150066.

Gachet, A., Haettenschwiler, P., 2003. Developing intelligent decision support systems: a bipartite approach. In: International Conference on Knowledge-Based and Intelligent Information and Engineering Systems. Springer, Berlin, Heidelberg, pp. 87–93.

Ge, X., Zhang, L., Shu, J., Xu, N., 2014. Short-term hydropower optimal scheduling considering the optimization of water time delay. Electric Power Systems Research, 110, 188-197. http://dx.doi.org/10.1016/j.epsr.2014.01.015

Georgakakos, A.P., 1989. The value of streamflow forecasting in reservoir operation. Journal of the American Water Resources Association, 25(4), 789-800.

Georgakakos, A. P., 2006. Decision Support Systems for Water Resources Management: Nile Basin Applications and Further Needs. 1–22, Atlanta, Ga.

Georgakakos, K., Graham, N., Carpenter, T., and Yao, H., 2005. Integrating climate-hydrology forecasts and multi-objective reservoir management for Northern California. Eos Trans. AGU, 86(12), 122–127.

Georgakakos, K.P., Graham, N.E., Georgakakos, A.P., Yao, H., 2007. Demonstrating Integrated Forecast and Reservoir Management (INFORM) for northern California in an operational environment. IAHS Publication 313, 439.

Georgakakos, K.P., Graham, N.E., 2008. Potential benefits of seasonal inflow prediction uncertainty for reservoir release decisions. Journal of Applied Meteorology and Climatology 47(5), 1297-1321.

Georgiou, P.E., Papamichail, D.M., 2008. Optimization model of an irrigation reservoir for water allocation and crop planning under various weather conditions. Irrig. Sci. 26, 487–504. doi:10.1007/s00271-008-0110-7.

Giuliani, M., Li, Y., Cominola, A., Denaro, S., Mason, E., Castelletti, A., 2016. A Matlab toolbox for designing Multi-Objective Optimal Operations of water reservoir systems. Environ. Model. Softw. 85, 293–298. https://doi.org/10.1016/j.envsoft.2016.08.015

Global Forecast System (GFS) | National Centers for Environmental Information (NCEI) formerly known as National Climatic Data Center (NCDC), 2018. https://www.ncdc.noaa.gov/data-access/model-data/model-datasets/global-forcast-system-gfs (accessed December 30, 2017).

Global Surface Summary of the Day - NOAA Data Catalog [WWW Document], 2018. URL https://data.noaa.gov/dataset/dataset/global-surface-summary-of-the-day-gsod (accessed 1.30.18).

Global PHES Atlas, 2020. http://re100.eng.anu.edu.au/global/ (accessed Nov 15, 2020).

Goddard, Y. Aitchellouche, W. Baethgen, M. Dettinger, R. Graham, P. Hayman, M. Kadi, R. Martínez, H. Meinke, 2010. Providing Seasonal-to-Interannual Climate Information for Risk Management and Decision-making. Procedia Environ. Sci. 1, 81–101. doi:10.1016/j.proenv.2010.09.007.

Golembesky, K., Sankarasubramanian, A., and Devineni, N., 2009. Improved drought management of Falls Lake Reservoir: Role of multimodel streamflow forecasts in setting up restrictions. Journal of Water Resources Planning and Management, 135(3), 188-197.

Govindaraju, R.S., Rao, A.R., 2000 (Eds.). Artificial Neural Networks in Hydrology. Kluwer Academic Publishers, Dordrecht, Netherlands.

Grill, G. et al., 2015. An index-based framework for assessing patterns and trends in river fragmentation and flow regulation by global dams at multiple scales. Environmental Research Letters 10(1), 015001.

Grumet, 2016. How Germany’s Combined Wind And Hydropower Plant Will Work - GE. https://www.ge.com/reports/unique-combo-wind-hydro-power-revolutionize-renewable-energy/ (accessed December 3, 2017).

Gu, R.,McCutcheon, S., Chen, C.J., 1999. Development of weather-dependent flow requirements for river temperature control. Environmental Management, 24(4), 529-540.

Hamill, T. M., Bates, G. T., Whitaker, J.S. et al., 2013. NOAA's second-generation global medium-range ensemble reforecast data set. Bull Amer. Meteor. Soc., 94, 1553-1565. http://dx.doi.org/10.1175/BAMS-D-12-00014.1

Hamlet, A.F., Huppert, D., Lettenmaier, D.P., 2002. Economic Value of Long-Lead Streamflow Forecasts for Columbia River Hydropower. J. Water Resour. Plan. Manag. 128, 91–101. doi:10.1061/(ASCE)0733-9496(2002)128:2(91).

Handcock, R.N., Torgersen, C.E., Cherkauer, K.E., et al., 2012. Thermal infrared remote sensing of water temperature in riverine landscapes. Fluvial remote sensing for science and management, 1, 85-113.

Harrison, J., 2019. New Collection Facility Improves Passage for Salmon and Steelhead on Oregon's North Fork Santiam River, https://www.nwcouncil.org/news/fish-passage-north-fork-santiam-river-improves-new-collection-facility (accessed December 2019).

Heide, D., von Bremen, L., Greiner, M., Hoffmann, C., Speckmann, M., Bofinger, S., 2010. Seasonal optimal mix of wind and solar power in a future, highly renewable Europe. Renew. Energy, 35, 2483–2489. doi:10.1016/j.renene.2010.03.012.

Haxton, T.J., Findlay, C.S., 2008. Meta-analysis of the impacts of water management on aquatic communities. Canadian Journal of Fisheries and Aquatic Sciences 65(3), 437-447.

Hecht, J.S. et al., 2019. Hydropower dams of the Mekong River basin: A review of their hydrological impacts. Journal of Hydrology 568, 285-300.

Holmes, K.J. and Papay, L., 2011. Prospects for electricity from renewable resources in the United States. Journal of Renewable and Sustainable Energy, 3(4), 042701. https://doi.org/10.1063/1.3613947

Hossain, F., Degu, A.M., Yigzaw, W. et al., 2012. Climate Feedback–Based Provisions for Dam Design, Operations, and Water Management in the 21st Century. J. Hydrol. Eng. 17, 837–850. doi:10.1061/(ASCE)HE.1943-5584.0000541.

Hsu, N.S., Wei, C.C., 2007. A multipurpose reservoir real-time operation model for flood control during typhoon invasion. J. Hydrol. 336, 282–293. doi:10.1016/j.jhydrol.2007.01.001.

Humphrey, G.B., Maier, H.R., Wu, W., Mount, N.J., Dandy, G.C., Abrahart, R.J., Dawson, C.W., 2017. Improved validation framework and R-package for artificial neural network models. Environmental Modelling and Software, 92, 82-106. doi:10.1016/j.envsoft.2017.01.023

Hutton, C.J., Kapelan, Z., 2015. A probabilistic methodology for quantifying, diagnosing and reducing model structural and predictive errors in short term water demand forecasting. Environ. Model. Softw. 66, 87–97. https://doi.org/10.1016/j.envsoft.2014.12.021

Hydropower Vision: A New Chapter for America's 1st Renewable Electricity Source | Department of Energy, 2016. https://www.energy.gov/eere/water/articles/hydropower-vision-new-chapter-america-s-1st-renewable-electricity-source (accessed November 21, 2016).

Imboden, D.M., Wuest, A. 1995. “Mixing mechanisms in lakes” in Physics and chemistry of lakes, A. Lerman, D. M. Imboden, J. R. Cat, Eds. (Springer Verlag), pp. 83–138.

Jacobson, M.Z., 2009. Review of solutions to global warming, air pollution, and energy security. Energy Environ. Sci. 2, 148–173. doi:10.1039/b809990c.

Jacobson, M.Z. Delucchi, M.Z., 2011. Providing all global energy with wind, water, and solar power, Part I: Technologies, energy resources, quantities and areas of infrastructure, and materials. Energy Policy. 39, 1154–1169. doi:10.1016/j.enpol.2010.11.040.

Jacobson, M.Z., Delucchi, M.A., Bauer, Z.A.F., Goodman, S.C., Chapman, W.E. et al., 2017. 100% Clean and Renewable Wind, Water, and Sunlight All-Sector Energy Roadmaps for 139 Countries of the World. Joule, 1, 108–121. doi:10.1016/j.joule.2017.07.005.

Jacobson, M.Z., Delucchi, M.A., Cameron, M.A., Mathiesen, B. V., 2018. Matching demand with supply at low cost in 139 countries among 20 world regions with 100% intermittent wind, water, and sunlight (WWS) for all purposes. Renew. Energy. 123, 236–248. doi:10.1016/j.renene.2018.02.009.

Jacobson, M.A. Delucchi, A.R. Ingraffea, R.W. Howarth, G. Bazouin, et al., 2014. A roadmap for repowering California for all purposes with wind, water, and sunlight. Energy, 73 875–889. doi:10.1016/j.energy.2014.06.099.

Jakeman, A.J., Letcher, R.A., Norton, J.P., 2006. Ten iterative steps in development and evaluation of environmental models. Environ. Model. Softw. 21, 602–614. https://doi.org/10.1016/j.envsoft.2006.01.004

Jain, A., Maier, H.R., Dandy, G.C., Sudheer, K.P., 2009. Rainfall runoff modelling using neural networks: State-Of-The-Art and future research needs. ISH J. Hydraul. Eng. 15, 52–74. https://doi.org/10.1080/09715010.2009.10514968

Ji, Y., Lei, X., Cai, S., Wang, X., 2016. Hedging rules for water supply reservoir based on the model of simulation and optimization. Water (Switzerland). 8. doi:10.3390/W8060249.

Jiang, B., Wang, F., Ni, G., 2018. Heating Impact of a Tropical Reservoir on Downstream Water Temperature: A Case Study of the Jinghong Dam on the Lancang River. Water, 10(7), 951.

Jiménez-Muñoz, J.C., Sobrino, J.A., 2003. A generalized single-channel method for retrieving land surface temperature from remote sensing data. Journal of Geophysical Research, 108, 4688.

Jiménez-Muñoz, J.C, Sobrino, J.A., Sòria, G. et al., 2008. Revision of the single-channel algorithm for land surface temperature retrieval from Landsat thermal-infrared data. IEEE Transactions on geoscience and remote sensing, 47(1), 339-349.

Jones, J., 2015. Efficient wetland surface water detection and monitoring via Landsat: Comparison with in situ data from the everglades depth estimation network. Remote Sensing, 7(9), 12503-12538. https://doi.org/10.3390/rs70912503

Jordan, F.M., Boillat, J.-L., Schleiss, A.J., 2012. Optimization of the flood protection effect of a hydropower multi-reservoir system. Int. J. River Basin Manag. 10, 65–72. https://doi.org/10.1080/15715124.2011.650868

Jothiprakash, V., Arunkumar, R., 2014. Multi-reservoir optimization for hydropower production using NLP technique. KSCE J. Civ. Eng. 18, 344–354. doi:10.1007/s12205-014-0352-2.

Kareiva, P., 2012. Dam choices: analyses for multiple needs. Proceedings of the National Academy of Sciences 109(15), 5553-5554.

Khu, S.T., Madsen, H., 2005. Multiobjective calibration with Pareto preference ordering: An application to rainfall-runoff model calibration. Water Resour. Res. 41, doi:10.1029/2004WR003041.

King, J.M., Tharme, R.E., Brown, C.A., 1999. Definition and Implementation of Instream Flows, Thematic Report for the World Commission on Dams. Southern Waters Ecological Research and Consulting, Cape Town, South Africa.

Kirtman, B.P., Min, D., Infanti, J.M., Kinter III, J.L., et al., 2014. The North American multimodel ensemble: phase-1 seasonal-to-interannual prediction; phase-2 toward developing intraseasonal prediction," Bulletin of the American Meteorological Society, 95(4), 585-601. http://dx.doi.org/10.1175/BAMS-D-12-00050.1

Kişi, Ö., 2005. Daily River Flow Forecasting Using Artificial Neural Networks and Auto-Regressive Models. Turkish J. Eng. Env. Sci. 29, 9–20.

Kişi, Ö., 2007. Streamflow forecasting using different artificial neural network algorithms. J. Hydrol. Eng. 12(5), 532-539.

Kougias, I., Szabó, S., Monforti-Ferrario, F., Huld, T., Bódis, K., 2016. A methodology for optimization of the complementarity between small-hydropower plants and solar PV systems. Renew. Energy. 87, 1023–1030. doi:10.1016/j.renene.2015.09.073.

Krzysztofowicz, R., 2001. The case for probabilistic forecasting in hydrology. Journal of hydrology, 249(1-4), 2-9.
Labadie, J.W., 2004. Optimal Operation of Multireservoir Systems: State-of-the-Art Review. J. Water Resour. Plan. Manag. 130, 93–111. doi:10.1061/(ASCE)0733-9496(2004)130:2(93).

Labadie, J.W., 2004. Optimal operation of multireservoir systems: state-of-the-art review. Journal of Water Resources Planning and Management 130 (2), 93–111. doi:10.1061/(ASCE)0733- 9496(2004)130:2(93).

Lee, S.-Y., Hamlet, A.F., Fitzgerald, C.J., Burges, S.J., 2009. Optimized Flood Control in the Columbia River Basin for a Global Warming Scenario. J. Water Resour. Plan. Manag. 135, 440–450. https://doi.org/10.1061/(ASCE)0733-9496(2009)135:6(440)

Le Ngo, L., Madsen, H., Rosbjerg, D. 2007. Simulation and optimisation modelling approach for operation of the Hoa Binh reservoir, Vietnam. J. Hydrol. 336, 269–281. doi:10.1016/j.jhydrol.2007.01.003.

Lehmkuhl, D.M., 1974. Thermal regime alteration and vital environmental physiological signals in aquatic organisms. In AEC symposium series (CONF 730505) 261-222.

Lehner, B., Liermann, C.R., Revenga, C. et al., 2011. Global reservoir and dam (GRanD) database, Version 1.1, Bonn, Germany: Global Water System Project.

Lehner, B., Liermann, C.R., Revenga, C., Vörösmarty, C., Fekete, B., Crouzet, et al., 2011. High-resolution mapping of the world's reservoirs and dams for sustainable river-flow management. *Frontiers in Ecology and the Environment*, *9*(9), pp.494-502.

Li, F.F., Qiu, J., 2015. Multi-objective reservoir optimization balancing energy generation and firm power. Energies 8, 6962–6976. doi:10.3390/en8076962.

Li, H., Deng, X., Kim, D.Y., Smith, E.P., 2014. Modeling maximum daily temperature using a varying coefficient regression model. Water Resources Research, 50(4), 3073-3087.

Li, Q., Yu, M., Zhao, J., Cai, T., Lu, G., Xie, W., Bai, X., 2012. Impact of the Three Gorges reservoir operation on downstream ecological water requirements. Hydrology Research, 43(1-2), 48-53.

Li, H.Y., Ruby Leung, L., Tesfa, T. et al., 2015. Modeling stream temperature in the Anthropocene: An earth system modeling approach. Journal of Advances in Modeling Earth Systems, 7(4), 1661-1679.

Li, X., 2005. Diversification and localization of energy systems for sustainable development and energy security. Energy policy 33(17), 2237-2243.

Liang, X., Lettenmaier, D.P., Wood, E.F., Burges, S.J., 1994. A simple hydrologically based model of land surface water and energy fluxes for general circulation models. J. Geophys. Res. 99, 14415. doi:10.1029/94JD00483.

Liang, X., Wood, E.F., Lettenmaier, D.P., 1996. Surface soil moisture parameterization of the VIC-2L model: Evaluation and modification. Glob. Planet. Change. 13, 195–206. doi:10.1016/0921-8181(95)00046-1.

Ligon, F. K., Dietrich, W. E., Trush, W. J., 1995. Downstream Ecological Effects of Dams. BioScience, 45(3), 183–192 (1995). http://dx.doi.org/10.2307/1312557

Ling, F., Foody, G., Du H. et al., 2017. Monitoring thermal pollution in rivers downstream of dams with Landsat ETM+ thermal infrared images. Remote Sensing, 9(11), 1175.

Lippmann, R.P., 1987. An introduction to computing with neural nets. IEEE ASSP Mag. 4–22.

Liu, H., 2010. On the Levenberg-Marquardt training method for feed-forward neural networks. Proceedings of 6th International Conference on Natural Computation 1, 456-460. https://doi.org/10.1109/ICNC.2010.5583151

Liu, P., Guo, S., Xu, X., Chen, J., 2011. Derivation of aggregation-based joint operating rule curves for cascade hydropower reservoirs. Water resources management, 25(13), 3177-3200.

Livneh, B., Rosenberg, E.A.., Lin, C., Nijssen, B., Mishra, V., Andreadis, K.M., Maurer, E.P., Lettenmaier, D.P., 2013. A Long-Term Hydrologically Based Dataset of Land Surface Fluxes and States for the Conterminous United States: Update and Extensions. J. Clim. 26, 9384–9392. doi:10.1175/jcli-d-12-00508.1.

Lohmann, D., Nolte-Holube, R., Raschke, E., 1996. A large-scale horizontal routing model to be coupled to land surface parametrization schemes. Tellus, Ser. A Dyn. Meteorol. Oceanogr. 48, 708–721. doi:10.3402/tellusa.v48i5.12200.

Lohmann, D., Raschke, E., Nijssen, B., Lettenmaier, D.P., 1998. Regional scale hydrology: I. Formulation of the VIC-2L model coupled to a routing model, Hydrol. Sci. J. 43 (1998) 131–141. doi:10.1080/02626669809492107.

Lorrai, M., Sechi, G.M., 1995. Neural nets for modeling rainfall–runoff transformations. Wat. Resour. Man. 9, 299–313.

Lund, J.R., and Guzman, J., 1999. Derived operating rules for reservoirs in series or in parallel. Journal of Water Resources Planning and Management, 125(3), 143-153.

Madsen, H., Richaud, B., Pedersen, C.B., Borden, C., 2009. A Real-Time Inflow Forecasting and Reservoir Optimization System for Optimizing Hydropower Production. Waterpower XVI 1–12.

Maier, H. R., Dandy, G. C., 1996. The Use of Artificial Neural Networks for the Prediction of Water Quality Parameters. Water Resour. Res. 32(4), 1013–1022. https://doi.org/10.1029/96WR03529

Maier, H.R., Dandy, G.C., 2000. Neural networks for the prediction and forecasting of water resources variables: A review of modelling issues and applications. Environ. Model. Softw. 15, 101–124. https://doi.org/10.1016/S1364-8152(99)00007-9

Maier, H.R., Jain, A., Dandy, G.C., Sudheer, K.P., 2010. Methods used for the development of neural networks for the prediction of water resource variables in river systems: Current status and future directions. Environ. Model. Softw. 25, 891–909. https://doi.org/10.1016/j.envsoft.2010.02.003

Manyari, W.V., de Carvalho Jr, O.A., 2007. Environmental considerations in energy planning for the Amazon region: Downstream effects of dams. Energy Policy, 35(12), 6526-6534.

Marques, G. F., Tilmant, A., 2013. The economic value of coordination in large-scale multireservoir systems: The Parana River case. Water Resour. Res., 49, 7546–7557. http://dx.doi.org/10.1002/2013WR013679.

Matek, B., Gawell, K., 2015. The benefits of baseload renewables: a misunderstood energy technology. The Electricity Journal, 28(2), 101-112.

Maurer, E. P., Lettenmaier, D. P., 2004. Potential effects of long-lead hydrologic predictability on Missouri River main-stem reservoirs. J. Clim., 17(1), 174–186.

Mayne, D.Q., Rawlings, J.B., Rao, C.V., Scokaert, P.O., 2000. Constrained model predictive control: Stability and optimality. Automatica, 36(6), 789-814.

McCartney, M., 2009. Living with dams: Managing the environmental impacts. Water Policy, 11(1), 121–139. https://doi.org/10.2166/wp.2009.108

Mehta, S., 2008.The Kosi Disaster: Millions Flooded Out. Available from: https://www.internationalrivers.org/resources/the- kosi-disaster-millions-flooded-out-3599 (accessed 6 October 2018).

Mekong River Commission (MRC), 2009. Economic, Environmental and Social Impact Assessment of Basin-Wide Water Resources Development Scenarios, Assessment Methodology. Mekong River Commission, Vientiane Lao PDR.

Mekong River Commission (MRC), 2012. Hydropower Project Database.

Miao, Y., Chen, X., Hossain, F., 2016. Maximizing hydropower generation with observations and numerical modeling of the atmosphere. J. Hydrol. Eng. 21, 2516002. https://doi.org/10.1061/(ASCE)HE.1943-5584.0001405

Mohammadzadeh-Habili, J. et al., 2009. Derivation of reservoir's area-capacity equations. Journal of Hydrologic Engineering, 14(9), 1017-1023.

Mohseni, O., Stefan, H.G., Erickson, T.R., 1998. A nonlinear regression model for weekly stream temperatures, Water Resources Research, 34(10), 2685-2692.

Montanari, A., Grossi, G., 2007. Estimating the uncertainty of hydrological forecasts: A statistical approach. Water Resources Research, 44(12).

Monthly Charts for Grand Lake O' The Cherokees, Pensacola Dm [WWW Document], 2018. URL http://www.swt-wc.usace.army.mil/PENScharts.html (accessed 8.21.17).

Monteiro, C., Ramirez-Rosado, I.J., Fernandez-Jimenez, L.A., 2013. Short-term forecasting model for electric power production of small-hydro power plants. Renewable Energy, 50, 387-394.

Moran, E.F., Lopez, M. C., Moore, N., Müller. N., Hyndman, D.W., 2018. Sustainable hydropower in the 21st century, Proceedings of the National Academy of Sciences, 115(47), 11891-11898

Moré, J.J., 1978. The Levenberg-Marquardt algorithm: Implementation and theory. Numer. Analysis 630, 105-116. https://doi.org/10.1007/BFb0067700

Murphy, J., 2000. Predictions of climate change over Europe using statistical and dynamical downscaling techniques. Int. J. Climatol. 20, 489–501. doi:10.1002/(SICI)1097-0088(200004)20:5<489::AID-JOC484>3.0.CO;2-6.

National Marine Fisheries Service, Willamette Basin Biological Opinion—Endangered Species Act Section 7(a)(2) Consultation: National Oceanic and Atmospheric Administration Fisheries Log Number F/NWR/2000/02117, 2008, https://www.westcoast.fisheries.noaa.gov/fish_passage/willamette_opinion/ (accessed Oct 2019).

Neelakantan, T.R., Pundarikanthan, N.V., 1999. Hedging Rule Optimisation for Water Supply Reservoirs System. Water Resour. Manag. 13, 409–426. doi:10.1023/A:1008157316584.

Neumann, D.W., Rajagopalan, B., Zagona, E.A., 2003. Regression model for daily maximum stream temperature. Journal of Environmental Engineering, 129(7), 667-674.

Niemeyer, R.J., Cheng, Y., Mao, Y., Yearsley, J.R., Nijssen, B., 2018. A thermally stratified reservoir module for large-scale distributed stream temperature models with application in the Tennessee River Basin. Water Resources Research, 54, 8103–8119. https://doi.org/10.1029/2018WR022615.

Nilsson, C., Reidy, C.A., Dynesius, M., Revenga, C., 2005. Fragmentation and flow regulation of the world's large river systems. Science 308(5720), 405-408.

NHAAP | Existing Hydropower Assets, 2017. https://nhaap.ornl.gov/existing_hydropower_assets (accessed December 8, 2017).

NRLD, National Register of Large Dam, Under of Central Water Commission, 2012. http://www.indiaenvironmentportal.org.in. Accessed 22 July 2020

Oklahoma City, OK Electricity Rates | Electricity Local, 2018. https://www.electricitylocal.com/states/oklahoma/oklahoma-city/ (accessed August 21, 2018).

Olden, J.D., Naiman, R.J., 2010. Incorporating thermal regimes into environmental flows assessments: modifying dam operations to restore freshwater ecosystem integrity. Freshwater Biology, 55(1), 86-107.

Oregon Electricity Rates | Electricity Local, 2018. https://www.electricitylocal.com/states/oregon/ (accessed May 11, 2018).

Oregon Water Resources Department and U.S. Army Corps of Engineers, Small-scale water supply allocation process Willamette River Basin, 2012, https://digital.osl.state.or.us/islandora/object/osl:14841 (accessed October 2019).

Oregon Department of Environmental Quality, Willamette Basin Total Maximum Daily Loads (TMDLs) - Chapter 4: Temperature - Mainstem TMDL and Subbasin Summary, 2006, https://www.oregon.gov/deq/FilterDocs/chpt4temp.pdf (accessed November 2019).

Pacific Northwest Mesoscale Model Numerical Forecast Information, 2017. https://www.atmos.washington.edu/wrfrt/info.html (accessed November 23, 2017).

Padmanabhan, V., 2018. Kerala Floods Highlight India's Poor dam Management. Available from: https://www.livemint.com/ Politics/oSkzuw37GHm9u0UvbD0C5H/Kerala-floods-highlight-Indias-poor-dam-management.html (accessed 6 September 2018).

Peel, M.C., Finlayson, B.L., McMahon, T.A., 2007. Updated world map of the Köppen-Geiger climate classification. Hydrol Earth Syst Sc 11: 1633–1644.

Piman, T, et al., 2013. Assessment of flow changes from hydropower development and operations in Sekong, Sesan, and Srepok rivers of the Mekong basin. Journal of Water Resources Planning and Management 139(6), 723-732.

Piman, T., Cochrane, T.A., Arias, M.E., 2016. Effect of proposed large dams on water flows and hydropower production in the Sekong, Sesan and Srepok rivers of the Mekong basin. River Research and Applications 32(10), 2095-2108

Poole, G.C., Berman, H., 2001. An ecological perspective on in-stream temperature: natural heat dynamics and mechanisms of human-caused thermal degradation. Environmental Management 27, 787–802.

Preece, R.M., Jones, H.A., 2002. The effect of Keepit Dam on the temperature regime of the Namoi River, Australia. River Research and Applications 18, 397–414.

Qi, Y.T., Luo, J.G., Wei, Y.X., Miao, Q.G., 2017. Maximizing Hydropower Generation in Flood Control Operation using Preference Based Multi-Objective Evolutionary Algorithm. IOP Conf. Ser. Earth Environ. Sci. 86. https://doi.org/10.1088/1755-1315/86/1/012037

Query Timeseries from USACE Northwestern Division, Dataquery 2.0, 2017. http://www.nwd-wc.usace.army.mil/dd/common/dataquery/www/ (accessed October 17, 2017).

Quinn, J.D., Reed, P.M., Giuliani, M., Castelletti, A., 2019. What is controlling our control rules? Opening the black box of multireservoir operating policies using time-varying sensitivity

analysis. Water Resources Research, 55(7), pp.5962-5984. https://doi.org/10.1029/2018WR024177

Rani, D., Moreira, M.M., 2010. Simulation–Optimization Modeling: A Survey and Potential Application in Reservoir Systems Operation. Water Resour. Manag. 24, 1107–1138. doi:10.1007/s11269-009-9488-0.

Raso, L., Schwanenberg, D., van de Giesen, N. C., van Overloop, P. J., 2014. Short-term optimal operation of water systems using ensemble forecasts. Adv. Water Resour., 71, 200–208.

Räsänen, T.A. et al., 2017. Observed river discharge changes due to hydropower operations in the Upper Mekong Basin. Journal of Hydrology 545, 28-41

Reddy, M.J., Kumar, D.N., 2006. Optimal Reservoir Operation Using Multi-Objective Evolutionary Algorithm. Water Resour. Manag. 20, 861–878. doi:10.1007/s11269-005-9011-1.

Reddy, M.J., Kumar, D.N., 2007. Multi-objective particle swarm optimization for generating optimal trade-offs in reservoir operation. Hydrol. Process. 21, 2897–2909. doi:10.1002/hyp.6507.

Rheinheimer, D.E., Null, S.E., Lund, J.R., 2014. Optimizing selective withdrawal from reservoirs to manage downstream temperatures with climate warming. Journal of Water Resources Planning and Management, 141(4), 04014063.

Ribeiro, M.T., Singh, S., Guestrin, C., 2016. "Why should I trust you?" Explaining the predictions of any classifier. In Proceedings of the 22nd ACM SIGKDD international conference on knowledge discovery and data mining 1135-1144.

Richter, B.S. et al., 1998. A spatial assessment of hydrologic alteration within a river network. Regulated Rivers: Research & Management 14(4), 329-340.

Rose, J. 2016. Remembering Oregon's epic 1996 flood: 20 years ago (photos). OregonLive.com. Available from: https://www. oregonlive.com/history/2016/02/oregon_flood_of_1996_20_ years.html (accessed 6 October 2018).

Rujivanarom, P. Can Laos afford to be the 'Battery of Asia'? | Earth Journalism Network, https://earthjournalism.net/stories/can-laos-afford-to-be-the-battery-of-asia (accessed September 2019).

Saad, M., Turgeon, A., Bigras, P., and Duquette, R., 1994. Learning disaggregation technique for the operation of long-term hydroelectric power systems. Water Resources Research, 30(11), 3195-3202.

Sadati, S.K., Speelman, S., Sabouhi, M., Gitizadeh, M., Ghahraman, B., 2014. GA-Optimal irrigation water allocation using a genetic algorithm under various weather conditions. Water (Switzerland), 6, 3068–3084. doi:10.3390/w6103068.

Saha, S., Moorthi, S., Wu, X., Wang, J., Nadiga, S., Tripp, P., Behringer, D., Hou, Y.T., Chuang, H.Y., Iredell, M., Ek, M., 2014. The NCEP climate forecast system version 2. Journal of Climate, 27(6), 2185-2208.

Sankarasubramanian, A., Lall, U., Devineni, N., Espinueva, S., 2009. The role of monthly updated climate forecasts in improving intraseasonal water allocation. Journal of Applied Meteorology and Climatology, 48(7), 1464-1482.

Schmitt, R.J., Bizzi, S., Castelletti, J. J. Opperman, G. M. Kondolf, 2019. Planning dam portfolios for low sediment trapping shows limits for sustainable hydropower in the Mekong. Science advances 5(10), eaaw2175.

Sechi, G.M., Sulis, A., 2009. Water System Management through a Mixed Optimization-Simulation Approach. J. Water Resour. Plan. Manag. 135 (2009) 160–170. doi:10.1061/(ASCE)0733-9496, 135:3(160).

Shamseldin, A.Y., 1997. Application of neural network technique to rainfall-runoff modelling. J. Hydrol., 199(3–4), 272–294.

Shaw, A.R., Sawyer, H.S., LeBoeuf, E.J. et al., 1983. Hydropower Optimization Using Artificial Neural Network Surrogate Models of a High-Fidelity Hydrodynamics and Water Quality Model. Water Resources Research, 53(11), 9444-9461.

Sikder, S., Ahmad, S.K., Hossain, F., Gebregiorgis, A., Lee, H., 2019. Case Study: A Rapid Urban Inundation Forecasting Technique Based on Quantitative Precipitation Forecast for Houston and Harris County Flood Control District. Journal of Hydrologic Engineering. https://doi.org/10.1061/(ASCE)HE.1943-5584.0001807.

Sikder, S., Hossain, F. 2016. Assessment of the weather research and forecasting model generalized parameterization schemes for advancement of precipitation forecasting in monsoon-driven river basins. J. Adv. Model. Earth Syst. 8, 1210–1228. doi:10.1002/2016MS000678.

Skamarock, W.C., Klemp, J.B., Dudhia, J., Gill, D.O., Barker, D.M., Duda, M.G., Huang, X.-Y., Wang, W., Powers, J.G., 2008. A Description of the Advanced Research WRF Version 3. doi:10.5065/D68S4MVH.

Sørensen B., 1981. A combined wind and hydro power system, Energy Policy, 9 (1981), 51-55.

Souza, T.M., Diniz, A.L., 2012. An Accurate Representation of Water Delay Times for Cascaded Reservoirs in Hydro Scheduling Problems. IEEE.

Spector, J., 2015. The Environmentalist Case Against 100% Renewable Energy Plans - CityLab, (2015). https://www.citylab.com/environment/2015/07/the-environmentalist-case-against-100-renewable-energy-plans/398906/ (accessed March 19, 2017).

Sreekanth, J., Datta, B., Mohapatra, P.K., 2012. Optimal short-term reservoir operation with integrated long-term goals. Water resources management, 26(10), 2833-2850.

Stanley, E.H., Doyle, M.W., 2003. Trading off: the ecological effects of dam removal, Frontiers in Ecology and the Environment, 1(1), 15-22.

Stensrud, D.J., 2007. Parameterization schemes: keys to understanding numerical weather prediction models, Cambridge University Press.

Stevens, L.E., Shannon, J.P., Blinn, D. W., 1997. Colorado River benthic ecology in Grand Canyon, Arizona, USA: dam, tributary and geomorphological influences. Regulated Rivers: Research & Management, 13(2), 129-149.

Sudheer, K.P., Gosain, A.K., Ramasastri, K.S., 2002. A data-driven algorithm for constructing artificial neural network rainfall–runoff models. Hydrol. Proc. 16, 1325–1330. https://doi.org/10.1002/(ISSN)1099-1085

Sudheer, K.P., Nayak, P.C., Ramasatri, K.S., 2003. Improving peak flow estimates in artificial neural network river flow models. Hydrol. Proc. 17, 677–686. https://doi.org/10.1002/hyp.5103

Sun, Y., Wendi, D., Kim, D.E., Liong, S.Y., 2016. Application of artificial neural networks in groundwater table forecasting–a case study in a Singapore swamp forest. Hydrology and Earth System Sciences 20(4),1405-1412.

Taylor, K.E., Stouffer, R.J., Meehl, G.A., 2012. An overview of CMIP5 and the experiment design. Bull. Am. Meteorol. Soc. 93, 485–498.

Teutschbein,C., Wetterhall, F., Seibert, J., 2011. Evaluation of different downscaling techniques for hydrological climate-change impact studies at the catchment scale. Clim. Dyn. 37, 2087–2105. doi:10.1007/s00382-010-0979-8.

Tharme, R.E., 2003. A global perspective on environmental flow assessment: emerging trends in the development and application of environmental flow methodologies for rivers. River research and applications, 19(5-6), 397-441.

Tilt, B., Braun, Y., and He, D., “Social impacts of large dam projects: A comparison of international case studies and implications for best practice,” Journal of environmental management, 90, S249-S257 (2009).

Thomas J.J., Wallis, K.F., 1971. Seasonal variation in regression analysis. Journal of the Royal Statistical Society: Series A (General), 134(1), 57-72.

Turner, S.W. D, Bennett, J.C., Robertson, D.E., Galelli, S., 2017. Complex relationship between seasonal streamflow forecast skill and value in reservoir operations. Hydrology and Earth System Sciences 21(9), 4841-4859.

Toffolon, M. Piccolroaz, S., 2015. A hybrid model for river water temperature as a function of air temperature and discharge. Environmental Research Letters 10(11), 114011.

Turner, S. W. D., Galelli, S., 2016. Water supply sensitivity to climate change: An R package for implementing reservoir storage analysis in global and regional impact studies. Environ. Modell. Softw. 76, 13–19.

Xu, B., Zhong, P.-A., Stanko, Z., Zhao, Y., and Yeh, W. W.-G., 2015. A multiobjective short-term optimal operation model for a cascade system of reservoirs considering the impact on long-term energy production. Water Resour. Res., 51, 3353–3369. http://dx.doi.org/10.1002/2014WR015964

USBR (U.S. Bureau of Reclamation), Aspinall Unit Operations Final Environmental Impact Statement - Background Material (Bureau of Reclamation, Utah, 2004)

USBR (U.S. Bureau of Reclamation), Record of Decision for the Aspinall Unit Operations Final Environmental Impact Statement (Bureau of Reclamation, Utah, 2012b). Retrieved May 11, 2019, from https://www.usbr.gov/uc/envdocs/eis/AspinallEIS/ROD.pdf

USBR (U.S. Bureau of Reclamation), Aspinall Unit Operations Final Environmental Impact Statement (Bureau of Reclamation, Utah, 2012a). Retrieved June 8, 2019, from https://www.usbr.gov/uc/envdocs/eis/AspinallEIS/

U.S. Department of the Interior, Operation of Glen Canyon Dam: Final Environmental Impact Statement, 1995, U.S. Bur. of Reclamation, Salt Lake City, Utah.

U.S. Energy Information Administration, Electric Power Monthly: with data for June 2018, Washington DC, 2018. doi:10.2172/123200.

U.S. Energy Information Administration, International Energy Outlook 2019 with projections to 2050, Washington, D.C., 2019.

Van Vliet, M. T. H. et al., 2011. Global river temperatures and sensitivity to atmospheric warming and changes in river flow. Water Resources Research, 47(2), W02544.

Vieira, F., Ramos, H.M., 2009. Optimization of operational planning for wind/hydro hybrid water supply systems. Renew. Energy. 34 928–936. doi:10.1016/j.renene.2008.05.031.

Vörösmarty, C.J., Sharma, K.P., Fekete, B.M., et al., 1997. The storage and aging of continental runoff in large reservoir systems of the world. Ambio, 26, 210–219.

Wasimi, S.A., Kitanidis, P.K., 1983. Real-time forecasting and daily operation of a multireservoir system during floods by linear quadratic Gaussian control. Water Resources Research, 19(6), 1511-1522. doi:10.1029/WR019i006p01511.

Wei, C.C., 2016. Comparing single- and two-segment statistical models with a conceptual rainfall-runoff model for river streamflow prediction during typhoons. Environ. Model. Softw. 85, 112–128. https://doi.org/10.1016/j.envsoft.2016.08.013

Welsh, W.D., 2008. Water balance modelling in Bowen, Queensland, and the ten iterative steps in model development and evaluation. Environ. Model. Softw. 23, 195–205. https://doi.org/10.1016/j.envsoft.2007.05.014

Wilby, R.L., Wigley, T.M.L., 1997. Downscaling general circulation model output: a review of methods and limitations. Progress in physical geography 21(4), 530-548. https://doi.org/10.1177/030913339702100403

Wild, T.B., Loucks, D.P., 2014. Managing flow, sediment, and hydropower regimes in the Sre Pok, Se San, and Se Kong Rivers of the Mekong basin, Water Resources Research 50, 5141–5157.

Windsor, J.S., 1973. Optimization model for the operation of flood control systems. Water Resour. Res. 9, 1219–1226. doi:10.1029/WR009i005p01219.

Winemiller K.O., et al., 2016. Balancing hydropower and biodiversity in the Amazon, Congo, and Mekong. Science 351(6269), 28-129.

Wu, C.L., Chau, K.W., Li, Y.S., 2009. Predicting monthly streamflow using data-driven models coupled with data-preprocessing techniques. Water Resour. Res. 45(8). https://doi.org/10.1029/2007WR006737

Wu, W., Dandy, G.C., Maier, H.R., 2014. Protocol for developing ANN models and its application to the assessment of the quality of the ANN model development process in drinking water quality modelling. Environ. Model. Softw. 54, 108–127. https://doi.org/10.1016/j.envsoft.2013.12.016

Xie, Q., Liu, Z., Fang, X., Chen, Y., Li, C., MacIntyre, S., 2017. Understanding the temperature variations and thermal structure of a subtropical deep river-run reservoir before and after impoundment. Water, 9(8), 603.

Xu, B., Zhong, P. A., Zambon, R. C., Zhao, Y., Yeh, W. W. G., 2015. Scenario tree reduction in stochastic programming with recourse for hydropower operations. Water Resources Research, 51(8), 6359-6380.

Yang, S.L. et al., 2005. Impact of dams on Yangtze River sediment supply to the sea and delta intertidal wetland response. Journal of Geophysical Research: Earth Surface 110(F3).

Yang, T., Asanjan, A. A., Welles, E., Gao, X., Sorooshian, S., Liu, X., 2017. Developing reservoir monthly inflow forecasts using artificial intelligence and climate phenomenon information. Water Resour. Res., 53, 2786–2812. http://dx.doi.org//10.1002/ 2017WR020482

Yang, T., Gao, X., Sellars, S.L., Sorooshian, S., 2015. Improving the multi-objective evolutionary optimization algorithm for hydropower reservoir operations in the California Oroville-Thermalito complex. Environ. Model. Softw. 69, 262–279. https://doi.org/10.1016/j.envsoft.2014.11.016

Yasar, M., 2016. Optimization of Reservoir Operation Using Cuckoo Search Algorithm: Example of Adiguzel Dam, Denizli, Turkey. Math. Probl. Eng. 2016, 1–7. doi:10.1155/2016/1316038.

Yazicigil, H., Houck, M.H., Toebes, G.H., 1983. Daily operation of a multipurpose reservoir system. Water Resour. Res. 19(1), 1-13

Yearsley, J., 2012. A grid-based approach for simulating stream temperature. Water Resources Research, 48(3).

Yeh, W.W.-G., Becker, L., 1982. Multiobjective analysis of multireservoir operations. Water Resour. Res. 18, 1326–1336. doi:10.1029/WR018i005p01326.

Yeh, W. W.-G., 1979. Real-time reservoir operation: The California central valley project case study, paper presented at the National Work- shop on Reservoir Systems Operations. American Society of Civil Engineers (ASCE), Boulder, Colo.

Yeh, W.W.-G., 1985. Reservoir Management and Operations Models: A State-of-the-Art Review. Water Resour. Res. 21, 1797–1818. doi:10.1029/WR021i012p01797.

Yuba County Water Agency, Lower Yuba River Water Temperature Evaluation – Attachment B – Draft EIR/EIS, 2007.

Yüksel, I., 2009. Hydroelectric power in developing countries. Energy Sources, Part B: Economics, Planning, and Policy 4 (4), 377–386.

Zarfl, C., et al., 2019. Future large hydropower dams impact global freshwater megafauna. Scientific Reports 9(1), 1-10.

Zarfl, C., Lucía, A., 2018. The connectivity between soil erosion and sediment entrapment in reservoirs. Current Opinion in Environmental Science & Health 5, 53-59.

Zarfl, C., Lumsdon, A.E., Berlekamp, J., et al., 2015. A global boom in hydropower dam construction. Aquatic Sciences, 77(1), 161-170. https://doi.org/10.1007/s00027-014-0377-0

Zealand, C.M., Burn, D.H., Simonovic, S.P., 1999. Short term streamflow forecasting using artificial neural networks. J. Hydrol. 214(1-4), 32-48. https://doi.org/10.1016/S0022-1694(98)00242-X

Zemzami, M., Benaabidate, L., 2016. Improvement of artificial neural networks to predict daily streamflow in a semi-arid area. Hydrol. Sci. J. 61, 1801–1812. https://doi.org/10.1080/02626667.2015.1055271

Zhang, G., Patuwo, B.E., Hu, M.Y., 1998. Forecasting with artificial neural networks: the state of the art. Int. J. Forecasting 14, 35– 62. https://doi.org/10.1016/S0169-2070(97)00044-7

Zhao, T., Cai, X., Yang, D., 2011. Effect of streamflow forecast uncertainty on real-time reservoir operation. Advances in Water Resources 34(4), 495-504. https://doi.org/10.1016/j.advwatres.2011.01.004

Zhong, Y, Power, G., 1996. Environmental impacts of hydroelectric projects on fish resources in China. Regulated Rivers: Research and Management 12, 81–98.

Zhou, Y., Guo, S., Liu, P., Xu, C.Y., Zhao, X., 2016. Derivation of water and power operating rules for multi-reservoirs. Hydrological Sciences Journal, 61(2), 359-370.

Zhu, F., Zhong, P. A., Sun, Y., Yeh, W. W. G., 2017. Real-time optimal flood control decision making and risk propagation under multiple uncertainties. Water Resources Research 53 (12), 10635–10654.

Ziv G. et al., 2012.Trading-off fish biodiversity, food security, and hydropower in the Mekong River Basin. Proceedings of the National Academy of Sciences 109(15), 5609-5614

APPENDIX A: VALUE OF SHORT-TERM WEATHER FORECASTS IN MAXIMIZING HYDROPOWER PRODUCTION

A.1 WRF performance evaluation

The evaluation of dynamically downscaled forcings of precipitation, min/max temperature and wind speed from WRF was performed using Livneh daily CONUS near-surface gridded meteorological dataset (Livneh et al., 2013). For Detroit dam, due to the absence of Livneh dataset after 2014, WRF model evaluation was performed for the peak flow event of 16 January 2011. In the case of Pensacola dam, WRF model was set up for the peak inflow event of 20 March 2012. The GFS forecast fields corresponding to lead times of 1-16 days was processed for downscaling using WRF simulation for both the dams. The metrics of correlation, RMSE, Probability of detection (POD) and Frequency Bias (Chen et al., 2016) were calculated to assess the performance of downscaled variables at different lead times. POD is the measure of how well the simulation can capture the true positives while frequency bias measures the extent to which the simulated results are biased towards false positive/negative (both having best value of one). For both dams, performance of the forecast model deteriorates with lead time, with higher number of misses (true negatives) and false positives. The comparison maps of precipitation are shown in Figure A1 for the selected peak flow events and Table A1 summarizes metrics for both the dams. Results for lead times of 3, 5 and 7 days for Detroit dam, and of 4, 6 and 8 days for Pensacola dam are shown here.

Table A1**.** Metrics for evaluation of WRF downscaled forcings for lead times of 3-8 days (L3-L8)

Variable	Metric	Detroit Dam			Pensacola Dam		
		L3	L5	L7	L4	L6	L8
Precipitation	Correlation	0.85	0.84	0.19	0.61	0.31	-0.09
	RMSE (mm)	11.18	21.62	15.86	23.39	30.52	33.57
	POD	0.93	0.96	0.04	0.72	0.66	0.57
	Freq. Bias	2.28	2.56	0.04	0.76	0.67	0.58
Max. Temperature	Correlation	0.53	0.48	0.48	0.78	0.71	0.64
	RMSE (˚C)	4.88	4.65	6.05	3.73	4.82	5.19
Min. Temperature	Correlation	0.68	0.67	0.68	0.87	0.82	0.58
	RMSE (˚C)	5.45	5.34	3.46	2.07	2.26	3.23
Wind Speed	Correlation	0.16	0.36	0.01	0.61	0.45	-0.19
	RMSE (m/s)	2.26	2.03	2.56	1.70	1.88	2.76

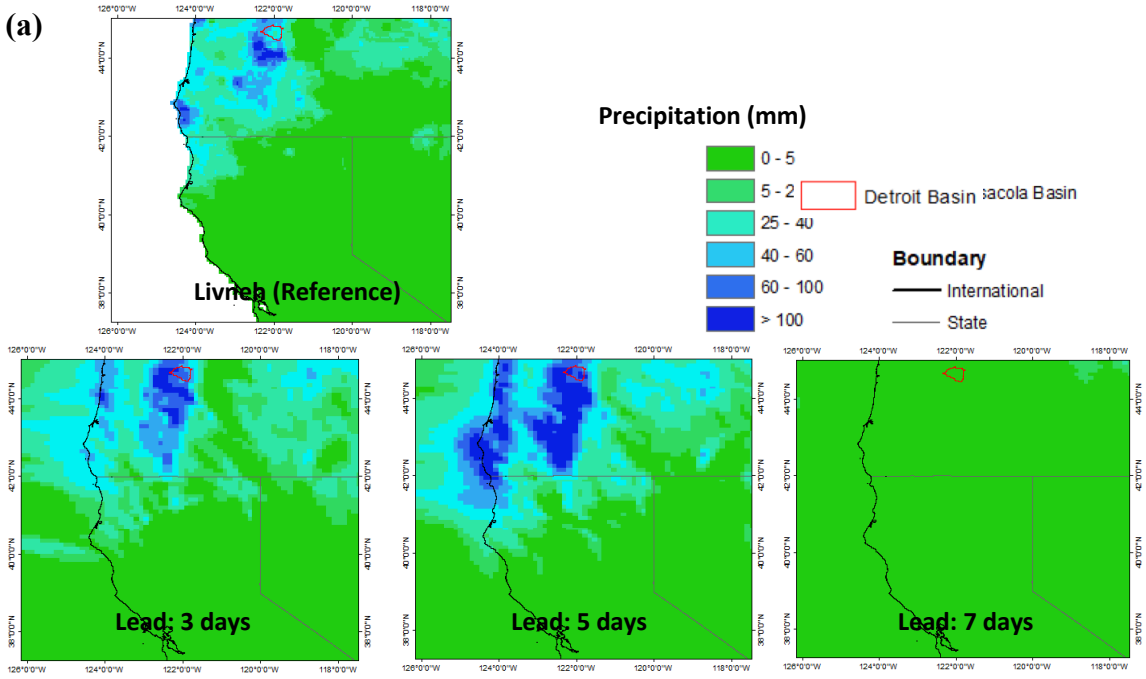

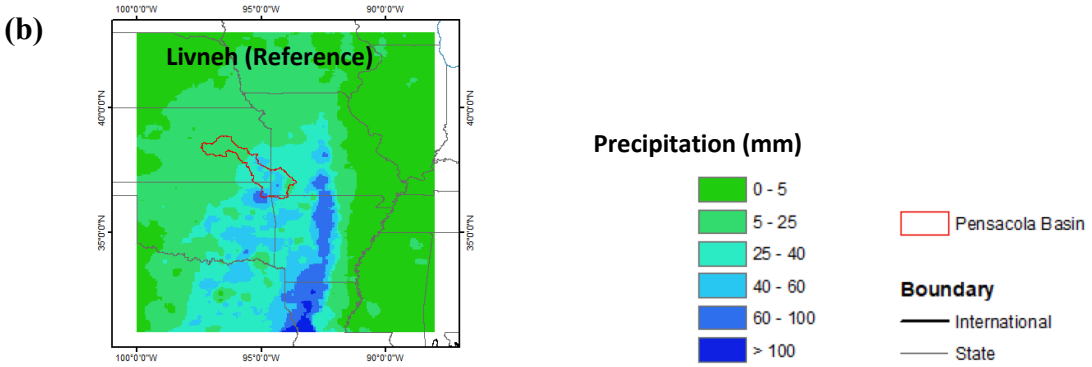

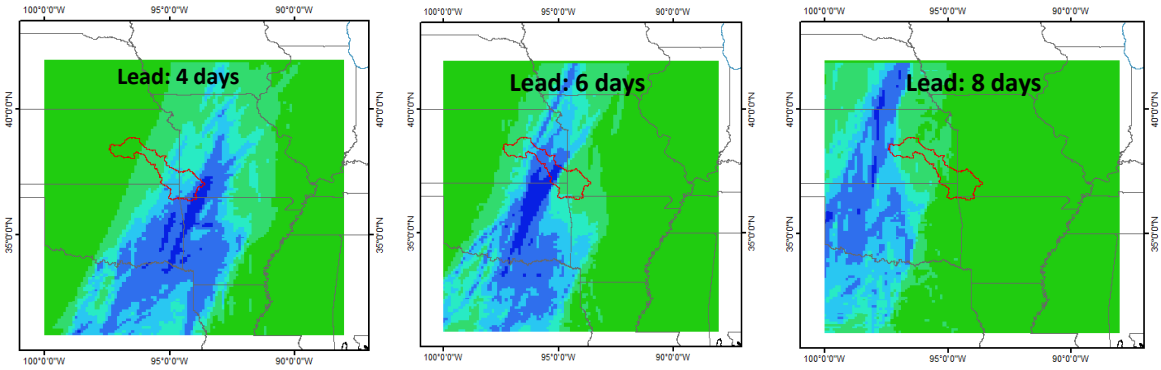

Figure A1. Assessment of WRF downscaled precipitation (0.1˚) with reference Livneh dataset over the events of 16 Jan 2011 and 20 Mar 2012 for (a) Detroit and (b) Pensacola dam.

A.2 VIC Model Setup

A.2.1 Detroit Dam

Calibration was performed on the period from 2009-11, and the validation over 2013-15. The first few months were ignored for calculating metrics considering the model spin-up period. Normalized RMSE is calculated as $\frac{RMSE}{\sigma_{obs}}$ (where σ_{obs} is standard deviation of the observed streamflow). The results for calibration and validation are shown in Figure A2. As the high flow events are of interest, normalized mean absolute error ($NMAE = \frac{1}{Num\ of\ peaks} \sum \frac{|Obs-Mod|}{Mod}$) specific to peaks (with flow exceeding turbine capacity of 9000 cfs) and percentage of times peaks were under/overestimated are also shown.

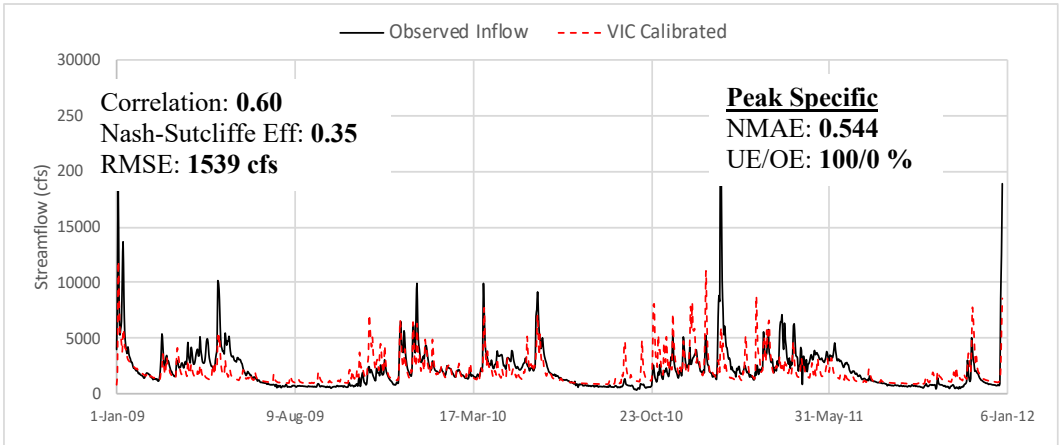

(a)

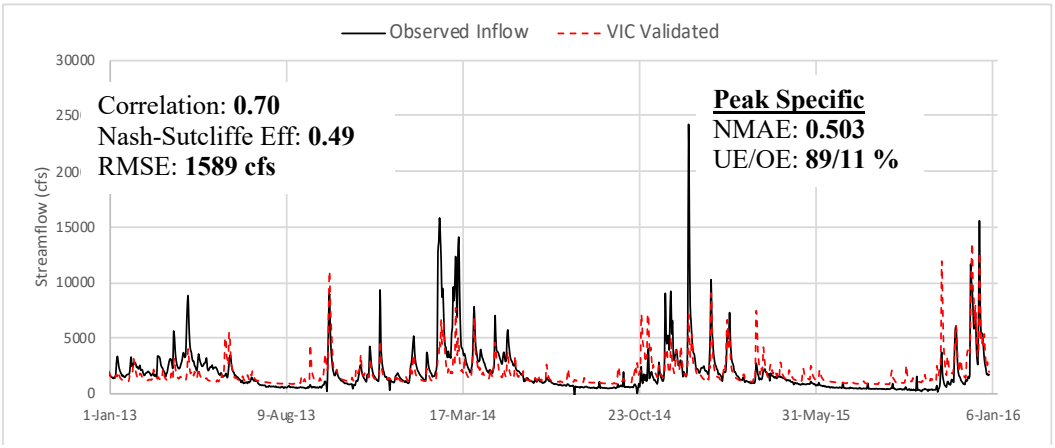

(b)

Figure A2. (a) VIC calibrated and (b) validated streamflow, along with metrics for Detroit Dam. NMAE is normalized mean absolute error, UE/OE is % times peak is under/overestimated. (1 cfs = 0.028 m^3/s)

A.2.2 Pensacola Dam

Daily inflow data from 2002-06 was used for calibration, while validation was performed over 2011-15. The calibration and validation results are shown below in Figure A3. The NMAE and percent times peak is overestimated (false positive) or underestimated (missed bias) over the considered period is obtained for events with flow exceeding 20,000 cfs (566 m^3/s).

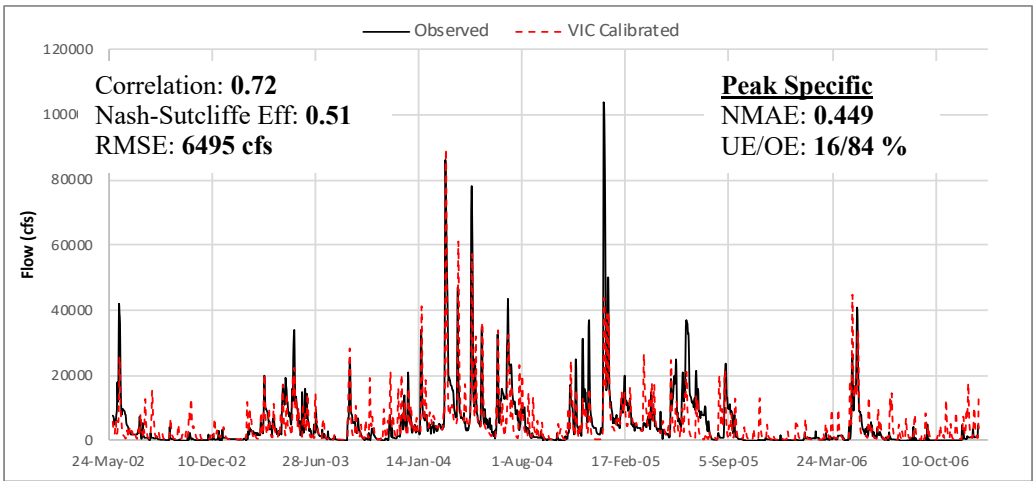

(a)

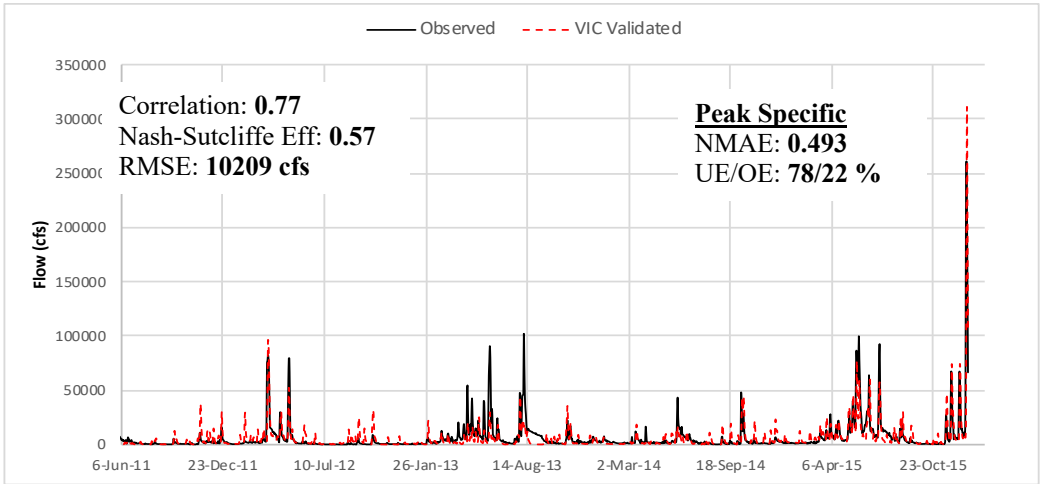

(b)

Figure A3. (a) VIC calibrated and (b) validated streamflow, with metrics for Pensacola Dam. NMAE is normalized mean absolute error, UE/OE is % times peak is under/overestimated. (1 cfs = 0.028 m^3/s).

The modeled real-time reservoir inflow forecasts over the Detroit dam generated by the operational system over Dec 2017 to Sep 2018, forcing the VIC model with WRF downscaled forcings, is compared with the observed inflow in Figure A4. The hindcast flow from VIC model is also plotted alongside for comparison. The metrics of comparison are summarized in Table A2.

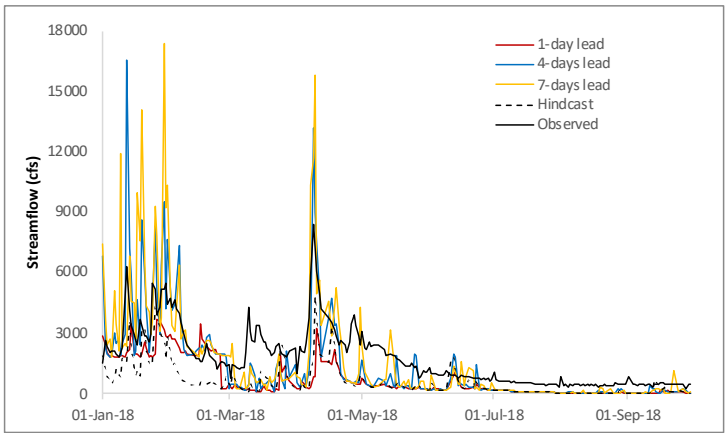

Figure A4. Comparison of the modeled daily forecast/hindcast flow for lead times of 1, 4 and 7 days over Jan-Sep 2018 against observed data for Detroit dam. (1 cfs = 0.028 m^3/s)

Table A2. Metrics for comparison of daily modeled forecast/hindcast flows against observed data over Jan-Sep 2018 for Detroit dam.

	Best value	**Lead 1**	**Lead 4**	**Lead 7**	**Lead 10**	**Hindcast**
RMSE (cfs)	0.0	1486.1	1459.8	1944.7	1882.3	1504.0
NRMSE	0.0	1.03	1.01	1.35	1.31	1.04
Correlation	1.0	0.64	0.78	0.71	0.67	0.72
NSE	1.0	0.35	0.37	-0.11	-0.04	0.34

A.3 Constraints for Optimization

1. Release from the turbines is constrained by the turbine capacity, P_{turb}.

$$R_{p,t} \leq P_{turb} \quad , \forall t \tag{A1}$$

2. The system follows storage-volume continuity (water-balance equation) which requires that in each period t,

$$S_{t+1} = S_t + [I_t - L_t - (R_{p,t} + R_{np,t})] \cdot \Delta t, \ \forall t \tag{A2}$$

However, as the optimization is performed at daily time steps ($\Delta t = 1$), the losses due to evaporation and seepage, L_t, were ignored.

3. Reservoir storage (S) was limited to ensure dam safety and avoid infeasible scenarios such as the reservoir running empty,

$$S_{min} \leq S_t \leq S_{max}, \ \forall t = 1,2,\dots,16 \quad \text{(A3)}$$

4. Daily hydropower production (HP) was limited by the powerplant's overload capacity (HP_{max}),

$$HP_t < HP_{max}, \ \forall t = 1,2,\dots,16 \quad \text{(A4)}$$

5. To prevent the downstream flooding hazards, the total release was constrained to a maximum limit, R_{max},

$$R_{p,t} + R_{np,t} \leq R_{max}, \forall t \quad \text{(A5)}$$

6. To avoid excessive and infeasible rates of non-power release via the spillway, the non-power release rate was limited to the spillway capacity,

$$R_{np,t} \leq Spill_{max}, \ \forall t \quad \text{(A6)}$$

7. Lastly, the releases made from reservoir should comply with the environmental flow limit, Q_{env},

$$R_{np,t} + R_{p,t} \geq Q_{env}, \forall t \quad \text{(A7)}$$

Table A4. Parameters/constraints for the optimization model setup for the two dams

Parameters	**Detroit Dam**	**Pensacola Dam**
Turbine Capacity	151.2 m^3/s (5340 cfs)	340 m^3/s (12,000 cfs)
Spillway Capacity	4,984 m^3/s (176,000 cfs)	14,866 m^3/s (525,000 cfs)
Minimum storage	1.67×10^8 m^3 (135.7 kaf)	1.56×10^8 m^3 (126.5 kaf)
Maximum storage	5.61×10^8 m^3 (455.1 kaf)	2.4937×10^9 m^3 (2021.7 kaf)
Maximum release	255 m^3/s (9000 cfs)	850 m^3/s (30,000 cfs)
Env. flow limit	42.5 m^3/s (1500 cfs)	28.3 m^3/s (1000 cfs)

APPENDIX B: DATA-DRIVEN TECHNIQUE FOR FORECASTING RESERVOIR INFLOW: APPLICATION FOR HYDROPOWER MAXIMIZATION

B.1 ANN Performance with Köppen Geiger Climate Classes

The climate classes used in this study are shown in Figure B1, with the distribution of selected dam sites. The markers for each site are sized with the NSE of ANN forecast at lead time of one day.

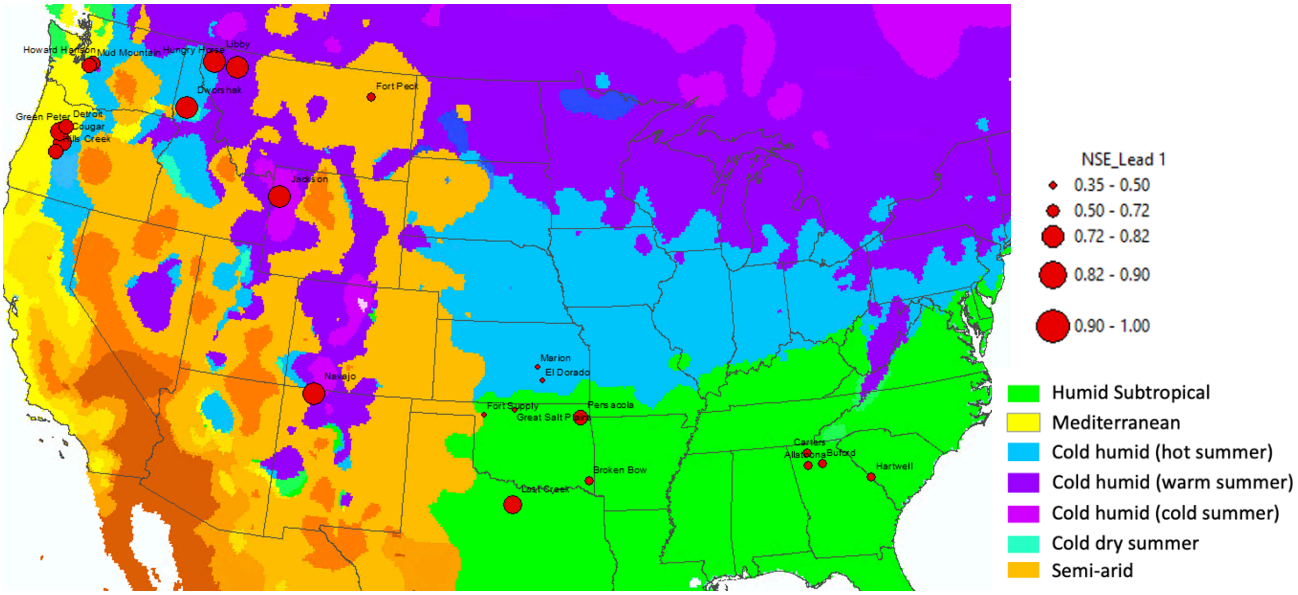

Figure B1. Map showing the Köppen Geiger Climate Classes used in this study and the selected dam sites with markers sized with NSE of ANN forecasted flow at lead time of 1 day.

B.2 Optimization Model Setup for Pensacola Dam

B.2.1 Constraints – Mathematical Formulation

We define the following constraints for the optimization model with the specific values summarized in Table B1.

1. Release from the turbines is constrained by the turbine capacity, P_{turb}.

$$R_{p,t} \leq P_{turb} \quad , \forall t \tag{B1}$$

2. The system follows storage-volume continuity (water-balance equation) which requires that in each period t,

$$S_{t+1} = S_t + [I_t - L_t - (R_{p,t} + R_{np,t})] \cdot \Delta t, \ \forall t \tag{B2}$$

However, as the optimization is performed at daily time steps ($\Delta t = 1$), the losses due to evaporation and seepage, L_t, were ignored.

3. Reservoir storage was limited to ensure dam safety and avoid infeasible scenarios such as the reservoir running empty.

$$S_{min} \leq S_t \leq S_{max}, \ \forall t \tag{B.3}$$

Here, S_{min} is set up considering the conservation pool of the reservoir to keep it at a suitable level above the inactive pool, while S_{max} denotes the active storage capacity till the reservoir's full pool.

4. To prevent the downstream flooding hazards, the total release was constrained to a maximum limit, R_{max},

$$R_{p,t} + R_{np,t} \leq R_{max}, \forall t \tag{B4}$$

5. To avoid excessive and infeasible rates of non-power release via the spillway, the non-power release rate was limited to the spillway capacity,

$$R_{np,t} \leq Spill_{max}, \ \forall t \tag{B5}$$

6. Lastly, the releases made from reservoir should comply with the environmental flow limit, Q_{env},

$$R_{np,t} + R_{p,t} \geq Q_{env}, \forall t \tag{B6}$$

Table B1. Constraints for Optimization for Pensacola dam, OK

Constraint	**Value**	**Comments**
Turbine Capacity	12,000 cfs	-
Spillway Capacity	525,000 cfs	-

Minimum storage	1,265,000 ac-ft	95% of 10-yr minimum
Maximum storage	2,021,679 ac-ft	Flood control pool
Maximum release	50,000 cfs if level exceeds 750 ft, otherwise 30,000 cfs	Avoid flooding at downstream station of Neosho River
Env. flow limit	500 cfs	-

B.2.2 Objective Functions – Mathematical formulation

The following two functions (objective and penalty) were defined for setting up the optimization problem:

1. *Energy Maximization*: Minimize the deficit in hydroelectric energy production (MWh) from the maximum generation capacity of the powerplant,

$$\min f_1 = HP_{max} - \sum_t \epsilon \cdot (HF_t - HT_t) \cdot R_{p,t} \cdot \Delta t_{turb} \quad \text{(B7)}$$

2. *Penalty Function:* Minimize the sum of the absolute value of storage deviations from the rule curve-specified value over a fixed number of days of the optimization horizon. It is represented as,

$$\min f_2 = \sum_t |S_t - T_t| \qquad (t = 3, 4 \ldots \ 7 \text{ days}) \quad \text{(B8)}$$

If a flood event is forecasted causing the reservoir level to reach the flood storage pool, the function is modified to minimize the uncontrolled spillway release,

$$\min f_2 = \sum_t R_{np,t} \qquad (t = 1, 2 \ldots 7 \text{ days}) \quad \text{(B9)}$$

where:

HP_{max} – Maximum hydropower generation capacity

HF – Reservoir forebay water level, obtained from area-elevation curve

HT – Reservoir tailrace water level

ϵ – Turbine efficiency

R_{np} – Spillway (non-power) release

R_p – Power (turbine) release

Δt_{turb} – Turbine operating hours

T – Target (rule curve specified) storage

S – Reservoir storage

t – Time step (days) over the period of optimization

APPENDIX C: FORECAST-INFORMED HYDROPOWER OPTIMIZATION AT LONG AND SHORT-TIME SCALES FOR A MULTIPLE DAM NETWORK

C.1 Skill Assessment of Short-term inflow forecasts

Using the selected ANN architecture, the training, validation and testing of the ANN base model was performed using the GFS forecast forcings for the Blue Mesa dam. The trained ANN model was then forced with 11-member ensemble forecast forcings from GEFS model to result into the ensemble streamflow forecasts for lead times of 1-7 days. The GEFS-based ensemble flow forecasts obtained using the trained ANN model are shown in Figure C1 for the period of analysis 2016-18. The selected period of analysis included an anomalously dry, intermediate and anomalously wet years. The performance of the average scenario of GEFS-based ensemble forecasts is compared against that obtained using GFS-based forecast. The evaluation metrics of Nash-Sutcliffe Efficiency (NSE), Correlation, Root Mean Squared Error (RMSE) and RMSE normalized with the mean of observed inflow (NRMSE) were used. The metrics are shown in Table C1.

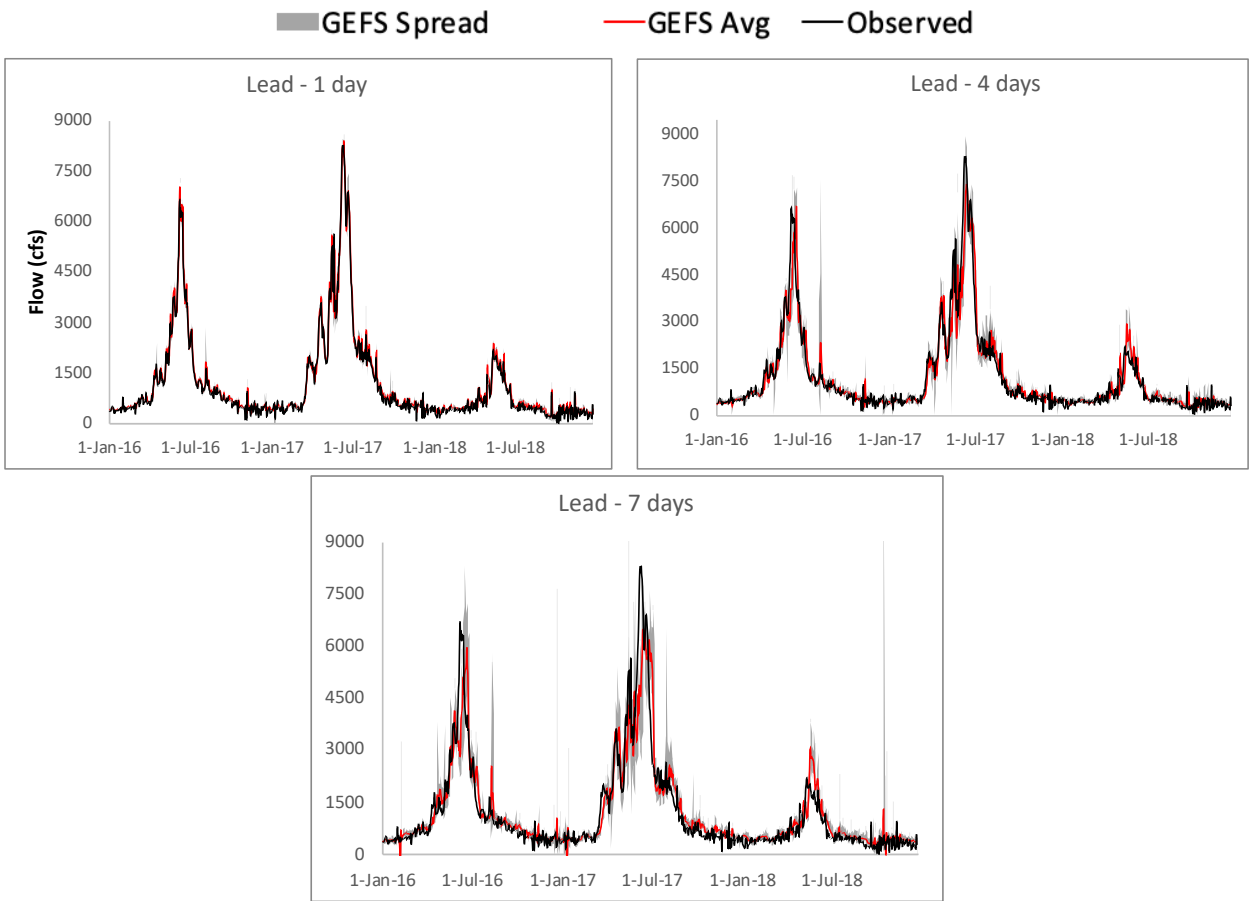

Figure C1. Daily ensemble inflow forecasts along with the observed flow and average scenario of the 11-member ensemble for Blue Mesa dam over 2016-18.

Table C1. Evaluation metrics comparing the GEFS-average and GFS based flow forecasts for lead times of 1, 4 and 7 days against the observed inflow for Blue Mesa dam.

Metric	GEFS average scenario			GFS		
	L1	L4	L7	L1	L4	L7
NSE	0.971	0.923	0.912	0.972	0.921	0.888
Correlation	0.986	0.963	0.956	0.986	0.960	0.943
RMSE (cfs)	215.1	350.9	375.6	188.7	313.5	368.1
NRMSE	0.120	0.196	0.209	0.120	0.199	0.233

C.2 Skill Assessment of Long-term inflow forecasts

The long-term ANN model was trained using the selected predictors and ensemble forecast forcings were used to result into the ensemble of flow forecasts. The modeled monthly flow

forecasts over the testing period are compared with the observed inflow in Figure C2(a). The spread in the ensemble forecasts for the lead time of 1 month for Blue Mesa dam is shown as boxplot in Figure C2(b). The average forecast scenario was used for performing the deterministic genetic algorithm-based optimization. The metrics evaluating the performance of average monthly forecast scenario against the observed values are tabulated in Table C2.

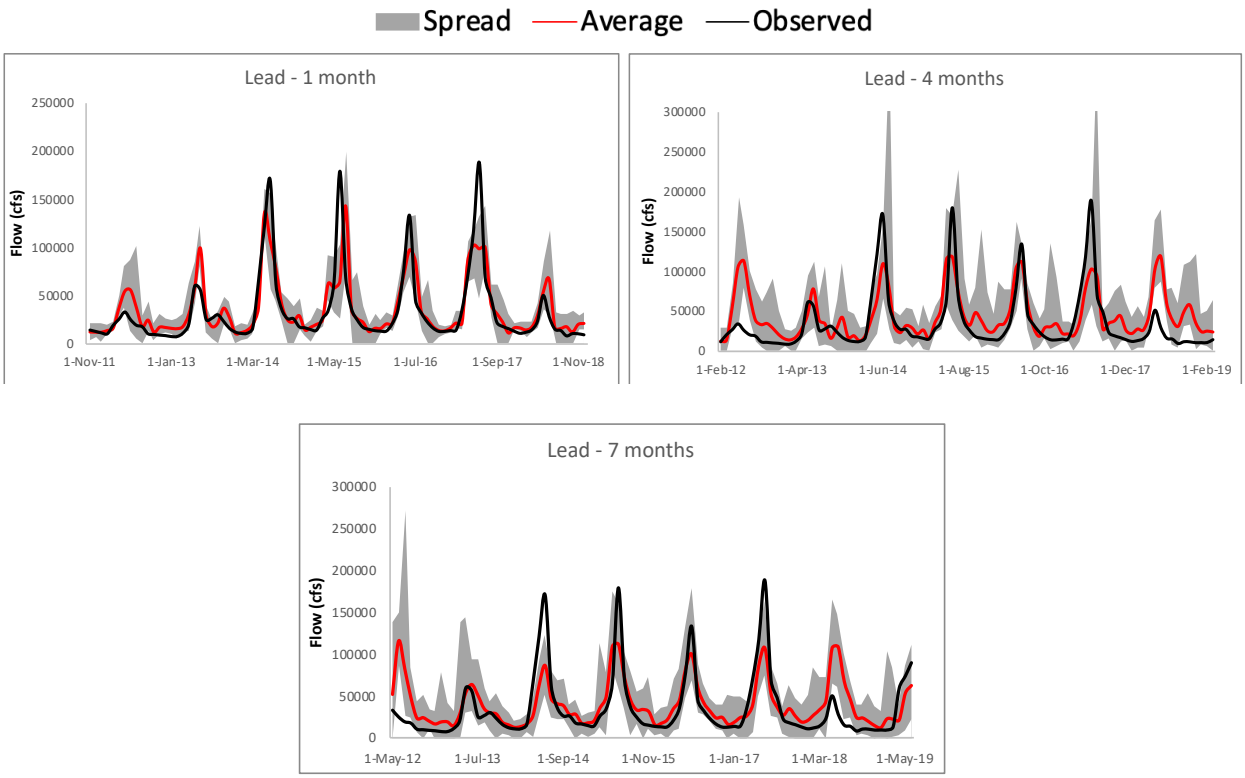

(a)

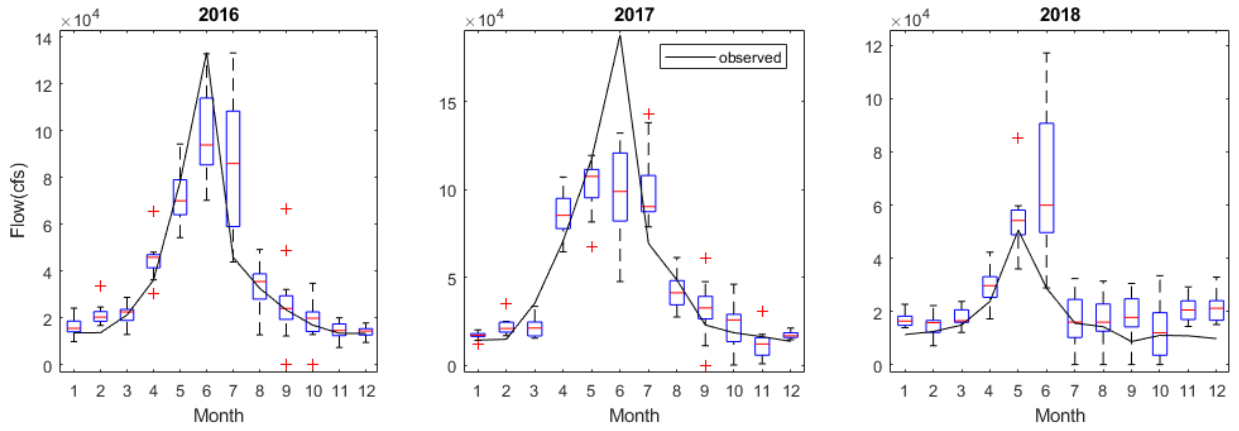

(b)

Figure C2. (a) Ensemble monthly flow forecasts using the ANN model compared against the observed inflows over the testing period for lead times of 1, 4 and 7 months; (b) Boxplots of the ensemble flow forecasts for 2016-18 showing the spread in the forecasts for lead time of 1-month.

Table C2**.** Evaluation metrics for assessing the performance of the average scenario from the ensemble of monthly flow forecasts over the testing period of ANN model.

Metric	**Lead 1 month**	**Lead 4 months**	**Lead 7 months**
NSE	0.63	0.53	0.58
Correlation	0.80	0.75	0.77

APPENDIX D: REALIZING ECOSYSTEM-SAFE HYDROPOWER FROM DAMS

D.1 Selected dams for remote sensing-based temperature estimation

Table D1. Summary of the selected dams, their approximate downstream river channel widths, Landsat-7 ETM+ scene path and row numbers, and USGS upstream and downstream stations for temperature measurements.

S. No.	Dam name	Lat (°N)	Lon (°W)	Normal Reservoir depth (m)	Down-stream river width (m; approx.)	Landsat 7 scene #		USGS station ID(s)		Analysis period	
						Path	Row	u/s	d/s	u/s	d/s
1.	Fort Peck, MT	48.0	106.4	67	250	35	27	06115200	06177000	2010-18	2002-04
2.	Palisades, ID	43.3	111.2	75	100	38	30	09205000	13032500	2015-19	2006-15
3.	Glen Canyon, AZ	36.9	111.5	170	150	37	34	09379500	09380000	2009-16	2009-16
4.	Dworshak, ID	46.5	116.3	192	75	42	28	13340600	13341000	2009-18	2009-18
5.	Detroit, OR	44.7	122.2	130	40	45	29	14179000, 14178000, 14180300	14181500	2010-19	2010-19
6.	Lower Monumental*, WA	46.6	118.5	165	300	43	28	13352595	13352600	2010-19	2010-19
7.	McNary*, WA	45.9	119.3	23	800	44	28	14019220	14019240	2010-19	2010-19
8.	Keystone, OK	36.2	96.2	22	250	27	35	07176950	07164500	2004-05	2009-19
9.	Green Peter, OR	44.7	122.5	100	35	45	29	14185900	14186200	2010-19	2010-19
10.	Holter, MT	47.0	112.0	15	115	39	27	06054500	06066500	2010-18	2010-18

* run-of-river dam

D.2 Hydrological characteristics and performance evaluation over selected years

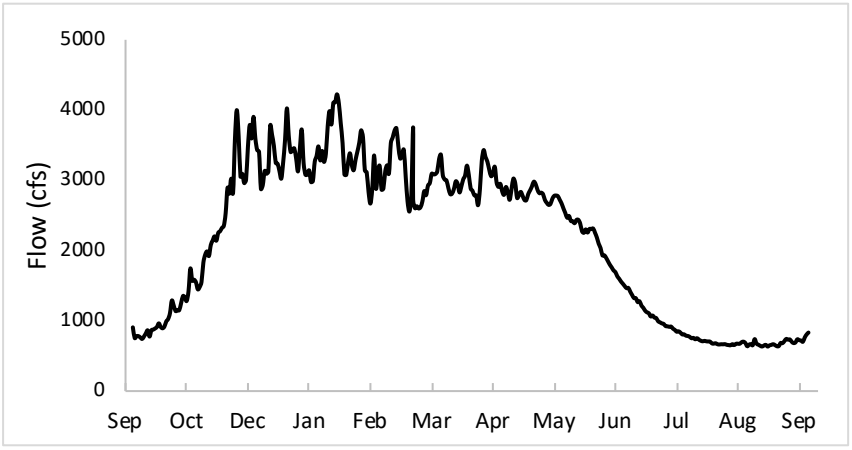

Figure D1. Flow climatology for Detroit dam, derived using 50 years of reservoir inflow data (1961-2010) (Source: USACE)

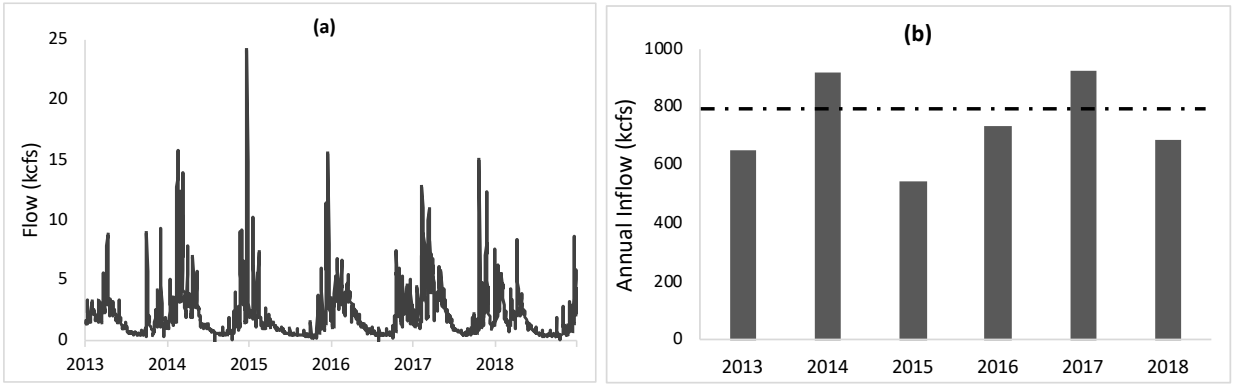

Figure D2. (a) Daily inflow into Detroit reservoir over selected years of analysis, (b) Corresponding annual inflow rates over each year, dashed line shows climatological average flow rate.

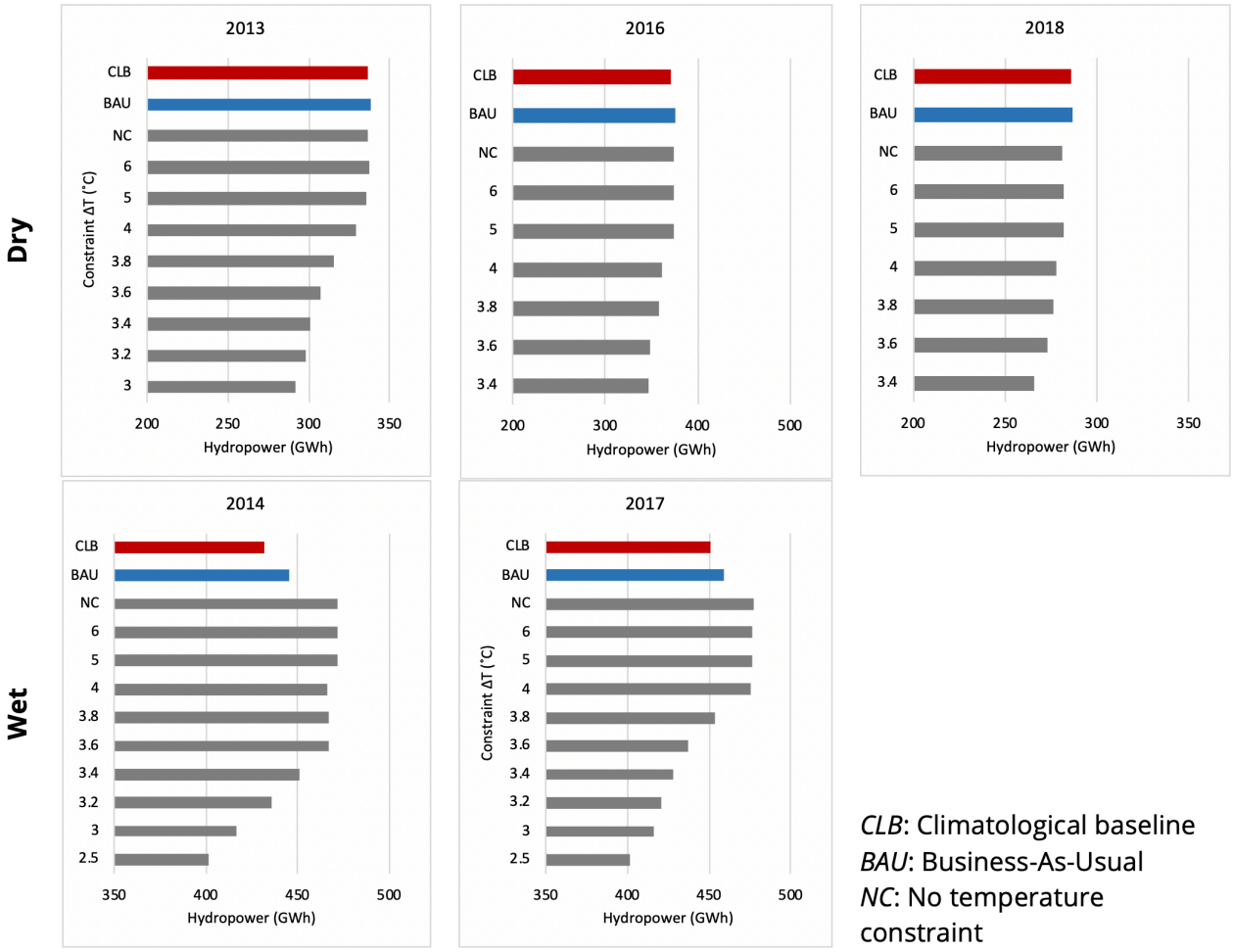

Figure D3. Hydropower generation from different constraints on allowable temperature difference, compared with those from scenarios of no temperature constraint (NC), CLB and BAU, over wet and dry years.

APPENDIX E: HOW MIGHT PLANNED HYDROPOWER DAMS ALTER RIVER TEMPERATURES AROUND THE WORLD?

E.1 Observed Trends in Thermal Impact of Existing Dams in US

Based on the historical record of observed temperature over hydropower dams in the U.S., we found contrasting impacts of dam operations during summer and winter seasons. Most hydropower dams tend to cool downstream rivers during JJA (Figure E6), the primary cause of which is the stratification of reservoirs with significant difference between the temperatures of surface water and that of deeper pools from which the water is released. Reservoirs with larger storage pool and small areal extent (and hence a small area to storage ratio) experience strong thermal stratification and such dams tend to have a severe cooling impact, as suggested by Figure E6a. In contrast, small storage reservoirs with large area have relatively uniform water pool leading to comparatively warmer release downstream. Also, deeper reservoirs (shown with larger markers in Figure E6a) tended to intensify the stratification and its cooling impact.

Considering the climate, hydropower dams lying in arid and warm regions with hotter summers (Köppen climate classes 7-9) tended to shift the thermal regime towards cooling (Figure E6b). This is likely as the surface water temperatures increase due to contact with warm air and high solar radiation that cannot penetrate the cooler bottom layer (hypolimnion). Dams located in more humid and snowy climates (Köppen climate classes 25, 26) experienced relatively cooler air temperatures, though not high enough to stratify the reservoir. Thus, such dams exhibited weaker cooling impact and even lead to warming in many cases.

During the winter months of DJF, reservoirs that experience strong stratification caused warming with positive thermal change. As the air temperature decreases with declining solar

radiation input during the winter season, reservoir's surface water begins to cool. This eventually leads to the top layer cooling down to a temperature similar or lower than the hypolimnion, breaking the thermal stratification. Thus, dams in such conditions exhibited a warming effect, although no strong relationship (p-value of 0.19) with the dam size could be observed (Figure E6c). In cases when the winter temperatures drop below 4˚C (for example, for dams in climate class 26), surface waters become lighter than the bottom warmer water and a so-called inverse stratification develops, again causing the release of warm water downstream (Figure E6d).

E.2 Development of Neural Network Model for FUTURIST Framework

The multilayer perceptron feedforward ANN model for predicting thermal regime changes was developed by first training the network over selected 107 existing dams in the U.S., followed by the validation over existing dams in data-limited regions of Southeast Asia, in particular, MRB and India.

The architecture of ANN was designed by hyperparameter tuning procedure. The search space comprised of a set of values of input nodes, varying number of dense layers (or hidden layers), and varying number of dense layer nodes. The resulting architecture comprised of an input layer with 7 nodes, two dense (hidden) layers with 16 and 8 hidden units, and an output layer with single node of thermal change to be predicted. To prevent the model from overfitting, we added a dropout layer with a dropout rate of 0.3. Dropout works by randomly setting the outgoing edges of hidden units to zero at each update of the training phase. Rectified linear unit (ReLU) was employed for the activation function for each layer. ReLU outputs the input directly if it is positive, and zero otherwise and is advantageous by reducing the likelihood of the gradient to vanish. All

inputs were normalized, and regularization was used to further prevent the ANN model from overfitting.

We also compared the performance of selected ANN architecture with two other models - one with 3 hidden layers (256, 16, and 4 nodes) representing a complex model, and other a simpler regression model with same input predictors for both. The resulting performance of ANN-derived thermal changes for validation over dams in Southeast Asia over months of JJA and DJF is shown in Table S1.

The training was performed using Adam Optimizer with a learning rate of 0.001. Adam optimization is a stochastic gradient descent method based on adaptive estimation of first-order and second-order moments. Because the purpose here is to predict the continuous variable of thermal change, loss functions pertinent to regression of mean absolute error and mean squared error were used during the training procedure. Iterations for 1200 epochs were simulated with a batch size of 5. The open-source Keras library was used to implement the model.

The validated model was then used for making predictions on planned dams. For the future hydropower dam locations, all the input nodes can be directly derived from dam height and its location. A toolbox was developed in ArcGIS software to automate the derivation of area-elevation relationship of any dam based on its height and location. A global DEM from Shuttle Radar Topography Mission (SRTM) was used, as it (the mission) was able to see a major portion of bathymetry above the existing river level for the future dams. The storage capacity was then derived by integrating that relationship from the river level to maximum dam height.

E.3 Models used for Climate Change Impact Assessment

The climate scenarios for projected rise in global air temperatures under RCP4.5, RCP8.5, and retrospective (historical) scenarios were acquired from 21 different models of General Circulation Model (GCM) runs conducted under CMIP5. These were acquired from Google Earth Engine (GEE) data catalog as NASA Earth Exchange (NEX) GDDP dataset (GEE product ID: "NASA/NEX-GDDP"). The processing of these models was performed using cloud computing platform of GEE to obtain ensemble mean of air temperatures over all the selected 216 dams for input to the FUTURIST ANN model.

The 21 CMIP5 models selected are as follows:

ACCESS1-0	inmcm4
bcc-csm1-1	IPSL-CM5A-LR
BNU-ESM	IPSL-CM5A-MR
CanESM2	MIROC-ESM
CCSM4	MIROC-ESM-CHEM
CESM1-BGC	MIROC5
CNRM-CM5	MPI-ESM-LR
CSIRO-Mk3-6-0	MPI-ESM-MR
GFDL-CM3	MRI-CGCM3
GFDL-ESM2G	NorESM1-M
GFDL-ESM2M	

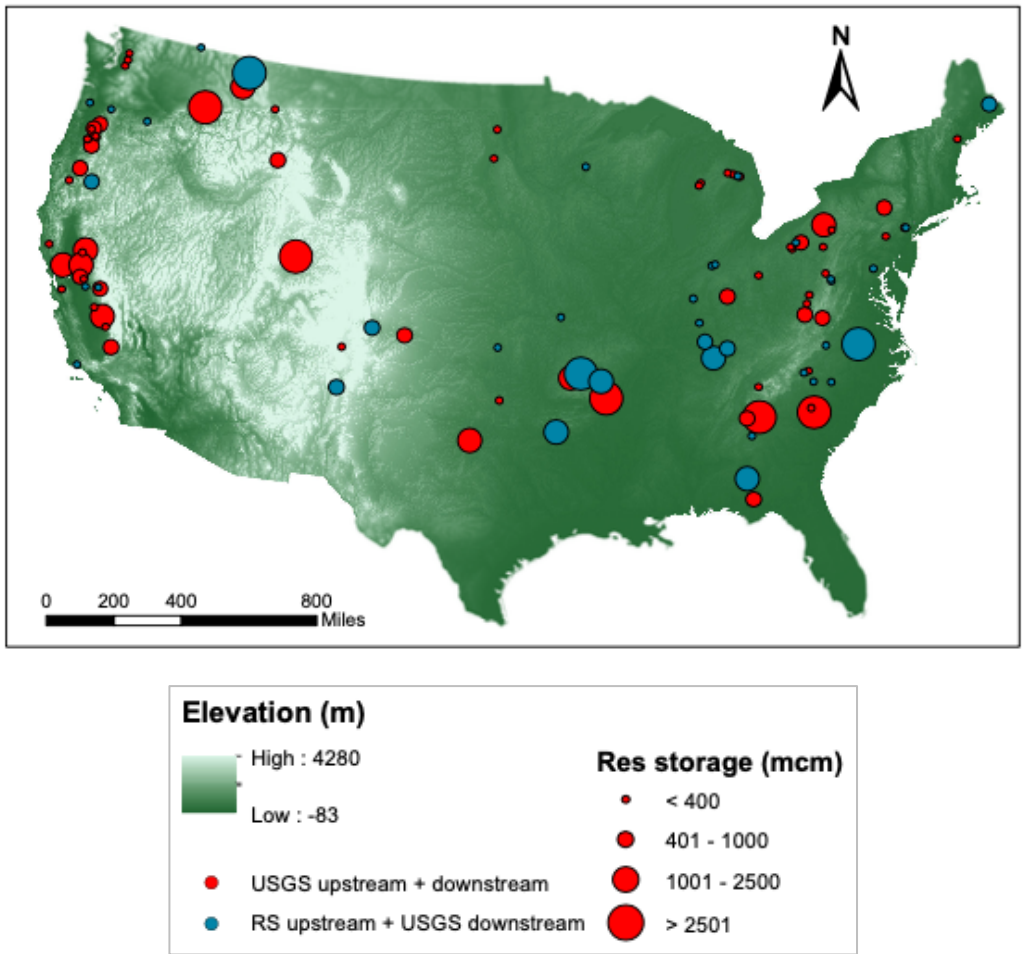

Figure E1. Location of selected existing dams in the U.S., sized with the reservoir storage capacity. Red markers indicate dams for which USGS temperature monitoring stations were available both upstream and downstream, while blue markers indicate dams for which only downstream USGS stations were present. Upstream water temperature was obtained using remote sensing for blue markers.

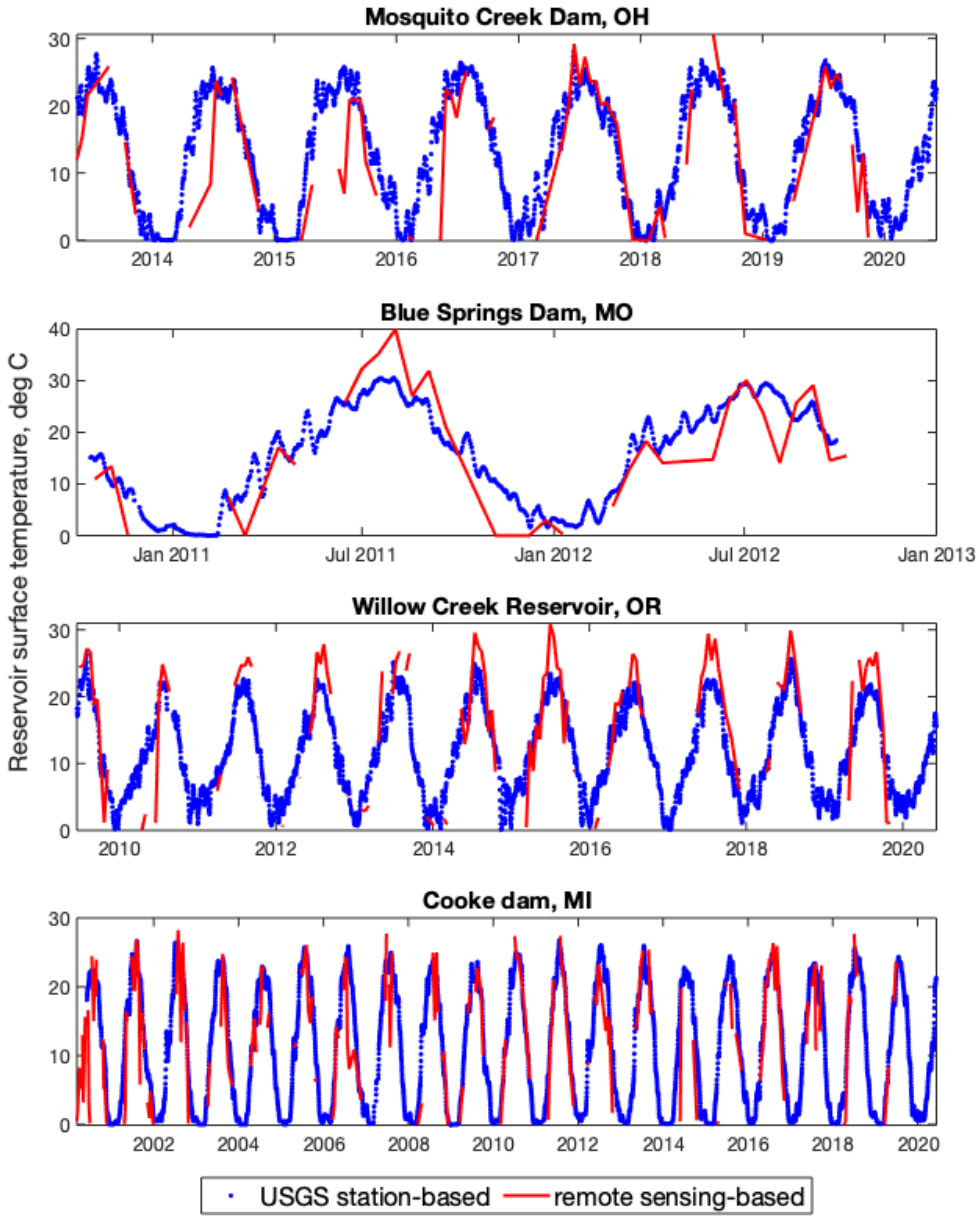

Figure E2. Comparison of reservoir surface temperature retrieved from USGS monitoring stations and remote sensing-based extraction algorithm for four dams in the U.S.

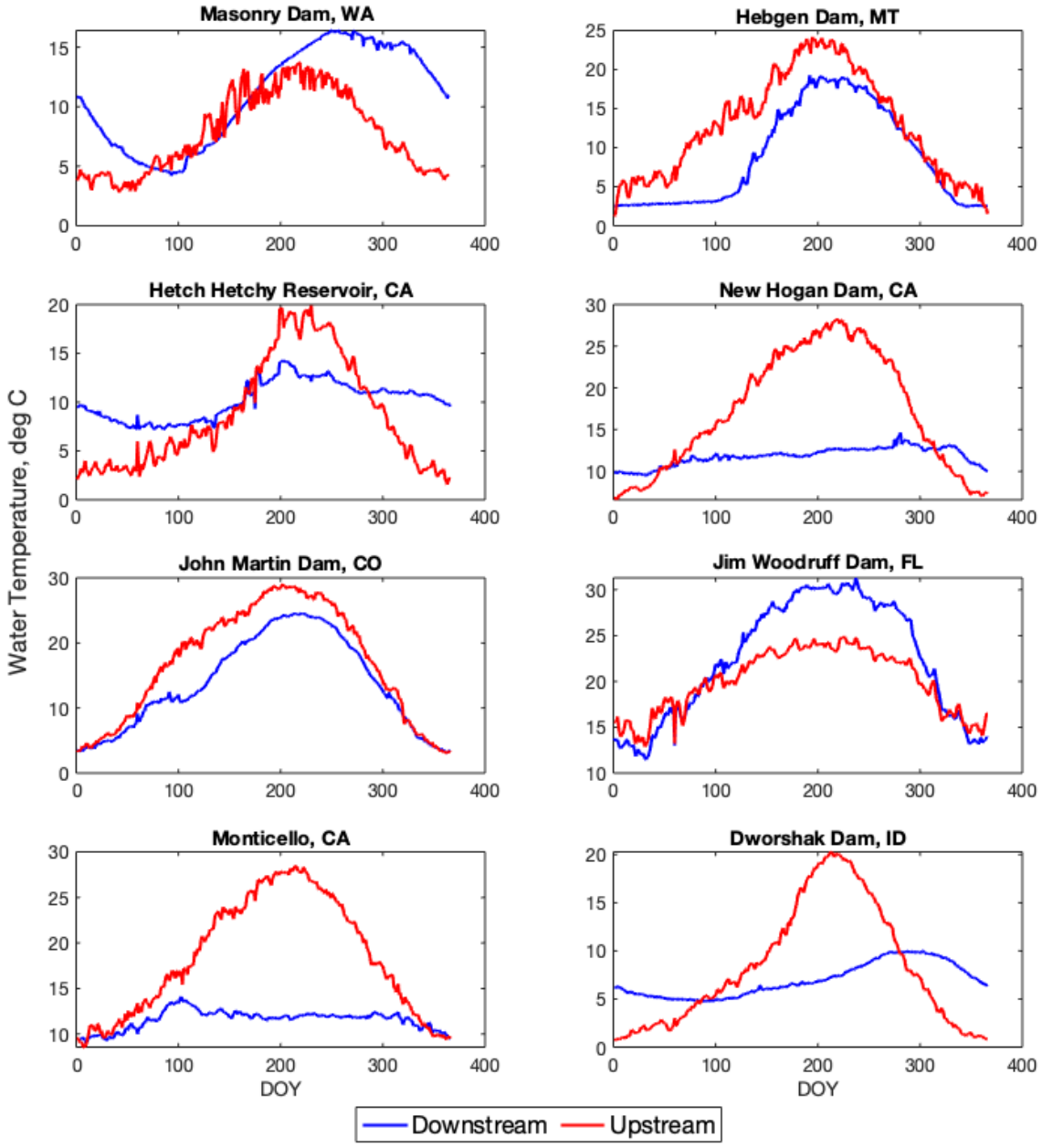

Figure E3. Annual-averaged water temperatures from USGS monitoring stations upstream and downstream of eight dams in the U.S. Difference in the temperature profiles underscores the diverse response of downstream river channels upstream to dam operations.

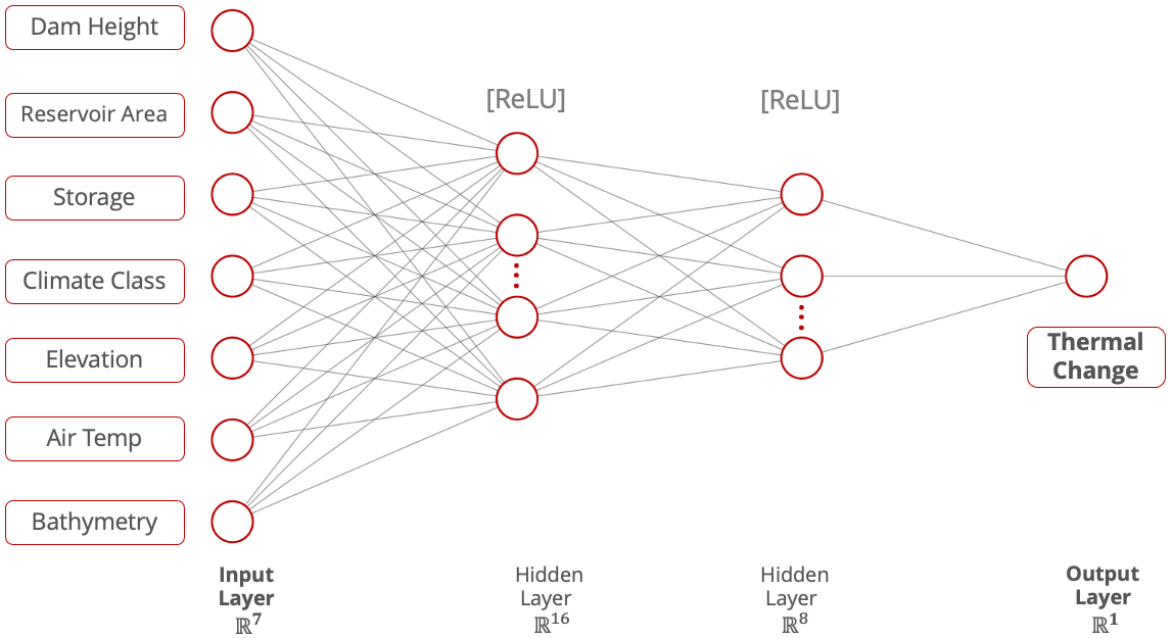

Figure E4. Feedforward Neural Network architecture with input, dense, and output layer configurations used for FUTURIST framework. 'ReLU' is the rectified linear unit, used as the activation function for the hidden layers.

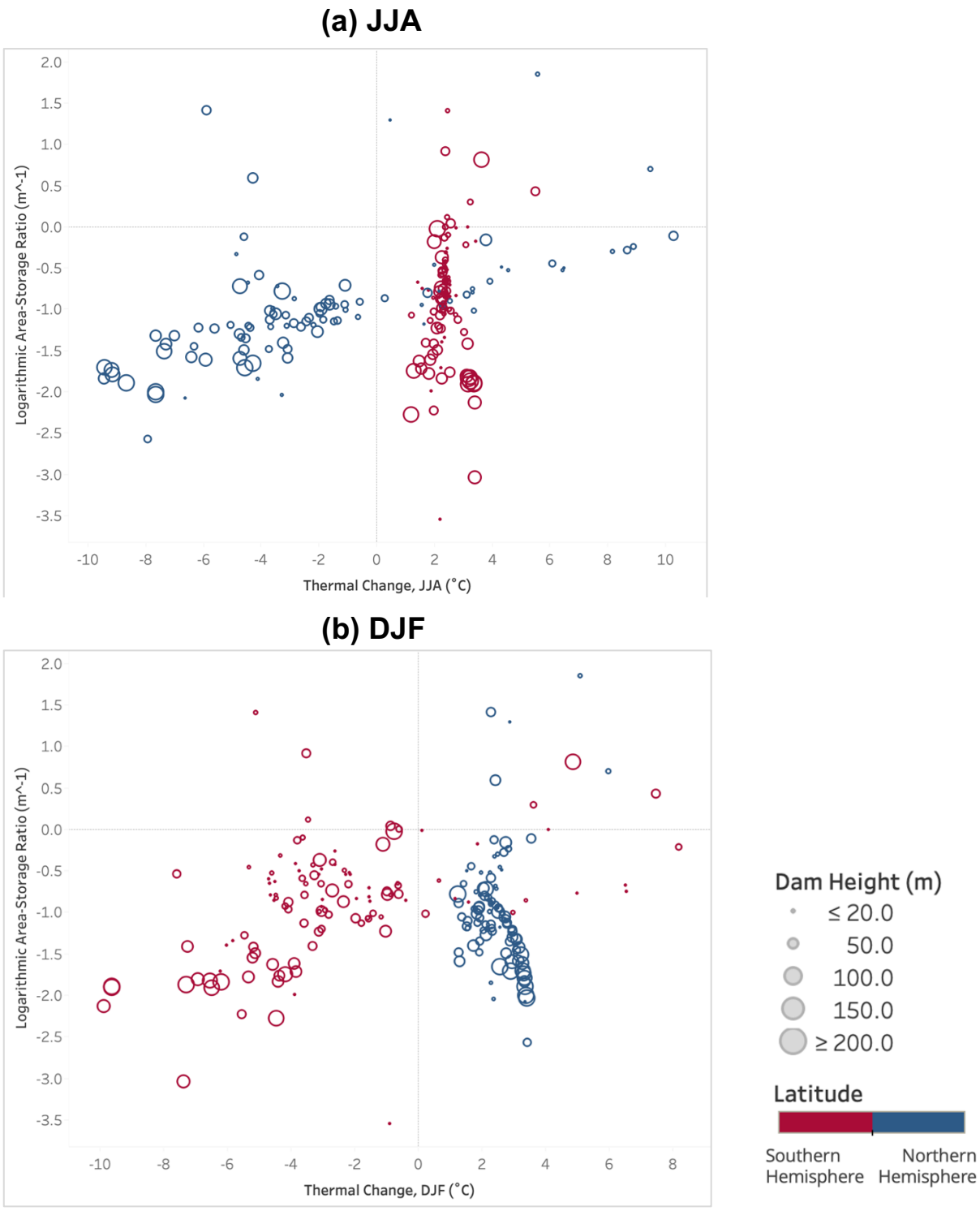

Figure E5. Trends in thermal regime change for 216 planned dams for months of JJA. Variations are plotted with (a) area-storage ratio (measure of reservoir's stratification), and (b) Köppen Geiger climate class. Dam heights, air temperature, and terrain elevation are also shown with marker size and colors.

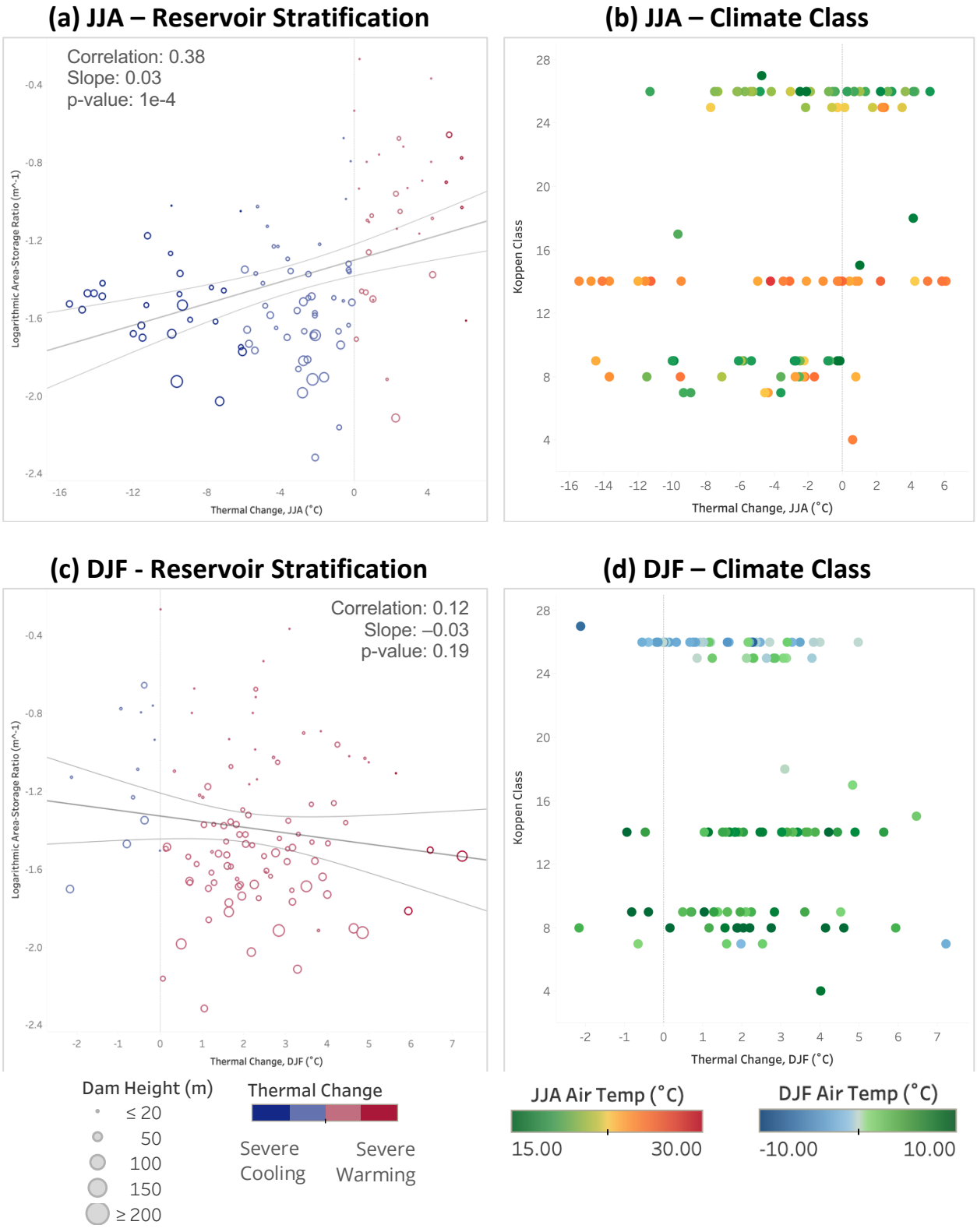
(a) JJA – Reservoir Stratification
Correlation: 0.38
Slope: 0.03
p-value: 1e-4
Logarithmic Area-Storage Ratio (m^-1)
Thermal Change, JJA (°C)
(b) JJA – Climate Class
Koppen Class
Thermal Change, JJA (°C)
(c) DJF - Reservoir Stratification
Correlation: 0.12
Slope: –0.03
p-value: 0.19
Logarithmic Area-Storage Ratio (m^-1)
Thermal Change, DJF (°C)
(d) DJF – Climate Class
Koppen Class
Thermal Change, DJF (°C)
Dam Height (m)
≤ 20
50
100
150
≥ 200
Thermal Change
Severe Cooling
Severe Warming
JJA Air Temp (°C)
15.00
30.00
DJF Air Temp (°C)
-10.00
10.00

Figure E6. Trends in thermal regime change (X-axis) observed for 107 existing dams in the U.S. for JJA (upper panel, a & b) and DJF (bottom panel, c &d). Left panel (a & c) shows trends with the log of area-storage ratio, as a measure of reservoir's thermal stratification and right panel (b & d) denote distribution of Köppen-Geiger climate class for the respective dams.

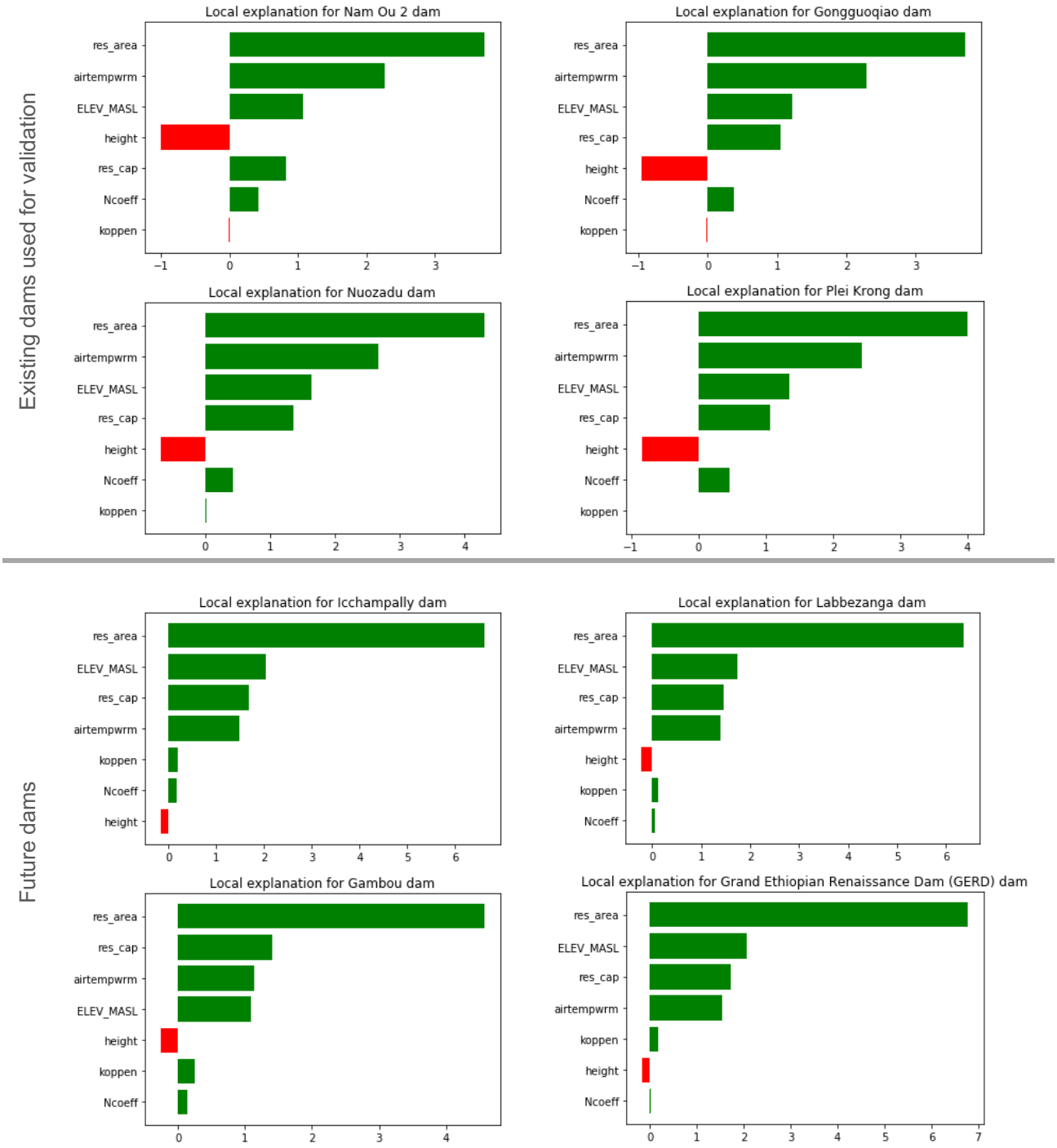

Figure E7. Contribution from input predictors of the trained NN model for a sample of existing dams used for validation and future dams used for prediction (variable names are as defined in Table E2).

Table E1. Comparison of performance in validation of ANN-derived thermal changes (both quantitative, shaded grey and categorical using four classes of thermal change) for ANN models with 2- and 3-hidden layers and a simpler multi-linear regression (MLR) model. Validation is performed over dams in Southeast Asia (MRB and India).

Metric	**JJA**			**DJF**		
	ANN: 2 hidden layers	ANN: 3 hidden layers	MLR	ANN: 2 hidden layers	ANN: 3 hidden layers	MLR
Correlation	0.64	0.62	0.51	0.16	0.11	- 0.11
MAE (˚C)	2.2	2.7	3.9	2.0	1.9	2.2
p-value	0.0003	0.0006	0.0062	0.45	0.60	0.60
Categorical Accuracy	77.8%	77.8%	62.9%	81.5	81.5	74.1
F1-score	0.76	0.80	0.61	0.73	0.73	0.70

Table E2. Description of input features used for training ANN model and in LIME model explanations (air temperature averaged for the respective season – warm/cold)

Variable title	**Description**
res_cap	Reservoir Storage Capacity (million m^3)
res_area	Reservoir area (km^2)
airtempwrm	Air temperature during JJA (˚C)
ELEV_MASL	Terrain elevation (meters above sea level)
height	Dam height (meters)
Ncoeff	Bathymetry coefficient (dimensionless)
koppen	Köppen-Geiger climate class